"ACTIVE CONTROL OF VEHICLE SUSPENSION"

by

Aly Maher Ahmed Abedel-Rehim Abouel-Nour

B.Sc& M.Sc Mech. Eng.

A Thesis submitted to the University of Leeds

in fulfillment of the requirements for the

Degree of Doctor of Philosophy

Department of Mechanical Engineering

The University of Leeds

Leeds, LS2 9JT

September 1989

ABSTRACT

Various types of actively controlled suspension systems for automotive or agricultural applications are theoretically studied on the basis of the well known quarter car model subjected to realistic inputs chosen to represent road surface/forward vehicle speed combinations for a range of different conditions. The vehicle response is evaluated through the performance criteria (the ride comfort, dynamic tyre load and suspension working space) and power requirements (the power input to actuator, power dissipated in damper or actuator and power fluctuation in spring and tyre). The range of suspension systems includes fully active, semi-active, slow-active, single state feedback active, two state switchable damper, continuously variable damper and conventional passive.

Computer programmes relating to the general dynamic modelling of ground vehicle suspension systems (generation of the artificial road, random process analysis and human response criteria) are designed. Computer programmes relating specifically to vehicle ride (linear or non linear), derivation of responses and power calculations for linear or non linear models, as well as performance criteria and optimal control of vehicle suspension are also designed.

The switchable damper system which involves continuously switching between two discrete settings is of considerable interest because such dampers are currently available. It is shown to offer worthwhile improvements over passive systems in terms of ride performance if a simple control law is followed.

Linear optimal control theory is used to obtain the optimal feedback gains of the fully active and slow-active suspension systems. The behaviour of the fully active linear control systems and the possibility of improving their performance by using a non-linear control law is investigated. The performances of the four and

two state feedback slow-active systems, using an actuator with limited frequency response up to 3 Hz, are similar. In terms of the power demand, there is little difference between the fully active and slow-active systems, configured with a conventional passive spring in parallel with the actuator, and their ride performances are also similar. The behaviour of the semi-active systems are evaluated with a control law based exactly on the optimal control of the fully active system, except that no power input is available.

A method of comparing performance and power requirements is based on the practical viewpoint that the suspension designer is essentially allocated a given amount of working space and must optimise the suspension within this constraint. Hence, all the competing systems are compared on the basis of equal workspace contours. Conclusions and suggestions for further work are discussed with particular reference to the relationship between the predictive models and their practical usefulness in assisting the designer of advanced suspension systems for on and off - road vehicles.

ACKNOWLEDGEMENTS

I would like to express my gratitude and sincere appreciation to my Project Supervisor, Dr. D.A. Crolla for his close supervision, enthusastic guidance, and helpful suggestions from the start to the finish of the period of research work. Many thanks are also due to Mr. R.S. Sharp and Mr. D.N.L. Horton for their assistance and knowledgeable encouragement.

Further thanks are extended to the academic, technical and secretarial staff of the Mechanical Engineering department for assisting me in one way or another to make this research possible.

I also wish to express my utmost thanks to the Misr government (Arab Republic of Egypt) who made this scholarship available and financially supported me throughout the period of this study. Many thanks also are due to Egyptian Education Bureau in London during the entire period of this research work.

Also, I would like to express my greatful gratitude to my family, my wife, my daughters Saffa and Radwha for their patience and support in writing this thesis.

Finally, I would like to dedicate this work to the Souls of my parents in memory of all they have done for me.

TABLE OF CONTENTS

ACTIVE CONTROL OF VEHICLE SUSPENSION

CHAPTER 6

CHAPTER 7

CHAPTER 8

CHAPTER 9

CHAPTER 10

NOMENCLATURE

This list of the principal symbols used within the thesis is intended to supplement the definitions given within the text. When a symbol occurs and is used to represent different variables in different parts of the thesis, all definitions are given.

a_f, a_r	Distances from body mass center to front and rear wheels [m]
a_v	Vehicle forward acceleration
A	Matrix defined in text
A_1	Matrix defined in text
A_d	Amplitude of the relative displacement of the damper [m]
A_f	Amplitude of the vibration force [m]
A_i	Amplitude of the periodical input
A_v	Amplitude of the vibration velocity [m/s]
AC_d	Coefficient of the damper which replaces the slow actuator
AK_s	Constant of the additional passive spring
b	Half distance between the right and left parallel tracks [m]
b_1, b_2	Control and disturbance vectors
C	Road roughness constant
C	Matrix defined in text
C_d	Passive damper coefficient [Ns/m]
C_m	Actuator displacement coefficient
C_r	Coefficient of the vehicle rolling resistance
C_s	Coefficient of the switchable damper [Ns/m]
C_v	Coefficient of the continuously variable damper [Ns/m]
d	Input vector

dx	Displacement interval
D	Disturbance input
E_v	RMS of the PSD road input velocities [m/s]
f	Frequency [Hz]
F	Suspension force [N]
F_d	Damping force [N]
F_n	Body natural frequency [Hz]
F_s	Restoring force of the spring [N]
g	Acceleration due to gravity $[m/s^2]$
GV	Constant representing the road roughness/speed combination
h	Subinterval
H_a	Complex response of the body acceleration
H_b	Complex responses of the vehicle body
H_d	Complex response of the dynamic tyre load
H_i	Periodical input
H_r	Complex response of the body/wheel relative workspace usage
H_w	Complex responses of the vehicle wheel
HC_d	Hard damper settings
HS_i	Periodical response of the suspension working space
HV_i	Periodical response of the suspension working velocity
I_b	Pitch inertia of the vehicle body $[kgm^2]$
J	Performance index
J_p	Performance index of the passive system
J_f	Performance index of the active system
K_{d1}, ..., K_{d4}	Feedback coefficients of the slow actuator

K_f	Vector of feedback gains
K_{f0}, ..., K_{fn}	Feedback coefficients of the force control law
K_s	Constant of the linear passive spring [N/m]
K_{s1}, ..., K_{sn}	Constants of the non linear passive spring
K_t	Tyre stiffness [Ns/m]
K_{v1}, K_{v3}	Variable feedback coefficients
m_f	Dimensionless mass factor
M	Auxiliary matrix
M_b	Mass of the vehicle body [kg]
M_w	Mass of the vehicle body [kg]
P	Matrix defined in text
P_{rr}	Power loss due to the vehicle rolling resistance
P_{ar}	Power loss due to the vehicle acceleration resistance
P(t)	Independent series
q_1, q_2, q_3	Weighting factors of the performance index
Q	Weighting matrix
Q(t)	Independent series
r	Weighting factor of the performance index
R_s	Dimensionless factor
R_x, R_y, R_z	Roll, pitch and yaw rotational axes
S	Transformed state vector
SC_d	Soft damper settings
u	Wavenumber [cycles/m]
u_a, u_b	Wavenumber [cycles/m]
U	Actuator control force
U_a	Actuator force [N]
U_d	Desired active damper force

U_s	Actuator demand signal
V	Vehicle forward speed [m/s]
W_b, W_c, W_d, W_e	Human weighting factors listed in table 2.3
W_c	Matrix defined in text
W_o	Matrix defined in text
W_g	Human weighting factors of ISO 1985 listed in table 2.3
X	Displacement [m]
$\dot{X}$	Velocity [m/s]
X_0	Absolute displacement of the road input conditions [m]
X_1, ..., X_4	State variable of the vehicle wheel and body
$X_a(t)$	Time history of the body acceleration
X_b	Absolute displacement of the vehicle body [m]
$\dot{X}_b$	Absolute velocity of the vehicle body [m/s]
$\ddot{X}_b$	Absolute acceleration of the vehicle body [m/s^2]
X_b, Y_b, Z_b	Orthogonal axes on the backrest of the human body
$X_d(t)$	Time history of the dynamic tyre load
X_f, Y_f, Z_f	Orthogonal axes on the feet of the human body
X(k)	Discrete random process for k=1, 2, ..., N
$X_r(t)$	Time history of the relative body/wheel workspace usage
X_s	Absolute displacement of the slow actuator
X_s, Y_s, Z_s	Orthogonal axes on the seat of the human body
X_{sb}	Required displacement of the slow actuator
X(t)	Continuous random process
X_w	Absolute displacements of the vehicle wheel [m]
$\dot{X}_w$	Absolute velocities of the vehicle wheel [m/s]
$\ddot{X}_w$	Absolute acceleration of the vehicle wheel [m/s^2]
Y	Vector of measurable states

$Y(t)$	Average profile between the right and left parallel tracks [m]
Z	output vector
Z_d	Desired value of output vector
$Z_r(t)$, $Z_l(t)$	Profiles of the right and left parallel tracks [m]
$Z(t)$	Tangent line between the right and left parallel tracks
α	Filter constant
γ	Damping ratio of the second order low-pass filter
κ_{v1}	Feedback coefficient for a given periodical input
κ_{v3}	Feedback coefficient for a given periodical input
ω	Frequency [rad/s]
ω_f	Natural frequency of the second order low-pass filter
ω_n	Body natural frequency [rad/s]
ϕ	Set of independent random radian phase angles
ψ	Phase angle between the vibration force and velocity
ψ_b	Phase angle between the body and road input
ψ_w	Phase angle between the wheel and road input
θ	Set of independent random radian phase angles
ζ	Damping ratio

ABBREVIATIONS

AP	Actuator power
arg	Arguments of the complex response
cm	Centimeter
COH	Coherence function between two parallel tracks
DFT	Direct Discrete Fourier transform
DP	Damper power
DTL	Dynamic tyre load
DTLP	Dynamic tyre load parameter
E	Expectation operator
FAC	fully active system
FP	Fluctuating power
i	imaginary part
IDFT	Inverse Discrete Fourier transform
ISO	International Standards Organization weighted
k	Kilo
kg	Kilogram weight
m	Meter
mag	Magnitudes of the complex response
max	Maximum
min	Minimum
mm	Millimeter
MP_-	Mean power dissipation
MP_+	Mean power demand
N	Number of points
N	Newton
ND	No data

NR	No result
o	Degree
P	Power
P_+, P_-	Power demand and dissipation
PAS	Passive system
PSD	Power spectral density
PSD_a	Power spectral density of an acceleration signal
PSD_b	Power spectral density of the vehicle body
PSD_c	Cross power spectral density between two parallel tracks
PSD_d	Direct power spectral density of the right or left track
PSD_d	Power spectral density of the dynamic tyre load
PSD_l	Direct power spectral density of the left track
PSD_r	Direct power spectral density of the right track
PSD_r	Power spectral density of the relative body/wheel work-space usage
PSD_{lr}	Cross power spectral density between the left and right tracks
PSD_{rl}	Cross power spectral density between the right and left tracks
PSD_w	Power spectral density of the vehicle wheel
PSD_y	Power spectral density of the average profile
PSD_z	Power spectral density of the tangent line
rad	Radian
RCP	Ride comfort parameter
RMS	Root mean square value
t	time
T	Time interval [s]

TDE	Time dissipating energy
TF_a	Transfer function of the body acceleration
TF_b	Transfer function of the vehicle body
TF_d	Transfer function of the dynamic tyre load
TF_r	Transfer function of the relative body/wheel workspace usage
TF_w	Transfer function of the vehicle wheel
s	Second
SAC	Semi-active system
SLA	Slow-active system
SLAF	Slow actuator force [N]
SLAWS	Slow actuator working space
SSFB	Single state feedback active system
SWD	Switchable damper system
SWS	Suspension working space [m]
SWV	Suspension working velocity [m/s]
W	Watt
∂	partial derivative
$\int$	Integration
$\sum$	Sum

SUPERSCRIPTS

n	Integer number
p	Exponent
T	Transpose

SUBSCRIPTS

a	Acceleration or actuator
b	Vehicle body
c	Cross
d	Direct track, damper or dynamic tyre load
l	Left track
r	Right track, or relative wheel/body workspace usage
s	Spring
w	Vehicle wheel

GENERAL LAYOUT AND PRESENTATION

This thesis is presented in accordance with the British Standard recommendations for the presentation of theses; BS4821:1972, and with the regulations of the University of Leeds.

All symbols and nomenclature, wherever possible, are in accordance with general and consistent usage and they are fully defined at their first appearance. A list of nomenclature is also included for ease of reference.

Equations, figures and tables are designated the number of the chapter in which they occur and by a secondary number denoting the order in which they appear in the chapter. Figures and tables are bound into the thesis near the appropriate text.

The references cited for the present research work are listed at the end of the thesis and numbered according to the year that they are quoted in each chapter.

Pages are numbered consecutively throughout the thesis including tables and figures.

IN LOVING MEMORY OF

MY PARENTS

CHAPTER 1

INTRODUCTION AND REVIEW OF PREVIOUS WORK

1.1 Introduction

If the loads applied between the rolling wheels of a vehicle and a road were transmitted directly to the chassis, not only would the vehicle's occupants suffer severely but also the structure would be subjected to an excessive degree of fatigue loading. Therefore, the primary function of the suspension system is to isolate the structure from shock loading and vibration due to irregularities in the road surface and it must do this without impairing the stability, steering or general handling qualities of the vehicle. The main components of the conventional passive suspension system are the spring and damper elements. In the case of active systems, an actuator will be used either instead of these passive elements or in parallel or in series with them.

For any vehicle, the suspension system must perform two main functions. First, it provides a high degree of isolation for the vehicle body from the loads applied between the wheels and road, tyre irregularities and wheel out-of-balance forces to ensure operator comfort and second, it keeps the wheels in close contact with the road surface to ensure adequate adhesion when accelerating, braking or cornering. These functions must then be optimised within several constraints: first, the minimum value of the relative body/wheel workspace usage; second, control of the vehicle attitude in manoeuvring; third, the minimum value of the riding height change with load change and finally, the minimum value of the power consumption. In fact, the conflict between these various aspects of vehicle behaviour is the main problem in the suspension systems design. It is well known for example that the best ride comfort can be obtained with a low value of spring stiffness which then implies large values of the working space usage relative to the ground/speed conditions. This in turn implies a vehicle which would suffer large attitude changes in manoeuvring and hard braking. In general, the problem can be

approached from the practical viewpoint that the suspension designer is essentially allocated a given amount of working space and must optimise the suspension ride behaviour within this constraint.

One of the important features of vehicle response predictions is the description of the road surface. The road, however, can be described by an infinite number of irregular spot heights which are considered as imposed displacements upon the tyre arising from the traversal of a given road surface. In general, the displacements imposed on the tyres at each corner of the vehicle are randomly varying functions of time and may be represented by power spectral density functions which describe the frequency content economically. Two other types of input may also be applied to the wheel, the first due to the wheel striking a bump and the second caused by the wheel falling into a pot-hole. The detailed effect of such bumps and pot-holes on the vehicle depends on their geometry and in general, vehicle response to such special features is treated separately from the response to random surfaces.

Human sensitivity to vibrations caused at the vehicle by these ground disturbances is complex. The vibration may cause many types of health disorders depending on its direction, frequency content, amplitude, duration and other environmental and human physical characteristics. Frequency-weighting curves and axis multiplying factors have been developed to evaluate the effects of vertical, longitudinal and lateral vibration with respect to driver comfort. Also, in order to make overall comparisons of vehicles, much research effort has been devoted to finding ways of reducing the complex vehicle vibration environment to a single figure of merit denoting the ride quality. A more detailed survey will be given in the next chapter to discuss road and comfort characteristics.

1.2 Literature survey

Many suspension systems have been studied using the well known quarter car model (see figure 3.3) in terms of performance criteria which typically include the root mean square values of vertical body acceleration (commonly ISO weighted, International Standards Organization ISO (1970)), dynamic tyre load variation or road holding (expressed as percentage ratio between dynamic and static tyre load) and suspension working space. Such systems, classified as passive, active, semi-active and slow-active systems, have been discussed extensively by many investigators and reviewed recently by Sharp and Crolla (1987-a) in terms of the performance. In (1987-b) the same authors introduced further results which attempted to quantify the overall benefits taking the attitude control and adaptation strategies into account. Some of the findings of the main contributions to the vehicle suspension design problem over recent years are reviewed in the following paragraphs.

The conventional passive suspension is the basic system used in most vehicles. It depends on passive elements, i.e. various types of spring and damper which provide forces that are linear or non linear functions of the relative displacements and velocities between the body and wheels of the vehicle. Thompson (1969) showed that for a given natural frequency (Fn=0.77 Hz) of the sprung mass of the quarter car model, the ratio between the optimum damper coefficients for minimising the road holding and minimising the body acceleration was 6.5, although recently, Crawford (1987) quoted that factor as 2.5 for a stiffer suspension (Fn=1.25 Hz). The factor is related to the natural frequency of the suspension system and represents one of the design compromises facing the suspension designer.

For a linear passive suspension system (one degree of freedom) excited by an input described by the power spectral density function of a real road, Ryba (1973) applied the superposition theory to obtain the root mean square values of the body

acceleration and working space of the system. In (1974), he calculated the performance criteria specified above of the well known quarter car model using the same technique. His results showed that a conflict exists between working space and comfort. The requirements of minimising suspension working space can be obtained by using stiff systems, whereas the requirements of maximising operator comfort can be obtained by soft systems. Another conflicting design requirement is the road holding, as influenced by the dynamic tyre/ground load variation, which has an optimum in between a stiff and soft spring system.

Sharp and Hassan (1984) confirmed the conflict between the performance criteria by their parametric studies of passive systems. Their results showed also that with a good passive system, a reduction of the unsprung mass is slightly beneficial to ride comfort and somewhat more beneficial to road holding, expressed as tyre/ground load variation. They also calculated results for a three degree of freedom model which had a vibration absorber on the unsprung mass. However, the benefits obtained were not sufficient with respect to the complexity and cost of the additional mass, spring and damper attached to the wheel mass. Furthermore, in (1986) they calculated those combinations of the natural frequency and damping ratio which gave the optimum passive system for given working spaces. They argued that this was particularly relevant to vehicle design, because the suspension designer was normally constrained with a fixed, restricted suspension working space.

Another feature of the performance of passive systems, which is of some importance, is the total energy dissipated. This manifests itself as an additional rolling resistance of the vehicle and this energy must, therefore, be provided by the engine. However, few studies of the total vehicle energy dissipation by the suspension systems have been made. Velinsky and White (1980) deduced that rough

roads lead to increases in rolling resistance as large as 20%. In (1985), Lu and Segel showed also that for a vehicle traversing a rough road at 30mph, the suspension system increases the rolling resistance by 10% when compared with a smooth road.

The switchable damper system is similar to a passive system except that the damper has two or more states. Two general classes for the control law of a switchable damper exist. The first, called continuously variable control, as discussed by Margolis et al (1975), requires a damper which can produce any desired force magnitude, the direction of this force being consistent with conventional dampers which can only dissipate energy. The second, called on-off control, discussed by Krasnicki (1981) for example, requires a switchable damper which need only produce two distinct levels of damping. This on-off control only requires a two position valve and, therefore, is less expensive than continuously variable control.

Margolis and Goshtasbpour (1984), discussed the performance of a single degree of freedom system with passive, on-off damping control and continuous damping control elements, and the frequency responses of these systems were compared. It was shown that the continuous control was superior to on-off control. They also discovered that the two-stage on-off control of a switchable damper would chatter between the on and off states. This chatter is dependent upon the switching algorithm which incorporates an n^{th} order time lag. In (1987), Crawford discussed the Ford variable dampers that were designed and developed by Armstrong Patents Ltd. The valves were designed to give high switching speed when changing from low to high rate. The switching time was reduced from 58 to 30 ms over the damper speed range from 0.1 to 1.0 m/s.

Active systems (see figure 3.4) use an actuator between the wheel and the body

instead of, or as well as, the spring and damper of the passive system. The actuator acts as a force producer according to some active control law. This active control law depends on the feedback signals of some or all of the state variables. The objective function of the feedback control is a quadratic integral performance index which is usually a weighted sum of the integral of body acceleration, road holding, working space and actuator force. Deriving a good or possibly optimal control law involves minimising this objective function. Typically, an active feedback control system consists of an external power supply, an actuator, transducers, signal processing, feedback and amplifying elements.

The idea of active feedback control used within the vehicle suspension system was first suggested in 1930, as pointed out by Hedrick and Wormley (1975), but the main developments have occurred over the last 20 years. State of the art reviews were produced by Hedrick and Wormley (1975) and Goodall and Kortum (1983). In general, the suspension design problem necessitates a compromise between a number of conflicting requirements, which are described by the performance categories of the suspension system mentioned previously. It is, therefore, an appropriate subject for the application of stochastic optimal control theory to obtain an optimal control law, which is a linear function of the state vector. The state vector includes all or some of the state variables of the suspension system, which are the physical state variables describing the vehicle and road input.

Thompson (1976) introduced a method of designing an active full state feedback control for the quarter car model. He assumed an integrated white noise to represent the road input and used classical optimal control theory, involving solution of the Riccati equation, to find the optimal feedback coefficients of all the state variables of the suspension system. The body acceleration represents the actuator force and this, therefore, was included in the performance index which was

described previously. The optimal control solution involves an obvious practical problem, i.e. that of measuring relative displacements from the road to the body and wheel.

Hac (1985) also derived the optimal control law for an active suspension system which contained passive elements in parallel with the actuator to reduce the actuator force. Consequently, the body acceleration and actuator force are represented separately in the performance index. His assumptions differed from those used of Thompson in the following ways. Firstly, the road input is described as high pass filtered white noise, i.e. it is integrated white noise which includes filtering to remove the infinite value that would otherwise occur at very low frequency. Then, the control law depends on the filter properties and the vehicle velocity. Secondly, the states of road input, body and wheel are measured as absolute variables. In addition, he used a numerical method involving solution of Liapunov equations to find the optimal feedback coefficients of all state variables.

Wilson et al (1986) presented a limited state feedback control technique for active suspension systems. Their technique differed from that used by Hac in the following ways. Firstly, the road surface can be described either as integrated white noise or filtered white noise. Secondly, the performance index is similar to that used by Thompson because the system has no passive elements. Thirdly, the absolute state variables of body and wheel are considered to be the only ones measured, i.e. no need to measure the road input to find the actuator force. Different forms of the optimal control laws, which include some or all of the relative state variables of the system, were obtained. They also carried out coordinate transformations which achieved the desired separation of state variables of the suspension system.

In practice, a conventional spring can be used in parallel with the actuator to support the static vehicle weight. The force demanded from the actuators, which is calculated from the control law, is significantly reduced by the removal of a spring force term from it, Crolla and Aboul Nour (1988a-b)

The concept of a semi-active system is the same as that of the fully active system, except that the latter is capable of supplying and dissipating energy and the semi-active system is capable only of dissipating energy. Consequently, the hardware and the control requirements of an active system can be used within a semi-active system except that the actuator in the active system is replaced by a continuously variable damper in parallel with a conventional spring. This damper is theoretically capable of tracking a force demand signal coming from state measurements and signal conditioning but when a power input is demanded the damper switches off. In general, this semi-active arrangement is a non linear system and the time domain must be used to obtain the response. Also, the process of switching between its on and off states typically involves some dynamic response which needs to be modelled. Obviously, the switchable damper system is similar to the semi-active system except the latter is based on the fully active system.

In Karnopp et al (1974) a single degree of freedom system of incorporating passive, skyhook, semi-active and active suspension types were discussed. The skyhook system uses a damper which provides force as a function of the absolute vertical velocity of the vehicle body rather than the relative wheel to body velocity. In the active system, the skyhook damper is replaced by an actuator between the body and wheel to provide a force similar to that of the skyhook damper, i.e. the actuator force depends on one state variable which is the velocity of the body. The results obtained from the semi-active and active systems (which used the same control force) were very close to each other.

The same comparison of the frequency responses between passive, semi-active and active systems was made by Margolis (1982) for a single degree of freedom model. The control law of the active element included only the body velocity. In (1983) he introduced the concept of semi-active control, which was a function of the body and wheel velocities, for a two degree of freedom model. His conclusion was that semi-active systems are quite capable of providing performance approaching that of the fully active systems.

Many versions of the semi-active system were studied by Sharp and Hassan (1986, 1987) for the quarter car model. These versions contain a feedback control law which includes some or all of the state variables and the switching between the on and off states included a first order time lag. The preferred system from a practical viewpoint (1987) was one which contained a conventional passive spring to support the static vehicle weight. They compared the semi-active system with other types of suspension system and the results of the fully active and semi-active systems were very close to each other at the lowest value of working space.

Slow-active systems (see figure 7.1) use an actuator which acts in series with a passive spring. A passive damper would typically be used between the body and wheel of the vehicle or in parallel with the spring in conjunction with this system. The actuator may be used to put energy in or take it out of the system over a certain limited bandwidth. The practical advantage of slow actuators with limited frequency response is that they are considerably cheaper than the high response actuators required for the other active systems. However, in the mathematical model, an idealised frequency limitation is imposed by a second order low pass filter, which enables the effect of various cut-off frequencies to be investigated. The control law of the limited actuator is based on a displacement demand signal which is a function of some or all the state variables of the system. The active feedback coeffi-

cients of a slow actuator can be found by applications of the linear stochastic optimal control theory in a similar fashion to that pertaining to the fully active systems.

In Sharp and Hassan (1987) the displacements and the velocities of the wheel and the body were assumed to be the measurable signals for the actuator displacement demand signal. Their results indicated that a system with a 3Hz bandwidth actuator and variable damping gave good ride performance over a wide range of road roughness conditions. They expected that the slow-active systems would be relatively inexpensive in terms of capital and energy consumption cost compared with the fully active systems.

1.3 Aim of the present work

The aim of the present work is the investigation of various types of intelligent suspension systems using the well known quarter car model, in terms of their performances and power consumptions. The systems are classified as passive, switchable damper, fully active, semi-active involving a continuously variable damper and slow-active. Therefore, the scheme of the present work involves the following procedures.

1- Presenting a good understanding of the subjects relating to the dynamic modelling of ground vehicle suspensions and designing appropriate computer programs. These subjects include the road surface description, the techniques for generating artificial roads, random process analysis and human response criteria.

2- Designing software programmes of vehicle ride (linear or non linear) models, calculating performance and power requirements for linear or non linear models, and deriving optimal control laws for vehicle suspensions.

3- Presenting parametric studies and discussing suspension performance capabili-

ties including the energy dissipation in passive systems.

4- Evaluating the possibility of improving the conventional passive system by using a two state switchable or continuously variable damper, instead of a fixed damper. The switchable damper system which involves switching between two discrete settings is of considerable interest because such dampers are currently available commercially.

5- Investigating the performance capabilities and power demand and dissipation requirements of the fully and slow active suspension systems.

6- Introducing an alternative searching method to find optimal variable feedback coefficients as functions of time for active systems.

7- Studying the performance capabilities and power dissipation of semi-active systems based on the optimal active feedback control.

8- Evaluating and correlating the energy losses of suspension systems, due to the road roughness, as a part of vehicle rolling and acceleration resistance.

The modelling procedure of these systems involves the following stages. Firstly, write the equations for the models together with equations describing the force producing elements. Secondly, derive appropriate -sometimes optimal- control laws. Thirdly, use a random disturbance input at the tyres. Fourthly, evaluate the performance and power requirements in terms of some random process criteria such as root mean square, mean and peak values. Fifthly, repeat these calculations over a range of road surfaces and vehicle speeds. Finally, compare all of these systems in terms of their performance and power consumption.

The work presented here is divided into ten chapters. In this first chapter, a survey of the previous work has been introduced. Chapter 2 gives a survey of subjects relating to the dynamic modelling of ground vehicle suspension systems. This survey covers a wide range of the road surface description, the techniques for generating artificial roads, random process analysis and human response criteria. The aim of chapter 3 is to outline the vehicle ride models, derivation of responses, power calculations, performance criteria and optimal control of vehicle suspension.

In chapter 4, linear analysis procedures are used to obtain the performance capabilities and damper power losses of passive systems. Also the behaviour of switchable damper systems is studied by using non linear analysis procedures. Parametric studies and comparisons for the passive and switchable systems are also presented.

The performance capabilities including the power requirements, of the fully active systems, using either a full or limited state feedback control law, are the subject of chapter 5. Although, an active system is considered to be a linear system, its power demand and dissipation must be obtained by using time domain analysis. Furthermore, the possibility of using feedback coefficients which are functions of time, i.e. recalculated at small time intervals, is investigated, whilst recognising the computational difficulties that this would involve in practice.

In chapter 6, the non linear analysis procedures are used to obtain the behaviour of various types of semi-active system which are based on the active feedback control laws obtained in the previous chapter. The performance capabilities and power dissipation for varying road input conditions, road roughness constants and vehicle forward velocities, of the semi-active systems are compared with the corresponding properties of the fully active systems.

The performance capabilities including the power requirements of the slow active system, using an actuator with limited frequency response up to 3 Hz, are presented in chapter 7. The validity of using simple state combination measurements of the active feedback control law are evaluated. This simple active feedback control law depends on measuring absolute velocities of the vehicle body and wheel or measuring only the relative displacement between the two ends of the actuator used.

The most difficult step is to interpret such results, which without some well-founded strategy can become an overwhelming task in view of the large volume of results, for all the suspension systems studied in the present work, which may easily be generated. One efficient method for comparing performance is based on the practical viewpoint that the suspension designer is essentially allocated a given amount of working space and must optimise the suspension within this constraint. Hence, competing systems are compared on the basis of equal workspace contours in chapter 8. In chapter 9, the power requirements, demand and dissipation, of the vehicle due to the road roughness and forward vehicle velocity are correlated and compared for all types of competing suspension systems. Finally, the conclusions and suggestions for further work are presented in chapter 10.

CHAPTER 2

ROAD DESCRIPTION, RANDOM PROCESS ANALYSIS AND HUMAN RESPONSE CRITERIA

In this chapter a survey of subjects relating to the dynamic modelling of ground vehicle suspension systems is presented. This survey is divided into four essential parts to cover the road profile description, generation of the artificial road, random process analysis and human response criteria.

The first part describes the displacement imposed on the tyres at each corner of the vehicle, measurement techniques, the spectral and coherence properties of the road profiles. The second part also gives the techniques used to generate the artificial road, for either one track or two parallel tracks, in order to use them in the time domain for non-linear analysis.

The third part indicates the practical tools for random vibration analysis, used to judge the response of the suspension system to a random input. A short survey is given to review some of those tools which include the mean, mean square and peak values of the random vibration. The fourth part indicates the human response to vehicle body acceleration. Measurement techniques and weighting of the comfort are explained, with a summary of the weighted value as a function of frequency, location and direction in respect to the human body.

2.1 Road profile description

When a vehicle traverses a particular road surface at constant speed the displacements imposed, i.e. vertical input excitation, on the tyres at each corner of the vehicle are related to the detailed spectral description of the profiles of that road surface. A designer of a suspension system, for example, needs some sort of description of a large number of roads in order to assess the performance of a vehicle suspension over a wide range of operating conditions. Other features of a road related to handling issues are: degree of traffic polishing of the road surface, consistent safety in dry and wet conditions, minimum spray generation, low noise gen-

eration and subsequent maintenance which are not included in this description. Therefore, a more detailed survey will be introduced to describe the road surface roughness features of prime concern to the ride problem including profile measurement, profile spectra and profile characteristics.

2.1.1 Profile measurement

During the past few years, several experimental investigations have been performed to study road surface profiles. Measurements of road surface profiles have been carried out using instrumentation on either a passenger car or a profile - following wheel on various test sections of roadway. The passenger car technique for two parallel tracks is discussed by Healey et al (1977). For each track, they used an accelerometer attached to the car body over the sensing wheel and a potentiometer for measuring the relative displacement between the car body and the sensing wheel. The accelerometer signal was integrated twice and summed with the potentiometer signal to obtain the absolute motion of the wheel. The profile following wheel method is discussed by Bulman (1979). He used a light beam as the reference level aimed across the profile to be measured.

These investigators obtained a reasonable record of the profiles for statistical analysis, with at least 200 metres sample length and vertical resolution of 0.01 metre. Some of these data have been recorded on magnetic tape for further analysis of a particular test track profile. Leeds University Vehicle Dynamics Group, for example, keeps copies of spot heights for a number of off-road tracks, measured for example by the A.F.R.C. Institute of Engineering, Silsoe or the Motor Industry Research Association, Nuneaton. The spot heights of surface texture may be transformed by Fourier analysis to characterise their frequency domain properties.

2.1.2 Profile spectra

The conversion of the road surface roughness data and many kinds of vehicle response data from time to frequency domain is common. This conversion for the numerical manipulation of 2^n sample values, where n is an integer, in a sequence obtained from a continuously varying signal at equal time intervals can be achieved by digital processing involving the Discrete Fourier Transform (DFT), Newland (1984). The result of the DFT process then is to give the amplitude and phase properties of a number of sine waves which add together to give precisely the original signal sample values at the sampling instants.

Dodds and Robson (1972) formulated the spectra of the two parallel tracks for a given road, which has profiles $Z_r(t)$ and $Z_l(t)$ and a distance between the tracks of 2b. They simplified the problem by considering the following variables;

$$Y(t) = \frac{Z_r(t) + Z_l(t)}{2} \qquad 2\text{-}1$$

$$Z(t) = \frac{Z_r(t) - Z_l(t)}{2b} \qquad 2\text{-}2$$

where Y(t) is the average profile and Z(t) is the tangent line between tracks as shown in Figure 2.1. Direct and cross spectral density were formulated as a function of wave number (u) as;

$$PSD_d(u) = PSD_r(u) = PSD_l(u) = PSD_y(u) + b^2\, PSD_z(u) \qquad 2\text{-}3$$

$$PSD_c(u) = PSD_{rl}(u) = PSD_{lr}(u) = PSD_y(u) - b^2\, PSD_z(u) \qquad 2\text{-}4$$

and the coherence function between tracks was found from,

$$COH(u) = \frac{PSD_c(u)}{PSD_d(u)} \qquad 2\text{-}5$$

Once the $PSD_d(u)$ and COH(u) are defined and different sets of independent

random radian phase angles are generated then the artificial track profiles, which are parallel to each other, can be simulated to represent a given isotropic road surface.

2.1.3 Profile characteristics

Based on a very large number of road and terrain measurements, the mean square displacement spectral density has been found to be inversely proportional to the wave number. Robson (1979) reviewed the state of the art of the approximate relationships used to describe road spectra and suggested the following description;

$$PSD(u) = C\,u_a^{-p} \quad \text{,if} \quad 0 < u \le u_a$$

$$PSD(u) = C\,u^{-p} \quad \text{,if} \quad u_a < u \le u_b$$

$$PSD(u) = 0 \quad \text{,if} \quad u_b < u \qquad \text{2-6}$$

where C is a roughness constant of a road, u (cycle/metre) is the wave number and u_a, u_b are suitable wave numbers to be determined and p is an exponent. Typical values of roughness constant for various roads are indicated in Table 2.1 for an exponent value p=2.5. He also indicated that curves of the coherence function as shown in Figure 2.2 represent the coherency relationship versus the frequency content of an isotropic surface for various track widths. The coherence function is inversely proportional to wave number and track width. Road surfaces cannot of course be expected to be precisely isotropic, and indeed it can easily be shown that they are not even precisely homogeneous. But in formulating the representative road model, where great precision would be of little avail, isotropy would seem to provide an acceptable basis.

The area under the curve PSD(u) over a given range of wave numbers is then the mean square value over that range. The PSD function may be expressed in

terms of the frequency f Hz and traversal vehicle velocity V meter/second instead of the wave number u by equating mean square values as follow;

$PSD(f)\,df = PSD(u)\,du$, and $f = uV$,then

$$PSD(f) = C\,V^{p-1} f^{-p} \quad \text{, say} \quad GV = C\,V^{p-1} \qquad 2\text{-}7$$

where GV is another constant representing the road roughness. A somewhat better than average minor road is used throughout this thesis and its power spectral density is plotted against the frequency f for various vehicle velocity V in Figure 2.3. The roughness constant of that road is 10^{-5}. The mean square values of the road input condition are also plotted versus vehicle speed, V, over a frequency range up to 15 Hz in Figure 2.4.

2.2 Generation of the artificial road input

In Cebon and Newland (1983), some methods of generating either one or more parallel track profiles of the road were presented by applying the inverse Fourier transform to the amplitude of the power spectral density function. In general, it is better to generate such tracks as a function of wave number to enable use of the track profiles at any vehicle velocity, V, directly.

2.2.1 Generation of one track random profile

An artificial time history of the track profile can be generated from the spectral density function PSD(u) of a given road by using digital processing involving the Inverse Discrete Fourier transform IDFT. The coefficients of series IDFT can be derived from that desired PSD(u) over a certain range of wave numbers u(k), k=[1,2....,N-1]. These coefficients are added to a set of independent random radian phase angles $\theta(k)$ uniformly distributed between 0 and 2π. The spot heights of the series $Z_1(t)$, t=[1,2....,N-1] , at regular closely spaced intervals, dx, along the track

are then:

$$Z_l(t) = \sum_{k=0}^{N-1} \sqrt{S(k)}\, e^{i[\theta(k) + u(k)\, dx\, t]} \qquad 2\text{-}8$$

where

$$S(k) = \frac{2\pi}{N\, dx} PSD[u(k)] \qquad \text{and} \qquad u(k) = \frac{2\pi k}{N\, dx}$$

In the work presented here, the artificial track used contains N=8192 points within a 300 metre track length as shown in Figure 2.5. To ensure that the artificial t-ack accurately represents the minor road which is used throughout, the power spectral density function PSD(u) of that artificial track Z_l is again converted by using the DFT process. The PSD(u) of that artificial road fits very closely to that of the original PSD(u) as shown in Figure 2.6.

2.2.2 Generation of random profiles for two parallel tracks

Suppose that both the spectral density PSD(u) and coherence function COH(u) of a given isotropic road are known. Then, it is possible to generate two artificial track profiles which are parallel to each other and a known distance apart. Various different techniques can be used to generate these track profiles by using the IDFT. The first technique derives from equations 2-3 and 2-4 but in (1983), Cebon and Newland gave another technique. This technique generates the first track Z_l from PSD(u) directly by using the equation 2-8, assuming that the Z_l track is the left track. Then the right track Z_r might be generated by summing together two independent series, one of them correlated and other uncorrelated with the left track. The correlated series P(t) uses the same phase angles $\theta(k)$, as that used in the left

track, and the uncorrelated series Q(t) uses a new independent set of radian angles $\phi(k)$ as;

$$P(t) = \sum_{k=0}^{N-1} COH(k)\ \sqrt{S(k)}\ e^{i[\theta(k) + \mu(k)\ dx\ t]}$$

$$Q(t) = \sum_{k-0}^{N-1} \sqrt{1 - COH^2(k)}\ \sqrt{S(k)}\ e^{i[\phi(k) + \mu(k)\ dx\ t]}$$

$$Z_r(t) = P(t) + Q(t) \qquad 2\text{-}9$$

thus, the left and right track profiles are $Z_l(t)$ and $Z_r(t)$.

2.3 Statistical criteria for use in the random response

Phenomena whose states at a future instant of time cannot be predicted are classified as non deterministic, and referred to as random. The response of a vehicle suspension system to a random excitation is also a random phenomenon. So, some statistical methods relating to random vibration analysis must be adopted. A short survey will be given to discuss these statistical tools which include mean, mean square and peak values.

2.3.1 Mean value

The mean value of the single random process at N given samples X(k), (k=1,2,.. ,N), over a certain time is obtained by simply summing up the values of the samples and dividing the result by the number of samples. For a continuous function X(t), the mean value can be obtained in some interval 0 to T by integrating and dividing the result by the interval T. The mean value can be written mathematically as;

$$Mean = \frac{1}{N}\sum_{k=1}^{N} X(k) \quad , \text{or} \quad Mean = \frac{1}{T}\int_{0}^{T} X(t)\,dt \qquad 2\text{-}10$$

However, because the suspension problem is mainly concerned with variations about a nominal mean value of zero, the mean square value is of more use.

2.3.2 Mean square value

The mean square value of a random variable provides a measure of the energy associated with the vibration described by that variable. The definitions of the mean square value for a given N samples X(k), (k=1,2.. ,N) and for a continuous function X(t) in the interval 0 to T are;

$$Mean\ \ square = \frac{1}{N}\sum_{k=1}^{N} X^2(k) \quad , \text{or} \quad Mean\ \ square = \frac{1}{T}\int_{0}^{T} X^2(t)\,dt \qquad 2\text{-}11$$

The positive square root of the mean square value is known as root mean square which is the same as the standard deviation in the case of the mean value of zero.

For the power spectral density of the road input, which is a function of frequency as shown in figure 2.6, the mean square value over a particular frequency range is calculated by integrating the area under the power spectral density curve over that range as in the following equation;

$$Mean\ \ square = \int_{f1}^{f2} PSD(f)\,df \qquad 2\text{-}12$$

Neither the mean nor the mean square values give complete information about the random process. Therefore, the peak values should be taken into account.

2.3.3 Peak value

The peak value of the single random process is the maximum value of the sam-

ple function. It can be used with linear or non-linear suspension systems to determine the maximum quantity of the random response, which might be displacement, force, working space, tyre load, energy, and power. A designer of an active suspension system, for example, needs to know the maximum demanded power, which would be used in designing the actuator.

One of the most common examples of a probability distribution is the Normal or Gaussian distribution. It is interesting to note that for a random process of the Normal distribution only 1 peak in 100 peaks exceeds three times the standard deviation on average, Newland (1984). In general, the response of a vehicle suspension system is a stationary Gaussian process because the input, i.e. the irregular spot heights of the road, is a Gaussian process.

2.4 Human response in relation to body acceleration

A vehicle must carry at least one passenger and most are suitable for several passengers in addition. Discomfort and annoyance for both driver and passengers are not desirable and must therefore be minimised. Therefore, a measure of passenger comfort is one of the more subjective areas with which vehicle designers become involved. The comfort involves everything in the driver's environment to ensure the continued carrying out of his or her complicated task without unnecessary distraction. The driving environment includes whole-body vibration, noise, temperature, handling, decor etc. However, having noted that many factors affect overall comfort, this study is only concerned with the human comfort due to vibration of the vehicle body, which is the factor over which the suspension designer can exert some control.

2.4.1 Comfort measurement

Investigations of human response to whole body vibration have been approached experimentally as follows. Volunteers were requested to assess a range of sinusoidal vibrations with increasing amplitudes in terms of levels of perception, discomfort, annoyance etc. Results of these studies have been reviewed by many investigators. Jones and Saunders (1972) summarised the causes of the sometimes large discrepancies in the results including the differing experimental environments. In their study, a method of adjustment was employed to derive equal comfort curves for whole body vertical vibration of the subject at different acceleration peak levels, from 0.1 to 0.6, of gravitational acceleration and frequency range 4-80 Hz with 20 Hz reference frequency. These results were compared with the results of other investigators and International Standards Organization ISO (1970).

Griffin (1986) gave a definition of a comfort model with twelve axes as shown in Figure 2.7. The model assumed that the principal vibration inputs influencing the vibration discomfort of a seated person occur at three locations; the supporting seat surface, the backrest, and the feet. At each of the input positions the vibrations may occur in three orthogonal translational axes defined relative to the orientation of the human body such that X_s, Y_s and Z_s on the seat, X_b, Y_b and Z_b on the backrest and X_f, Y_f, and Z_f at the feet. The rotational vibrations also on the seat may be assessed. These are the roll R_x, pitch R_y and yaw R_z axes. He summarized the frequency-weighting and axis multiplying factors which were derived by many investigators to evaluate the vibration with respect to comfort as shown in Tables 2.2 and 2.3. The frequency-weighting values should be multiplied by this axis factor to obtain the weighted value for the required axis.

2.4.2 Frequency weighting

The constant comfort curves of the vertical, lateral, and longitudinal vibration are given by the ISO standards (1974) which are shown in Figure 2.8. These curves represent the relation between RMS acceleration values versus frequency for various exposure times, assuming a simple sinusoidal excitation.

The standards gave two alternative approaches to determine the weighting criterion as follows. First, by analysis of the acceleration into octave band levels, weighting the levels in individual bands and recombination. Second, by direct use of electrical filters in a frequency-weighting "ride meter". Pollard and Simons (1984) considered the most appropriate one for railways involving the following procedure. Firstly, a power spectral density of the acceleration signal PSD_a of interest is calculated by using, for example, the DFT. Secondly, analyse each PSD_a acceleration into 1/3 octave components over the frequency range 1 to 80 Hz. Thirdly, average the root mean square value of each frequency component $PSD_a(f)$ over the duration specified for the measurement. Fourthly, multiply the 1/3 octave values by the weighting factors W(f) listed in table 2.3/Wg and calculate a weighted acceleration value which is the root mean square value ride comfort parameter (RCP) for each vibration recording as in the following equation;

$$RCP = \sqrt{\sum_{f=1}^{80} PSD_a(f)\, W(f)\, df} \qquad 2\text{-}13$$

The standard ISO (1985) was only defined over the range from 1 to 80 Hz and the values are defined as the ratio of the acceleration band value at 4-8 Hz. In general, for any vehicle one can determine a time history of the acceleration adjusted to give the proper human comfort weighted at all frequencies as discussed.

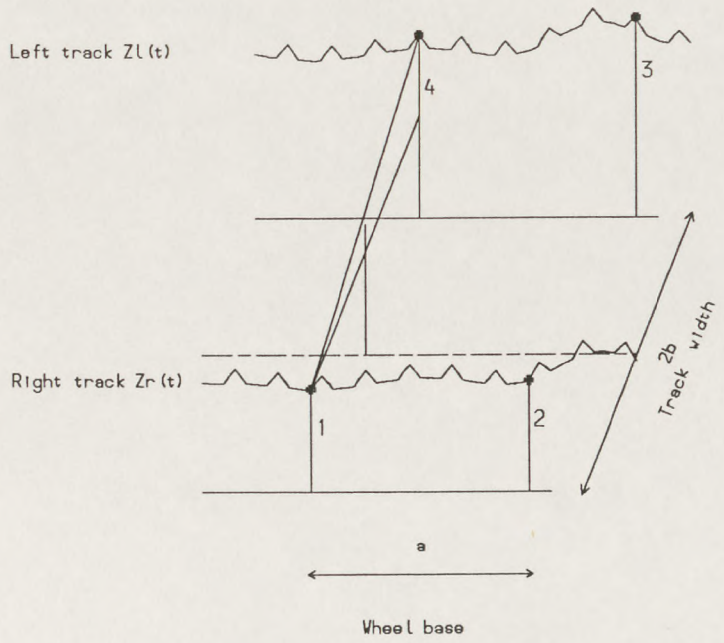

Figure 2.1 Two parallel track profiles and the four imposed displacements at the vehicle wheels.

Road type	Range	Mean
Motorway	$3\ 10^{-8}$ - $50\ 10^{-8}$	$10\ 10^{-8}$
Main road	$3\ 10^{-8}$ - $800\ 10^{-8}$	$50\ 10^{-8}$
Minor road	$50\ 10^{-8}$ - $3000\ 10^{-8}$	$500\ 10^{-8}$

Table 2.1 Roughness constant range for different types of road surface.

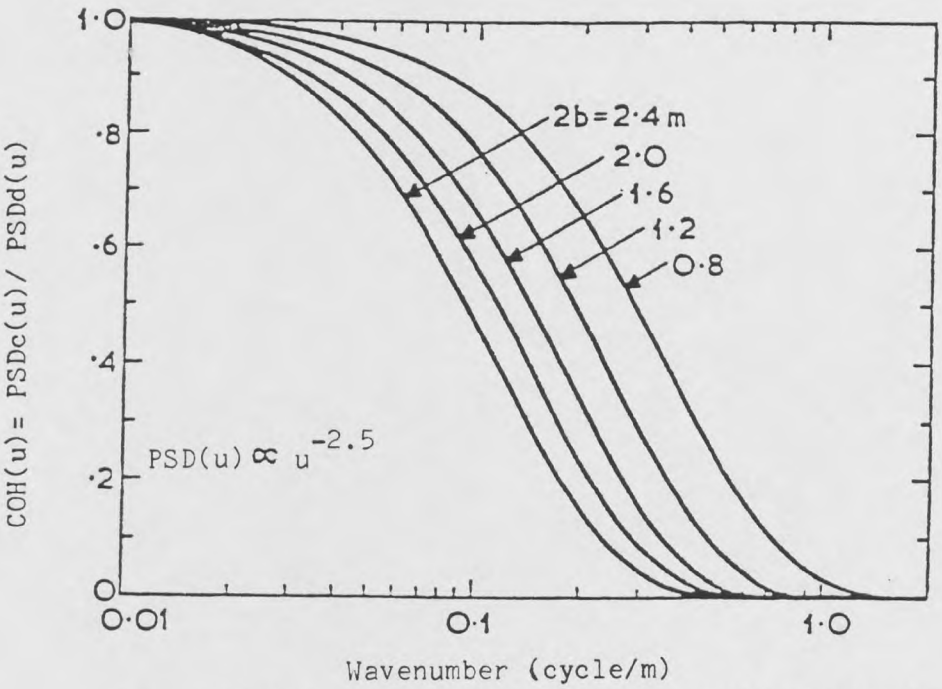

Figure 2.2 Coherency curves for an isotropic surface for various track widths 2b [from Robson (1979)]

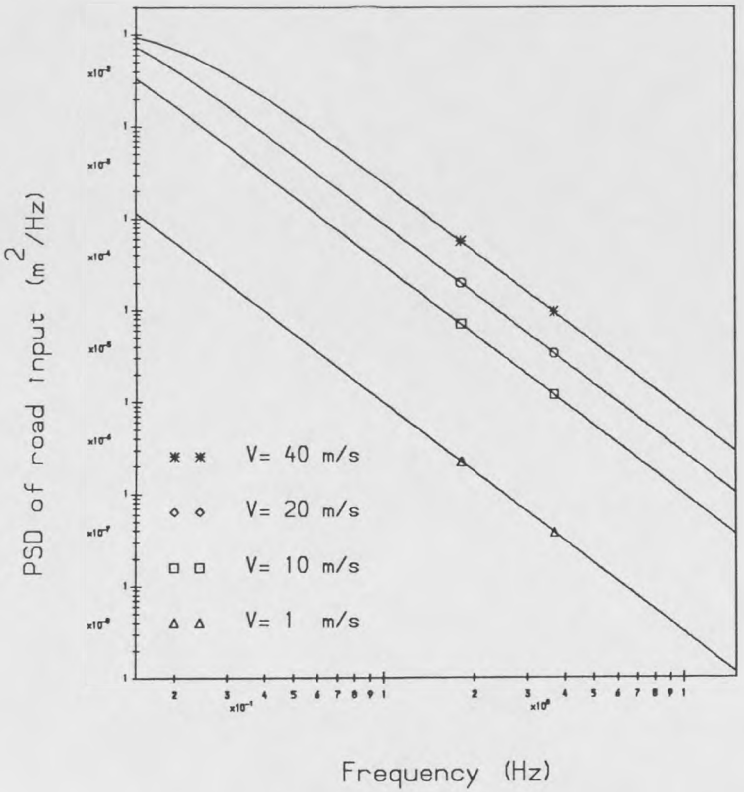

Figure 2.3 Displacement power spectral densities for a minor road traversed at different velocities.

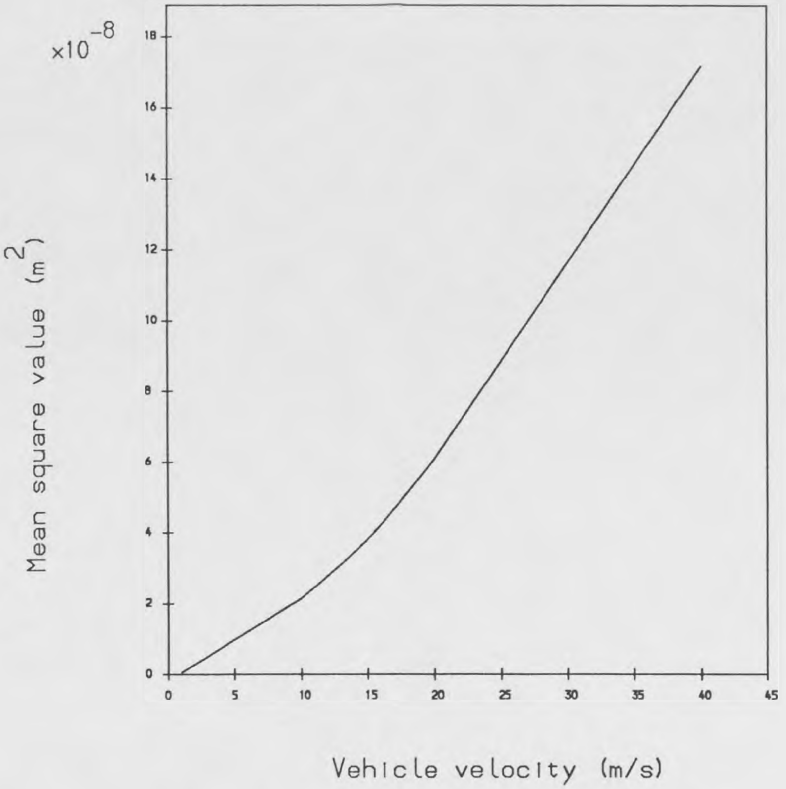

Figure 2.4 The mean square value of the road elevation versus vehicle velocity.

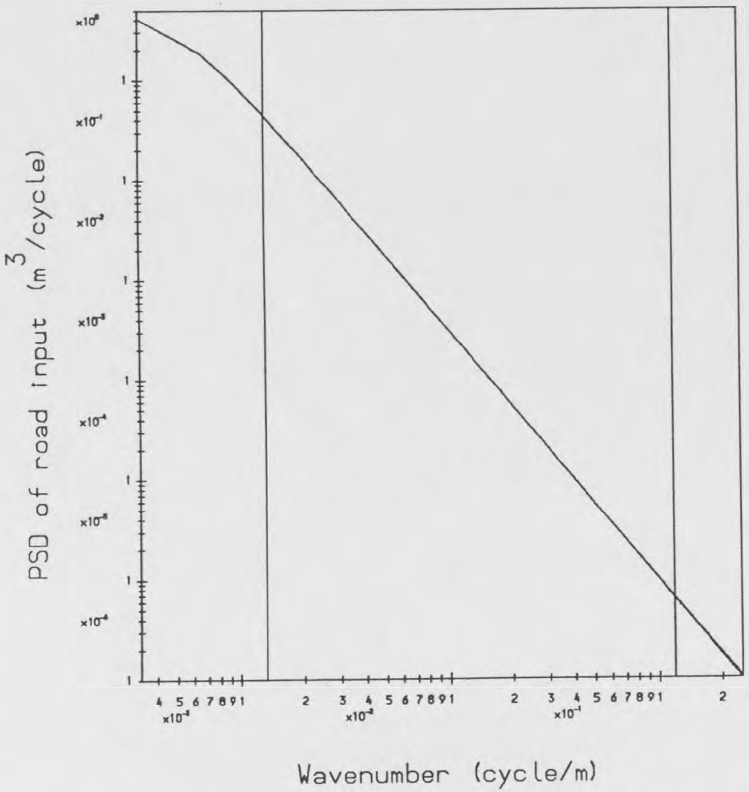

Figure 2.6 Displacement power spectral densities for a minor road {continuous} and artificial track profile {broken}, showing those lines coincide exactly.

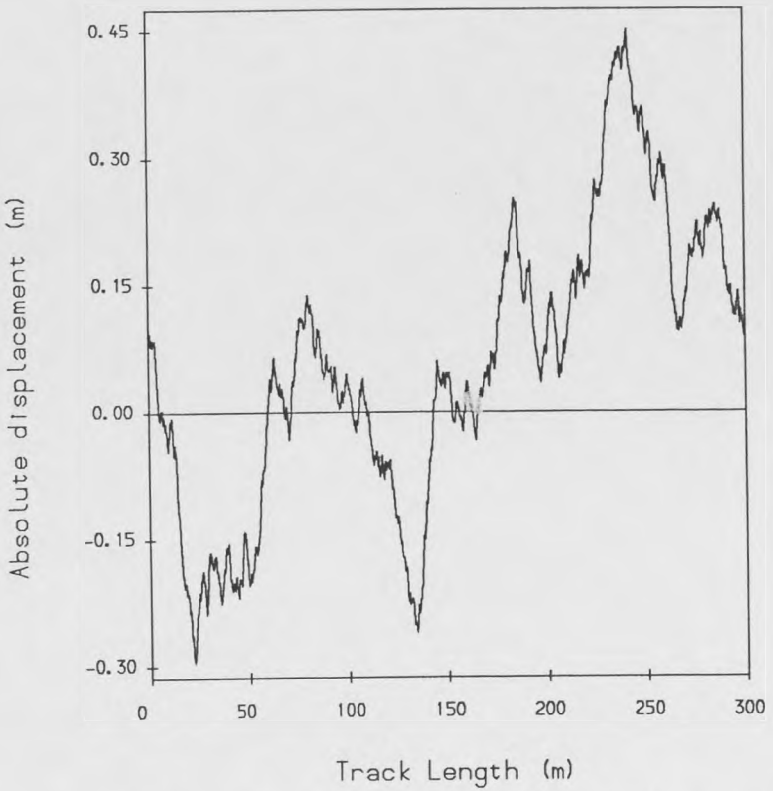

Figure 2.5 The spot heights of the track profile.

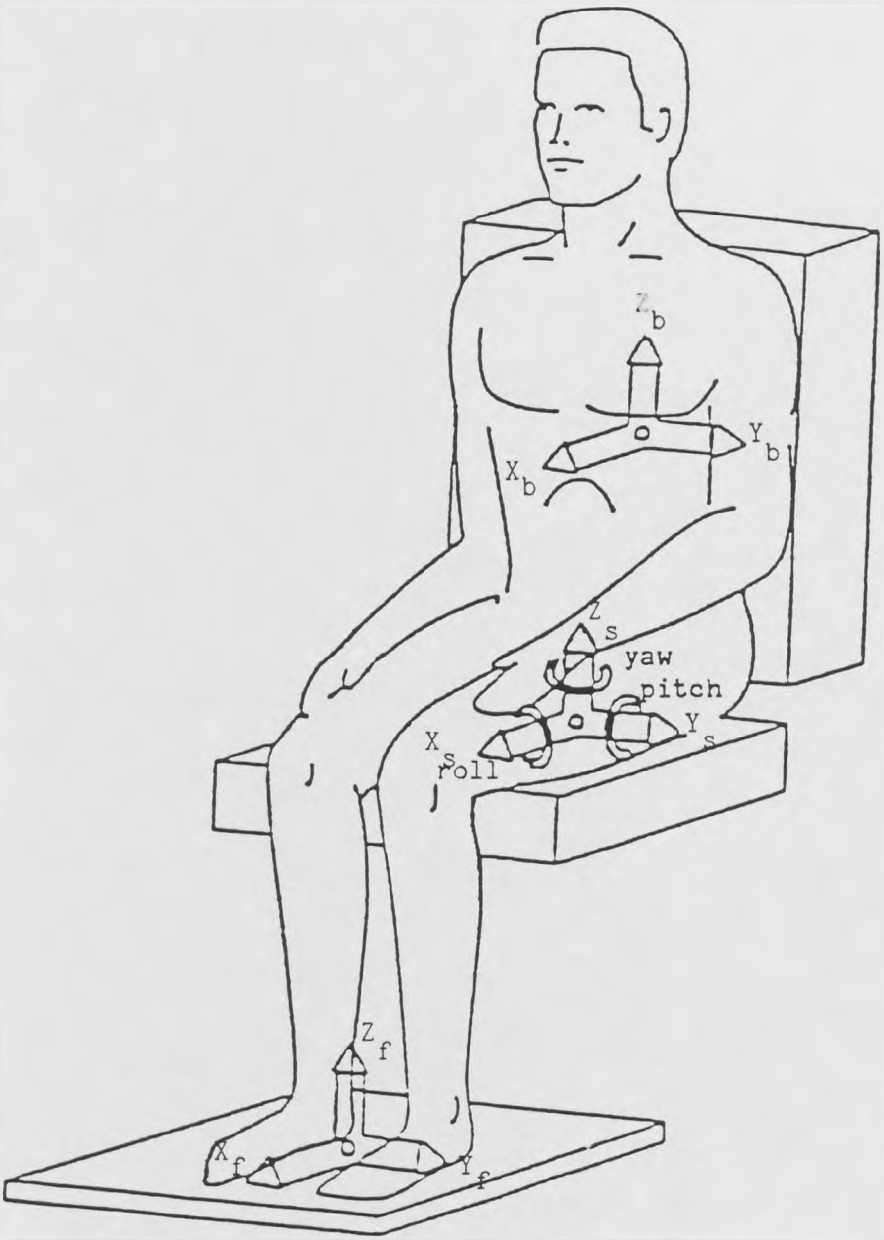

Figure 2.7 Twelve axes of vibration included in tne model of vibration discomfort [from Griffin (1986)].

Table 2.3 Frequency-weighting W(f) as a function of frequency f (Hz) for different weighting schemes.

Code name	Frequency from	to	Weighting W(f)
Wb	0.5	2.0	0.4
	2.0	5.0	f/5.0
	5.0	16.0	1.0
	16.0	80.0	16.0/f
Wc	0.5	8.0	1.0
	8.0	80.0	8.0/f
Wd	0.5	2.0	1.0
	2.0	80.0	2.0/f
We	0.5	1.0	1.0
	1.0	20.0	1.0/f
Wg	1.0	4.0	$(f/4)^{0.5}$ ISO 1985
	4.0	8.0	1.0
	8.0	80.0	8.0/f

N.B. W(f) = 0.0 where not otherwise defined, such that f is the frequency of vibration.

Table 2.2 Axes multiplying factors for all locations.

Location	Axis	Code name	Multiplying factors
Seat	X, Y	Wd	1.0
	Z	Wb	1.0
	R_x, R_y, R_z	We	0.63, 0.4, 0.2
Back	X	Wc	0.80
	Y, Z	Wd	0.5, 0.4
Feet	X, Y, Z	Wb	0.25, 0.25, 0.4

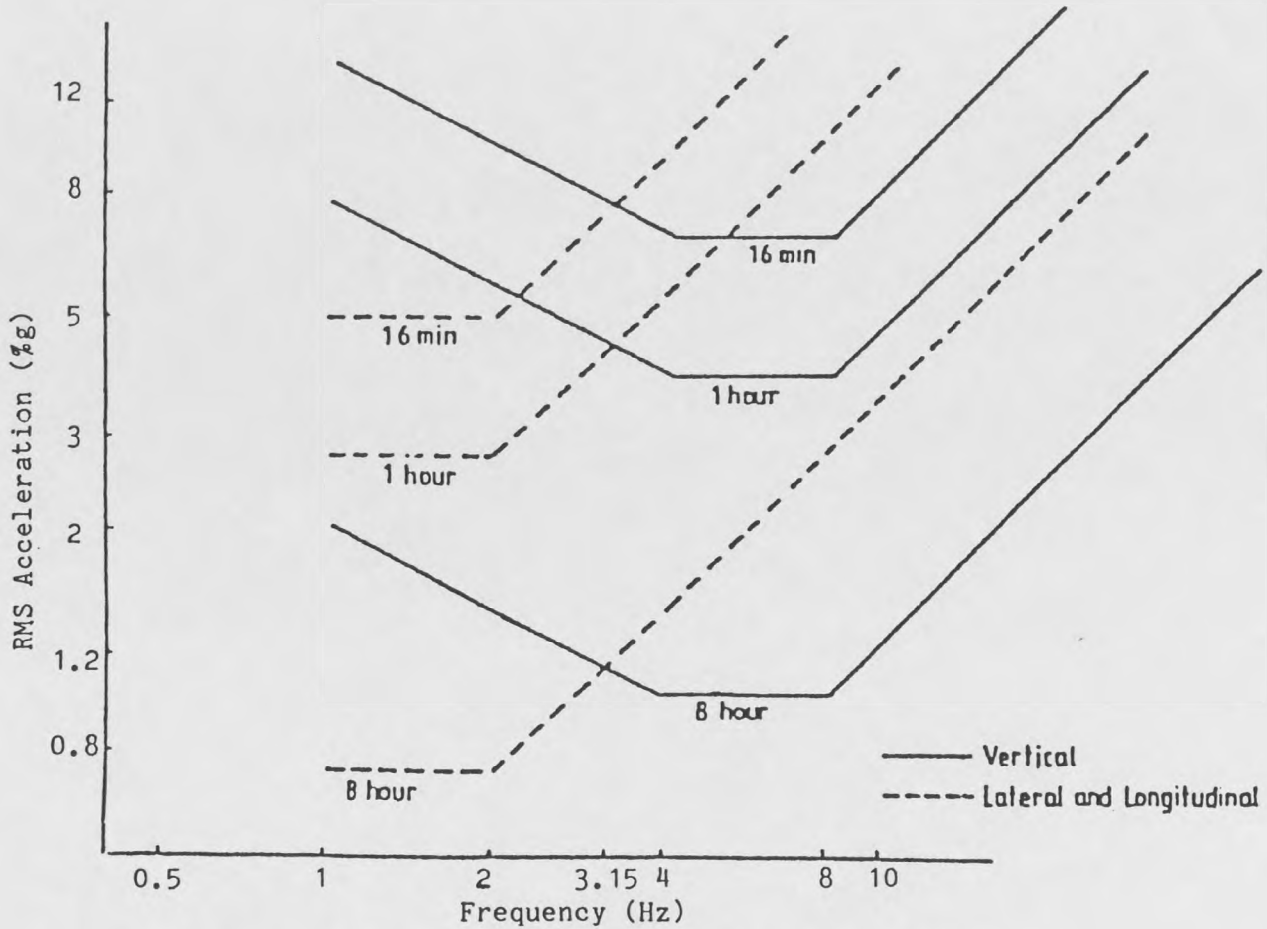

Figure 2.8 ISO reduced comfort boundaries of 1974.

CHAPTER 3

MODELLING, SIMULATION AND CONTROL OF THE VEHICLE SUSPENSION

The aim of this chapter is to describe the simulation of vehicle ride vibrations, derivation of responses, power calculations, performance criteria and optimal control of a vehicle suspension. The chapter is divided into five main parts. In the first part, a short survey is given to describe three different models for suspension studies, which are the well known full, half and quarter car models.

Based on the well known quarter car model, the procedures for obtaining the response and the power of the models depend on their characteristics (linear or non-linear) and the type of excitation. The second part describes the derivation of responses for the linear and non-linear models. The power calculations are introduced in the third part. The fourth part summarizes the performance criteria of the vehicle suspension systems and the quadratic integral performance index of the suspension systems is also included. The last part describes the application of optimal control theory to the vehicle suspension problem.

3.1 Modelling of the suspension

Vehicles are complex mechanical systems with many degrees of freedom and they may incorporate linear or nonlinear springs and various types of damping characteristic. For the investigation of the dynamic interaction between vehicles and the track or road, the following important assumptions are used with the ride models. Firstly, the vehicle is split into three basic components: masses, springs and damping elements. Secondly, the whole range of vibration elements and components such as engine, gear box and drive, exhaust, etc, are not taken into account. Thirdly, the deformation of vehicle body may also be neglected because the frequency range used is only up to 15 Hz.

The vehicle mass may be assumed to be concentrated into several lumped masses upon which all gravitational and external forces are assumed to be acting. The

individual parts of a vehicle are connected in general by springs and damper elements. The restoring force of the linear spring F_s depends on the deformation X and the constant of the spring K_s, but for nonlinear springs the restoring force may be represented by,

$$F_s = K_{s1} X + K_{s2} X^2 + ... + K_{sn} X^2 \qquad 3\text{-}1$$

where K_{s1}, K_{s2}, ..., K_{sn} are constants. The third important components of vehicles are the damping elements. The purpose of the dampers is to absorb vibrational energy. In the damper, the damping force F_d depends on the velocity $\dot{X}$ of the vibration and the damper coefficient C_d, although practical dampers may have more complicated, non-linear characteristics.

In the active system, an actuator is used with or without passive springs and damping elements between the car body and wheel masses. In what follows a short survey will be given, attempting to describe the well known full, half and quarter models of the vehicle.

3.1.1 Full car model

A seven degree-of-freedom model of the vehicle suspension is simulated as shown in Figure 3.1. The vehicle body may be represented as a rigid plate with uniform mass distribution. Attached to this are masses representing the individual suspended wheels. The body mass is supported on the wheels via the active or passive elements and the wheels are supported on the road via the tyres. The tyres themselves are modelled as springs and dampers which are permanently in contact with the road.

The seven degrees of freedom of the full car model are vertical, pitch and roll motions of body, plus the vertical motions of the four wheels. The equations of

motion of the model can be obtained from the basic equations of Newton and Euler, concerning linear and angular momenta, for the individual free bodies.

3.1.2 Half car model

The four degree of freedom model of the half vehicle is shown in Figure 3.2. This model differs from the full vehicle model in that the roll motion interactions between left and right tracks are omitted. The real problem approximates to this model only for long wavelength, low frequency inputs but for higher frequencies the coupling of the two wheels through the body motion is not so important because the body motions are not so large. Anti-roll bars provide a direct coupling of two wheels of course. In the special case when the pitch inertia I_b of the vehicle body mass M_b is $I_b = M_b a_f a_r$ where a_f and a_r are longitudinal distances from body mass centre to front and rear wheels, the interactions between front and rear wheels do not occur and the single wheel model is perfect, Mitschke (1961).

3.1.3 Quarter car model

A two degree of freedom system represents the suspension system at one corner of the vehicle as shown in Figure 3.3. The well known quarter car model consists of two masses, one of them representing the wheel mass M_w and other representing the body mass M_b. Passive elements or an active actuator are used to join the two masses. For the passive system, it is assumed that a linear spring with stiffness K_s and a damper with damping coefficient C_d are used to obtain the suspension force F. The tyre is modelled as a linear spring with stiffness K_t. The vertical displacement of the wheel is X_w and of the body is X_b. In the case of active systems, shown in Figure 3.4, the actuator control force U is a function of some or all the state variables $(X_0, X_w, X_b, \dot{X}_w, \dot{X}_b)$. The road input in this model is X_0. Then, the equations of motion of the two degree-of-freedom model are;

$$M_w \ddot{X}_w(t) + F(t) - K_t (X_0(t) - X_w(t)) = 0 \qquad 3\text{-}2$$

$$M_b \ddot{X}_b(t) - F(t) = 0 \qquad 3\text{-}3$$

where:

$$F(t) = K_s (X_w(t) - X_b(t)) + C_d (\dot{X}_w(t) - \dot{X}_b(t)) \qquad \text{(If passive)}$$

$$F(t) = U(t) \qquad \text{(If active)}$$

Sharp and Crolla (1987a) summarize the advantage of using a simple model over more complex models in terms of: first, being described by few design parameters second, having few performance parameters third, having only a single input, leading to ease of computation of performance and ease of application of optimal control theory to derive control laws and final, ease of mapping and understanding of the relationships between design and performance. Healey et al (1977) predicted the performance of the full, half and quarter car models in response to excitation by road profiles. Their comparisons between the calculated responses of seven, four and two degree of freedom systems support the employment of the simple model up to 10 Hz. For that reason, the quarter car model will be utilised throughout this thesis as a fundamental basis for studying the various suspension systems. A forward speed of 12 m/s is used over road roughness specified by equation 2-7 and other vehicle data, which refers to a farm transport vehicle studied by Crolla et al (1987) for on and off road use, are as follows:

$$\textit{Body mass } (M_b) = 2500.0 \ kg$$

$$\textit{Wheel mass } (M_w) = 330.0 \ kg$$

$$\textit{Tyre stiffness } (K_t) = 700.0 \ kN/m \qquad 3\text{-}4$$

3.2 Derivation of responses

In the case of a linear system, it is possible to obtain the responses of ride models in the frequency domain by using the principles of the superposition theory. But the study of non-linear systems is considerably more complicated and then the time domain treatments must be used to obtain the response of the ride models. Subsequently, the transformation of time responses into frequency domain can be obtained by using the Fourier analysis.

3.2.1 Linear model

The equations 3-2 and 3-3 will now be considered and the displacement inputs to the model will be taken as random. Hence, the amplitude of the input can be calculated from the power spectral density function of the road (equation 2-7) as;

$$X_0(\omega) = \sqrt{2\, PSD(\omega)\, d\omega} \qquad 3\text{-}5$$

where $d\omega$ is the frequency subinterval in radian/second. Having;

$$X_0(t) = X_0(\omega)\, e^{i\,\omega\, t} \qquad 3\text{-}6$$

The response of wheel $X_w(t)$ and body $X_b(t)$ are then;

$$X_w(t) = X_w(\omega)\, e^{i\,(\omega\, t + \psi_w(\omega))} \qquad 3\text{-}7$$

$$X_b(t) = X_b(\omega)\, e^{i\,(\omega\, t + \psi_b(\omega))} \qquad 3\text{-}8$$

where ψ_w and ψ_b are the phase angles. By inserting equations 3-6 to 3-8 and their first and second derivatives into 3-2 and 3-3 yields

$$-M_w\, \omega^2\, X_w(\omega) + F(\omega) + K_t\, X_w(\omega) \qquad = K_t\, X_0(\omega) \qquad 3\text{-}9$$

$$-M_b\, \omega^2\, X_b(\omega) - F(\omega) \qquad = 0\,, \qquad 3\text{-}10$$

where:

$$F(\omega) = K_s\,(X_w(\omega) - X_b(\omega)) + i\,\omega\,C_d\,(X_w(\omega) - X_b(\omega)) \quad \text{, or} \quad F(\omega) = U(\omega)$$

The complex frequency response can be obtained by solving equations 3.9 and 3.10 over the frequency range of interest. The complex responses of the wheel $H_w(\omega)$ and the body $H_b(\omega)$ are;

$$H_w(\omega) = \frac{X_w(\omega)}{X_0(\omega)} \qquad 3\text{-}11$$

$$H_b(\omega) = \frac{X_b(\omega)}{X_0(\omega)} \qquad 3\text{-}12$$

The transfer function of the wheel $TF_w(\omega)$ and the body $TF_b(\omega)$ are given by the magnitudes of their complex responses as;

$$TF_w(\omega) = mag(H_w(\omega)) \qquad 3\text{-}13$$

$$TF_b(\omega) = mag(H_b(\omega)) \qquad 3\text{-}14$$

The power spectral density function of the wheel $PSD_w(\omega)$ and the body $PSD_b(\omega)$ can then be obtained from the input power spectral density and the transfer function as;

$$PSD_w(\omega) = (TF_w(\omega))^2\,PSD(\omega) \qquad 3\text{-}15$$

$$PSD_b(\omega) = (TF_b(\omega))^2\,PSD(\omega) \qquad 3\text{-}16$$

3.2.2 Non-linear model

The two second order differential equations 3-2 and 3-3 may be transformed into four first order equations by defining the new variables: $X_1 = X_w$, $X_2 = X_b$, $X_3 = \dot{X}_w$ and $X_4 = \dot{X}_b$, *so that* $\dot{X}_1 = X_3$ and $\dot{X}_2 = X_4$. The new formulation for a quarter car model can then be written as;

$$\dot{X}_1(t) = X_3(t) \qquad 3\text{-}17$$

$$\dot{X}_2(t) = X_4(t) \qquad 3\text{-}18$$

$$\dot{X}_3(t) = \frac{K_t\,(X_0(t) - X_1(t)) - F(t)}{M_w} \qquad 3\text{-}19$$

$$\dot{X}_4(t) = \frac{F(t)}{M_b} \qquad 3\text{-}20$$

Integration of the system of first order ordinary differential equations over a range with suitable initial conditions to find the time responses of the ride model is achieved with the NAG routine D02PAF (1987), which uses a Runge-Kutta-Merson method, for each time input step $X_0(t)$. A computer program was also written using the Euler method of approximate integration to find the responses of the ride model in some interval 0 to T as follows. First, divide this interval into N subintervals h by a sequence of points t_1, t_2, ..., t_n and then, for any subinterval (X_{n-1}, X_n) the solution is;

$$X_n = X_{n-1} + f(t_{n-1}, X_{n-1})\,h, \qquad n = 2, 3, ..., N \qquad 3\text{-}21$$

In general, the power spectral density functions of the time responses can be obtained by using the transformation procedures as follows. Firstly, the time responses of the model must be tapered at the ends by a window function. Secondly, the power spectral density of wheel $PSD_w(\omega)$ and body $PSD_b(\omega)$ can be obtained by using a DFT process. Finally, the resulting (one sided) spectral density is obtained by taking the N/2 values in the frequency range 0 to 1/2h Hz.

To ensure the responses obtained from the frequency and time domain are comparable, an example solution of the passive system was solved with spring and damper parameters K_s= 160 kN/m and C_d= 18 kNs/m respectively. The power spectral densities of the predicted performances obtained by both frequency and time domain are shown in Figure 3.5 and can be seen to be very similar.

3.3 Power calculations

The energy losses associated with the dynamic tyre deflection and suspension damper stroking appear eventually as a part of the vehicle rolling resistance. The instantaneous power of a force-producing elements, e.g. spring, damper, actuator, is;

$$P(t) = F(t)\, V(t) \qquad 3\text{-}22$$

where P, F, and V are the instantaneous power, relative force, and relative velocity respectively. The energy is the integral of the power with respect to time through a certain interval T as;

$$E(t) = \int_0^T F(t)\, V(t)\, dt \qquad 3\text{-}23$$

For the special case in which the force and velocity are sinusoidal then;

$$F(t) = A_f(\omega) \sin(\omega t + \psi(\omega)) \qquad 3\text{-}24$$

$$V(t) = A_v \sin(\omega t) \qquad 3\text{-}25$$

where A_f and A_v are the amplitude of force and velocity. Also ω and ψ are the radian frequency and phase angle between the force and velocity. The instantaneous power formula can be written as;

$$P(t) = A_f(\omega)\, A_v(\omega) \sin(\omega t + \psi(\omega)) \sin(\omega t)$$

$$P(t) = 0.5\, A_f(\omega)\, A_v(\omega)\, [\cos \psi(\omega) - \cos(2\omega t + \psi(\omega))] \qquad 3\text{-}26$$

The formula for the power consists of two terms. The first term indicates the mean power value and second term gives a fluctuating power value at twice the relevant frequency, indicating that power alternately flows into and out of the particular element. The mean power value can be obtained over a time interval T from equations 2-10 and 3-26 as;

$$Mean\ power\ (\omega) = \frac{A_f(\omega)\, A_v(\omega)}{2\,T} \int_0^T [\cos \psi(\omega) - \cos (2\,\omega\, t + \psi(\omega))]\, dt \qquad 3\text{-}27$$

The second term in the integral is zero so that the mean power is

$$Mean\ power\ (\omega) = 0.5\, A_f(\omega)\, A_v(\omega) \cos \psi(\omega) \qquad 3\text{-}28$$

If the system is linear, it is possible to calculate the total mean power value in the frequency domain over a specified radian frequency range ω_k, k=[1,2,...,N]. Assuming that the complex responses of the force $F(\omega_k)$ and the velocity $V(\omega_k)$ are known for each frequency, then the amplitudes of force $A_f(\omega_k)$ and velocity $A_v(\omega_k)$ and the phase difference $\psi(\omega_k)$ can be found from the magnitude and arguments;

$$A_f(\omega_k) = mag(F(\omega_k)), \qquad A_v(\omega_k) = mag(V(\omega_k)) \qquad 3\text{-}29$$

$$\psi(\omega_k) = \arg(F(\omega_k)) - \arg(V(\omega_k)) \qquad 3\text{-}30$$

A convention of using a negative sign to indicate power dissipated and a positive sign to indicate power demand is used throughout. Then, the total mean power is the sum of the powers calculated at individual frequency components as follows;

$$Mean\ power = -\,0.5 \sum_{k=1}^{N} A_f(\omega_k)\, A_v(\omega_k) \cos \psi(\omega_k) \qquad 3\text{-}31$$

3.3.1 Passive elements

Because the phase angle between the force and the velocity of the passive spring is 90°, then the mean power value is zero and its fluctuating power is;

$$P(t) = -\,K_s(X_1(t) - X_2(t))\,(X_3(t) - X_4(t)) \qquad 3\text{-}32$$

The phase angle between the force and the velocity of the passive damper is 0°, so that the mean power value of the linear damper at the required frequency ω_k,

k=1,..,N can be obtained from the solution of the equations 3-9 and 3-10 as;

$$A_d(\omega_k) = mag(X_w(\omega_k) - X_b(\omega_k)) \qquad 3\text{-}33$$

then ;

$$Mean\ power = -0.5\, C_d \sum_{k=1}^{N} (\omega_k A_d(\omega_k))^2 \qquad 3\text{-}34$$

For a non-linear damper, the dissipation power must be calculated in the time domain as;

$$P(t) = -C_d (X_3(t) - X_4(t))^2 \qquad 3\text{-}35$$

and the mean power value may be obtained by equation 2-10

3.3.2 Active elements

The mean power value of the active system can be derived using the same procedure mentioned previously. However in this case, the designer needs to know the power demand and dissipation of the actuator. Hence, the time domain was used to compute the power demand P_+ and dissipation P_- of active system which can be obtained from the actuator power P as;

$$P(t) = -U(t)\,(X_3(t) - X_4(t)) \qquad 3\text{-}36$$

$$If \quad P(t) \le 0 \quad then \quad P_-(t) = P(t), \qquad or$$

$$If \quad P(t) > 0 \quad then \quad P_+(t) = P(t).$$

Two examples of the passive and active models are given to indicate the dynamic power properties of the systems in response to a sinusoidal frequency of 29 mm amplitude and 1Hz frequency as shown in Figures 3.6 and 3.7. For the passive system, the parameters of the spring and damper are 160 kN/m and 16 kNs/m

respectively. The power figure of most interest in the mean power dissipated by the damper. The power of the spring and damper elements are summed together to represent the total power of the passive suspension which can be compared with the corresponding power of the active system. For the active system, the feedback coefficients, K_{f1}, ..., K_{f4}, of the actuator are 944080, -316228, 18279 and -54766. The results show the following features. Firstly, the mean values of the spring fluctuating power characteristics, which are the power, relative body-wheel displacement and velocity, and suspension force are similar to that of the input. Secondly, the mean power value of the damper represents the average power dissipation of the passive system. Finally, the total power of the passive suspension elements is similar to that of the active actuator element and therefore, the active actuator is dissipating vibrational energy from the system during most of the working time.

3.4 Performance criteria of the vehicle suspension

A vehicle suspension system performs two main functions within several constraints. The functions are first, it must provide a high degree of isolation for the vehicle body from the road surface, tyre irregularities, and wheel out-of-balance forces to ensure operator comfort and second, it must maintain the wheels in close contact with the road surface to ensure adequate adhesion when accelerating, braking or cornering. The constraints are first, it must minimise the relative body-wheel usage second, it must keep vehicle attitude control and finally, it must minimise the power requirements for power consuming systems.

3.4.1 Performance calculations

The performance criteria of suspension systems can be obtained as follows. The complex responses of body acceleration $H_a(\omega)$, dynamic tyre load $H_d(\omega)$ and relative body/wheel workspace usage $H_r(\omega)$ are;

$$H_a(\omega) = \omega^2 H_b(\omega) \tag{3-37}$$

$$H_d(\omega) = \frac{K_t (X_0(\omega) - X_w(\omega))}{X_0(\omega)} \tag{3-38}$$

$$H_r(\omega) = \frac{(X_w(\omega) - X_b(\omega))}{X_0(\omega)} \tag{3-39}$$

and the transfer functions of these complex responses are;

$$TF_a(\omega) = mag(H_a(\omega)) \tag{3-40}$$

$$TF_d(\omega) = mag(H_d(\omega)) \tag{3-41}$$

$$TF_r(\omega) = mag(H_r(\omega)). \tag{3-42}$$

The power spectral density functions of body acceleration $PSD_a(\omega)$, dynamic tyre load $PSD_d(\omega)$ and relative body/wheel workspace usage $PSD_r(\omega)$ are;

$$PSD_a(\omega) = TF_a^2(\omega)\, PSD(\omega) \tag{3-43}$$

$$PSD_d(\omega) = TF_d^2(\omega)\, PSD(\omega) \tag{3-44}$$

$$PSD_r(\omega) = TF_r^2(\omega)\, PSD(\omega) \tag{3-45}$$

In the case of non-linear systems, the body acceleration $X_a(t)$, the dynamic tyre load $X_d(t)$ and the relative body/wheel workspace usage $X_r(t)$ can be obtained in the time domain as;

$$X_a(t) = \dot{X}_4(t) \tag{3-46}$$

$$X_d(t) = K_t (X_0(t) - X_1(t)) \tag{3-47}$$

$$X_r(t) = X_1(t) - X_2(t) \tag{3-48}$$

and the transformation into the frequency domain can also be obtained by the DFT process.

As a measure of the comfort, the power spectral density of the body accelera-

tion must be weighted for the human sensitivity weighting factor W(f) (Table 2.3/Wg) as;

$$RCP(\omega) = PSD_a(\omega)\, W^2(\omega) \qquad 3\text{-}49$$

The root mean square values of the comfort, the dynamic tyre load and the suspension working space can be obtained by using a limited integral as in equation 2-11. In addition, the dynamic tyre load variation may be expressed as a percentage ratio between dynamic and static tyre load as;

$$DTL\ variation = \frac{RMS\ dynamic\ tyre\ load}{static\ tyre\ load}\ 100 \qquad 3\text{-}50$$

3.4.2 Performance index

The optimization problem of a suspension system involves a quadratic objective function called the performance index. The quadratic integral performance index employed is the weighted sum of the mean integral square quantities which represent the requirements of the suspension system performance. The performance index contains three or four quantities, each one of them representing the mean square value multiplyed by a weighting factor. Therefore, the performance index of the quarter car model can be written as;

$$J = \lim_{t\to\infty} E\,[q_1\,(X_0 - X_w)^2 + q_2\,(X_w - X_b)^2 + r\,(U)^2 + (\ddot{X}_b)^2] \qquad 3\text{-}51$$

where E is the expectation operator and q_1, q_2 and r are the weighting factors. The four terms in the performance index represent dynamic tyre load, relative body-wheel displacement, actuator force and body acceleration.

3.5 Optimal control of the suspension

The optimal control problem is aimed at obtaining a suspension control system that is the best possible with respect to a certain performance index or design criterion. Among the many different types of optimal control design problems, the time optimal control and minimum-integral control are the most general. In recent years much research effort has been expended on the analytical design of active isolation systems with special applications for active vehicle suspensions.

Consider the active system shown in figure 3.4. The dynamic equations can be rewritten in a state space form as;

$$\dot{X}(t) = A\,X(t) + b_1\,U(t) + b_2\,D(t) \qquad \textit{state equation} \qquad 3\text{-}52$$

$$Z(t) = C\,X(t) \qquad \textit{output equation} \qquad 3\text{-}53$$

where X is the state variable vector which will be measured, U is the control force which is assumed to be applied equally to the body and wheel, D is the disturbance input and Z is the output vector. Initially, the state variable of the road input X_0 is considered to be a unit step and other state variables of the model are assumed to be zero, i.e. the transpose of the vector X is [1 0 0 0 0]. The system should have zero steady state following errors for this input and the desired value of output vector is defined as:

$$Z_d = [1 \;\; 1]^T X_0 \qquad 3\text{-}54$$

The steady state linear stochastic regulator problem consists of determining the control law which minimises the performance index. This control law is obtained by different techniques as described in the following sections.

3.5.1 Full state feedback, method 1

The full state feedback active control of the quarter car model was obtained by Thompson (1976) as follows. The state and output equations 3-52 and 3-53 were used and the performance index in equation 3-51 was simplified to;

$$J = \lim_{t \to \infty} E\,[q_1\,(X_0 - X_w)^2 + q_2\,(X_w - X_b)^2 + r\,(U)^2] \qquad 3\text{-}55$$

He described the road surface as integrated white noise and, therefore, the state variables of the system are $S_1 = X_1 - X_0$, $S_2 = X_2 - X_0$, $S_3 = X_3$ and $S_4 = X_4$. Then, the new state and output vectors may be written as;

$$\dot{S} = A\,S + b_1\,U \qquad 3\text{-}56$$

$$Z = C\,S \qquad 3\text{-}57$$

The system matrix A and the vectors S, b_1 and b_2 are;

$$A = \begin{pmatrix} 0 & 0 & 1 & 0 \\ 0 & 0 & 0 & 1 \\ \dfrac{-K_t}{M_w} & 0 & 0 & 0 \\ 0 & 0 & 0 & 0 \end{pmatrix}, \qquad S = \begin{pmatrix} X_1 - X_0 \\ X_2 - X_0 \\ X_3 \\ X_4 \end{pmatrix}, \qquad b_1 = \begin{pmatrix} 0 \\ 0 \\ -\dfrac{1}{M_w} \\ \dfrac{1}{M_b} \end{pmatrix}.$$

The output matrix C and weighting matrix Q are;

$$C = \begin{pmatrix} 1 & 0 & 0 & 0 \\ 1 & -1 & 0 & 0 \end{pmatrix}, \qquad Q = \begin{pmatrix} q_1 & 0 \\ 0 & q_2 \end{pmatrix} \qquad 3\text{-}58$$

In terms of the new coordinates, the performance index was given by;

$$J = 0.5 \int_0^\infty [S^T\,C^T\,Q\,C\,S + r\,U^2]dt \qquad 3\text{-}59$$

The solution of this problem involves solving the algebraic Riccati equation which is;

$$A^T P + P A + C^T Q C - \frac{P b_1 b_1^T P}{r} = 0 \qquad 3\text{-}60$$

where P is a positive definite symmetric matrix, the pair (A, b_1) defines a stable system and the pair (A, C) defines a detectable system. Then the optimal control law U is given by;

$$U = - \frac{b_1^T P S}{r} = K_f^T S = \sum_{i=1}^{4} K_{fi} S_i \qquad 3\text{-}61$$

where K_f is the vector of feedback gains. In this study, the technique used to find the vector K_f is based on a numerical solution of the Riccati equation by the negative exponential method described by Kuo (1975) and then, a computer program was written to solve the algebraic Riccati equation enabling the feedback gains for any conditions to be found.

3.5.2 Full state feedback, method 2

Hac (1985) introduced another method for the full state feedback control of the quarter car model which contains passive elements in parallel to the active actuator. He described the road surface as a integrated filtered white noise, i.e. the road surface displacement spectral density is represented by;

$$PSD(f) = \frac{CV}{[(\alpha V)^2 + f^2]} \qquad 3\text{-}62$$

where α is a constant implying that displacements remain finite for vanishingly small frequency f (Hz) and V is a vehicle speed. He also assumed that the state displacements of the road input, body and wheel can be measured as absolute variables. Therefore, the performance index, state and output equations 3-51 to 3-53

were used. In this technique the vector of feedback gains requires solving the Riccati and Liapunov equations.

3.5.3 Limited state feedback

In practice, the relative displacements of the body and wheel to the road or the absolute displacement of road input can not be easily measured. Therefore, the control law based on limited state feedback depends on ignoring some of the state variables. Wilson et al (1986) considered the control law as;

$$U = -K_f Y \qquad 3\text{-}63$$

where K_f is the vector of feedback gains and Y is defined by;

$$Y = M X \qquad 3\text{-}64$$

where the desired state variables to be measured are specified by the auxiliary matrix M.

The input disturbance of road roughness used in their technique was defined as integrated filtered white noise;

$$\dot{X}_0(t) = -2\pi\alpha V X_0(t) + W(t) \qquad 3\text{-}65$$

where α is taken as 0.005. Then the state equations were deduced by substituting equations 3-63 to 3-65 into 3-52 as;

$$\dot{X} = A X + d \qquad 3\text{-}66$$

where

$$A = A_1 - b_1 K_f M \qquad 3\text{-}67$$

The matrix A_1 and the vectors X, b_1 and d were given by;

$$A_1 = \begin{pmatrix} -2\pi\alpha V & 0 & 0 & 0 & 0 \\ 0 & 0 & 0 & 1 & 0 \\ 0 & 0 & 0 & 0 & 1 \\ \dfrac{K_t}{M_w} & \dfrac{-K_t}{M_w} & 0 & 0 & 0 \\ 0 & 0 & 0 & 0 & 0 \end{pmatrix}, \quad X = \begin{pmatrix} X_0 \\ X_1 \\ X_2 \\ X_3 \\ X_4 \end{pmatrix}, \quad b_1 = \begin{pmatrix} 0 \\ 0 \\ 0 \\ \dfrac{-1}{M_w} \\ \dfrac{1}{M_b} \end{pmatrix}, \quad d = \begin{pmatrix} GV \\ 0 \\ 0 \\ 0 \\ 0 \end{pmatrix}.$$

The output matrix C and the weighting matrix Q are;

$$C = \begin{pmatrix} -1 & 1 & 0 & 0 & 0 \\ 0 & -1 & 1 & 0 & 0 \end{pmatrix}, \quad Q = \begin{pmatrix} q_1 & 0 \\ 0 & q_2 \end{pmatrix} \qquad 3\text{-}68$$

The performance index can be formulated as;

$$J = trace\,[W_c\,(C^T Q\, C + M^T K_f^T K\, M\, r)] = trace\,[W_o\, d\, d^T], \qquad 3\text{-}69$$

where;

$$A\, W_c + W_c A^T + d\, d^T = 0 \qquad 3\text{-}70$$

and

$$A^T W_o + W_o A + C^T Q\, C + \frac{M^T K_f^T K_f M}{r} = 0 \qquad 3\text{-}71$$

By applying the gradient search technique described by Wilson et al (1986) to the performance index with respect to any elements K_{fij} (i=1,.. ,p and j=1,.. ,m), the values of K_f can be found from;

$$\frac{\partial J}{\partial K_f} = 2\,[r\, K_f M\, W_c M^T - b_1^T W_0\, W_c M^T] \qquad 3\text{-}72$$

One difficulty of this technique is how to obtain the initial estimate for vector K_f but this can be overcome by selecting the value obtained from the full state feed-

back solution. In this study, a computer program was written to solve the Liapunov equations 3-70 and 3-71 and the feedback gain vector K_f was obtained by the NAG routine E04DBF (1987), which uses the conjugate gradient search method developed by Fletcher and Reeves (1964). This technique of solving the Liapunov equation differed from that of solving Riccati equation to find the feedback gains in that the stability test is included during the iteration process by which the control law K_f is found. The NAG routine F02AGF (1987), which uses the QR algorithm for real Hessenberg matrices (Wilkinson and Reinsch (1971)), is used to ensure closed loop stability of the limited state feedback active systems.

In this study, the control laws of limited, types 1 and 2, state feedback active systems were obtained by using different auxiliary matrices M as follows.

$$M = \begin{pmatrix} 0 & 1 & 0 & 0 & 0 \\ 0 & 0 & 1 & 0 & 0 \\ 0 & 0 & 0 & 1 & 0 \\ 0 & 0 & 0 & 0 & 1 \end{pmatrix}, \qquad \text{and } M = \begin{pmatrix} 0 & 0 & 0 & 0 & 0 \\ 0 & 1 & -1 & 0 & 0 \\ 0 & 0 & 0 & 1 & -1 \\ 0 & 0 & 0 & 0 & 0 \end{pmatrix} \qquad \text{3-73}$$

If the auxiliary matrix M is replaced by a unit matrix then the Liapunov equation becomes the Riccati equation and the control law of the full state feedback active system can also be found.

3.5.4 Comparison of the control strategies.

The performances of the active systems using all the control strategies described above are compared by using two different sets of weighting parameters, [q_1= 4, q_2= 500, $r = 10^{-8}$] and [q_1= 2500, q_2= 22.5, $r = 10^{-8}$], for the performance index in equation 3.51. The road input and basic elements of the model are the same as described in 2-7 and 3-4. The control system and actuator are assumed to have a flat frequency characteristic up to 15 Hz, which is the upper limit of the cal-

culation range and the performance index, J, of the systems is calculated in terms of the ride behaviour as follows;

$$J = \int_{\omega=1}^{90} [\frac{q_1 PSD_d(\omega)}{K_t^2} + q_2 PSD_s(\omega) + r RCP(\omega)] d(\omega) \qquad 3\text{-}74$$

where $PSD_d(\omega)$, $PSD_s(\omega)$ and $RCP(\omega)$ are the PSD curves of the system as a function of frequency ω radian/second. The active systems are classified as follows.

1- Full state feedback control law, method 1

2- Full state feedback control law, method 2

3- Limited state feedback control law, type 1

4- Limited state feedback control law, type 2

The limited state feedback system, type 2, is designed to represent the optimum passive system relative to the corresponding active systems. The natural frequency and damping ratio of the optimum passive systems are 0.26 Hz and 1.72 or 0.54 Hz and 0.5 respectively. Tables 3.1 and 3.2 give the feedback gains, reduction of the performance index compared with the optimum passive system, and the individual performances described by the RMS road holding, ride comfort and working space. The reduction of the performance index, J%, is obtained as follows.

J_p = The performance index of the optimum passive system,

J_f = The performance index of the corresponding active system and

$$J\,\% = \frac{(J_f - J_p)}{J_p} 100 \qquad 3\text{-}75$$

It must be noted that the performance calculations for all the systems are subject to the following restrictions. First, the performances of all the systems are obtained for a road input which differs from that used to obtain the optimal control law of all the systems, i.e. the slope of the PSD ground description used in generating the optimal control law is limited to -2, whereas a slope of -2.5 was used to represent the surface input conditions in this study. Second, the term of the body acceleration used in the performance index when deriving the control law is replaced by the ISO weighted body acceleration in the performance index which is used to judge the overall performance of the various systems. The results indicate that the full state feedback control strategy, method 2, gives the biggest improvement in the performance index. The full state feedback, method 1, gives a similar improvement of the performance index but the limited, type 1, state feedback only gives a little improvement of the performance index with relatively small dynamic tyre load. Finally, the improvements of performance index for all the control systems relative to the optimal passive system increase by decreasing the suspension working space.

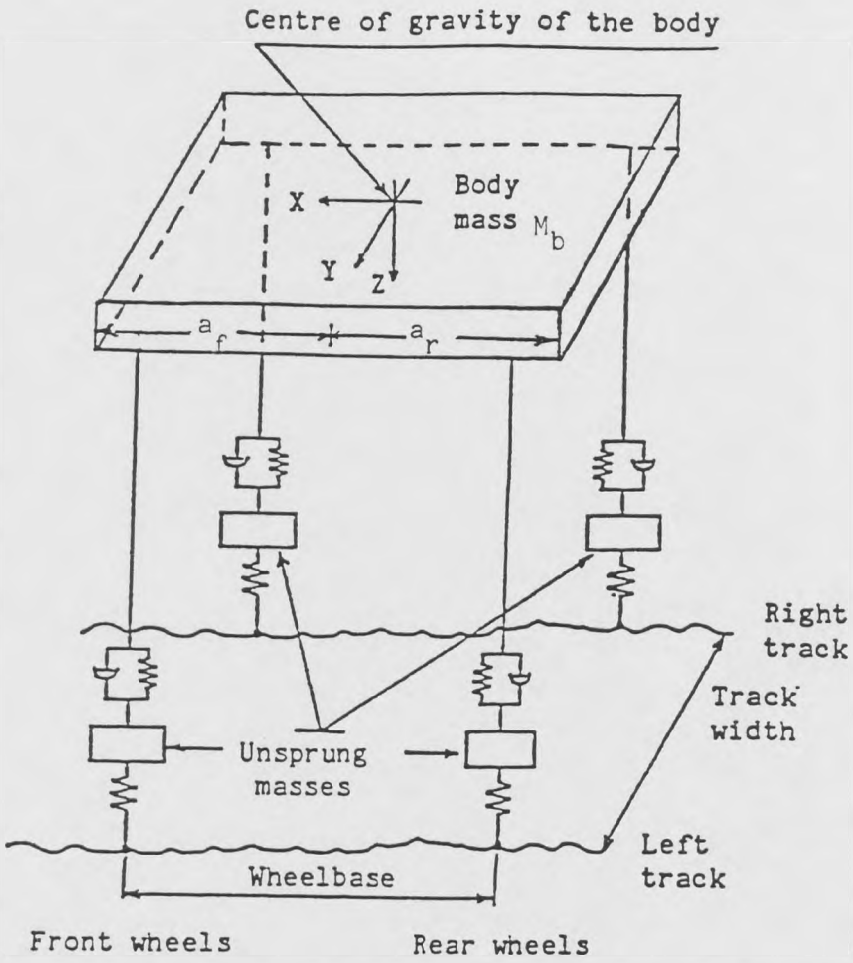

Figure 3.1 Full car passive suspension system.

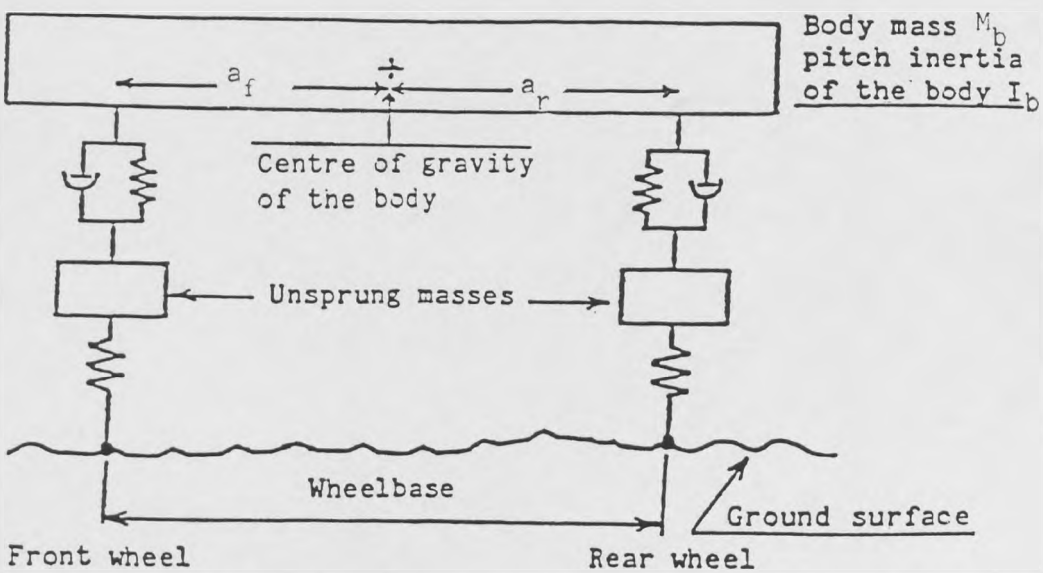

Figure 3.2 Half car passive suspension system.

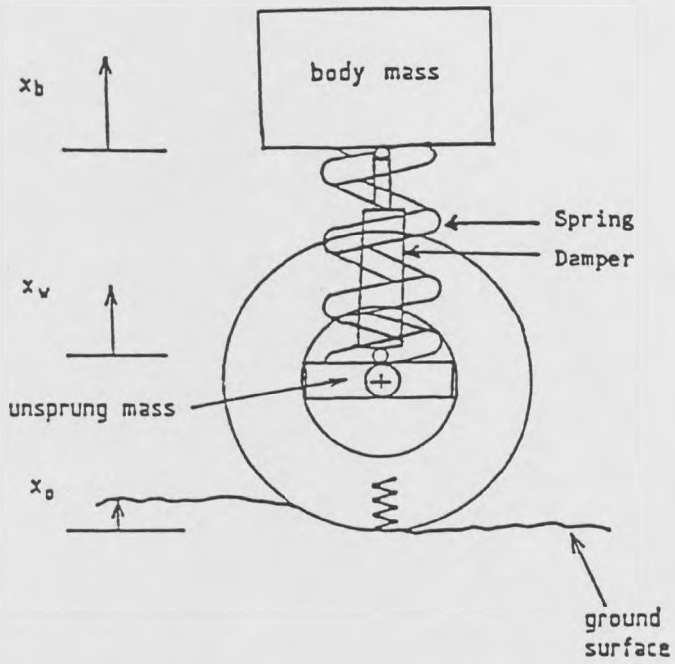

Figure 3.3 Quarter car passive suspension system.

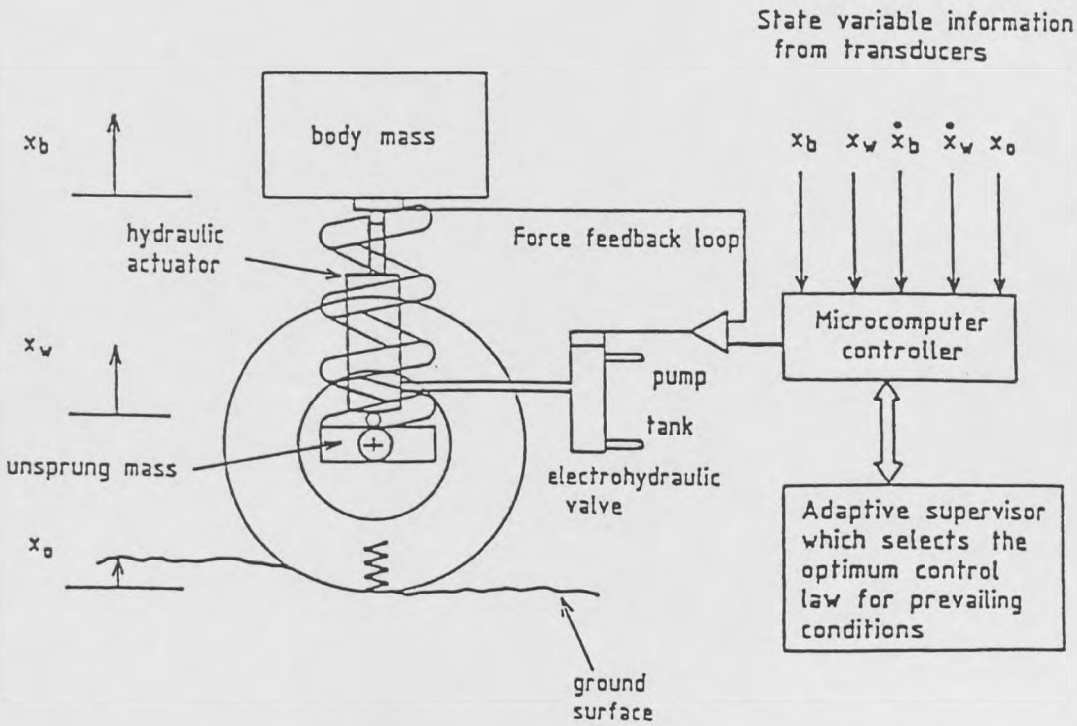

Figure 3.4 Quarter car fully active suspension system.

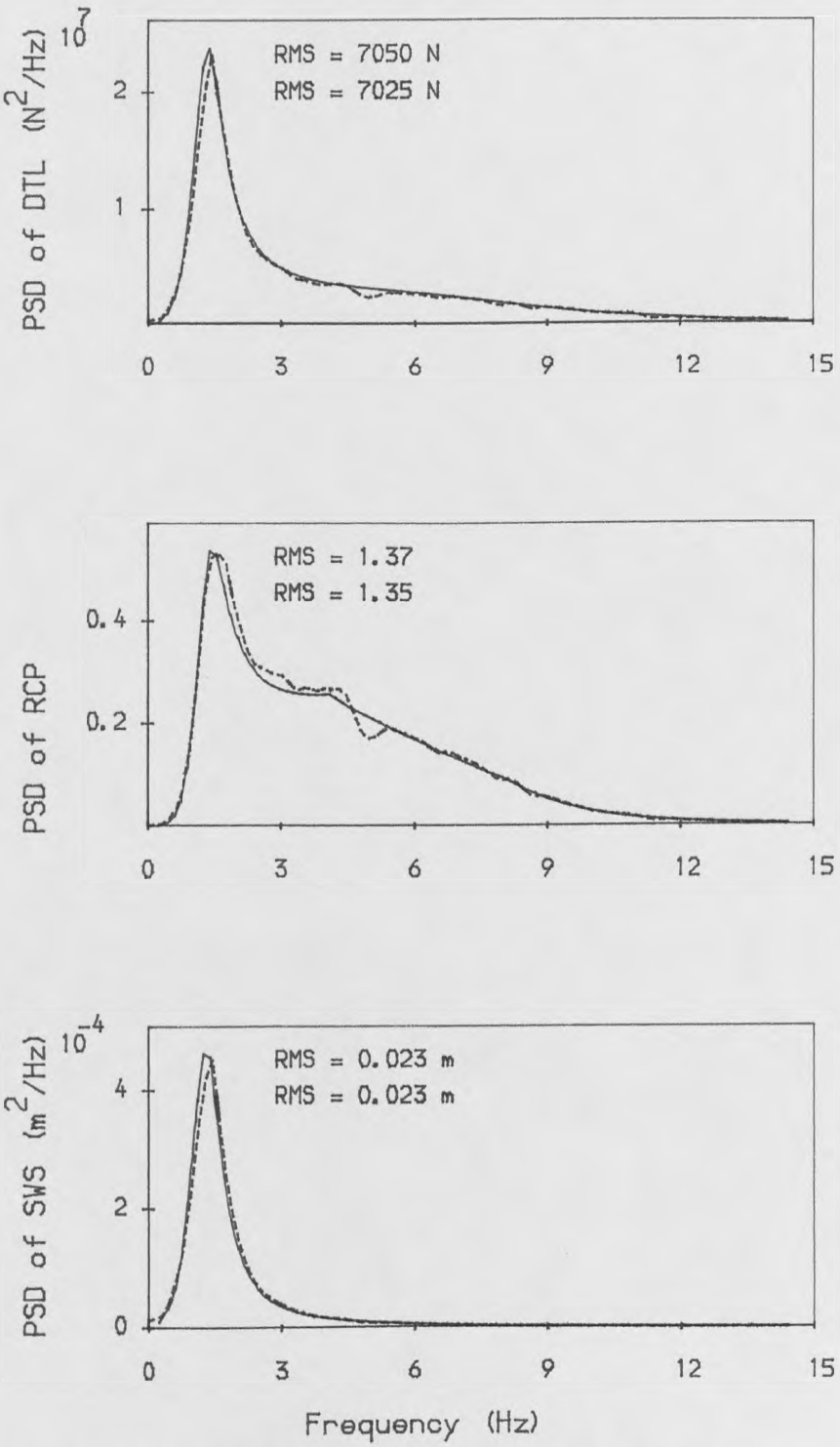

Figure 3.5 Comparison of PSD curves for passive quarter car model solved in the frequency (continuous line) and time (broken line) domain.

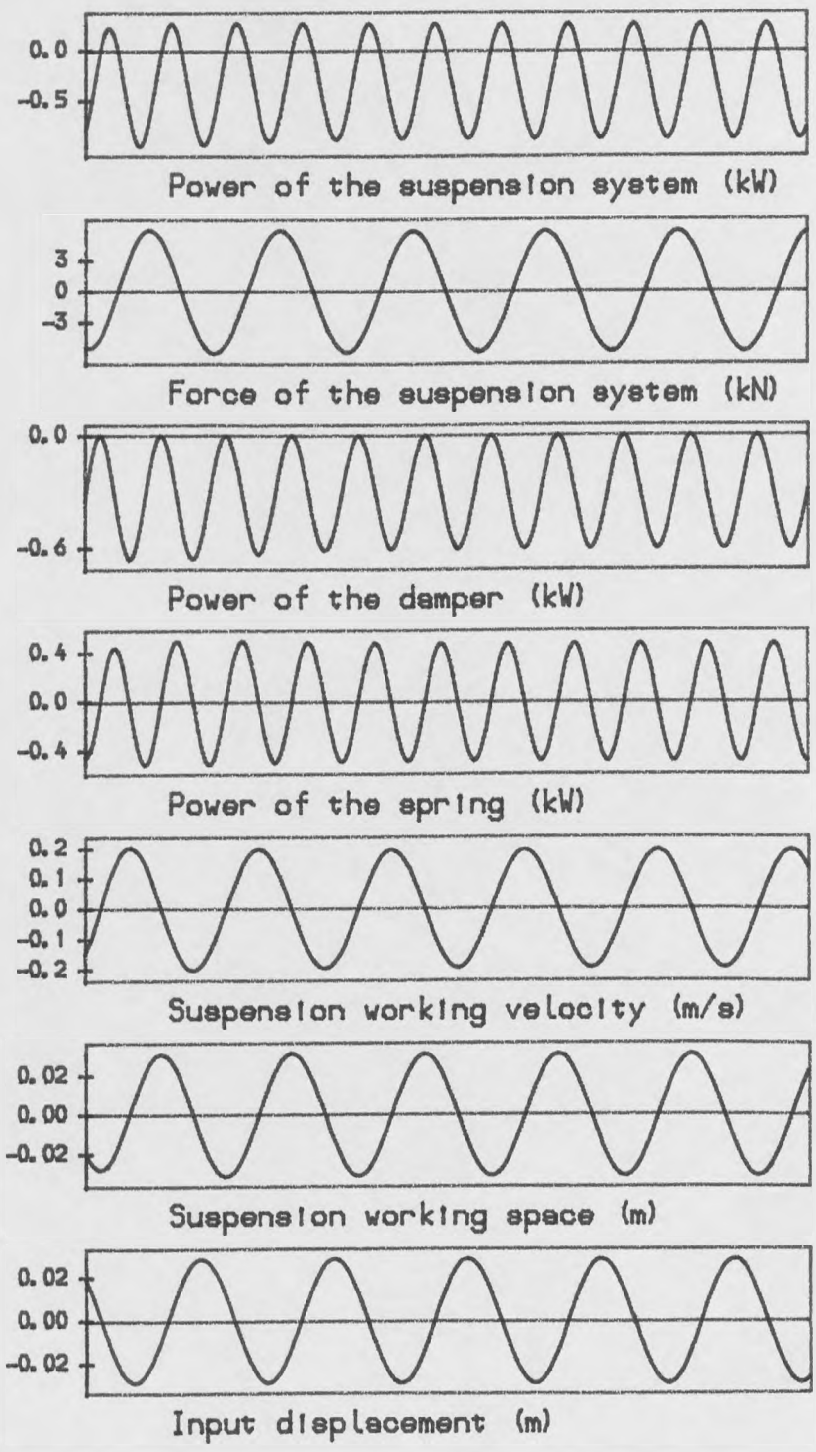

Figure 3.6 The dynamic power properties of the passive system in response to a sinusoidal ground input of 29 mm amplitude and 1Hz frequency.

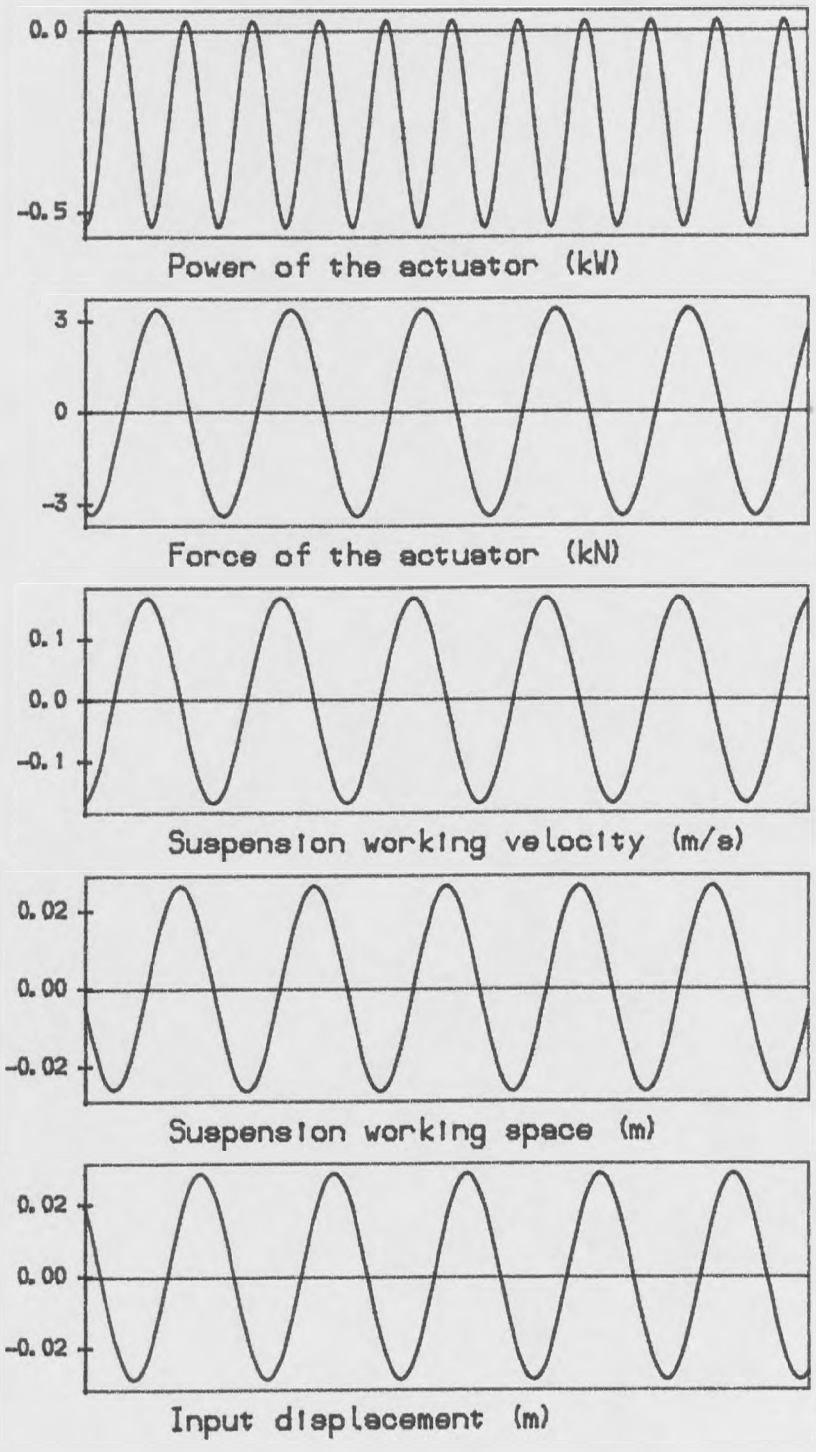

Figure 3.7 The dynamic power properties of the active system in response to a sinusoidal ground input of 29 mm amplitude and 1 Hz frequency.

Table 3.1 Comparison of control strategy and performance of systems are full state feedback control law, methods 1 and 2, and limited state feedback control law, types 1 and 2, for q1= 4.0, q2= 500.0 and r= 10^{-8} weighting parameters.

Control strategy	Control law = $K_{f0}X_0+K_{f1}X_w+K_{f2}X_b+K_{f3}\dot{X}_w+K_{f4}\dot{X}_b$					RMS Performances of dynamic tyre load% DTLP, ride comfort RCP, working space SWS (mm)			Reduction % of J compared with O.P.
	K_{f0}	K_{f1}	K_{f2}	K_{f3}	K_{f4}	DTLP	RCP	SWS	
Full state feedback, method 2	134647	79715	-223606	4556	-29802	23.83	0.89	25.1	23
Full state feedback, method 1	$-(K_{f1}+K_{f2})$	79720	-223600	4557	-29800	23.87	0.91	25.3	22
Limited state feedback, type 1	Zero	181249	-190168	7027	-28634	21.05	0.91	25.7	19
Limited state feedback, type 2	Zero	6685	-6685	14042	-14042	21.63	1.08	28.6	Optimal passive

Table 3.2 Comparison of control strategy and performance of systems are full state feedback control law, methods 1 and 2, and limited state feedback control law, types 1 and 2, for q1= 2500, q2= 22.5 and r= 10^{-8} weighting parameters.

Control strategy	Control law = $K_{f0}X_0+K_{f1}X_w+K_{f2}X_b+K_{f3}\dot{X}_w+K_{f4}\dot{X}_b$					RMS Performances of dynamic tyre load% DTLP, ride comfort RCP, working space SWS (mm)			Reduction % of J compared with O.P.
	K_{f0}	K_{f1}	K_{f2}	K_{f3}	K_{f4}	DTLP	RCP	SWS	
Full state feedback, method 2	-170808	215936	-47434	9845	-17154	19.18	0.84	32.9	20
Full state feedback, method 1	$-(K_{f1}+K_{f2})$	215900	-47430	9846	-17150	19.17	0.84	34.0	19
Limited state feedback, type 1	Zero	1329772	-1333884	-2349	-365068	19.64	0.86	35.5	14
Limited state feedback, type 2	Zero	28454	-28454	8568	-8568	21.30	0.85	37.8	Optimal passive

CHAPTER 4

PASSIVE SYSTEMS

4.1 Introduction

The suspension system of conventional passive spring and damper elements is widely used in most vehicles, although its performance is limited compared with other controlled suspension systems which require additional components, e.g. transducers, signal conditioning and power electronics equipment etc. The aim of this chapter is to investigate and understand the detailed behaviour of passive systems including power losses and to investigate the potential for improved performance by using either switchable dampers or variable rates of the damper instead of the conventional fixed rates.

The chapter is divided into three parts. The first part presents the frequency responses and performance capabilities, including the energy losses, of the conventional passive system using the well known quarter car model. The second part introduces a theoretical study of this system using variable rates of the damper elements to investigate the possiblity of improving the performance. It also indicates the control strategy and performance capability, including the energy losses, of the two state switchable damper and continuously variable damper systems. The third part gives a fair comparison of all systems in terms of the performances and power losses.

4.2 Conventional passive systems

The conventional suspension system involving passive spring and damper elements with linear, non-variable, rates is well known. It provides forces as linear or non linear functions of the relative displacement and velocity between the body and wheel of the vehicle. Specifically, the conventional passive systems involving passive elements with linear characteristics will only be considered in the present study. The layout of a passive system was shown in figure 3.3 and its equations of

motion indicated in equations 3-9 and 3-10. The transfer functions of the body and wheel are the output/input ratio as shown in equations 3-13 and 3-14. In more detail, the transfer functions between the body/wheel $TF_{bw}(\omega)$, the wheel/input $TF_{w}(\omega)$ and the body/input $TF_{b}(\omega)$ are;

$$TF_{bw}(\omega) = mag\left(\frac{1 + i\,2\zeta\left(\frac{\omega}{\omega_n}\right)}{1 - \left(\frac{\omega}{\omega_n}\right)^2 + i\,2\zeta\left(\frac{\omega}{\omega_n}\right)}\right) \qquad 4\text{-}1$$

$$TF_{w}(\omega) = mag\left(\frac{1}{1 - \frac{\omega^2\,(M_w + TF_{bw}\,M_b)}{K_t}}\right) \qquad 4\text{-}2$$

$$TF_{b}(\omega) = mag\left(\frac{X_b}{X_w}\right) = TF_{bw}\;TF_{w} \qquad 4\text{-}3$$

where ω, ω_n and ζ are the exciting frequency, natural frequency and damping ratio of the system;

$$\omega_n = \sqrt{\frac{K_s}{M_b}} \qquad rad/s, \text{ and}$$

$$\zeta = \frac{C_d}{2\,M_b\,\omega_n}$$

In what follows, a parametric study of conventional passive systems will be given, attempting to describe the effect of the model parameters on the performances. The study covers three categories of the performance: root mean square values of suspension working space, vertical body acceleration and dynamic tyre load variation. It also covers three terms of the power losses: root mean square values of the fluctuating power of the spring and tyre and the mean value of the dissipating

damper power as mentioned previously. In general, the performance criteria including the power loss of the conventional suspension depend on seven parameters. Five of them are related to the basic components of the model and the other two parameters represent the road input condition. Because the conventional suspension system is a linear one, the parameters related to the basic components of the model will only be considered in this parametric study. Table 4.1 gives the comparison of the performances of four groups of the conventional passive systems with various parameters values for an average minor road which is specified by equation 2-7 and a vehicle forward speed of 12 m/s. Figures 4.1 to 4.4 show the transfer functions between body/wheel, body/input and wheel/input of the systems in table 4.1. In more detail, the power spectral density PSD functions of the systems are also shown to represent the performances in response to the road input conditions.

Figure 4.1 shows the transfer functions and PSD performances of the systems in group A which uses springs which result in body natural frequencies of 12, 6 or 3 rad/s and the damper to give a constant damping ratio of 0.45. The systems are classified according to their spring stiffness as: stiff A1, soft A2 and very soft A3. The results indicate the following important features. For the body/wheel and body/input ratios, the frequency of the body resonance peaks increases with increasing stiffness of the spring. The highest peak of PSD working space is obtained with the A3 system, but the highest peak of PSD ride comfort is obtained with the A1 system. For the wheel/input ratio, neither the A1 nor A3 system gives the lowest peaks and therefore, the lowest PSD curve and RMS value, table 4.1, of tyre load is obtained with the A2 system. Figure 4.2 shows the transfer functions and PSD performances of the systems in group B which uses a damper with damping ratio of 0.8, 0.4 or 0.2 and the spring to give a constant body natural frequency of 8 rad/s. The systems are classified by their damping ratio as: very hard B1, hard

B2 and soft B3. These results indicate the following features. For the body/wheel and body/input ratios, the peak values decrease by increasing the damping ratio and therefore, the highest peak of PSD working space is obtained with the B3 system, but the conflict between working space and ride comfort alters as damping changes. For the wheel/input ratio, neither the B1 nor B3 system gives the lowest peaks and therefore, the lowest PSD curve and RMS value, table 4.1, of tyre load is obtained with the B2 system.

The transfer functions and PSD performances of the systems in group C which uses tyre stiffnesses of 350, 700 or 1400 kN/m are shown in Figure 4.3. The natural frequency and damping ratio of the systems are 7 rad/s and 0.45. The soft tyre system C1 gives better ride comfort and tyre load than the stiff tyre system C3 but with a relatively small working space as well. Finally, the effect of the body and wheel masses on the performances are also studied. Figure 4.4 shows the transfer functions and PSD performances of the systems in group D which uses the body/wheel mass ratio of 10.0, 7.6 or 5.0. The natural frequency and damping ratio of the systems are 7 rad/s and 0.45. Improvements in the performance can be obtained by increasing the body/wheel mass ratio.

The relative performances including the power losses of the conventional passive systems are generated for the data indicated in section 3-4. The root mean square values of the ride comfort, dynamic tyre load variation and fluctuating power of the spring and tyre, as well as the mean power dissipation of the damper and the natural frequency of the systems are plotted versus the root mean square value of suspension working space in Figure 4.5. The results confirm the conflict between the performance criteria as mentioned previously. In terms of the power requirements, the results indicate the following important features. The fluctuating power of the spring increases as its stiffness decreases and the power dissipation of

the damper decreases as its coefficient decreases, with both these trends causing an increase in the suspension working space. The fluctuating power of the tyre is higher than the fluctuating power of the passive spring and the difference between them decreases by increasing the suspension working space. The level of the fluctuating power of the passive spring and tyre are higher than the level of the dissipation power of the passive damper because the passive spring and tyre must generate higher forces since they carry the static load of the vehicle.

4.3 Switchable and continuously variable damper systems

These systems are similar to the conventional passive system except the damper is either a switchable damper, on-off control, or continuously variable damper. There are many other possible strategies of the variable damper systems, e.g. semi-active types, which are dealt with later in the thesis. Again, the two state switchable and continuously variable damper systems differ from the semi-active system in that the control law of the latter is based on the corresponding fully active one. In this chapter, the study of switchable and variable damper systems is aimed at evaluating their improvements in performance over the passive system. The behaviour of such systems is non-linear because of the switching process of the switchable and variable damper. Therefore, a non-linear procedure is used for predicting the performance properties including the power losses of the systems as discussed in chapter 3. In order to accommodate the fact that the switchable and variable dampers cannot switch between their modes instantaneously, a first order time lag is included in the model to control switching between the states. The following study will discuss the switchable and variable damper which can be used within the vehicle suspension system instead of the fixed damper.

4.3.1 Two state switchable damper

This damper only has two distinct levels of damping to produce the desired force magnitude. The control law which Hrovat and Margolis (1981) used to switch the damper between its hard and soft settings is indicated in Figure 4.6, i.e. the effective damper coefficient C_s is described by the following equations;

$$C_s = hard\ coefficient \qquad \text{if } \dot{X}_b \times (\dot{X}_b - \dot{X}_w) \text{ is positive} \qquad 4\text{-}4$$

$$C_s = soft\ coefficient \qquad \text{if } \dot{X}_b \times (\dot{X}_b - \dot{X}_w) \text{ is negative} \qquad 4\text{-}5$$

This control law is used throughout this thesis. Other control laws of the switchable damper systems were discussed by many investigators e.g. Krasnicki (1981), Lizell (1988) and Miller (1988). In comparison with the other controlled systems, the two state switchable damper approach is the simplest and involves hardware which is currently available, Crawford (1987), Parker and Lau (1988), Moore (1988), Lizell (1988), Meller et al (1988) and Hine and Pearce (1988).

4.3.2 Continuously Variable Damper

This damper can produce any desired force magnitude which only enables the damper to dissipate the energy from the system. In this section, one possible control strategy is developed from the two state switchable system principle. The damper of this system provides two functions. The first function is the same as that of a two state switchable damper system while the second function enables the damper to dissipate part of the stored spring energy instead of restoring it to the car body and wheel, i.e. the damper acts more in the case of dissipating the stored energy of the spring which otherwise would cause further acceleration of the masses. The control laws used to switch the damper between its states are,

$$C_v = C_s \qquad \text{if } (SWS \times SWV) \text{ is positive} \qquad 4\text{-}6$$

$$C_v = C_s - \frac{R_s K_s SWS}{SWV} \qquad \text{if } (SWS \times SWV) \textit{ is negative} \qquad 4\text{-}7$$

where K_s is the spring stiffness, R_s is a dimensionless factor, $SWS = X_w - X_b$ and $SWV = \dot{X}_w - \dot{X}_b$. The R_s factor represents how much stored energy of the spring must be dissipated by the damper, as indicated by a positive value less than or equal to one.

4.4 Comparison of all Systems

The results for the passive, two state switchable damper and continuously variable damper systems are generated for the following conditions. Firstly, a ground roughness coefficient described by equation 2-7 representing an average minor road and a forward speed of 12 m/s. Secondly, the switching dynamics used for the switchable and variable damper are assumed to be represented by a first order lag with a time constant of 0.011 seconds. Thirdly, a two state switchable damper has a hard setting which is the same as the fixed damper and a soft setting which is 25% of that setting. Finally, the continuously variable damper system is assumed to have a value for R_s of 0.75. These settings used for the switchable and variable damper were selected on an empirical basis in that they provided good performance, but they are not claimed to represent the optimum ratios.

The power spectral density functions are obtained for the passive, two state switchable damper and continuously variable damper systems used with a suspension of body natural frequency 1.27 Hz and the damping ratio of the fixed damper is 0.25. In terms of the dynamic tyre load variation, suspension working space, vertical body acceleration and mean value of the power dissipation of the damper, the results shown in Figures 4.7 indicate that the continuously variable damper system is better than the two state switchable damper, which in turn is better than the fixed damper system.

Another advantage of the continuously variable damper over the two state switchable damper systems as shown in Figure 4.8 is that the continuously variable damper system offers an improvement in the performance even when the time lag constant is as high as 150 ms. By comparison, the two state switchable damper system only offers a worthwhile improvement in the performance if the time lag constant is about 11 ms or less. Because the behaviour of two state switchable damper and continuously variable damper systems is non-linear, the RMS performance categories of these systems are obtained for different roads as shown in Figure 4.9. The results indicate that the relative performances of the non-linear damper systems on different roads can be directly correlated, as for the linear systems, with the RMS value of the roughness constants of these roads. Therefore, the percentage improvement in performance for the non-linear damper systems compared with the conventional passive system is constant over a wide range of road surfaces.

The RMS results of the non-linear damper systems attempt to provide the overall flavour of what might be achieved by the various systems using the same fair basis for comparison. Table 4.2 shows a comparison between a suspension of conventional stiffness fitted with fixed, switchable or variable damper for a natural frequencies of 1.03, 1.27 and 1.43 Hz. In terms of the performance categories, the switchable and variable dampers always offer worthwhile improvements in performance over the fixed damper. The two state switchable damper gives an improvement in ride comfort for the same values of dynamic tyre load and working space, while the continuously variable damper gives also an improvement in all the performance categories. Another comparison is done between a passive system using a conventional suspension at 1.03 Hz natural frequency with 0.25 damping ratio and the continuously variable damper system using a stiff suspension with 1.27 Hz natural frequency. The continuously variable damper system using a stiff suspension offers a worthwhile improvement in performance over the conventional

fixed damper system. Another way of viewing the advantage offered by the variable damper is that for the same level of ride comfort as offered by a passive system, the spring stiffness could be set higher, thus providing better body attitude control.

Finally, the RMS values of the ride comfort and dynamic tyre load variation of the three competitive systems are given for 35 mm working space restriction as shown in Figure 4.10. The benefits in performance offered by non-linear damper systems over passive systems and their suspension parameters are also summarised in Table 4.3.

4.5 Concluding remarks

The performance of the passive systems is related to the passive spring and damper elements, e.g. stiffer springs or harder dampers tend to reduce the working space at the expense of a deterioration in ride comfort. Passive systems with an intermediate range of spring stiffness and damper coefficients give the best dynamic tyre load. Small improvements in the performance of the passive system can be obtained by reducing the tyre stiffness or increasing the body/wheel mass ratio. The mean power dissipation of the fixed damper decreases and RMS fluctuating power of the passive spring and tyre all in general increase as the working space increases.

A significant improvement in ride performance can be obtained using a switchable damper rather than a fixed damper, and the continuously variable damper offers a further improvement in ride performance over a two state switchable damper. The continuously variable damper system offers an improvement in the performance even when the time lag constant is as high as 150 ms whereas the two state switchable damper system only offers improvement if the time lag constant is

about 11 ms. Summaries of the performance capabilities of passive, switchable damper and other systems will be given in more detail in chaper 8 and the power consumption of all systems will also be given in chaper 9.

Group	System	K_t kN/m	M_w kg	M_b/M_w	F_n Hz	C_d kNs/m	RMS Performances of dynamic tyre load % DTLP, ride comfort parameter RCP and working space SWS (mm)		
							DTLP	RCP	SWS
A	A 1	700	330	7.6	1.91	27.0	35.2	1.93	17.8
	A 2				0.95	13.5	22.1	1.12	27.6
	A 3				0.48	6.8	22.5	0.75	43.9
B	B 1	700	330	7.6	1.27	32.0	30.3	1.71	16.8
	B 2					16.0	25.0	1.32	24.4
	B 3					8.0	27.2	1.22	35.1
C	C 1	350	330	7.6	1.11	15.8	19.4	0.95	26.0
	C 2	700					23.7	1.24	24.9
	C 3	1400					31.0	1.51	24.2
D	D 1	700	250	10.0	1.11	15.8	22.2	1.21	24.7
	D 2		330	7.6			23.5	1.24	24.9
	D 3		500	5.0			26.6	1.29	25.6

Table 4.1 Comparison of performances of four groups of the conventional passive system with various parameters.

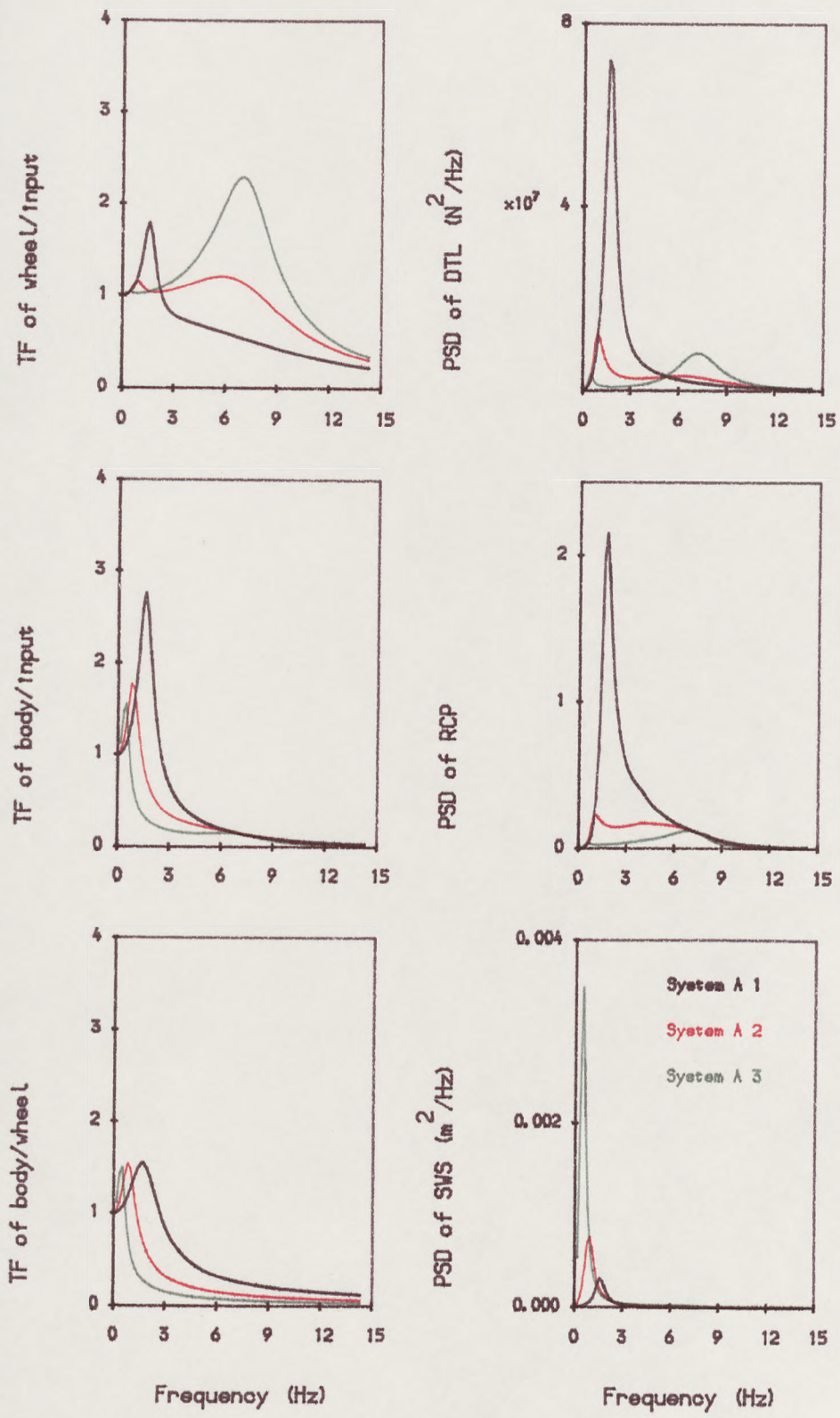

Figure 4.1. The transfer functions and PSDs of the passive systems in group A.

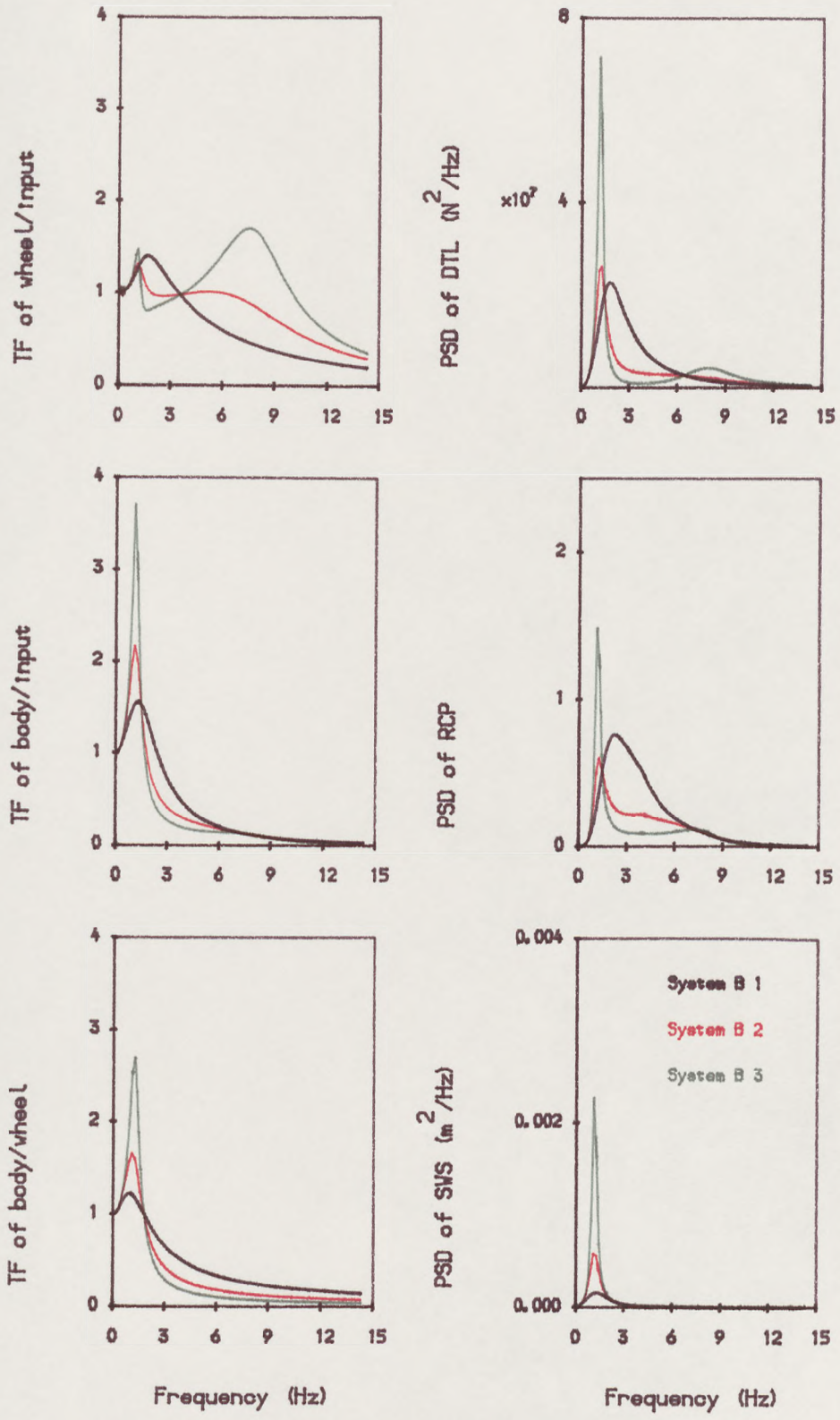

Figure 4.2. The transfer functions and PSDs of the passive systems in group B.

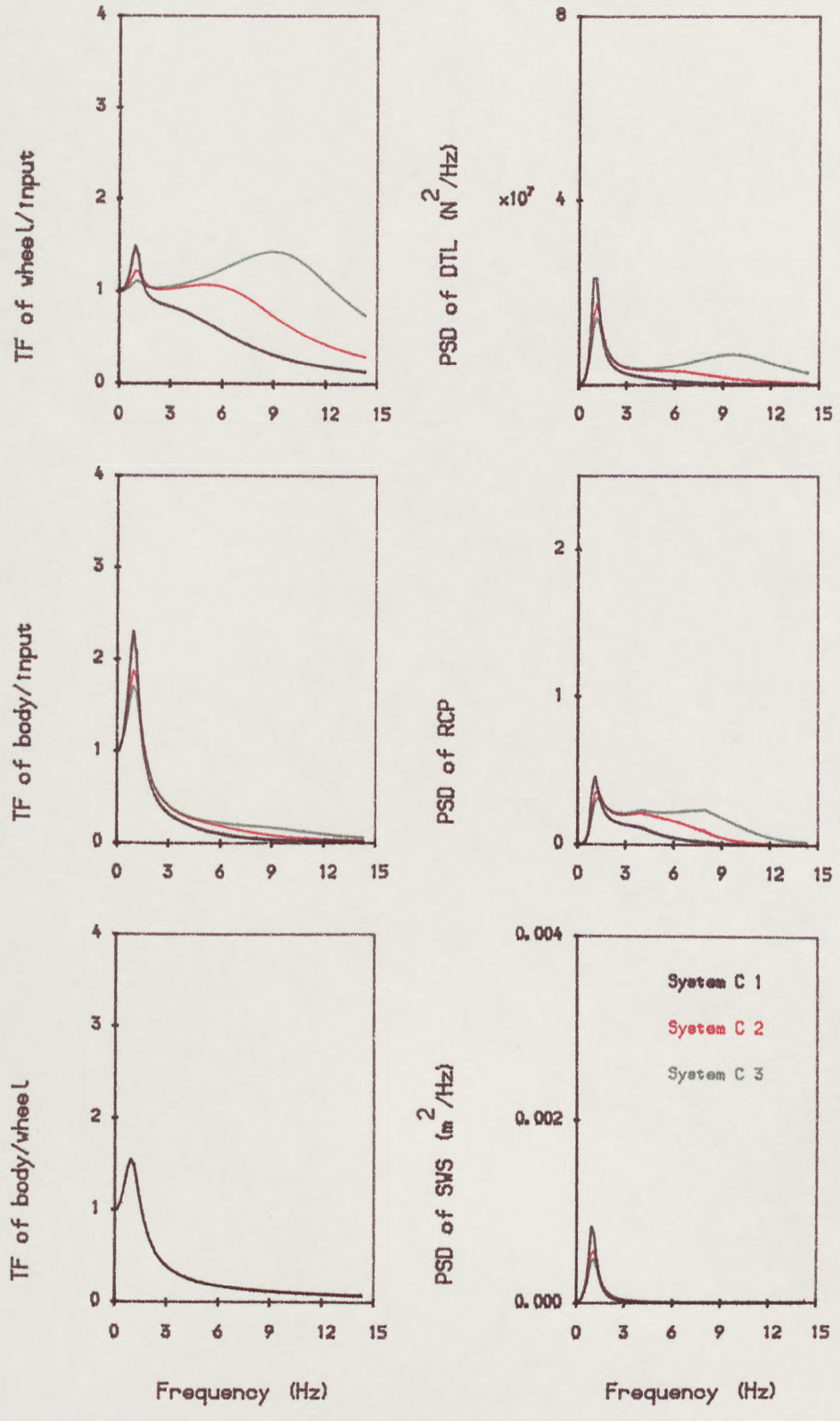

Figure 4.3. The transfer functions and PSDs of the passive systems in group C.

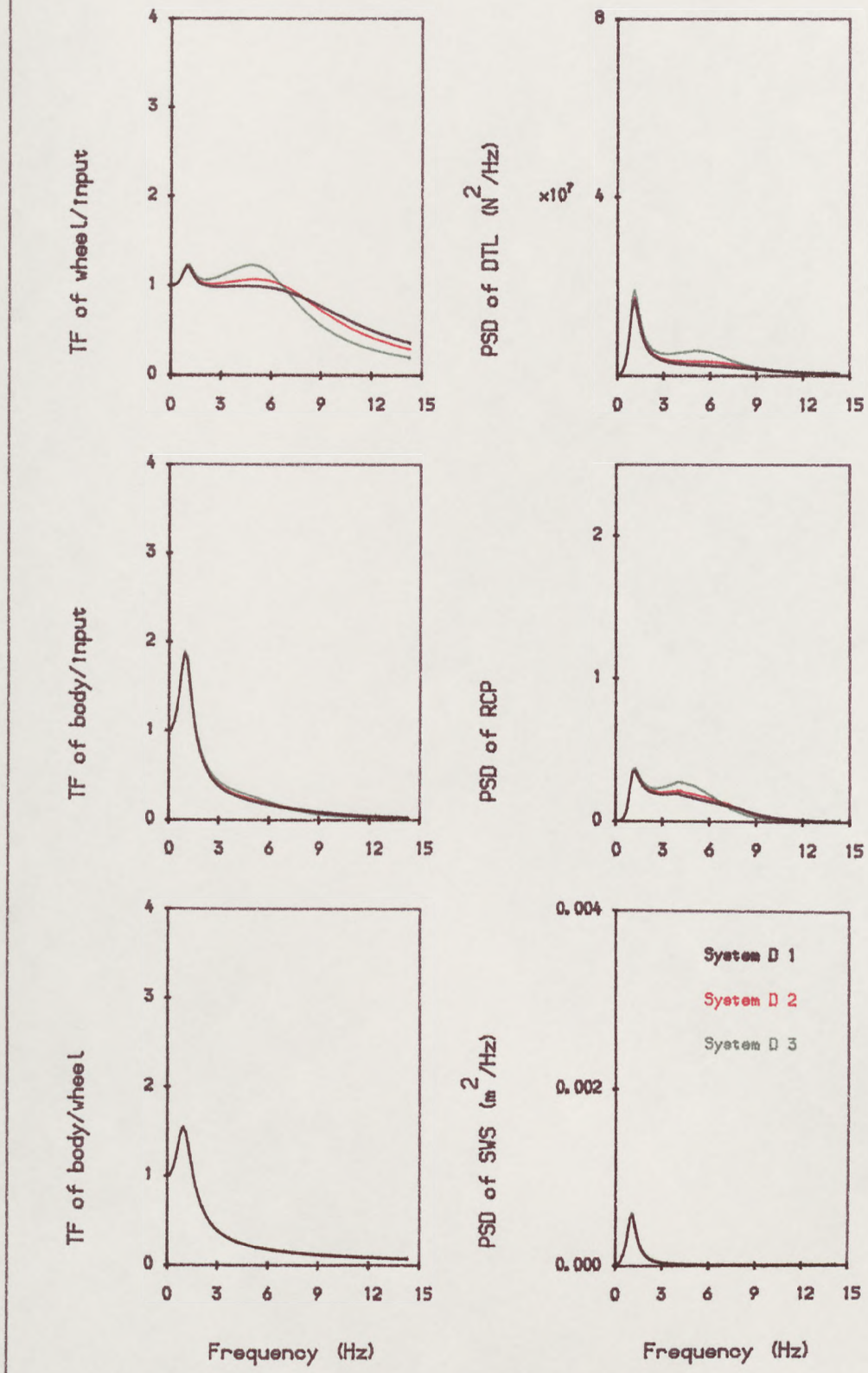

Figure 4.4. The transfer functions and PSDs of the passive systems in group D.

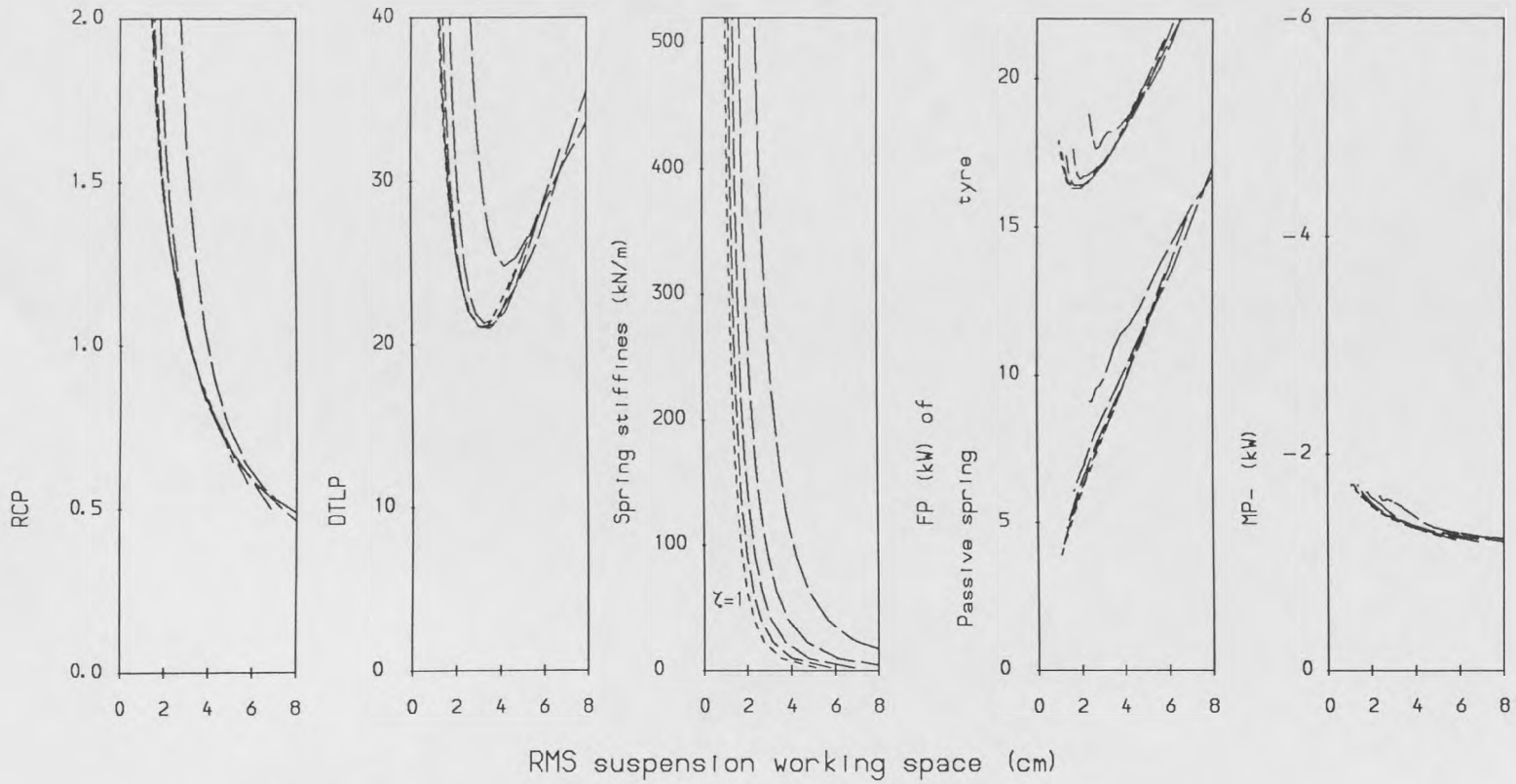

Figure 4.5. Passive systems performances and powers in the spring/damper and tyre at damping ratio {0.2, 0.4, 0.6, 0.8 and 1.0}.

Figure 4.6 Strategy for switching a two state damper.

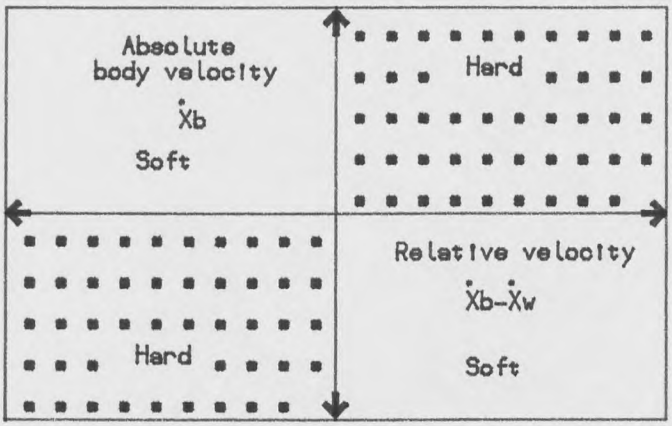

Figure 4.7 Comparison of passive and switchable damper systems.

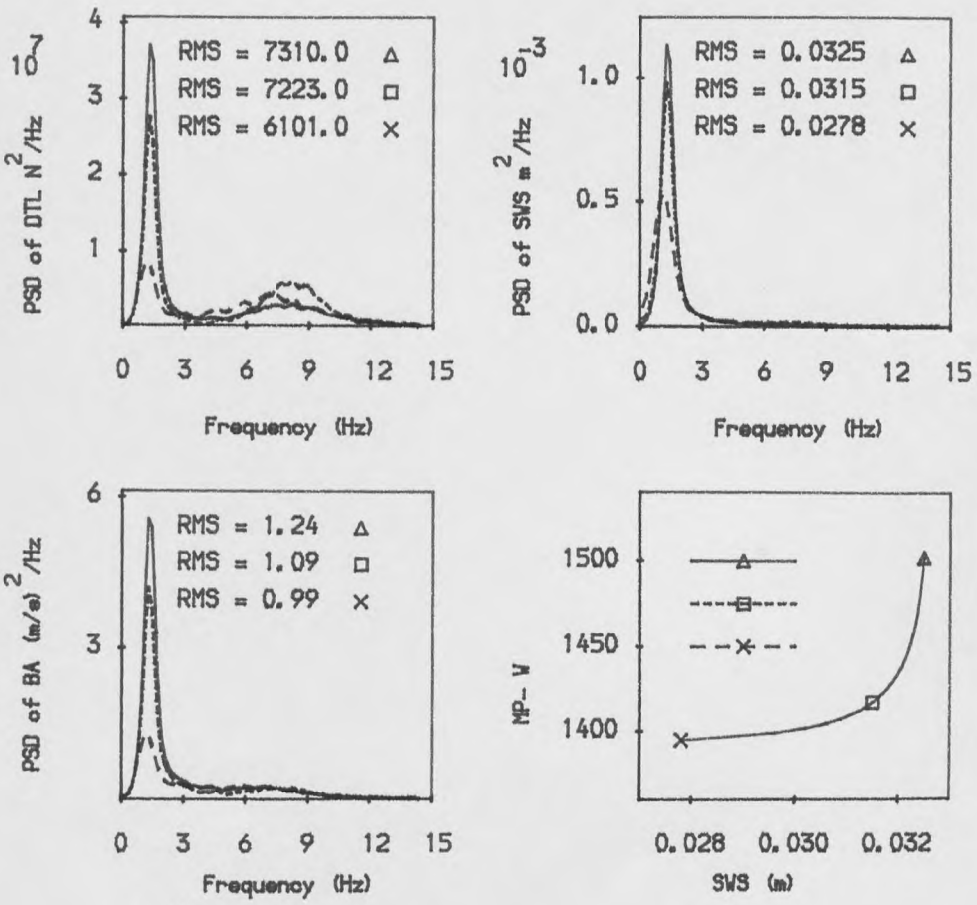

△ Passive
□ Two state switchable damper
× Continuously variable damper

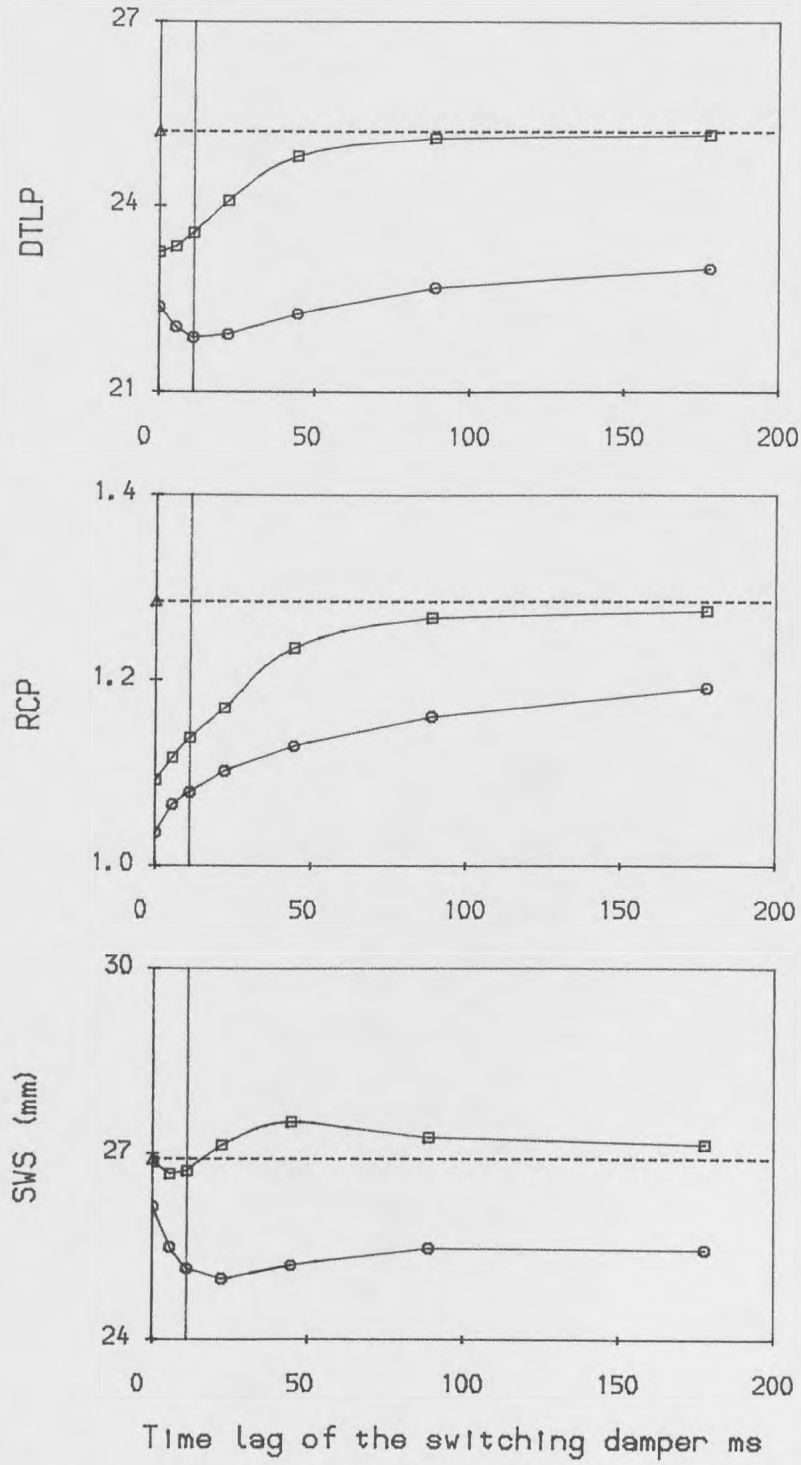

Figure 4.8 Performance of switchable and variable damper systems relative to passive system for a range of values of time lag. Body natural frequency = 1.27 Hz and damping ratio= 0.25 for fixed damper.
△---△ Passive □ □ Two state switchable
o o Continuously variable damper

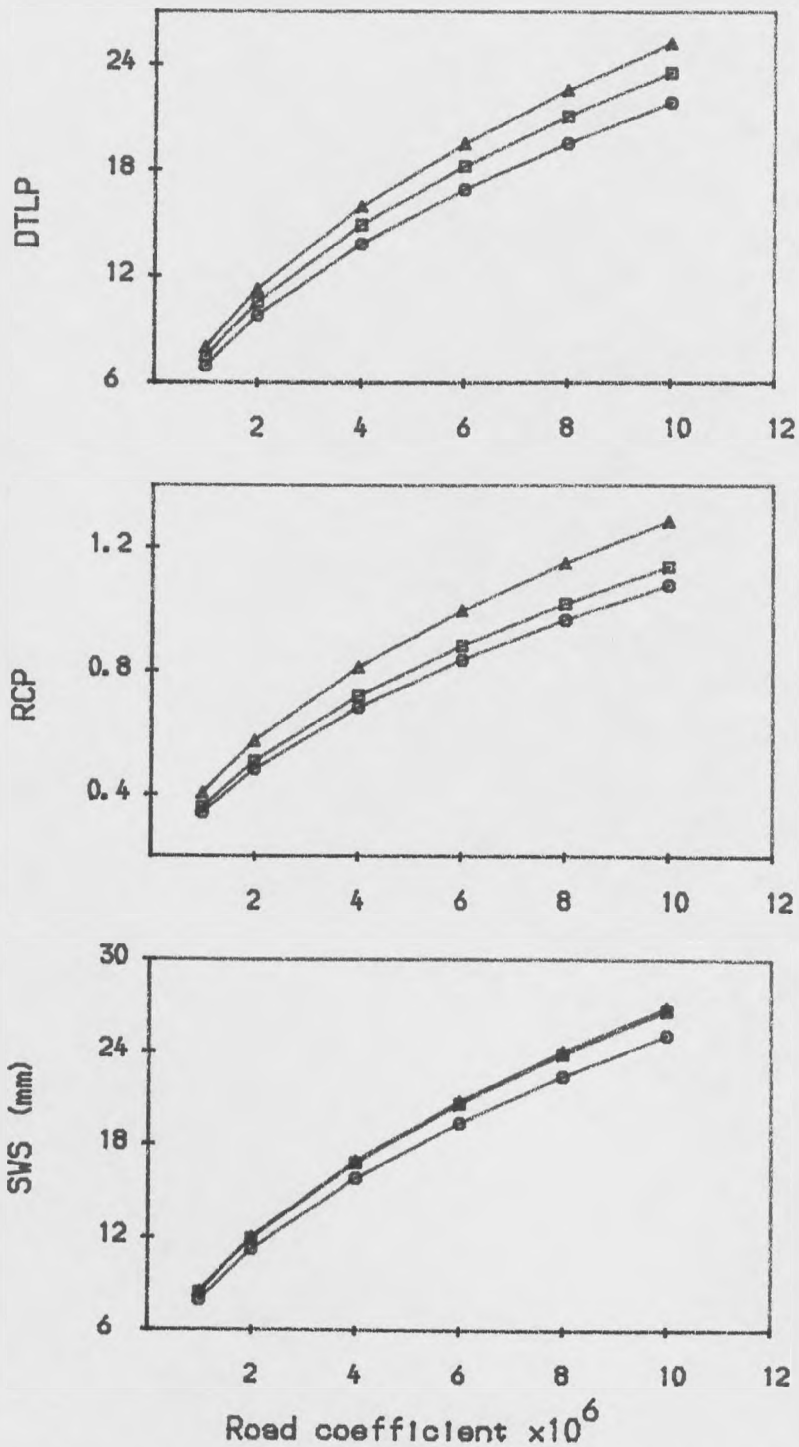

Figure 4.9 Performance of passive, switchable and variable damper systems versus road coefficient. Body natural frequency = 1.27 Hz and damping ratio = 0.25 for fixed damper.

△ △ Passive □ □ Two state switchable

o o Continuously variable damper

F_n Hz	ζ	System	RMS Performance of dynamic tyre load % DTLP, ride comfort parameter RCP and working space SWS (mm)			Improvement i.e. reduction for switchable system compared with passive %		
			DTLP	RCP	SWS	DTLP	RCP	SWS
1.03	0.45	Passiv.	22.8	1.18	26.6			
		Two st.	21.8	1.00	27.6	4.3	15.1	-3.9
		Contin.	21.5	1.08	26.0	5.4	8.0	2.0
	0.35	Passiv.	22.5	1.08	30.5			
		Two st.	22.4	0.94	30.3	0.3	13.4	0.5
		Contin.	21.2	0.99	28.5	5.7	8.8	6.5
	0.25	Passiv.	23.6	1.01	36.4			
		Two st.	24.5	0.90	35.2	-4.0	10.5	3.4
		Contin.	22.4	0.84	32.6	5.3	16.3	10.4
1.27	0.45	Passiv.	25.6	1.37	23.4			
		Two st.	23.2	1.18	23.9	9.5	13.5	-2.1
		Contin.	22.5	1.16	23.7	12.4	14.9	-1.2
	0.35	Passiv.	25.2	1.28	26.9			
		Two st.	23.6	1.14	26.7	6.5	11.4	0.7
		Contin.	21.9	1.08	25.1	13.3	16.0	6.6
	0.25	Passiv.	26.3	1.24	32.5			
		Two st.	26.0	1.09	31.5	1.2	12.3	3.0
		Contin.	22.0	0.99	27.8	16.5	19.9	14.5
1.43	0.45	Passiv.	27.9	1.50	21.7			
		Two st.	24.4	1.22	23.4	12.7	18.5	-8.0
		Contin.	23.4	1.26	21.7	16.0	16.2	0.0
	0.35	Passiv.	27.5	1.43	24.9			
		Two st.	25.1	1.22	25.4	8.8	14.3	-1.9
		Contin.	22.6	1.17	23.1	17.8	17.9	7.3
	0.25	Passiv.	28.9	1.41	30.1			
		Two st.	27.5	1.27	29.4	4.9	10.1	2.2
		Contin.	22.6	1.06	26.2	21.6	25.2	13.1

Table 4.2 Comparison of performance of passive, switchable and variable damper systems. The hard setting of the two state damper is the same as the fixed damper and the ratio Csoft/Chard is 0.25. The Rs value for variable damper is 0.75.

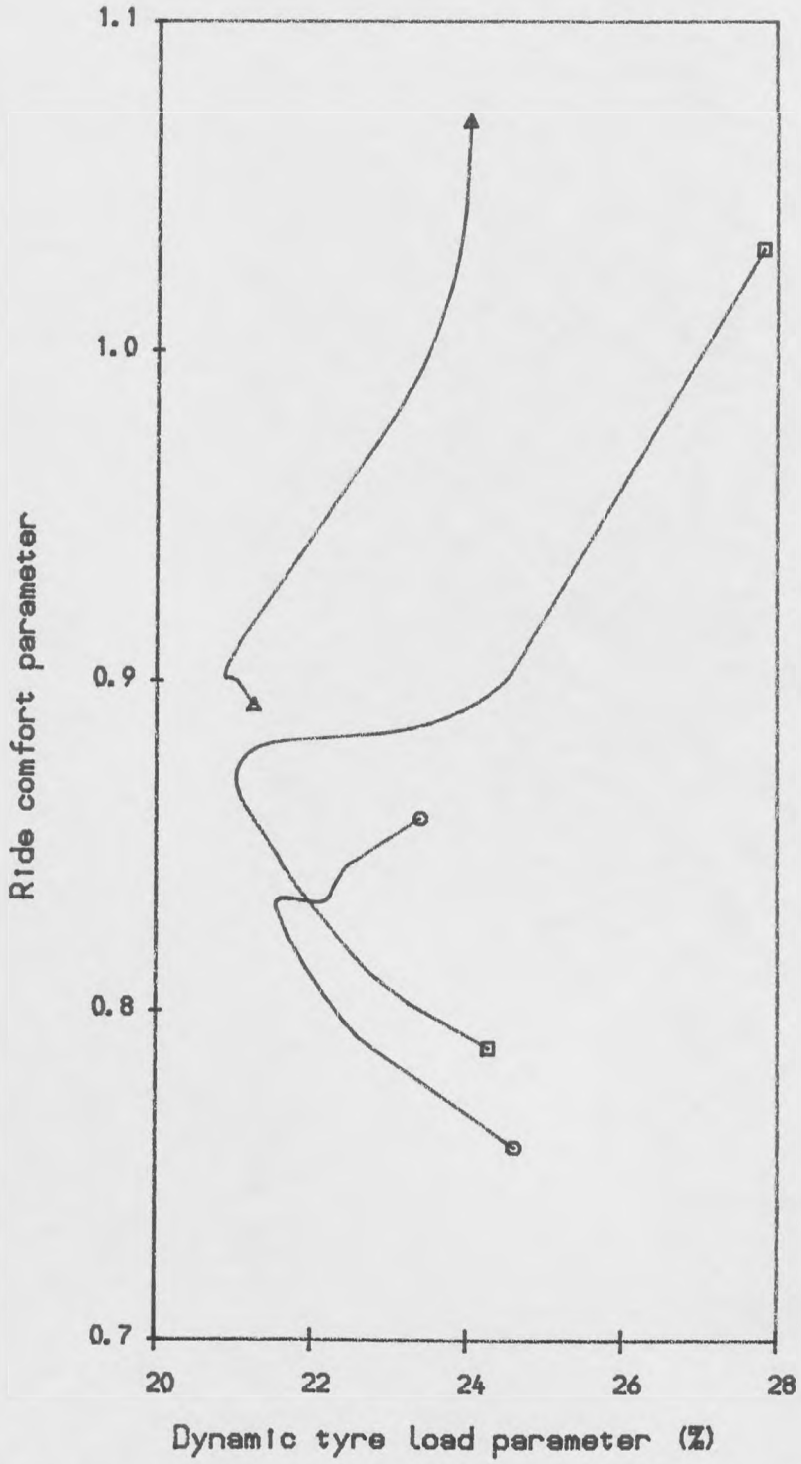

Figure 4.10. Comparison of passive, switchable and variable damper systems at a RMS suspension working space of 35 mm.

△ △ Conventional passive

□ □ Two state switchable damper

o o Continuously variable damper

Group	System	F_n Hz	ζ	Csoft/ Chard ratio	RMS Performance of dynamic tyre load % DTLP and ride comfort parameter RCP	
					DTLP	RCP
Passive	P 1	0.72	0.40	/	21.3	0.89
	P 2	0.56	0.55		21.0	0.90
	P 3	0.40	0.75		21.1	0.91
	P 4	1.03	0.25		23.5	1.00
	P 5	1.11	0.25		24.0	1.07
Two state	T 1	0.88	0.30	0.25	24.3	0.79
	T 2	0.80	0.35	0.50	22.6	0.82
	T 3	0.72	0.40	0.75	21.5	0.85
	T 4	0.48	0.70	0.75	21.2	0.88
	T 5	1.03	0.25	0.25	24.5	0.90
	T 6	1.19	0.20	0.00	27.8	1.03
Contin. variab.	C 1	1.03	0.20	0.00	24.6	0.76
	C 2	0.88	0.30	0.25	22.6	0.79
	C 3	0.80	0.30	0.75	21.5	0.83
	C 4	0.88	0.35	0.25	22.2	0.83
	C 5	1.03	0.20	0.50	22.5	0.84
	C 6	1.11	0.15	0.50	23.4	0.86

Table 4.3 Comparison of performance between passive, switchable and variable damper systems at a RMS suspension working space of 35 mm. The Rs value for the variable damper is 0.75.

CHAPTER 5

ACTIVE SYSTEMS

5.1 Introduction

The interest in intelligent suspension systems is currently high throughout the vehicle industry, motivated by the limitations of passive designs in meeting the conflicting requirements of a vehicle suspension. Most of the large vehicle companies are involved in investigation and development to improve suspension systems which are intelligent in the sense that they employ controllable active elements to provide improved isolation between the wheel and the body of the vehicle according to some control law instead of spring and damper elements of the conventional passive systems. The aim of this chapter is to study the behaviour of active linear control systems and the possibility of improving their performance by using a non-linear control law. The study covers three categories of the performance: root mean square values of suspension working space, vertical body acceleration and dynamic tyre load variation. It also covers four terms of the power losses: root mean square values of the fluctuating power of the spring, which is used to support the static vehicle weight, and tyre and the mean values of the actuator demand and dissipated power.

This chapter is divided into four parts. The first part presents the behaviour of active linear control systems. The linear control law uses only one set of the feedback gains of the some or all state variables of the system, but the non-linear control law uses for each time step a different set of the feedback gains. The second part introduces an alternative searching method to find the feedback gains of the non-linear control systems at each time step. In the third part, a comparison between both active linear and non-linear control systems is made in terms of the performance and power requirements. The last part summarises the important concluding remarks obtained throughout the calculations of the systems.

5.2 Active linear control systems

The layout in figure 3.4 shows the active linear control system which uses a fully active actuator in parallel with a passive spring between the body and wheel of the vehicle. The fully active actuator is controlled by a high frequency response servovalve and which involves a force feedback loop. The force demand signal, typically generated in a microprocessor, is governed by an optimal linear control law which is normally obtained by application of various forms of optimal control theory as discussed previously. The behaviour of the full and limited state feedback forms of the fully active systems will be discussed in terms of their performance and power requirements. The basic model and road input which were described in 3-4 are used to investigate the performance of these systems. Although these systems are linear and, therefore performance can be done in the frequency domain, this does not allow total power to be separated into power demand and dissipation components and therefore, a time history solution must be used to predict the separate components of the power usage.

5.2.1 Full state feedback systems

The control law of the full state feedback active system, method 1, can be re-written from equation 3-61 as;

$$U(t) = K_{f1} X_w(t) + K_{f2} X_b(t) + K_{f3} \dot{X}_w(t) + K_{f4} \dot{X}(t) - (K_{f1} + K_{f2}) X_0(t) \qquad 5\text{-}1$$

where K_{f1}, K_{f2}, K_{f3} and K_{f4} are the feedback coefficients. By inserting equation 5-1 into equations 3-2 and 3-3, the equation of motion of the active systems can be obtained and therefore, the behaviour of the system can also be calculated.

Table 5.1 gives the root mean square values of the performance criteria and the mean values of the actuator demand and dissipated power of four groups of the full

state feedback systems. These systems refer to different sets of the weighting parameters in the performance index, denoted q_1, q_2 and r. Figures 5.1 and 5.2 show the transfer functions and PSD curves of systems in groups AF and BF. The systems in group AF are chosen to give the same value of dynamic tyre load (20%) whereas the systems in group BF are chosen to give the same value of the suspension working space (3.5 cm). For group AF, the conflict between ride comfort and suspension working space is shown clearly both in the Table and in Figure 5.1, whereas for group BF, the direct conflict between ride comfort and dynamic tyre load is highlighted (figure 5.2).

In terms of the power requirements, the calculations therefore reveal how much power would be used by a 100% efficient system with a flat frequency characteristic up to 15 Hz, which is the upper frequency limit of the calculations. Results for a fully active system over a wide range of suspension workspace are included in group CF. In fact, the practical implementation of the systems may be an actuator only (Ac1), or an actuator in parallel with a spring designed to give a natural frequency of 1.27 (Ac2) or 1.01 Hz (Ac3). In all cases, the performance is the same but the power flows are different as shown in figure 5.3. In particular, the actuator in version Ac1 must generate higher forces since it carries the static load of the vehicle. The requirements of the actuator force, $U_a(t)$, of the Ac1 version and other versions are;

$$U_a(t) = \textit{Static load of vehicle body} + U(t) \qquad 5\text{-}2$$

$$U_a(t) = U(t) - \textit{Spring force} \qquad 5\text{-}3$$

The only realistic implementation of the fully active system from a practical viewpoint involves the inclusion of a spring in parallel giving a mean power demand of < 1.5 kW for version Ac2 and < 0.5 kW for version Ac3. The mean

powers dissipated by these versions are similar to those dissipated by the damper of the passive system. The mean power demand and dissipation of the actuator, RMS fluctuating power of the passive spring and tyre all generally increase with increasing working space. The calculation of mean power levels does not, however, tell the complete story. The time histories of power demand for groups AF and BF are shown in Figures 5.4 and 5.5 and for power dissipation in figures 5.6 and 5.7. The results indicate the following important points. The power requirement is related to the dynamic tyre load. The mean power demand generally increases with increasing workspace or dynamic tyre load. For group AF, the lowest value of mean power dissipation is obtained at 3.5 cm suspension working space (system AF2). The time histories of the power demand or dissipation look remarkably similar for all systems within a group and high peak levels occur which are of the order of 20 times the mean power levels. For group BF, the mean power dissipation increases as ride comfort decreases and again, the distributions of the peak power demand and dissipation are similar.

Figure 5.8 shows the design and power requirements of the systems in group DF versus the road input condition GV for forward speeds of 12 and 17 m/s. The systems are chosen to give 3.5 cm suspension working space RMS and 20% dynamic tyre load RMS. The results indicate the following features. The mean power dissipation of these systems is increased by operating on a rough road, while the mean power demand is increased by operating on a smooth road. The feedback coefficients of the systems are increased by operating on a rough road or operating with higher speed. For the fully active system, the outputs are proportional to the input conditions, GV, but the power demand and dissipation results are not related in a similar way. The power demand and dissipation of the systems DF2, DF4 and DF5 are shown in Figure 5.9 and 5.10. The figures indicate some important features of the actuator power requirements when operating on two different road

input conditions. The curves look remarkably similar and high peak power demand and dissipation levels occur. Ignoring the transient features during the initial two seconds of the trace, peak values of around twenty times the mean power and the peak power demands up to 4 kW and peak power dissipation up to 20 kW are indicated.

The performance properties of the full state feedback systems are displayed in Figure 5.11 for different types of road input conditions at a working space of 3.5 cm. Because the response of a linear suspension system follows the law of superposition, the RMS performances of all the active systems are proportional to the road input conditions, so that the performance of any active system, studied for road surface/vehicle forward speed combinations other than those presented here can be scaled down or scaled up as shown in Figure 5.11. Since the results scale in the manner described, the significant parameter is, more precisely, the ratio of the RMS performance categories to road input condition which is represented by the road roughness spectral density constant and the vehicle forward speed. The ratio has the values 2.0, 1.414, 1.18 and 1.0 respectively for curves GV= 4.2×10^{-5}, 16.6×10^{-5}, 33.3×10^{-5} and 41.6×10^{-5}. For example, if the smoother road were multiplied by 4, all the performance categories which lies on that curve would be multiplied by 2, except the power demand and dissipation of the systems.

5.2.2 Limited state feedback systems

The control law of the limited state feedback active systems can be re-written from equation 3-63 as,

$$U(t) = K_{f1} X_w(t) + K_{f2} X_b(t) + K_{f3} \dot{X}_w(t) + K_{f4} \dot{X}_b(t) \qquad 5\text{-}4$$

where K_{f1}, K_{f2}, K_{f3} and K_{f4} are the feedback coefficients. The equations of motion and the behaviour of the limited state information system can then be obtained as

described previously.

The performances of the limited state feedback fully active systems are summarised for four groups in Table 5.2. These systems are chosen within the same constraints used for the active systems indicated in Table 5.1. Comparison of the two Tables indicates that the behaviour of the limited and full state feedback systems are similar. Figures 5.12 and 5.13 show the transfer functions and PSD performances of the systems in groups AL and BL. The conflict between ride comfort and suspension working space is clearly shown in both the table 5.2 and figure 5.12, whereas the conflict between ride comfort and dynamic tyre load is also highlighted in figure 5.13. Figures 5.14 and 5.15 show the time histories of the power requirements of the system in group Bl. The mean power demand and dissipation increase as ride comfort decreases and the distribution of high peak power demand or dissipation is different. The reduction of the power requirements due to the use of a passive spring mounted in parallel to the actuator is shown in Figure 5.16 which represents the systems in group CL. Figure 5.17 shows the design and power requirements of the systems in group DL. The results indicate that the feedback coefficients are affected by the vehicle forward speed and, therefore for each road input condition, there are two sets of these feedback coefficients which use the same performance criteria for that system. The performance properties of the limited state feedback systems are also displayed in Figure 5.18 for different types of road input conditions at a working space of 3.5 cm. The responses of all the systems, provided they are linear, are proportional to the road roughness spectral density constant and vehicle forward speed as mentioned previously.

Finally, Figure 5.19 shows a comparison between the performance and power requirements of the full and limited state feedback systems at 3.5 cm of suspension working space. The figure merits some important comments as follows. The per-

formance of the full and limited state feedback systems are close to each other. The RMS of the fluctuating power of passive spring and wheel tyre are increased as the dynamic tyre load increases. The lowest value of the power dissipation and demand occurs at a dynamic tyre load RMS value of around 20%.

5.3 Active non-linear control systems

The conflict between the performance categories of the suspension systems could theoretically be reduced by using a control law in which the feedback gains were continuously varied rather than being fixed as described in section 5.2. Therefore, the aim of this section is to investigate the possibility of improving the performance of the active system by using a non-linear control law. In this system, the feedback gains are a function of time and need to be found for each time step. In practical terms, the difficulty would be in calculating these gains quickly enough, i.e., at each time step. With current levels of vehicle mounted processing capability this looks unlikely, but the idea is nevertheless worthy of investigation given the rapid changes which may occur in computing power. Thus, this control law is a non linear one, and non linear analysis procedures should be used to evaluate the performance capabilities including the power requirements of the system. In this study, the non-linear control law of a limited state feedback active system is considered as follows.

5.3.1 Limited state feedback systems

The following control law, which contains feedback gains of the relative displacements $K_{v1}(t)$ and velocity $K_{v3}(t)$ between the body and wheel of the quarter car model, will be used throughout.

$$U(t) = K_{v1}(t)\,[X_w(t) - X_b(t)] + K_{v3}(t)\,[\dot{X}_w(t) - \dot{X}_b(t)] \qquad 5\text{-}5$$

The procedure to determine the variable feedback gains is based on the definition of the random profile of an actual road surface which may be thought of as an infinite number of sine waves of different amplitudes added together using a set of random phase angles. From the fundamental design of vehicle suspension systems, the concern is for the vibration properties of the system in the frequency range 1 to 90 rad/s (0.2 to 15 Hz), as they dominate ride behaviour as discussed in earlier chapters. The road input, therefore, is assumed to be represented by a finite number, N, of sine waves to cover this frequency range. Let there be N= 512 periodical inputs, $H_i(t)$, which have different amplitudes, A_i, phase angles, θ_i, and frequencies, ω_i, within the effective frequency range, ω_i= 1, 1.175, 1.35, ..., 89.825, 90 rad/s. The road input, $X_0(t)$, can then be formulated as;

$$X_0(t) = \sum_{i=1}^{N} A_i \sin(\omega_i t + \theta_i)$$

i.e.

$$X_0(t) = \sum_{i=1}^{N} H_i(t) \qquad 5\text{-}6$$

It is assumed that the 2N samples of the road $X_0(t)$ can be measured by a height sensing instrument placed in the front of the vehicle as shown in figure 5.20. The Fourier content of the total length of surface shown (144 m) can be found by using, for example, a Fourier analysis procedure. This assumes that once a steady state condition is established, 1024 points are stored continuously, but are updated at each time step by reading in a new data point at the front of the vehicle and discarding the last point in the set. The corresponding instantaneous responses of the relative displacements $HS_i(t)$ and velocities $HV_i(t)$ between the wheel and body with respect to each periodical content $H_i(t)$ can also be found by the following

process. Let there be a stored set of the feedback coefficients, $\kappa_{v1}(\omega_i)$ and $\kappa_{v3}(\omega_i)$, each one of them being optimal for a particular frequency ω_i. The corresponding instantaneous responses of the relative displacement $HS_i(t)$ and velocity $HV_i(t)$ can be found by solving the equations of motion 3-2 and 3-3 of the system for each periodical input. For instance, the predicted values of the total relative displacement SWS(t) and velocity SWV(t) are;

$$SWS(t) = \sum_{i=1}^{N} HS_i(t) \qquad 5\text{-}7$$

$$SWV(t) = \sum_{i=1}^{N} HV_i(t) \qquad 5\text{-}8$$

Therefore, the variable feedback coefficients $K_{v1}(t)$ and $K_{v3}(t)$ are

$$K_{v1}(t) = \sum_{i=1}^{N} \frac{HS_i(t)\ \kappa_{v1}(\omega_i)}{SWS(t)} \qquad 5\text{-}9$$

$$K_{v3}(t) = \sum_{i=1}^{N} \frac{HV_i(t)\ \kappa_{v3}(\omega_i)}{SWV(t)} \qquad 5\text{-}10$$

In this technique, a stability test must be included during the calculation of $K_{v1}(t)$ and $K_{v3}(t)$ at each time step.

An example of the active non-linear control system was used to generate the time-history results shown in Figure 5.21 for the following conditions. Firstly, a ground roughness coefficient as described by equation 2-7 representing an average minor road at a forward speed of 12 m/s was used together with the data of the quarter car model as described in 3-4. Secondly, the 2N= 1024 samples of road input were assumed to be measured during a 12 second period, equating to the distance of 144m starting from the front of the vehicle as shown in Figure 5.20. Another sample must be taken at each time step of 11.7 ms and the last sample then

discarded. Thirdly, the stored set of the feedback coefficients $\kappa_{v1}(\omega_i)$ and $\kappa_{v3}(\omega_i)$ for all required frequency content of the system, ω_i= 1, 1.175, .., 90 rad/s, are assumed to be as follows;

$$\kappa_{v1}(\omega_i) = 22500 \quad \text{and } \kappa_{v3}(\omega_i) = 6750 \quad \text{if } 6 < \omega_i < 35$$

$$\kappa_{v1}(\omega_i) = 360000 \quad \text{and } \kappa_{v3}(\omega_i) = 27000 \quad \text{if } 6 \geq \omega_i \geq 35 \qquad 5\text{-}11$$

This set was selected on an empirical basis in that it provided good performance, but it is not claimed to represent an optimum set. In the case of the height sensing instrument of measuring the road inputs mounted 1m ahead of the front wheel (say for example at the front bumper), then the allowable time to calculate the gains and actuator desired force is up to 70 ms. The results indicate that the instantaneous values of feedback gains may be either positive or negative values, although the feedback coefficients $\kappa_{v1}(\omega_i)$ and $\kappa_{v3}(\omega_i)$ for a particular frequency content have only positive values. This means that the active actuator may be required to put energy in or take it out of the system. In practical terms, the main difficulties would be in using the height sensing instrument to obtain suitably accurate measurements of the ground profile and in performing the necessary calculations in the limited time available. The idealised system discussed here is also based on a single steady value of forward speed, whereas in practice this may commonly be varying.

5.4 Comparison of all active systems

In this section, the performance capabilities including the power requirements of the active linear control system and the active non-linear control system are compared with each other. The results are generated for the following conditions. Firstly, the road input conditions and the basic parameter of the model are the same

as described in 3-4. Secondly, the non linear analysis procedure was used to evaluate the responses of both systems for 12 seconds of the time history. Thirdly, the actuator of both systems was mounted in parallel with a spring which was designed to give a natural frequency of 1.01 Hz. Fourthly, the linear and non-linear systems were chosen to give similar dynamic tyre load RMS value of 16.3%. Fifthly, the active linear control system based on the full state feedback strategy has the feedback gains; 1770798, -547722, 23438 and -86738. Finally, the active non-linear control system is based on the feedback gains of the limited state feedback strategy outlined in section 5.3.

The underlying idea was to compare the non-linear system with a typical linear active system selected from the range discussed in section 5.2 on the basis that it gave good overall performance for the particular road/speed conditions used. Figure 5.22 shows the transfer functions and PSD performances of both systems. The results, obtained from studing one system for either linear or non-linear control laws, indicated the following features. For the linear system, the RMS value of ride comfort is 1.14 and of working space is 2.5 cm, whereas for the non-linear system, the RMS value of ride comfort is 0.88 and of working space is 1.9 cm. The non-linear system, therefore, gives significant improvements in both ride comfort (by 23%) and working space (by 24%) compared with the linear system for the same dynamic tyre load although its control law is not claimed to represent an optimal control, i.e., the full state feedback active non-linear control system should give more improvements in the performance.

Figure 5.23 shows the time histories of the power demand, power dissipation and actuator force of both the active linear and non-linear control system. The mean value of the power dissipation of the active non-linear control system is less than that of the active linear control system by 35%, although the mean values of

the power demand of both systems are similar. The peak values of power demand for both systems are up to 1.5 kW, whereas the peak values of the power dissipation of the linear and non-linear control systems are up to 10 and 7 kW respectively. Finally, the peak values of the actuator force of the active non-linear control system are less than those of the active linear control system by up to 30%.

5.5 Concluding remarks

It is important to note that throughout the calculations of the active systems, the mean power demand and dissipation were always reduced by using a passive spring placed in parallel with the active actuator without any change in the performance. The mean values of the power demand and dissipation increased as the working space or dynamic tyre load increased. The RMS values of the fluctuating power of the passive spring or tyre also increased as the working space or dynamic tyre load increased. For the linear systems, the performances of the full and limited state feedback were close to each other and the lowest value of the power demand and dissipation occured at a dynamic tyre load RMS value of around 20%. The mean power dissipation of the linear systems was increased by operating on a rougher road, while the mean power demand was increased by operating on a smoother road. Finally, the active non-linear control system provided a significant improvement in performance over the linear control system although it involves practical difficulties relating to ground profile measurement and amount of data processing required.

Group	System	weighting factor $r=10^{-8}$ and		RMS Performance of dynamic tyre load% DTLP, ride comfort RCP, working space SWS (mm) and mean power demand MP+ and dissipation MP- (W)				
		q_1	q_2	DTLP	RCP	SWS	MP+	MP-
AF	AF 1	2250	500	20.2	1.00	25.0	17	1400
	AF 2	1800	20	20.0	0.80	35.1	94	1378
	AF 3	1500	1	20.6	0.76	45.9	190	1470
BF	BF 1	17500	25	15.2	0.99	35.6	112	1385
	BF 2	800	40	22.5	0.72	35.5	125	1405
	BF 3	400	66	24.8	0.67	35.0	141	1427
CF	CF 1	4500	7000	29.3	1.69	15.3	7	1545
	CF 2	4000	500	19.3	1.02	25.4	19	1387
	CF 3	2500	22.50	19.2	0.84	34.4	75	1366
	CF 4	833	1.67	22.9	0.68	45.0	256	1501
	CF 5	500	0.18	25.5	0.61	55.8	532	1753
DF	DF 1	180	1	20.4	0.31	35.0	312	785
	DF 2	400	5	20.5	0.46	35.2	218	954
	DF 3	833	11.67	20.3	0.62	35.2	146	1153
	DF 4	1600	20	20.4	0.78	35.5	101	1384
	DF 5	1600	20	20.4	0.78	35.3	90	1359

Table 5.1 Comparison of performances and power requirements of the full state feedback fully active systems.

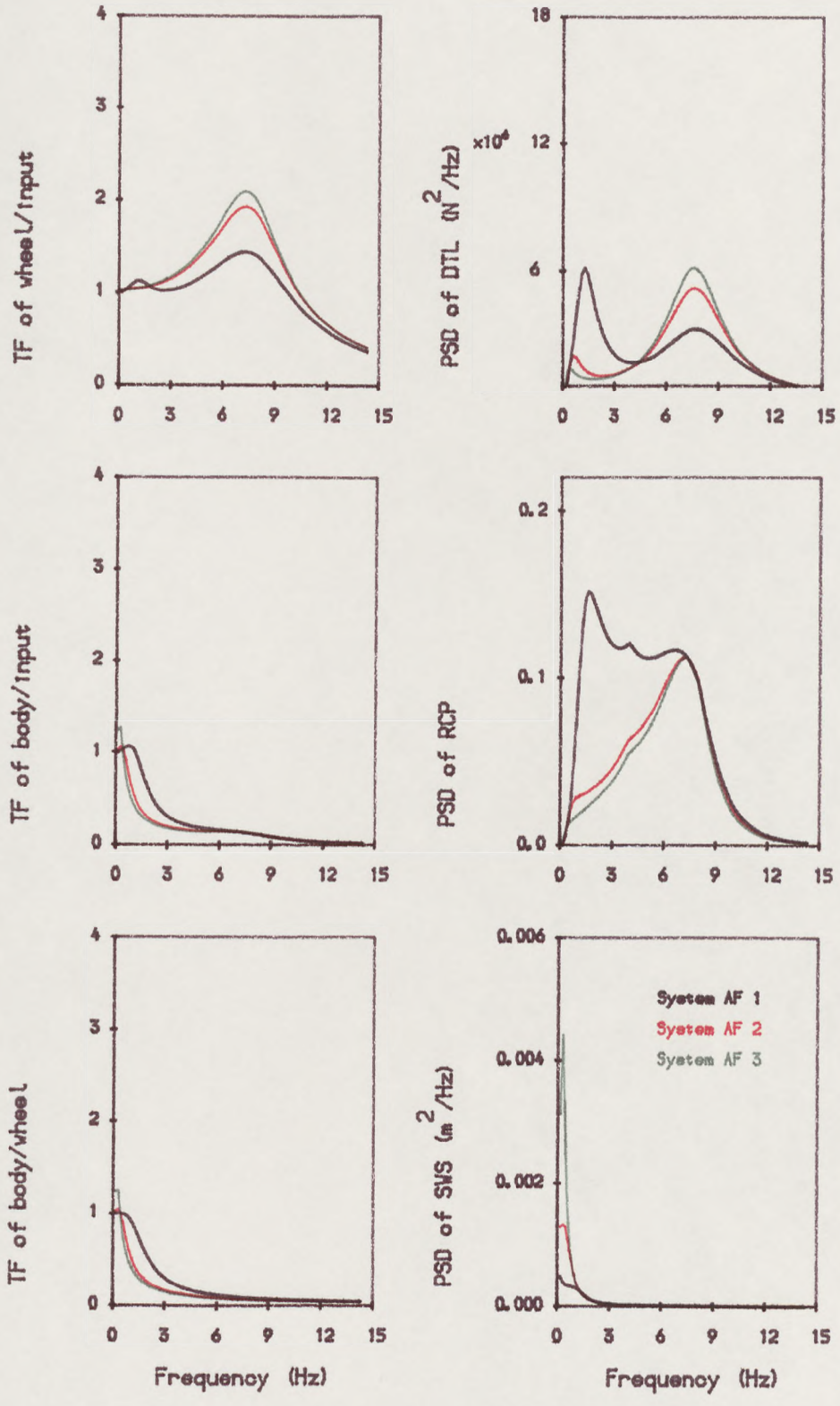

Figure 5.1. The transfer functions and PSDs of the full state feedback fully active systems in group AF.

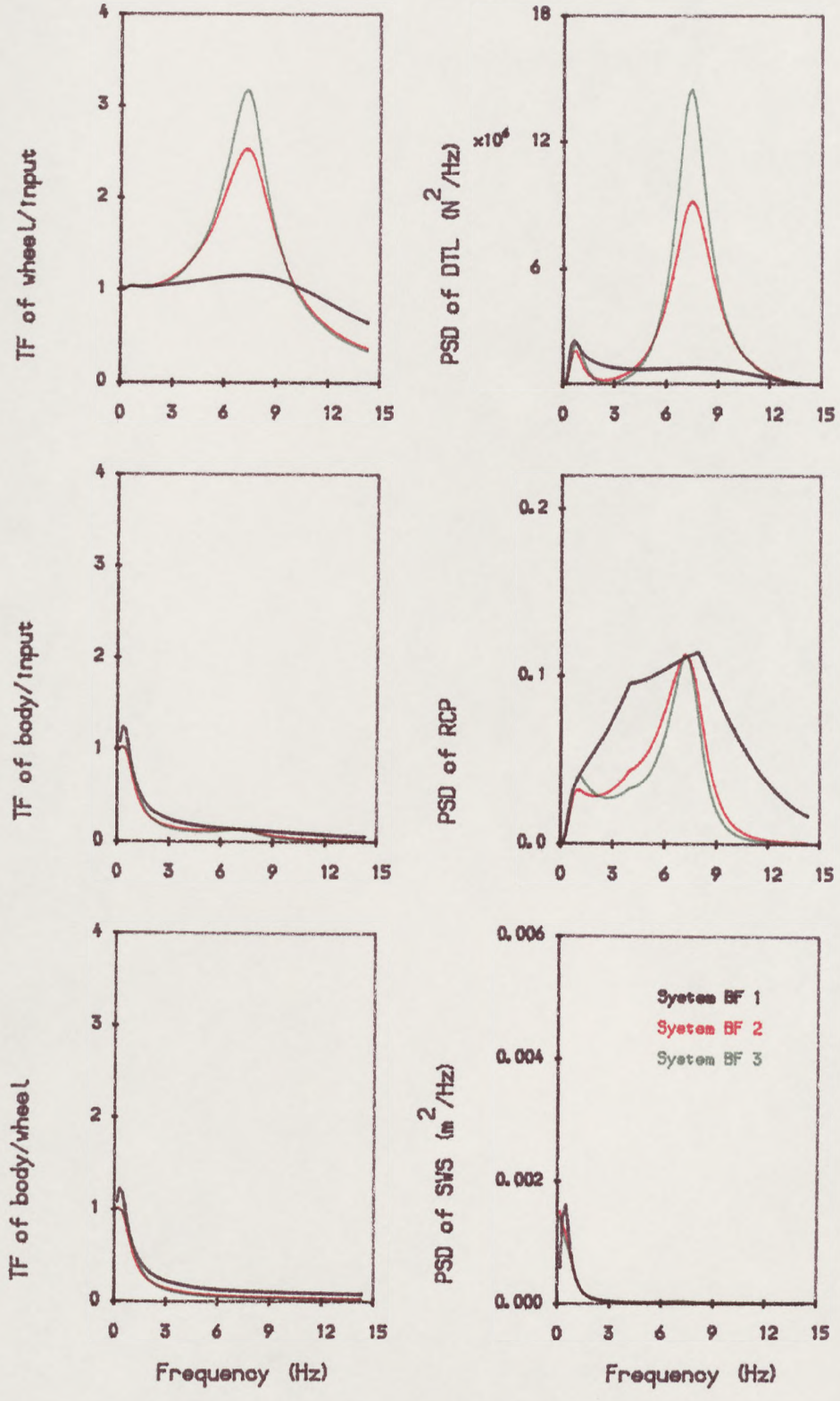

Figure 5.2. The transfer functions and PSDs of the full state feedback fully active systems in group BF.

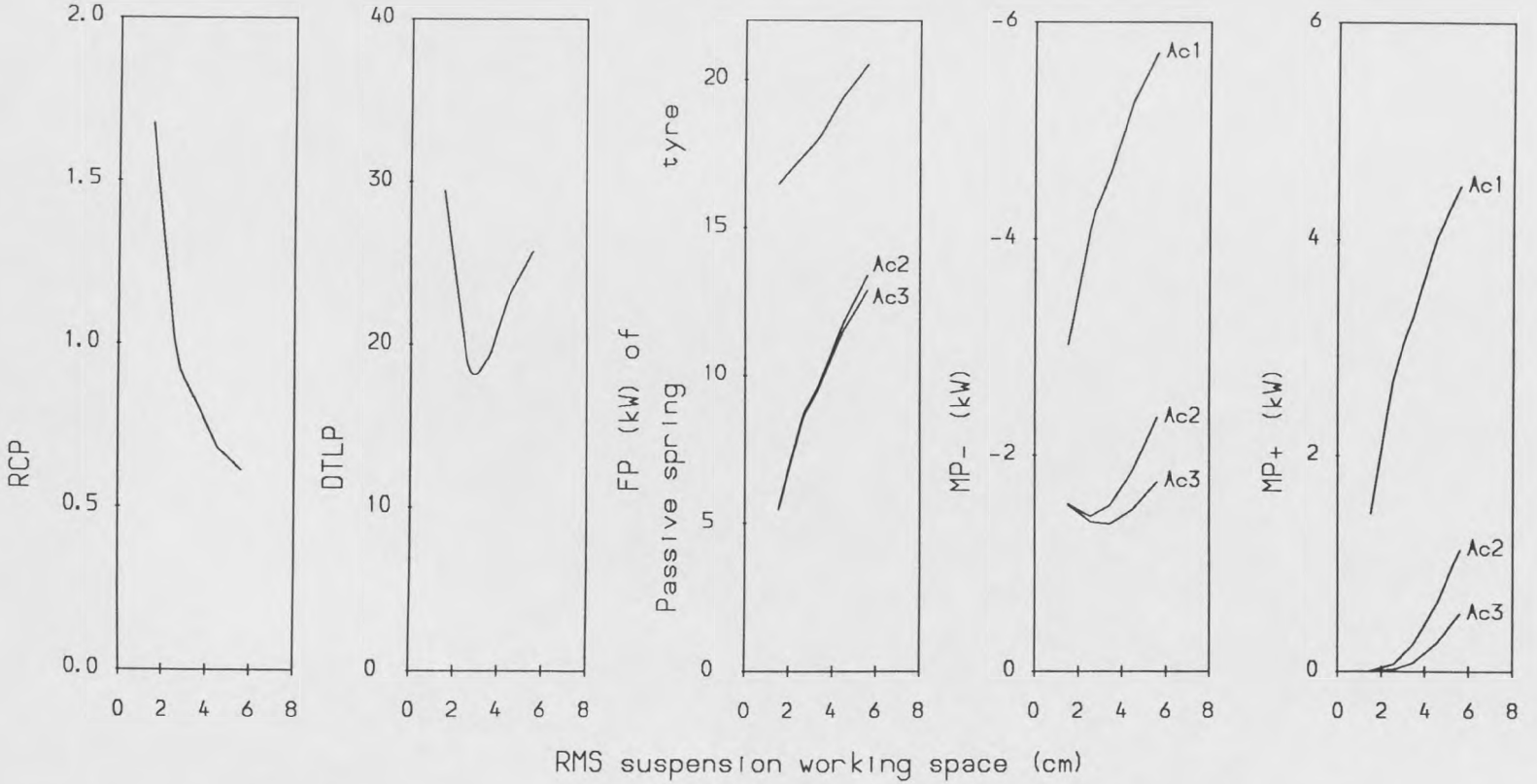

Figure 5.3. Comparison of full state feedback fully active systems: no passive spring Ac1, with additional spring at natural frequency 1.27 Ac2 and 1.01 Ac3, group CF.

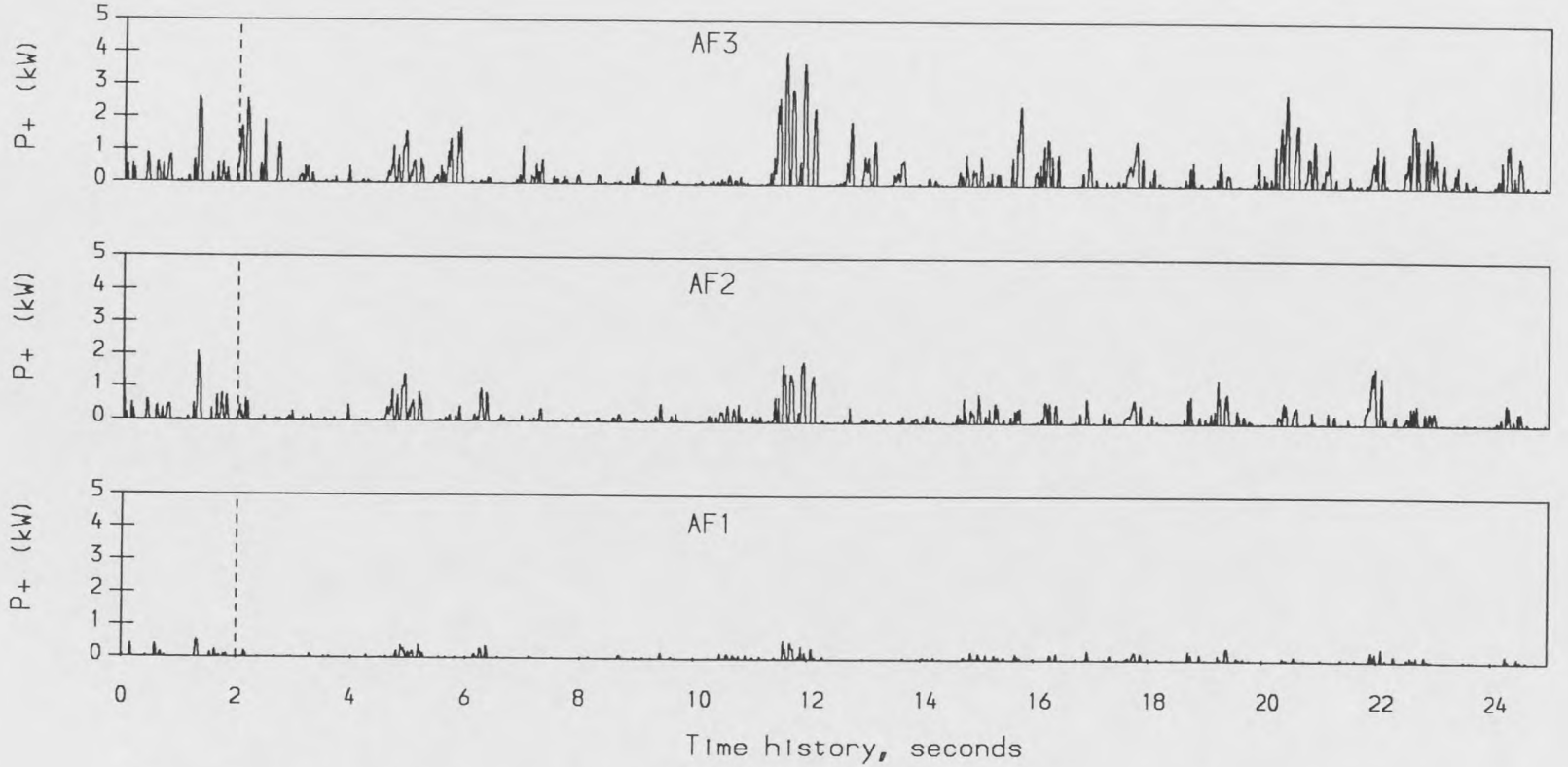

Figure 5.4. Time histories of the power demands of the full state feedback fully active systems: AF1, AF2 and AF3 in group AF.

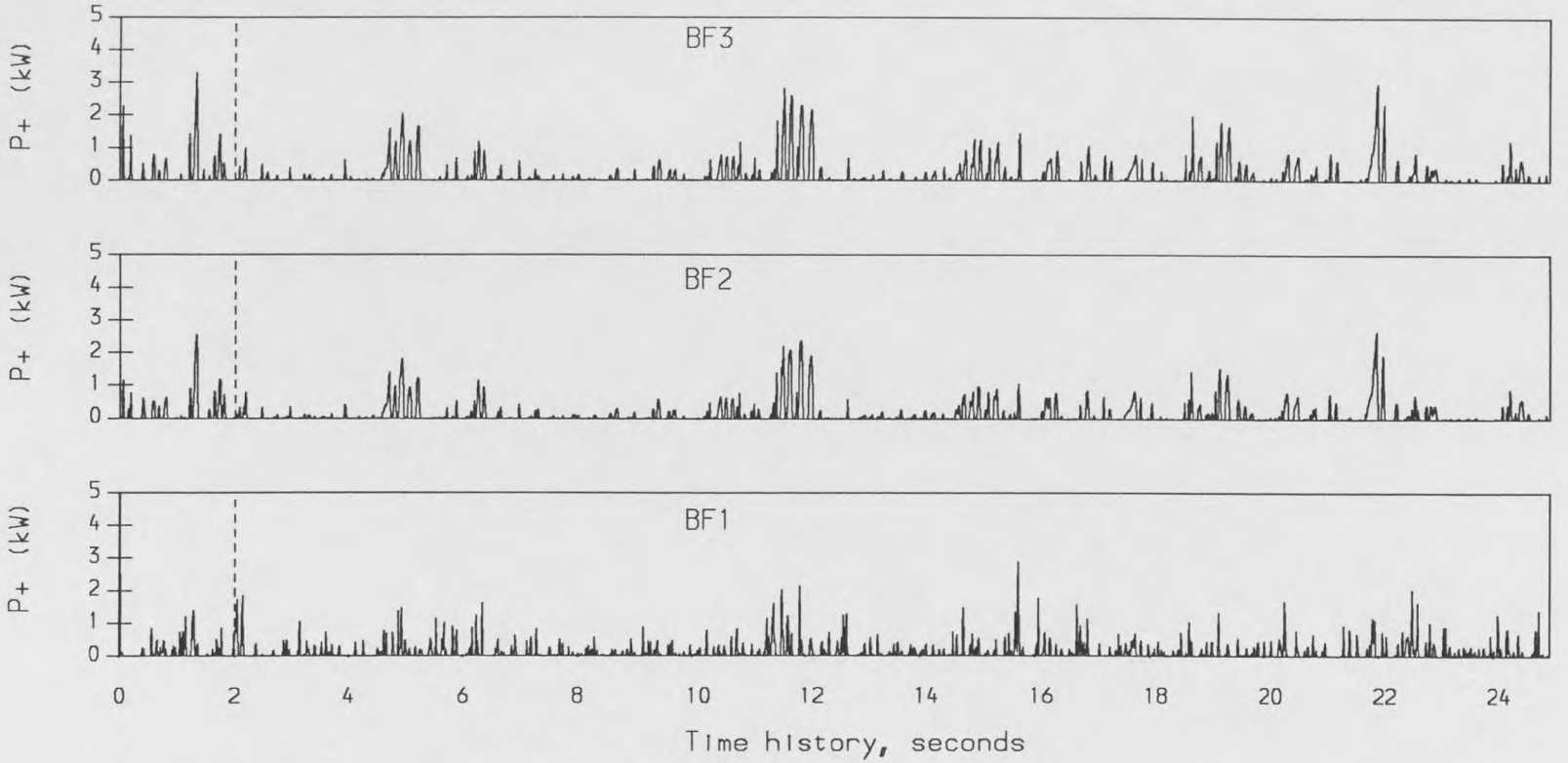

Figure 5.5. Time histories of the power demands of the full state feedback fully active systems: BF1, BF2 and BF3 in group BF.

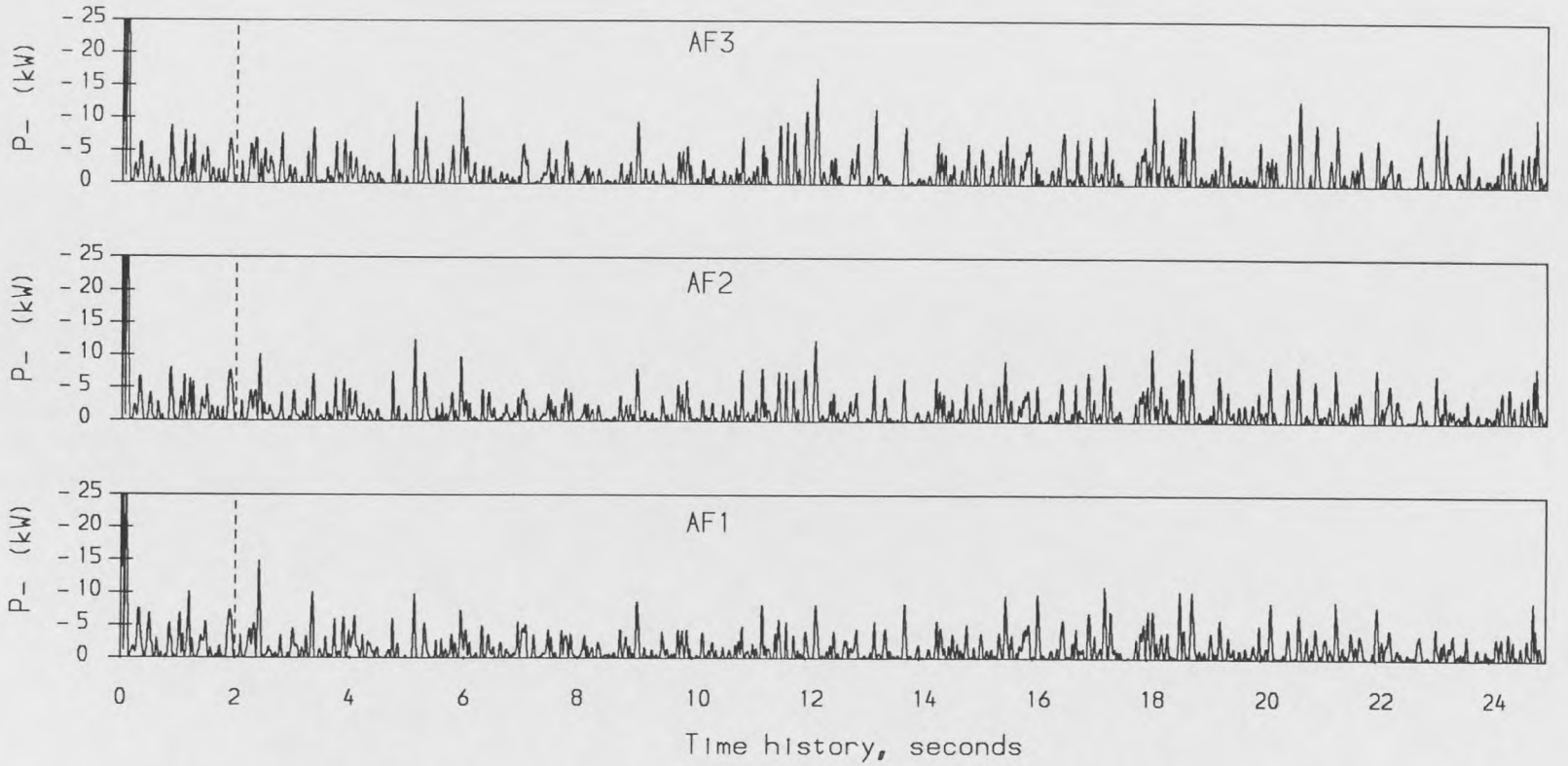

Figure 5.6. Time histories of the power dissipation of the full state feedback fully active systems: AF1, AF2 and AF3 in group AF.

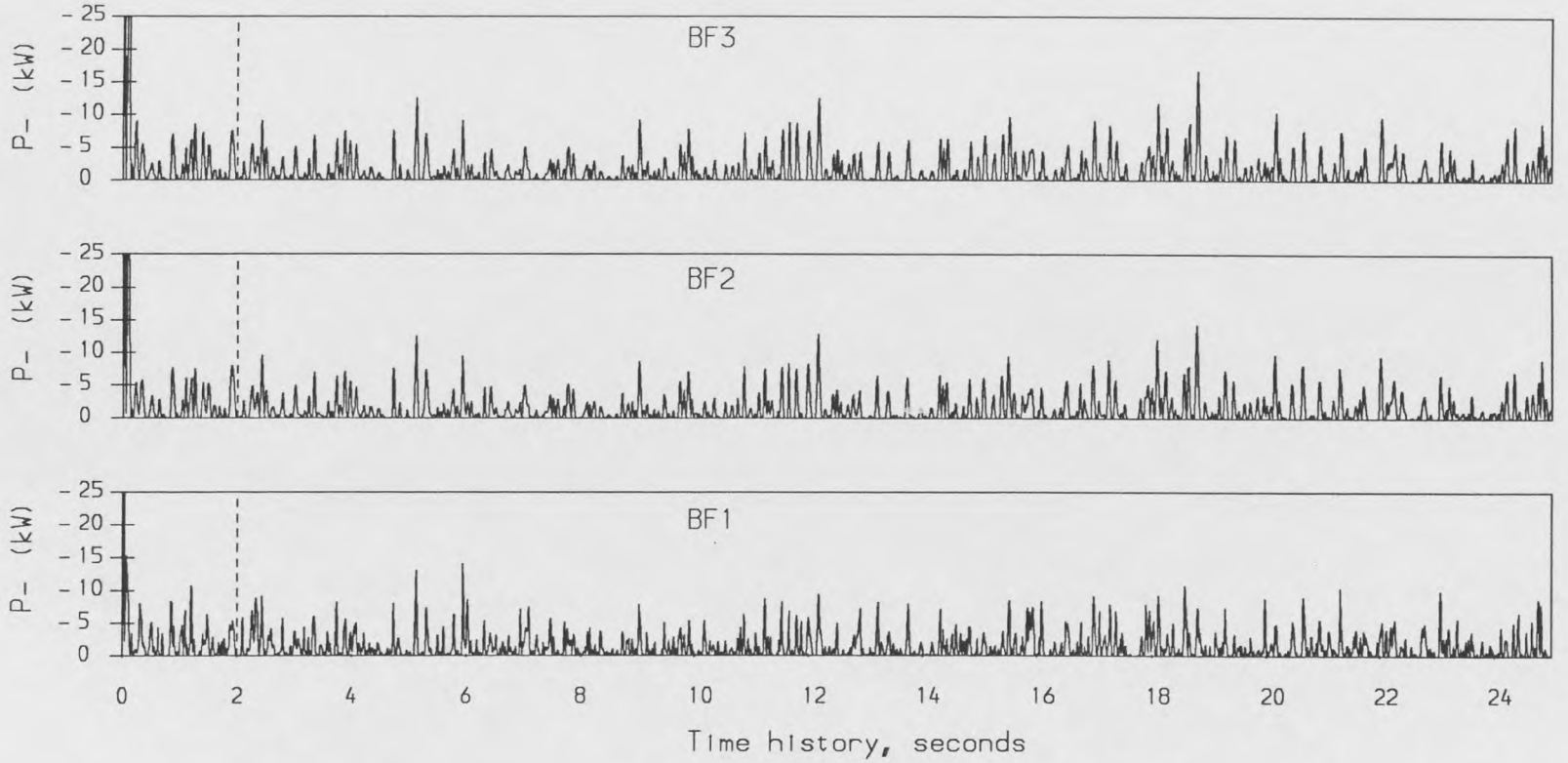

Figure 5.7. Time histories of the power dissipation of the full state feedback fully active systems: BF1, BF2 and BF3 in group BF.

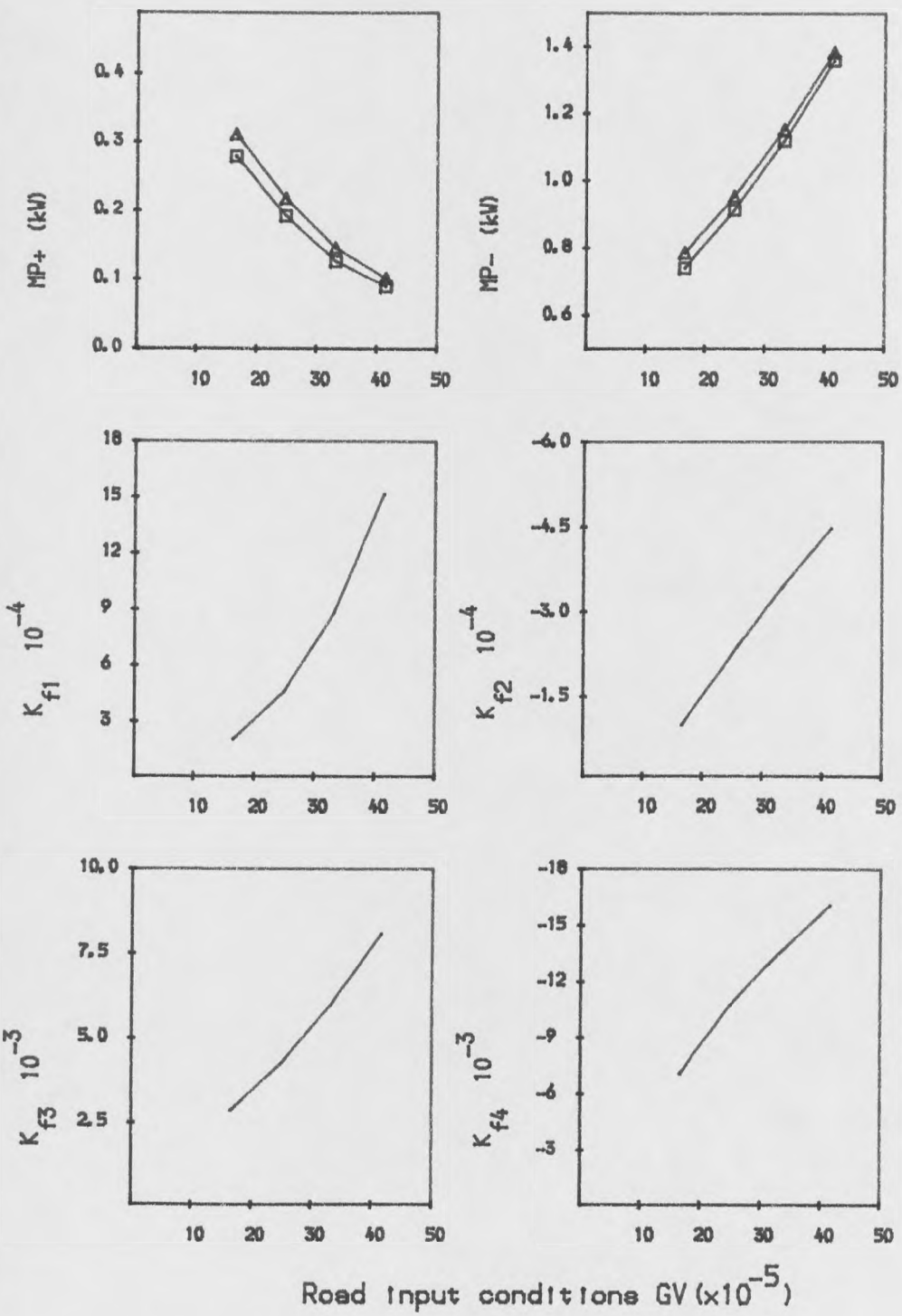

Figure 5.8. The design and power requirements of the full state feedback fully active systems at 3.5 cm RMS working space and 20% DTLP, group DF.

△ △ Forward speed 12 m/s

□ □ Forward speed 17 m/s

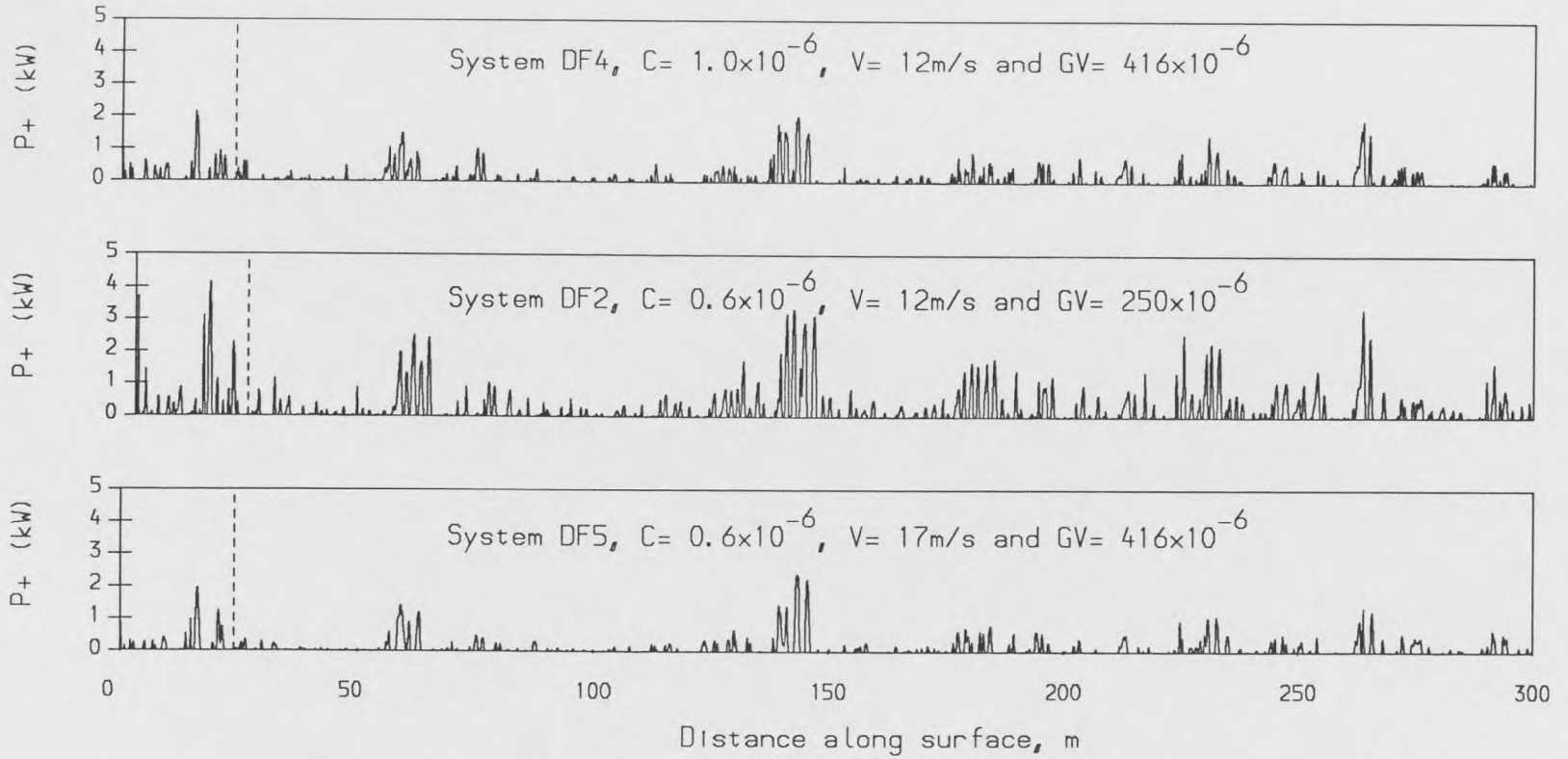

Figure 5.9. Power demands of the full state feedback fully active systems at 3.5 cm RMS working space and 20% DTLP, group DF, for 3 road input conditions.

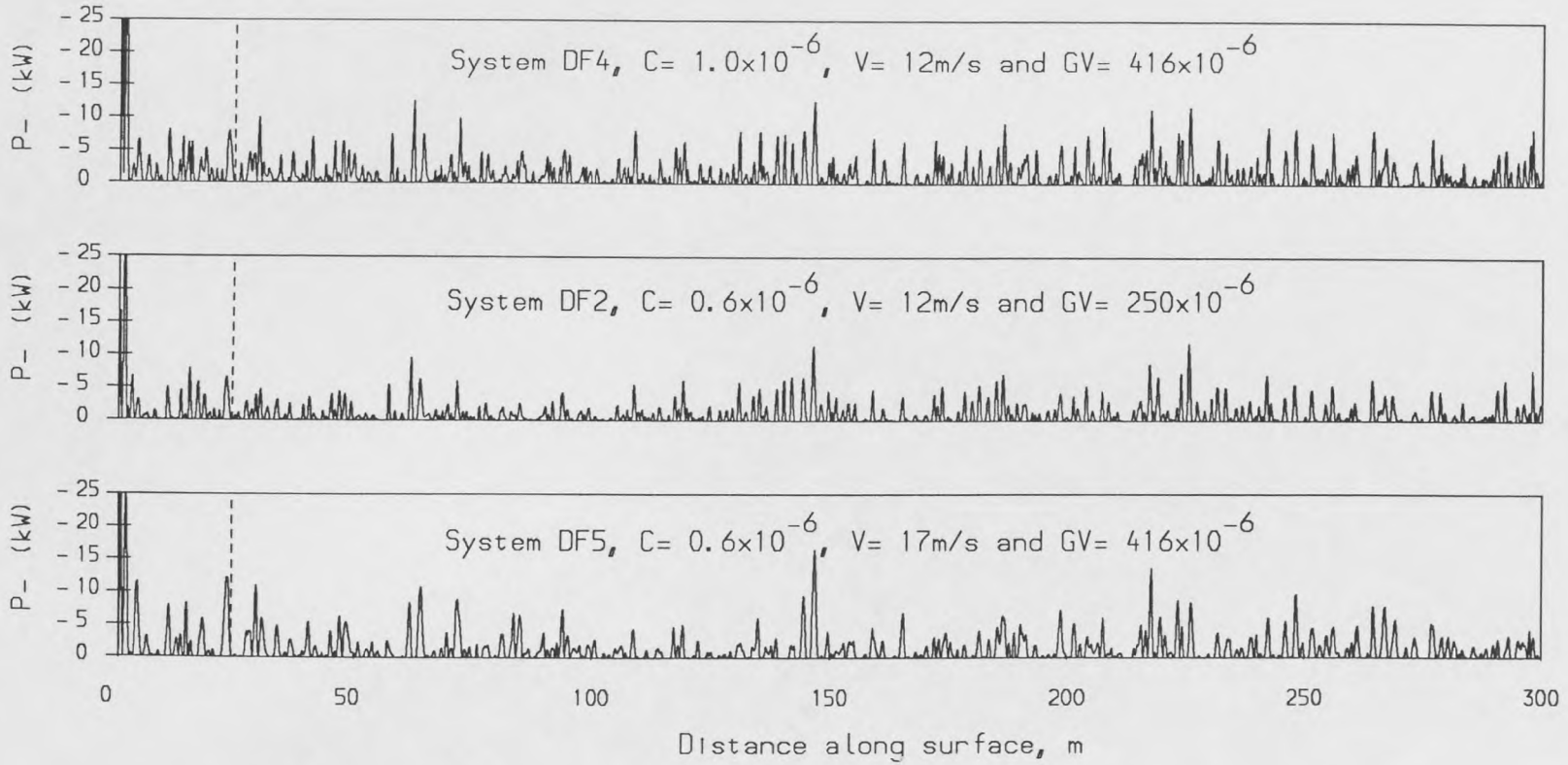

Figure 5.10. Power dissipation of the full state feedback fully active systems at 3.5 cm RMS working space and 20% DTLP, group DF, for 3 road input conditions.

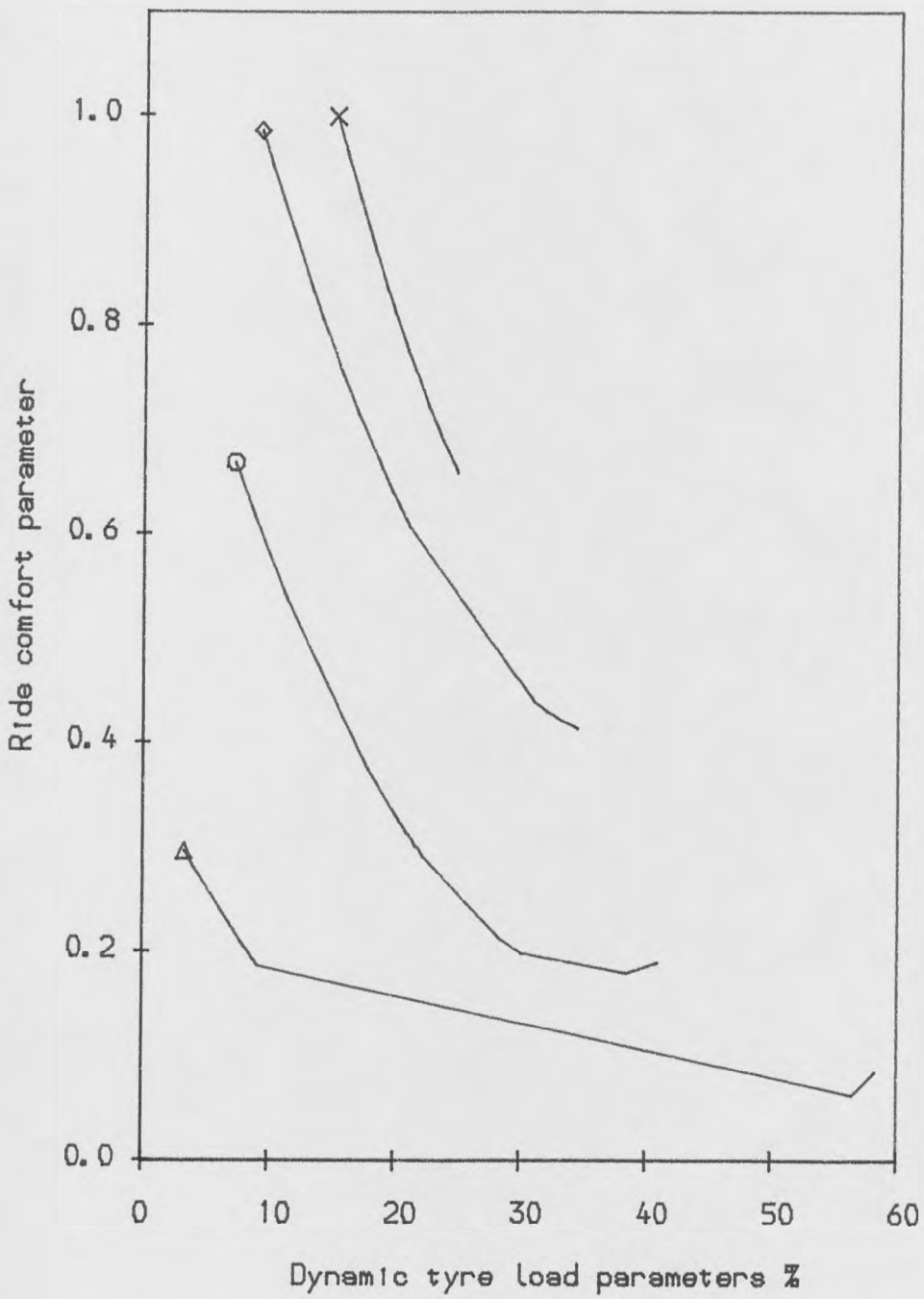

Figure 5.11. Comparison of performance of full state feedback fully active systems at 3.5 cm RMS working space.

△ △ GV= 4.20×10^{-5} o o GV= 16.6×10^{-5}

◇ ◇ GV= 33.3×10^{-5} × × GV= 41.6×10^{-5}

Group	System	weighting factor $r=10^{-8}$ and		RMS Performance of dynamic tyre load% DTLP, ride comfort RCP, working space SWS (mm) and mean power demand MP+ and dissipation MP- (W)				
		q_1	q_2	DTLP	RCP	SWS	MP+	MP-
AL	AL 1	6667	666.7	20.2	1.09	24.6	37	1417
	AL 2	1667	45	20.4	0.82	35.9	151	1430
BL	BL 1	16000	100	15.4	0.98	34.6	154	1412
	BL 2	1000	23.3	22.5	0.74	35.4	167	1448
	BL 3	500	40	24.7	0.66	35.4	183	1451
CL	CL 1	400	4000	29.3	1.68	15.3	4	1557
	CL 2	4000	500	20.6	1.03	24.2	28	1438
	CL 3	3333	66.7	18.7	0.90	34.1	113	1426
	CL 4	750	5	23.3	0.68	44.6	355	1635
	CL 5	533	0.2	25.1	0.62	55.2	764	2031
DL	DL 1	166	0.3	20.9	0.30	36.3	406	873
	DL 2	480	1.1	20.1	0.48	36.6	274	1007
	DL 3	800	5	20.9	0.62	36.9	224	1224
	DL 4	1857	12.8	20.8	0.81	35.6	142	1433
	DL 5	1857	12.8	20.8	0.81	35.6	119	1396

Table 5.2 Comparison of performances and power requirements of the limited state feedback fully active systems.

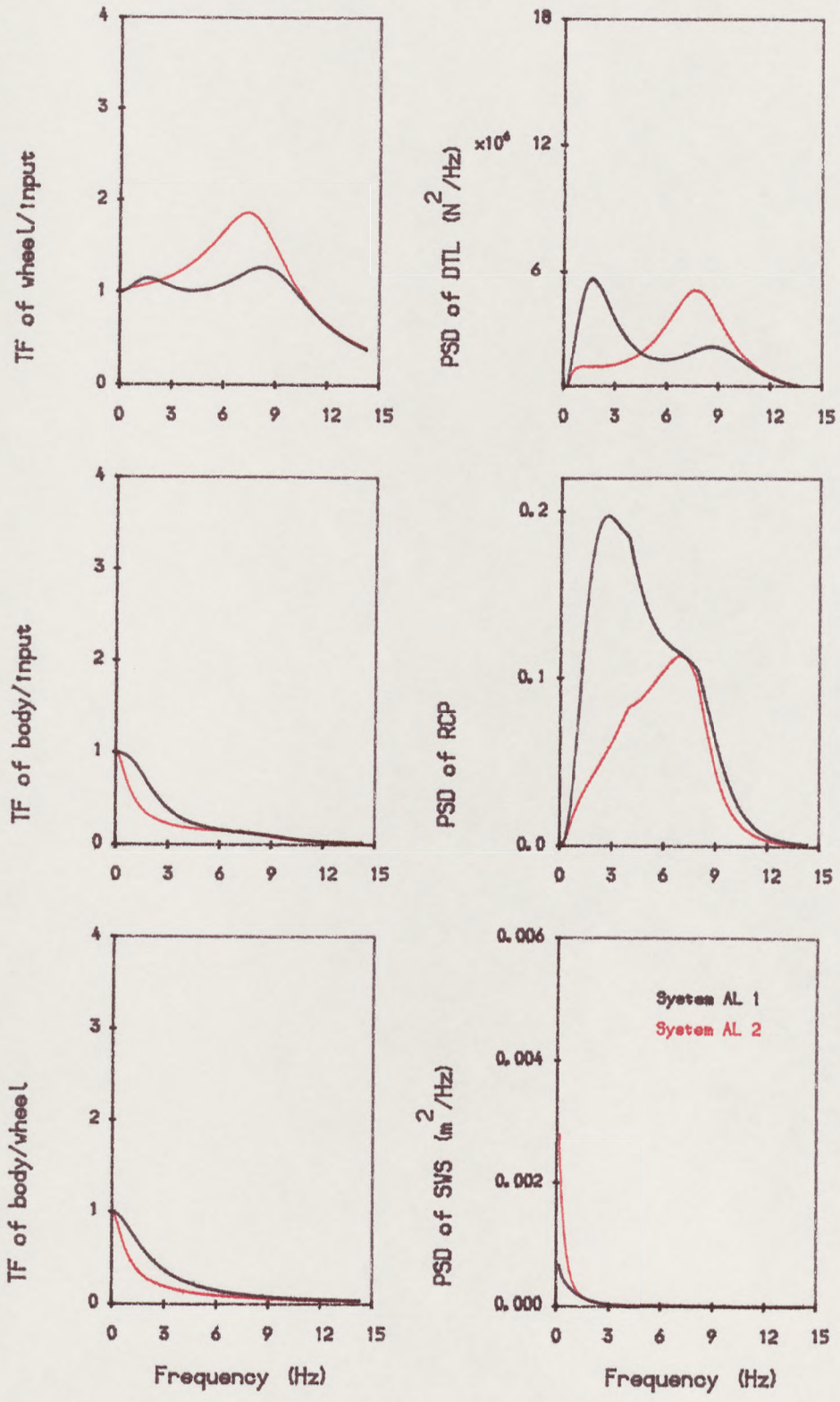

Figure 5.12. The transfer functions and PSDs of the limited state feedback fully active systems in group AL.

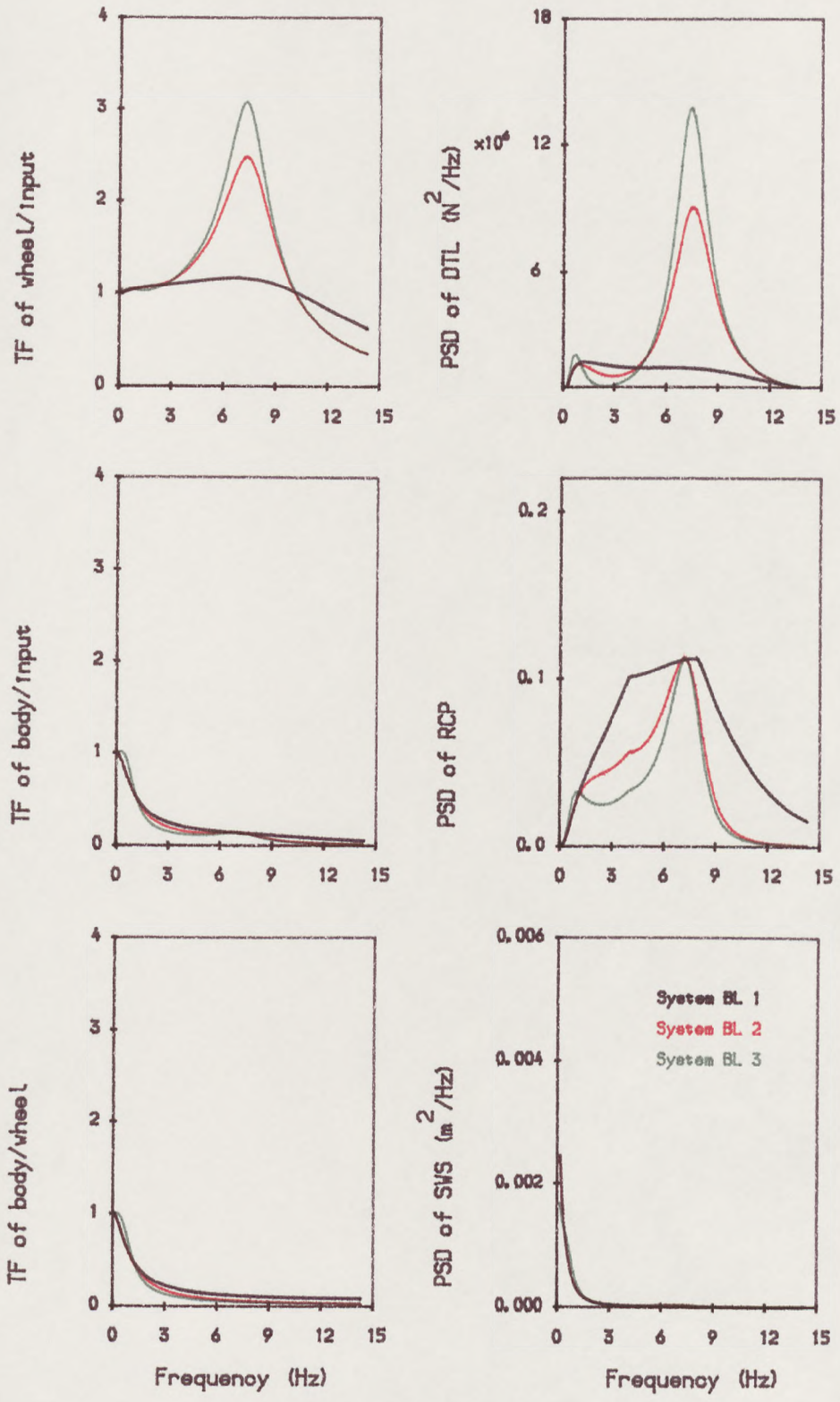

Figure 5.13. The transfer functions and PSDs of the limited state feedback fully active systems in group BL.

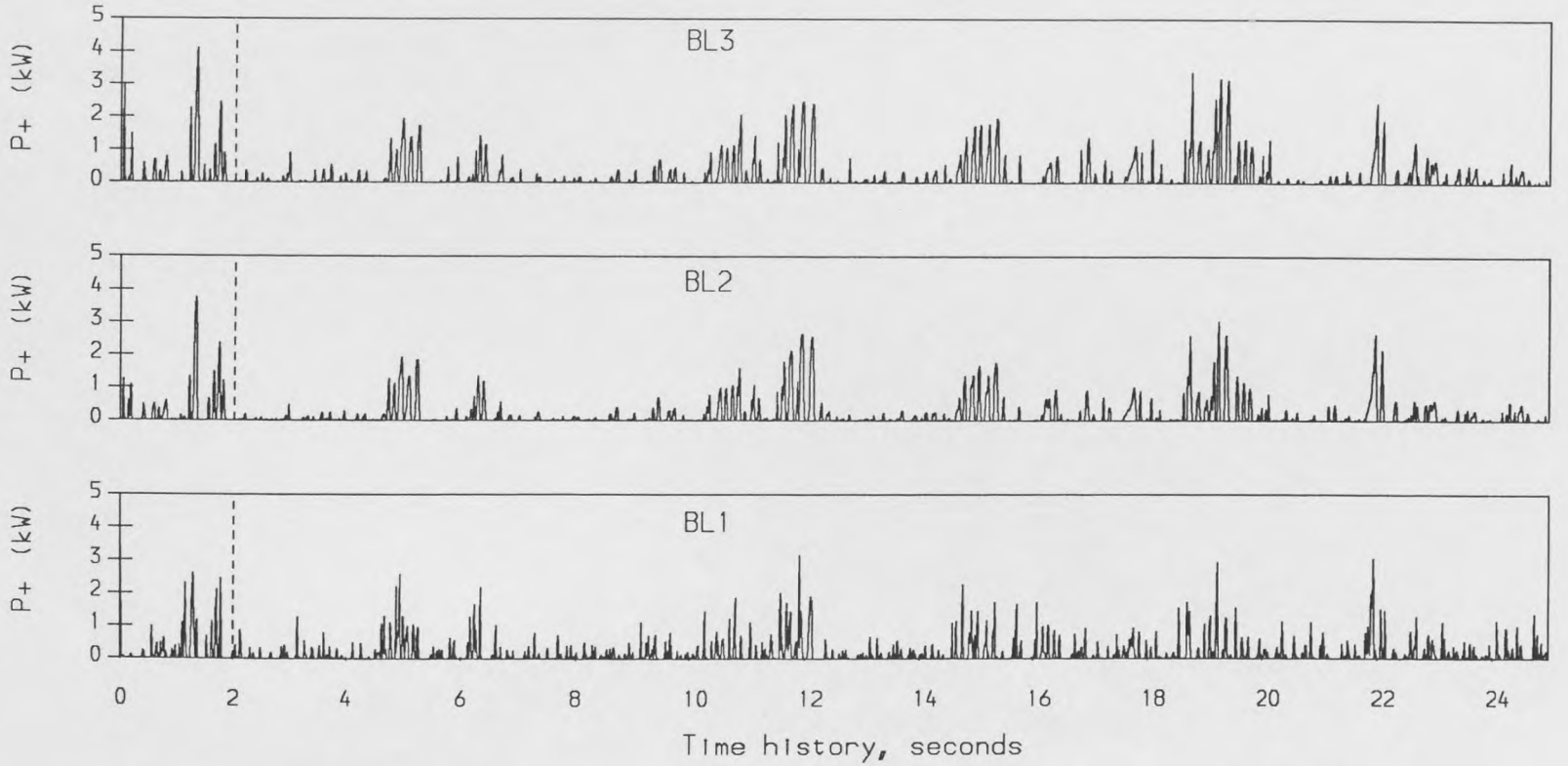

Figure 5.14. Time histories of the power demands of the limited state feedback fully active systems: BL1, BL2 and BL3 in group BL.

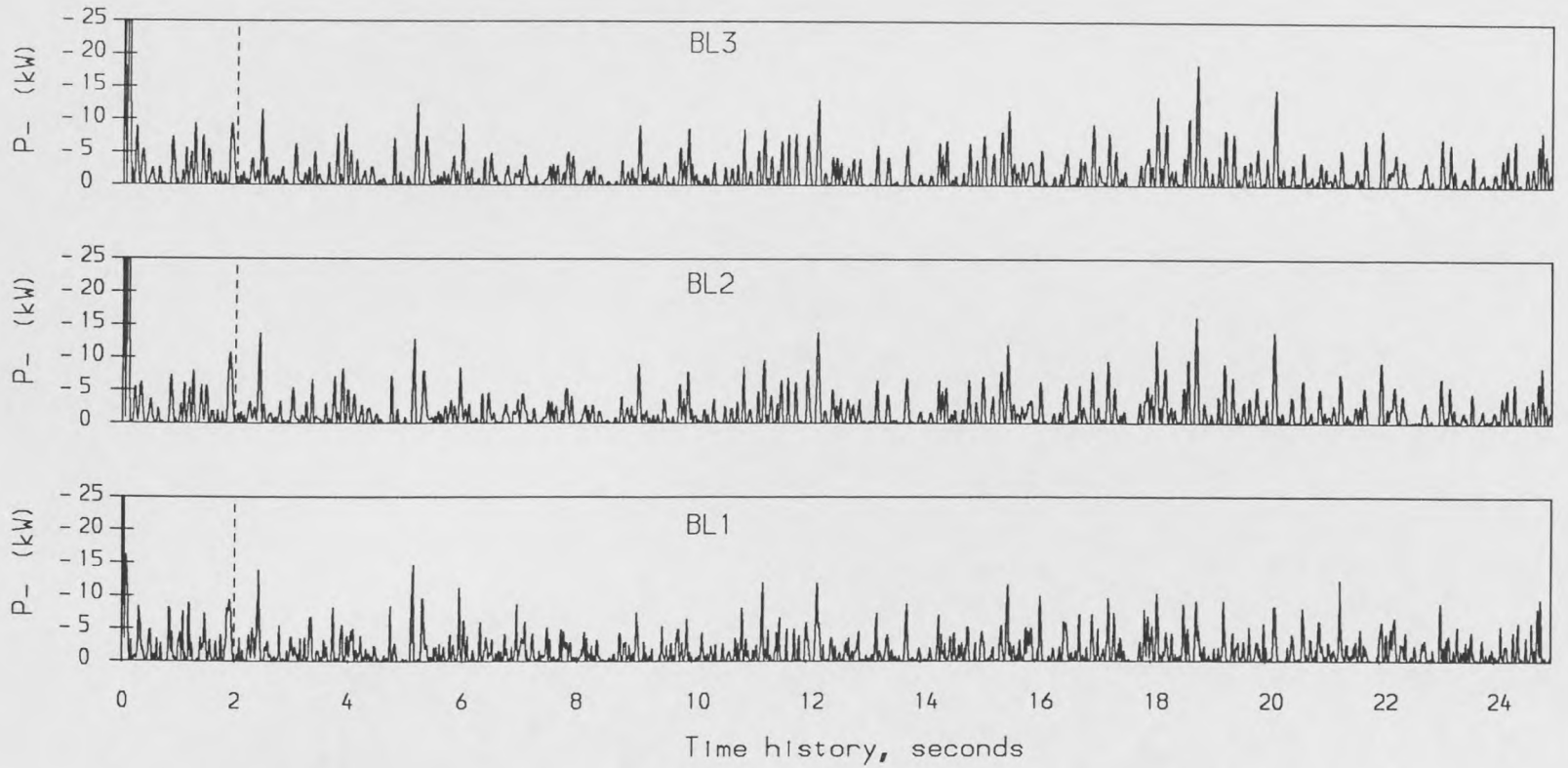

Figure 5.15. Time histories of the power dissipation of the limited state feedback fully active systems: BL1, BL2 and BL3 in group BL.

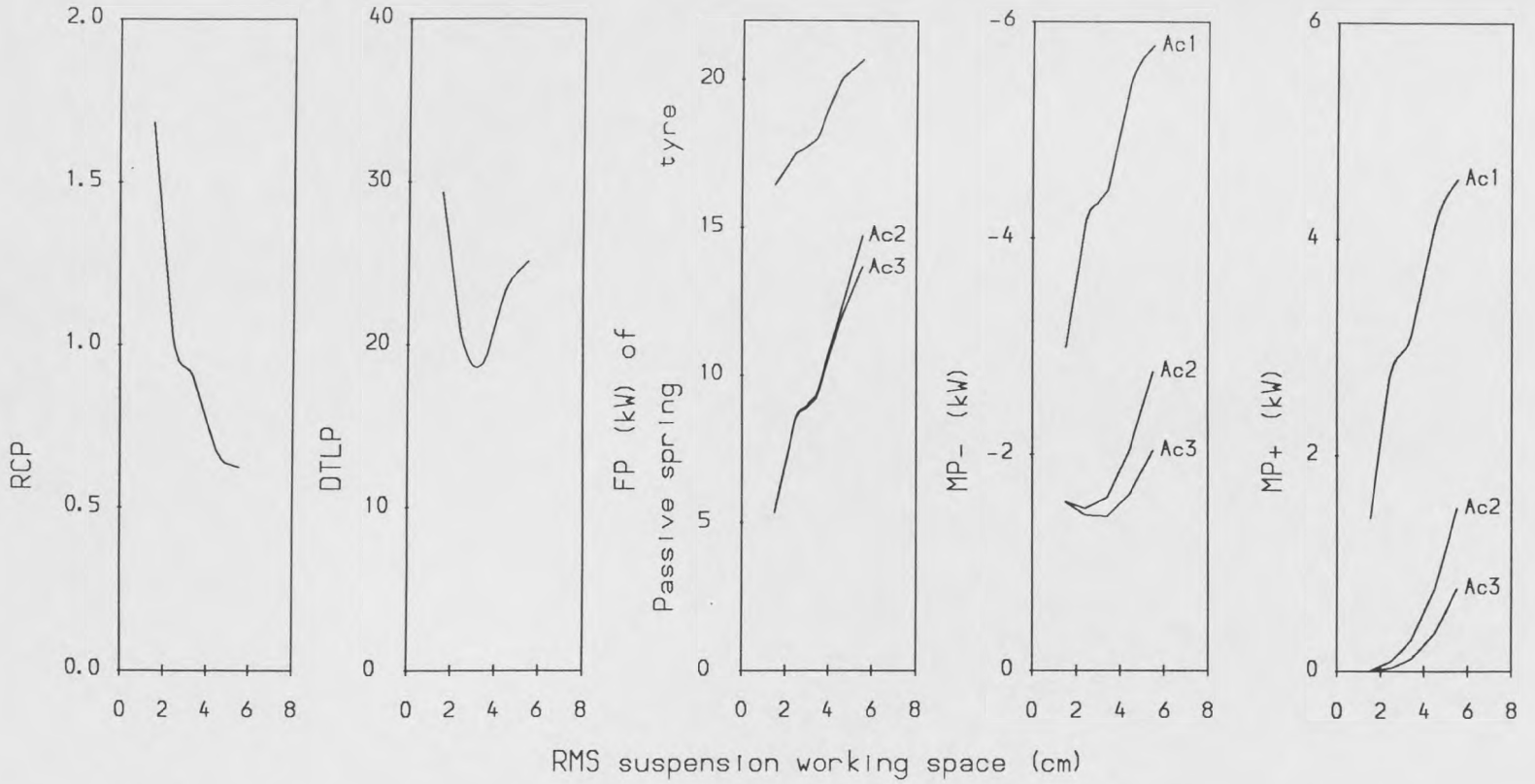

Figure 5.16. Comparison of limited state feedback fully active systems: no passive spring Ac1, with additional spring at natural frequency 1.27 Ac2 and 1.01 Ac3, group CL.

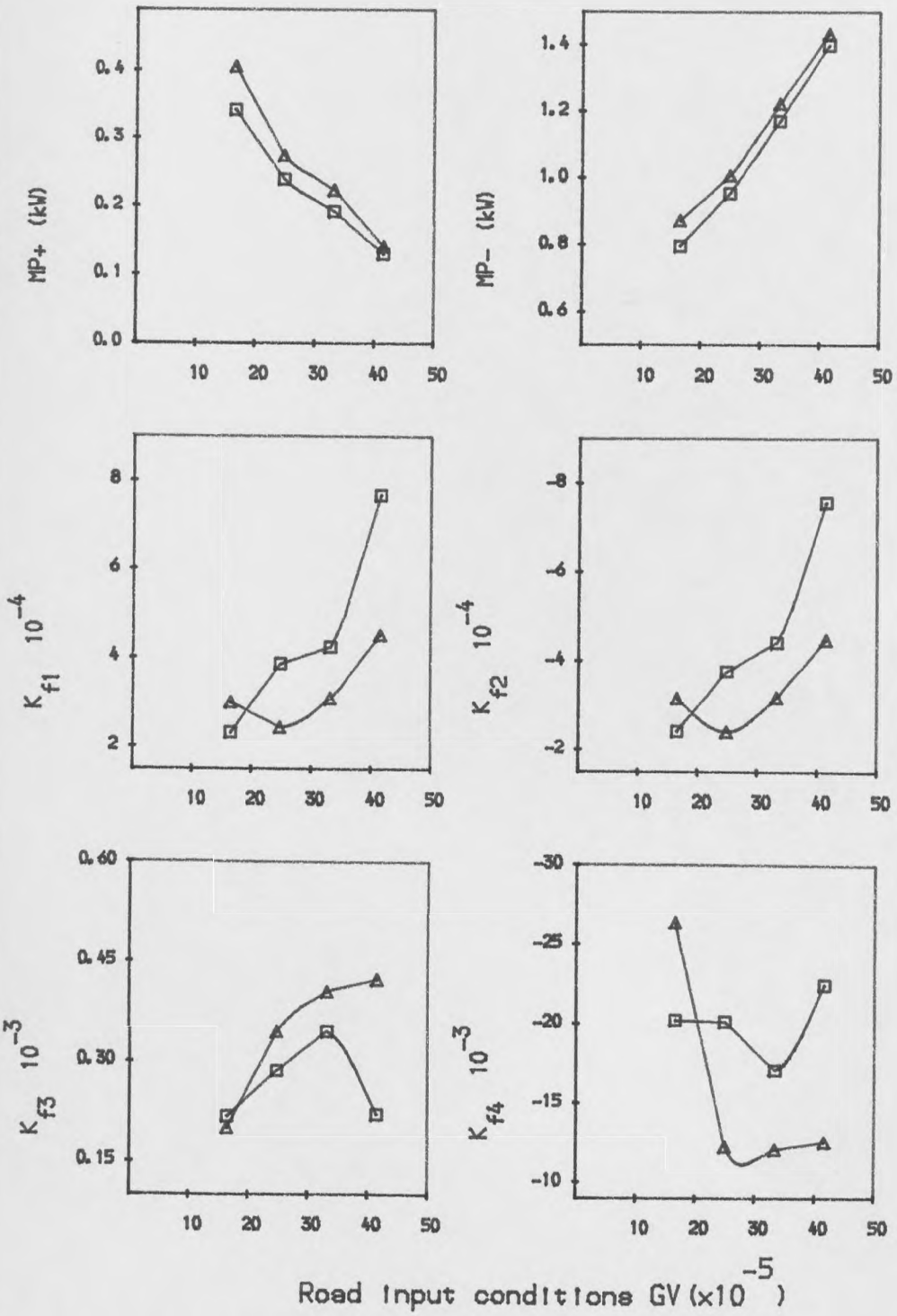

Figure 5.17. The design and power requirements of the limited state feedback fully active systems at 3.5 cm RMS working space and 20% DTLP, group DL.

△ △ Forward speed 12 m/s

□ □ Forward speed 17 m/s

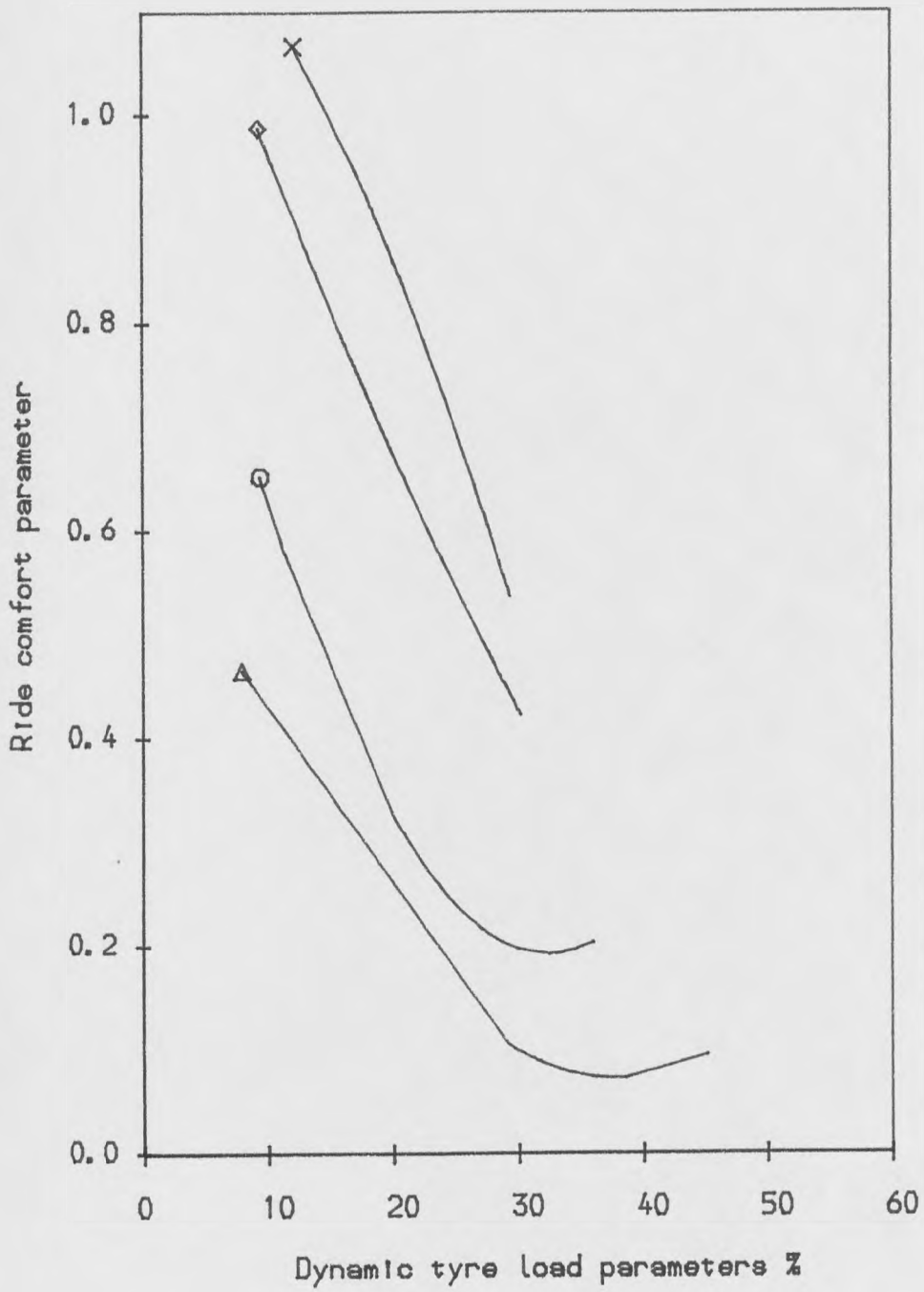

Figure 5.18. Comparison of performance of limited state feedback fully active systems at 3.5 cm RMS working space.

△ △ CV= 4.20×10^{-5} o o CV= 16.6×10^{-5}

◇ ◇ CV= 33.3×10^{-5} × × CV= 41.6×10^{-5}

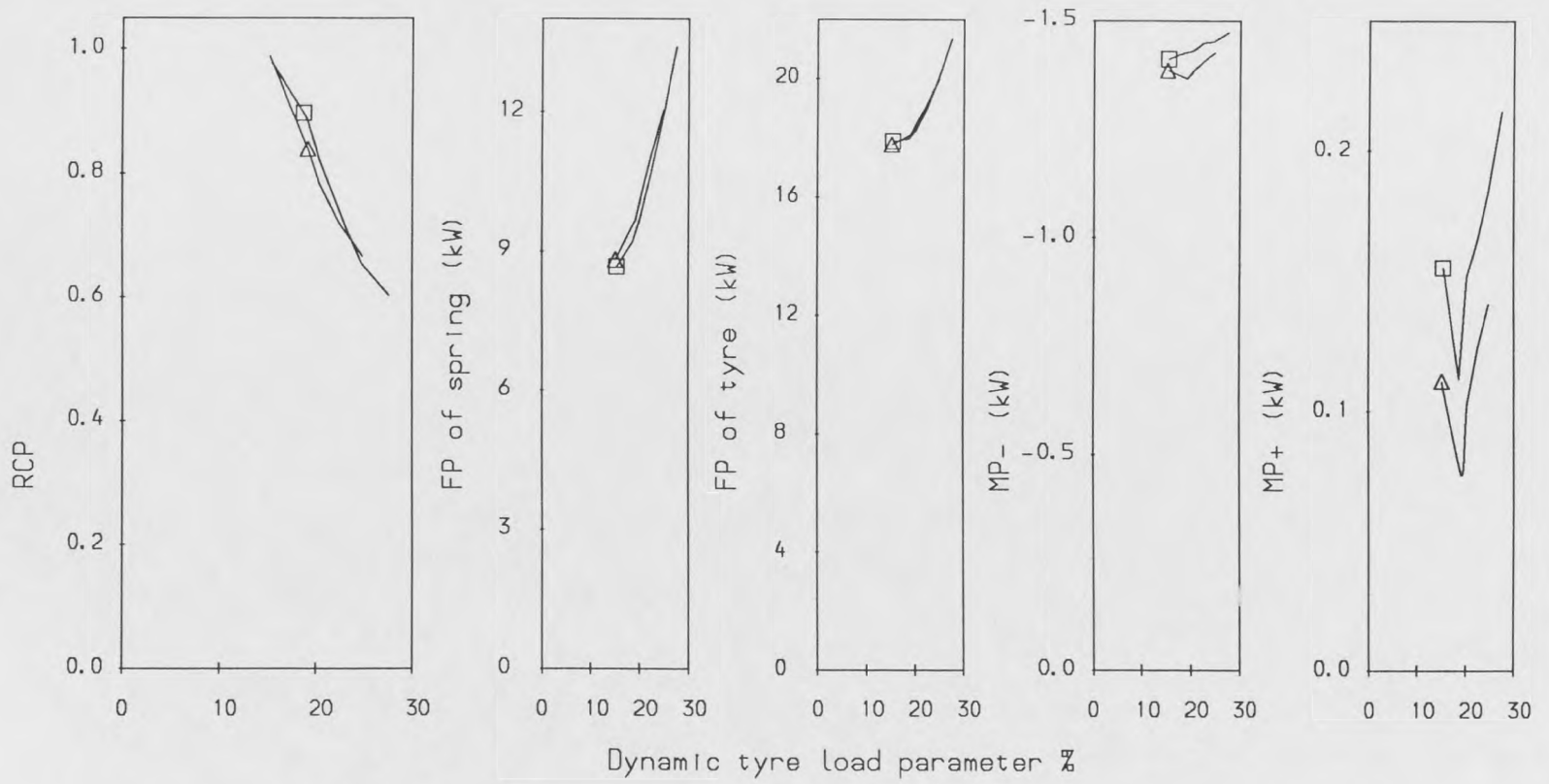

Figure 5.19. Comparison of performance and power requirements of full(Δ Δ) and limited(□ □) state feedback fully active systems at 3.5 cm working space.

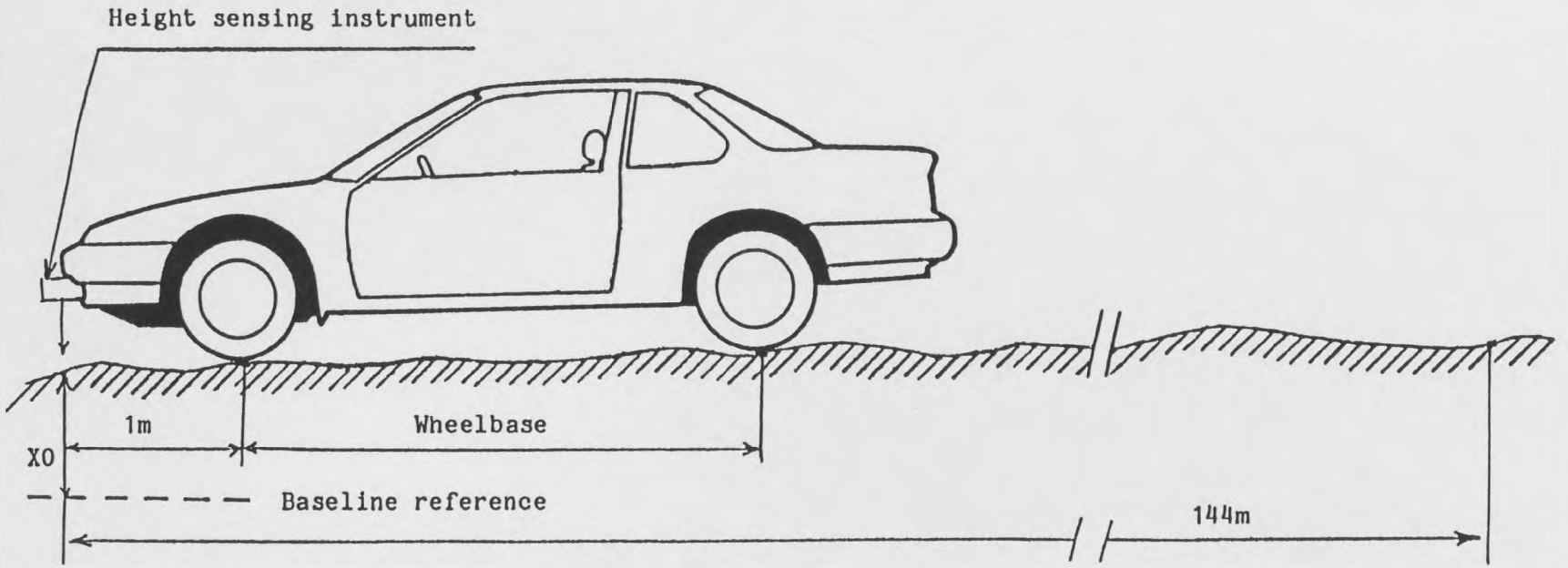

Figure 5.20 Active non-linear control system.

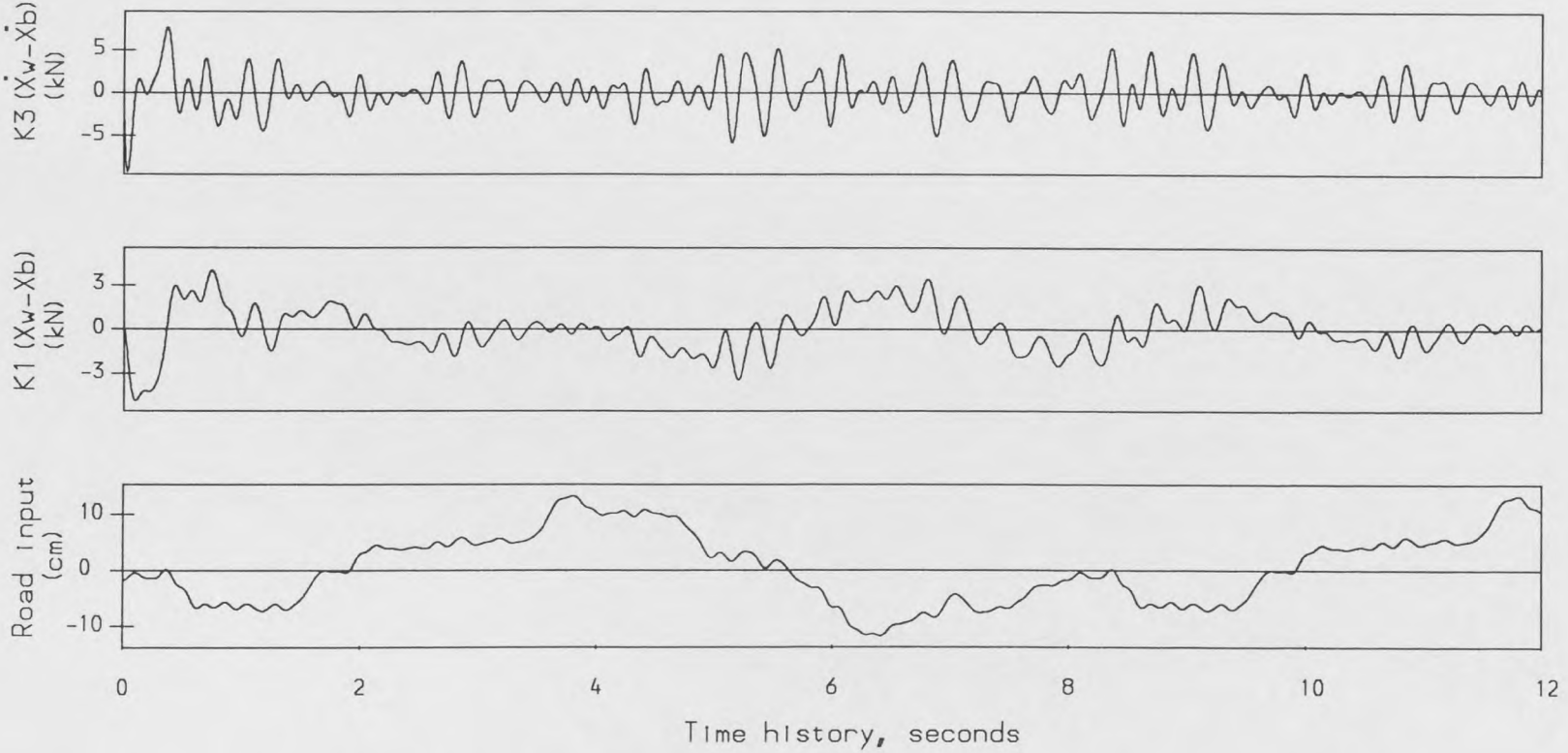

Figure 5.21. Time histories of the feedback coefficients of the active non-linear control system and the road input profile.

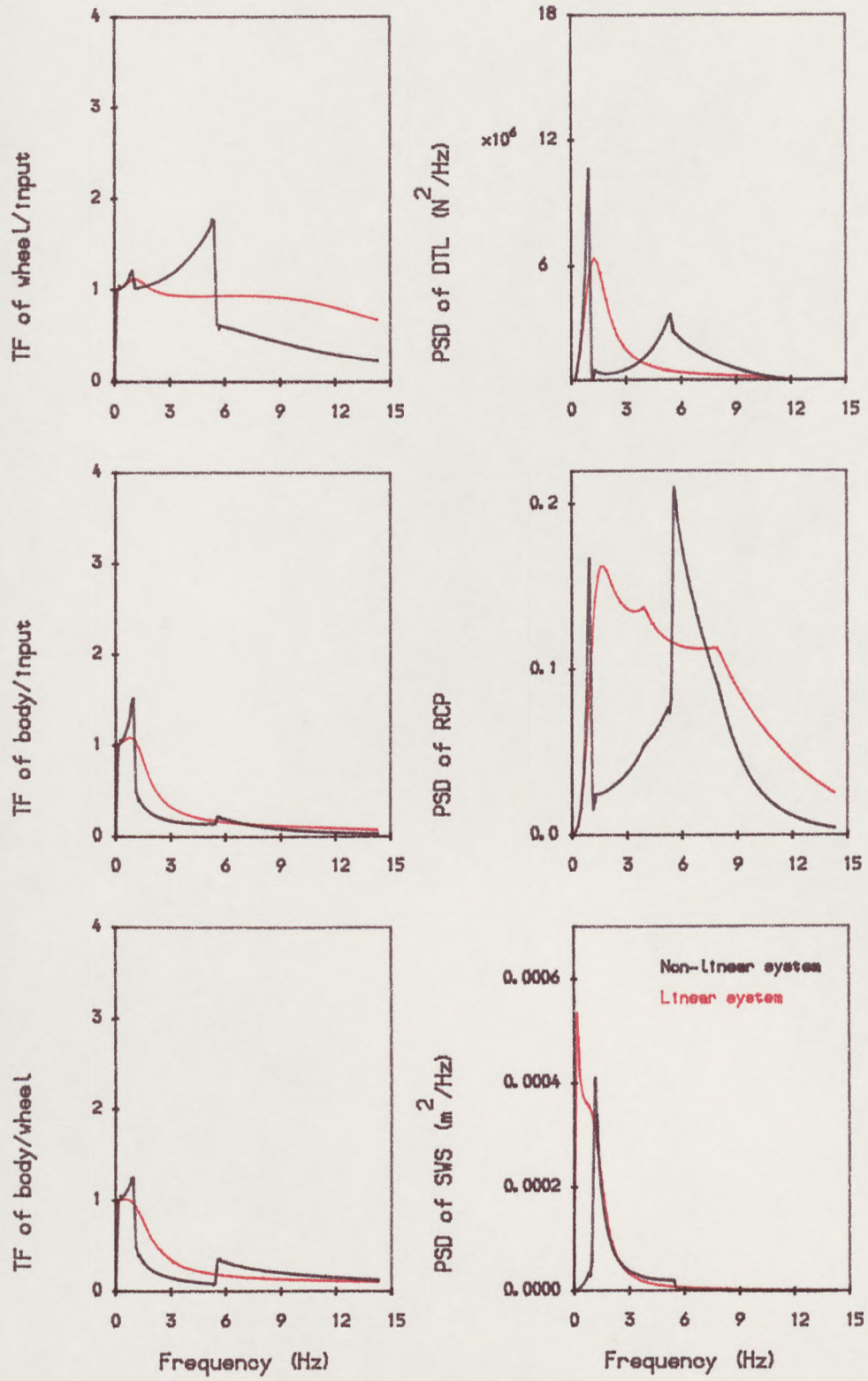

Figure 5.22. The transfer functions and PSDs of the active linear and non-linear control systems.

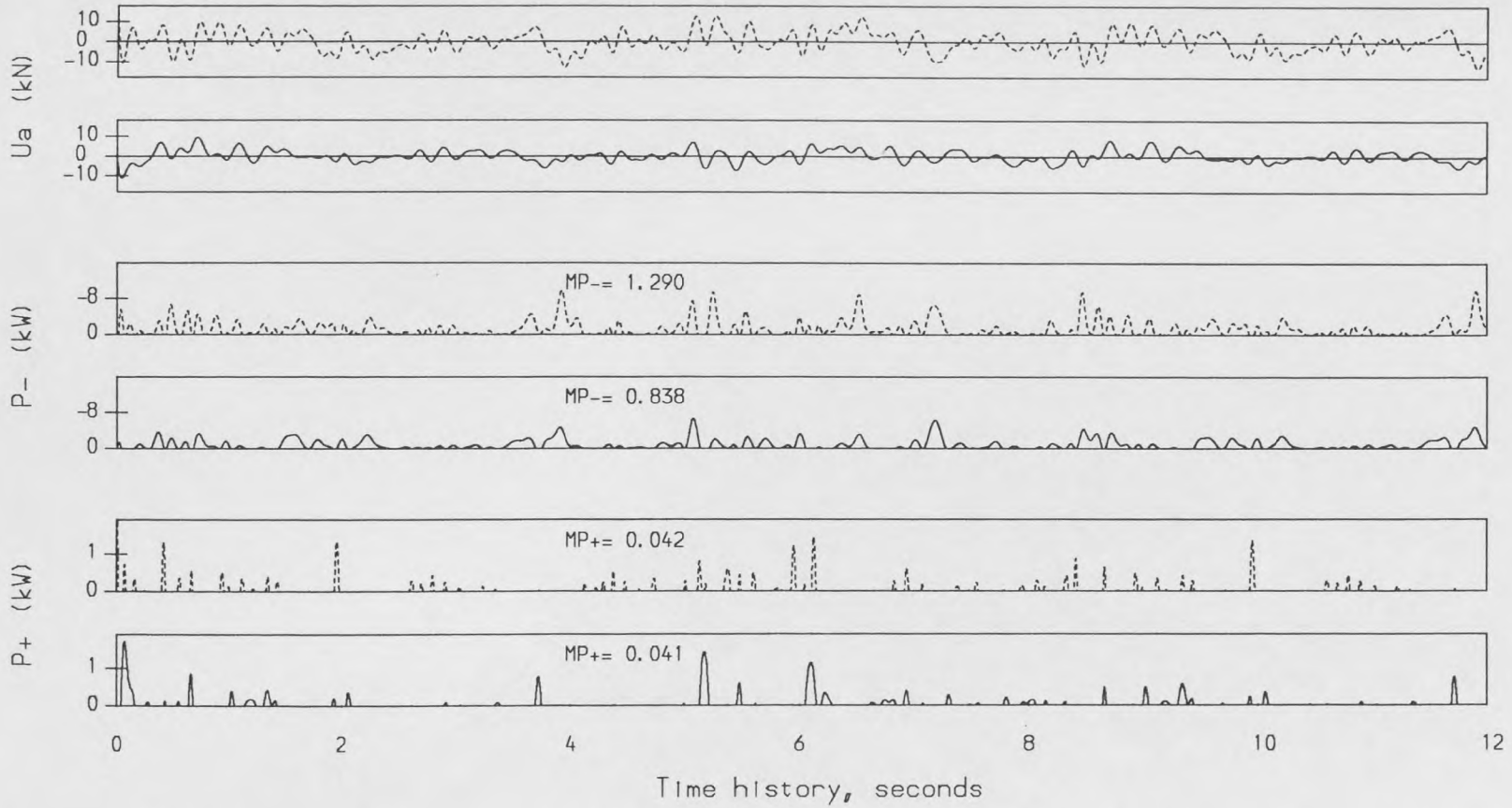

Figure 5.23. Time histories of the control forces and the power requirements of the active linear (broken line) and non-linear (continuous line) systems.

CHAPTER 6

SEMI-ACTIVE SYSTEMS

6.1 Introduction

The semi-active primary suspension consists of a conventional passive spring, to support the static weight of the vehicle body, in parallel with a device called an active damper. The term, semi-active, refers to a control system which is only capable of controlling the dissipation of energy from a suspension system. In this sense, the semi-active systems are similar to those referred to earlier as switchable and variable damper systems. However, the control strategy of the active damper differs from those of the switchable and variable damper systems by the following. The active damper generates a dissipative force according to some control policy based on the control law of the fully active system if energy dissipation of the system is required, otherwise when power is demanded it switches off. The behaviour of such systems is non-linear because of the switching process of the semi-active damper and the time domain must be used to obtain the performances, the fluctuating powers and the power losses of the various systems. A first order time lag is also included in the semi-active system to model the switching characteristic between the states of the damper since this cannot occur instantaneously in practice.

In this chapter, two different types of control law are used in studying semi-active systems. The first type is based on the active linear control law as discussed previously for either full or limited state feedback systems. The second type is based on the active non-linear control law which is only used in limited state feedback form in this study. Therefore, this chapter is divided into three parts. The first part presents the behaviour of the semi-active linear control system. The second part presents also the behaviour of the semi-active non-linear control system. A comparison between both semi-active linear and non-linear control systems is also made in terms of the performance and power losses. In the last part, the con-

clusions of the semi-active systems are summarised.

6.2 Semi-active linear control systems

Basically, the fully active linear control system is modified so that the actuator is only capable of dissipating power rather than supplying it as well. In practical terms, the actuator then becomes a continuously variable damper, i.e. an active damper, which is theoretically capable of tracking a force demand signal independently of instantaneous velocity across it. The behaviour of the full and limited state feedback forms of the semi-active systems will be discussed in terms of their performances and power requirements. The results for the semi-active systems are generated for the following conditions. Firstly, the road input and the basic elements of the model are the same as described in 2-7 and 3-4. Secondly, a conventional spring of 100 kN/m stiffness is mounted in parallel with the active damper between the body and wheel of the vehicle. The suspension force is equal to the sum of the spring and damper force when energy dissipation is required, otherwise the suspension force is equal to the spring force only with the damper switching to its off condition. Thirdly, the percentage time spent dissipating energy, TDE%, of the semi-active system is calculated as a percentage of the total time. It is a measure of the extent to which the performance of the semi-active systems is similar to the performance of the corresponding fully active systems. It also indicates that the percentage achievements of the corresponding fully active systems improve the performance only by "intelligent" dissipation of energy rather than putting power in. Fourthly, the switching dynamics used for the active damper are assumed to be represented by a first order lag with a time constant of 0.011 second. Finally, other than the limitation due to the switching delay, the control system and actuator are assumed to have a flat frequency characteristic up to 15 Hz, which is the upper limit of the calculation range.

6.2.1 Full state feedback systems.

The control law of the full state feedback semi-active system is the same as in equation 5-1 and the suspension force can be reformed as follows,

$$F(t) = U_d(t) + K_s\,(X_w(t) - X_b(t)) \qquad 6\text{-}1$$

where $U_d(t)$ is the desired active damper force which can be obtained by using equation 5-3 as;

$$U_d(t) = \textit{equation } 5\text{-}3, \qquad \text{for } U_a(t) \times (\dot{X}_b(t) - \dot{X}_w(t)) < 0 \qquad 6\text{-}2$$

$$U_d(t) = 0 \qquad \text{for } U_a(t) \times (\dot{X}_b(t) - \dot{X}_w(t)) > 0 \qquad 6\text{-}3$$

By inserting equation 6-1 into equations 3-2 and 3-3, the equations of motion of the semi-active system can be obtained.

Table 6.1 gives the root mean square values of the performance criteria and mean values of the power dissipation of five groups of the full state feedback semi-active systems. The semi-active systems in groups ASF, BSF, CSF and DSF are designed to correspond to those of the fully active systems in Table 5.1 in order to compare directly the fully active and semi-active systems. The percentage changes in all the performance categories of the fully active systems compared with the corresponding semi-active systems are also given in Table 6.1. The fully active system gives an improvement in a performance category (i.e. a reduction in the RMS value) over the corresponding semi-active system if the sign of the percentage change in the category is positive. Otherwise, a negative sign indicates that the semi-active system gives an improvement over the corresponding fully active system.

Figures 6.1 and 6.2 show the PSD performances of the systems in groups ASF and BSF. The power spectral densities of the semi-active system can be converted

from the time domain by using the direct Fourier transform DFT process. The mean values of the power dissipation are also plotted versus the RMS working space of the systems. The results indicate the following features. Firstly, the semi-active systems result in the same conflicts between the performance categories as the active systems. Secondly, the RMS working space, dynamic tyre load and mean power dissipation of semi-active systems are all in general improved compared with the corresponding active systems. Thirdly however, these improvement are achieved at the expense of an increase in the RMS ride comfort of semi-active systems compared with the corresponding active systems, except for the BSF1 system which is designed to give a very low value of the dynamic tyre load.

The effect of the spring stiffness on the performances is studied by using two versions of the semi-active systems as shown in Figure 6.3. The systems in group CSF in table 6.1 are calculated using a spring stiffness, Se2, designed to give a body natural frequency of 1.01 Hz. Repeat calculations using all the same parameters except that the spring stiffness, Se3, is designed to give a natural frequency of 1.27 Hz were made and the results are shown in Figure 6.3. These results indicate that the stiff version gives a reduction of the working space accompanied by an increase in the ride comfort parameter. Hence, the fluctuating power of the passive spring decreases as the working space decreases, but the mean power dissipation of both versions are similar. The percentage time dissipating energy decreases as the working space increases, this also resulting in an increase of power demand of the corresponding fully active system as shown earlier in figure 5.3. In order to compare the behaviour of the semi-active and the corresponding active systems CSF4, table 6.1, and CF4, table 5.1, further results for these systems are plotted out in Figures 6.4 and 6.5. Figure 6.4 shows the PSD performances and mean power dissipation versus RMS working space of both systems. Figure 6.5 shows also the time history of the control forces, power requirements of the active elements and

fluctuating power of the passive spring for both systems. The performances including the power dissipation of the semi-active system compared with the fully active system merit the following important comments. Firstly, the RMS working space and dynamic tyre load are reduced by 16% and 3% respectively but combined with an increase in RMS ride comfort of 14%. Secondly, the mean value and peak values of the power dissipation are reduced by 15% and 30% respectively. Thirdly, the shapes of the time histories of the control force or fluctuating power of both systems is similar when traversing the same surface.

The RMS working space, ride comfort parameter and dynamic tyre load as well as the percentage time dissipating energy of the semi-active systems in group DSF are plotted versus the road roughness parameter for forward speeds of 12 and 17 m/s in Figure 6.6. The performance of the semi-active systems compared with the corresponding active systems when operating on smoother roads indicate that the percentage improvement in RMS working space and dynamic tyre load as well as the percentage deterioration in RMS ride comfort are all increased. The percentage time dissipating energy is also decreased, also resulting in an increase of power demand of the corresponding active systems as shown earlier in figure 5.8.

The systems in group ESF are chosen to give dynamic tyre load figures of 20% at three values of the working space: 2.5, 3.5 and 4.5 cm. Figure 6.7 shows the RMS working space, ride comfort parameter and dynamic tyre load of the systems in group ESF versus the time lag constant of the active damper. The system ESF1 results in a similar performance to the corresponding active system for time lags up to 180 ms whereas systems ESF2 and ESF3 only offer similar performance up to 22 ms, as shown in figure 6.7. Figures 6.8, 6.9 and 6.10 show the following time histories of the semi-active system characteristics: switching between on and off, force and power dissipation for the systems ESF1, ESF2 and ESF3 respectively.

The results also include the following features. Firstly, the percentage time dissipating energy are: 99%, 97% and 93% for the systems ESF1, ESF2 and ESF3 respectively. Secondly, the peak values of the power dissipation or active damper force for systems in group ESF are similar.

The performance properties of the full state feedback semi-active systems are displayed in Figure 6.11 for different types of road for 12 m/s forward speed at a working space of 3.5 cm. The responses of all the systems are proportional to the road input conditions, so that the performance of any semi-active system, studied for smoother or rougher road surface/vehicle forward speed combinations than that assumed are scaled up or down. A comparison of the fully active and semi-active systems results shown in figure 5.11 and figure 6.11 respectively indicate two trends worthy of comment as follows. First, the performance output of the active systems are a function of the road input conditions GV which represent the road roughness parameter and vehicle forward speed whereas the outputs of the semi-active systems are separately related to either road roughness constant C or vehicle speed V and second, the active systems give improvements of the ride comfort over the semi-active systems for the same working space and dynamic tyre load, with the percentage improvement in ride comfort increasing when operating on the smoother roads.

6.2.2 Limited state feedback systems

The control law of the limited state feedback semi-active systems is the same as in equation 5-4 and therefore the suspension force can be reformed as equation 6-1. The performance criteria including power losses of the limited state feedback semi-active systems can be obtained as discussed previously. Table 6.2 summarises the RMS working space, ride comfort and dynamic tyre load, as well as the mean power dissipation and percentage changes in performance categories for five

groups of the limited state feedback semi-active systems. The systems in groups ASL, BSL, CSL and DSL are also designed to correspond to those of the fully active systems in Table 5.2 to give a fair comparison between the fully active and semi-active systems. In general, the results in tables 6.1 and 6.2 indicate that the behaviour of the full and limited state feedback semi-active systems are similar. Hence, the following discussion is restricted to those aspects of the results which are affected by having limited rather than full state information available in the control law.

For completeness, the full set of results for the limited state feedback systems is given in Figures 6.12 to 6.19. They vary only in detail from those presented previously for the full state feedback case. The conflict between the ride comfort and working space is clearly shown in Figure 6.12, whereas the conflict between ride comfort and dynamic tyre load is also indicated in Figure 6.13. The performances including power requirements of the semi-active systems are related to the body natural frequency in a similar way to that for the conventional passive systems, i.e. the stiff system increases the ride comfort and decreases the working space as shown in Figure 6.14. The percentage deterioration in ride comfort of the semi-active systems compared with the corresponding active systems increases when operating on smoother roads as shown in Figure 6.15.

The lower workspace system ESL1 gives a similar performance to that obtained by the corresponding fully active system for time lags up to 180 ms as shown in Figure 6.16. This is accompanied by an increase in the percentage time dissipating energy (98%) for system ESL1 as shown in Figure 6.17 compared with the higher workspace system ESL2 (93%) as shown in Figure 6.18. The performance of the limited state feedback semi-active systems studied for smoother or rougher road surface/vehicle speed combinations than that assumed are scaled up or

scaled down as shown in Figure 6.19 in a similar way of full state feedback case.

Finally, Figure 6.20 shows a direct comparison of the performances of the full and limited state feedback semi-active systems at 3.5 cm of working space. The first point to note is that the full state feedback systems give improvements of the ride comfort parameter over the limited state feedback systems for dynamic tyre loads up to 27%. This is accompanied by an increase in the percentage time dissipating energy for the full compared with the limited state feedback systems. Secondly however, despite this higher percentage of time, the total power dissipation of the full state feedback systems is actually lower than that of the limited state feedback systems.

6.3 Semi-active non-linear control systems

Based on the concept of the active non-linear control systems, which was discussed previously, a similar system was investigated based on the semi-active principle. This control law is again a non linear one because the feedback coefficients are function of time and need to be found for each time step as discussed in section 5.3.1. The control law of the limited state feedback semi-active non-linear control systems is the same as in equation 5-5 and therefore the suspension force can be also reformed as equation 6-1. The non-linear analysis procedures are again used to evaluate the performance capabilities of the systems.

The performance capabilities of the semi-active linear and non-linear control systems are compared to each other for the following conditions. Firstly, the basic elements and linear or non linear control law of the fully active models described in section 5.4 are used to design the semi-active systems when operating on an average minor road described in section 2-7 for forward speed of 12 m/s. Secondly, the switching dynamics of the active damper are assumed to be subject to constraints as

used before.

The results of this comparison indicate the following features. For the linear control system, the RMS values of ride comfort, dynamic tyre load and working space are 1.14, 17.8% and 2.5 cm respectively, whereas for the non-linear control system, the RMS values of ride comfort, dynamic tyre load and working space are 0.89, 16.7% and 2.4 cm. Thus, the non-linear control system gives significant improvements of the ride comfort by 36%, dynamic tyre load by 6% and working space by 6% over the linear control system. In terms of the power requirements, Figure 6.21 shows various time histories of the active damper characteristic, i.e. force, velocity and power dissipation for both linear and non-linear control systems. The mean power dissipation of the linear and non-linear control systems are 1.36 and 0.96 kW, i.e. the non-linear control system reduces the power dissipation by 30%. The peak dissipative power values of the linear and non-linear control systems are up to 15 and 10 kW respectively and the peak values of the active damper force for linear and non-linear control systems are up to 15 and 10 kN respectively. The peak values of the active damper relative velocities for both systems are similar. Again, similar practical difficulties apply to the semi-active version of this non-linear control system, as already outlined in section 5.4 for the active version.

6.4 Concluding remarks.

The calculations presented in this chapter reveal that, in general the semi-active systems give the same conflicts between the performance categories as the active systems. The semi-active systems give an improvement of the working space and reduction in power dissipation but coupled with a deterioration in ride comfort compared with the corresponding active system. The percentage improvement in working space and percentage deterioration in ride comfort increased when operating on smoother roads. When compared on the basis of equal working space

and dynamic tyre load, the fully active systems offer improvements of the ride comfort over the semi-active systems and again, these improvements are also increased when operating on smoother roads. The outputs of the semi-active systems are not related to the input conditions, GV, in the same proportional way in which the active linear systems are. The full state feedback semi-active systems result in only marginal improvements in performance over the limited state feedback semi-active systems.

In general, the semi-active system is as good as the fully active systems when the available suspension workspace is restricted relative to the ground/speed conditions and it is also satisfactory to use a conventional passive spring. In the most severe conditions when the vehicle is running on a rougher road at a high forward speed, the semi-active systems provide a similar performance to that obtained with the fully active systems for a limited workspace usage. High percentage time dissipating energy indicates that the fully active suspension achieves improvements mainly by "intelligent" dissipation not by putting power in. This is the reason why the semi-active system is virtually as good as the fully active system. Also, the semi-active system is not sensitive to the time lag of the damper (switching delay). Finally, the semi-active non-linear control system gives a significant improvement in the performance over the semi-active linear control system.

Typically, a semi-active system replaces an external power supply, for example hydraulic pump, and actuator used in a fully active system by an active damper, which would incorporate some from of continuously variable orifice. In practical terms, the main difficulties would be in designing a continuously variable damper to track a force demand signal independently of instantaneous velocity across it, and in particular generating either a very high force when velocity is small or very small force when velocity is high.

Group	System	weighting factor $r=10^{-8}$ and		RMS Performance of dynamic tyre load ZDTLP, ride comfort RCP, working space SWS (mm) and mean power dissipation MP- (W)				percentage improvement offered by fully active system compared with corresponding semi-active system		
		q_1	q_2	DTLP	RCP	SWS	MP-	DTLP	RCP	SWS
ASF	ASF 1	2250	500	20.1	1.01	24.6	1395	-1	1	-1
	ASF 2	1800	20	19.7	0.84	31.2	1314	-2	6	-11
	ASF 3	1500	1	20.5	0.84	39.3	1315	-1	10	-14
BSF	BSF 1	17500	25	16.7	0.98	32.5	1302	10	-1	-9
	BSF 2	800	40	21.5	0.80	31.1	1318	-5	12	-12
	BSF 3	400	66	23.1	0.77	31.0	1325	-7	16	-12
CSF	CSF 1	4500	7000	29.4	1.67	15.6	1538	0	-1	2
	CSF 2	4000	500	19.7	1.03	25.3	1384	2	1	-1
	CSF 3	2500	22.50	19.5	0.87	31.2	1316	2	4	-9
	CSF 4	833	1.67	22.3	0.78	37.8	1285	-3	14	-16
	CSF 5	500	0.18	24.5	0.78	44.2	1290	-4	27	-21
DSF	DSF 1	180	1	17.5	0.44	25.9	499	-14	42	-26
	DSF 2	400	5	18.9	0.56	28.2	764	-8	23	-20
	DSF 3	833	11.67	19.7	0.70	29.8	1033	-3	12	-15
	DSF 4	1600	20	20.4	0.84	31.7	1307	0	7	-11
	DSF 5	1600	20	21.0	0.84	33.1	1303	3	8	-6
ESF	ESF 1	3000	500	20.1	1.02	25.0	1390	2	1	0
	ESF 2	2295	4.10	19.8	0.86	35.3	1310	2	5	-9
	ESF 3	3000	0.27	20.4	0.93	45.8	1341	9	9	-42

Table 6.1 Results for various full state feeback semi-active systems including performances, power dissipation and percentage changes relative to corresponding fully active systems.

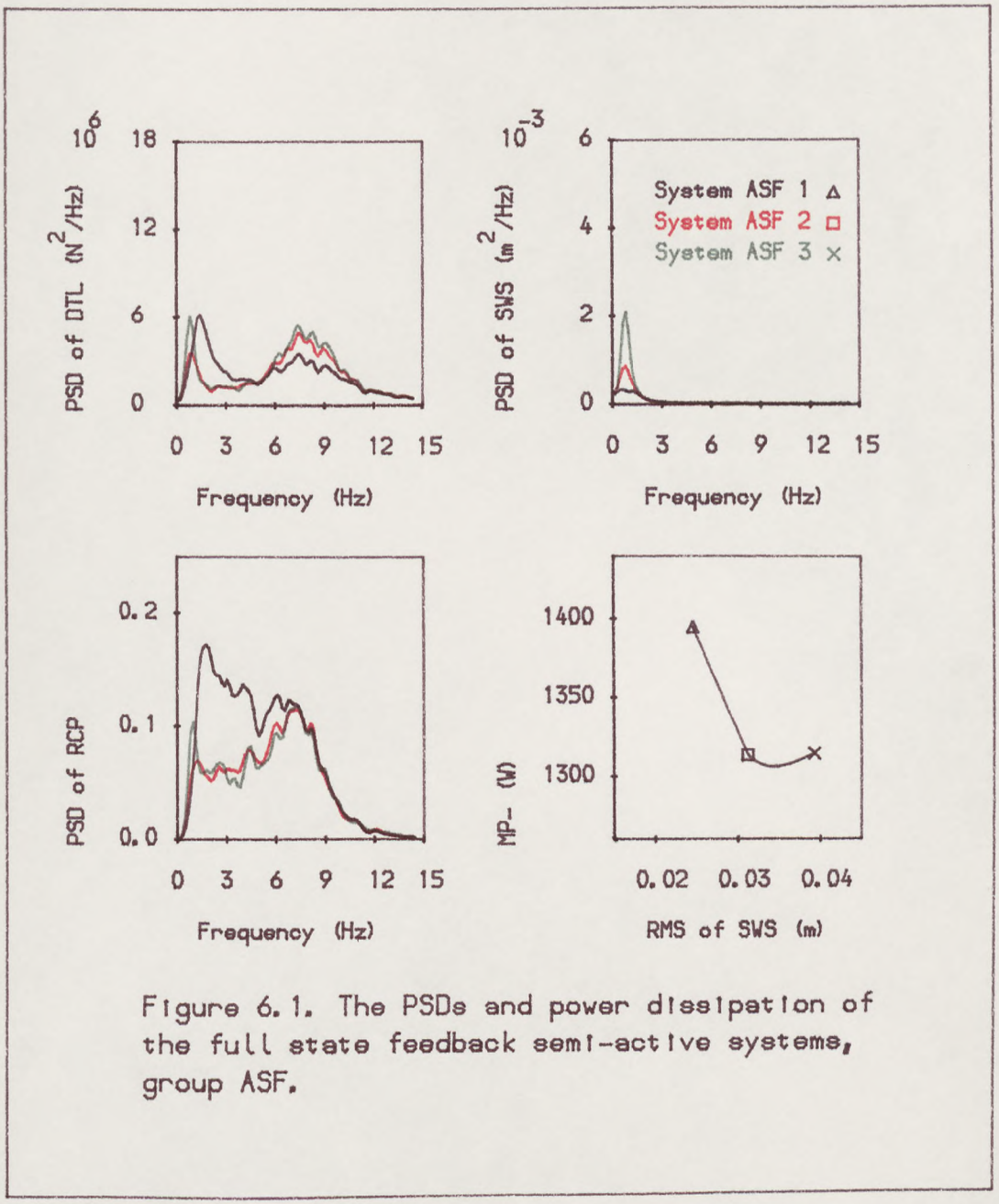

Figure 6.1. The PSDs and power dissipation of the full state feedback semi-active systems, group ASF.

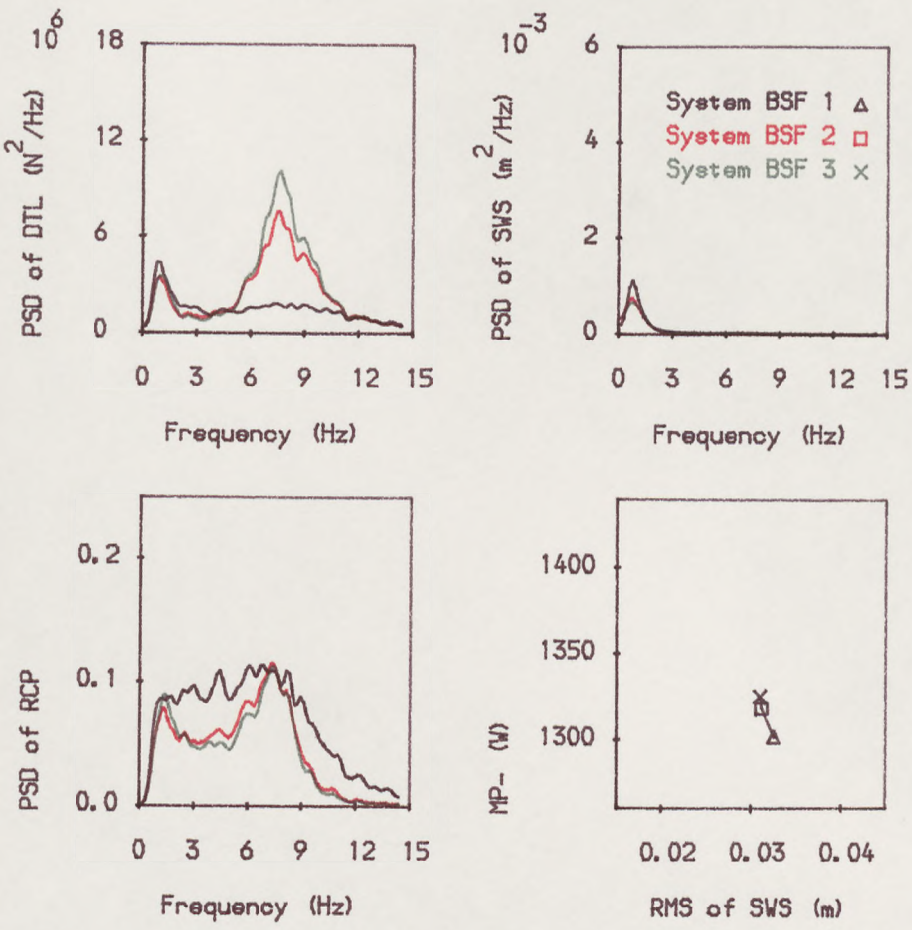

Figure 6.2. The PSDs and power dissipation of the full state feedback semi-active systems, group BSF.

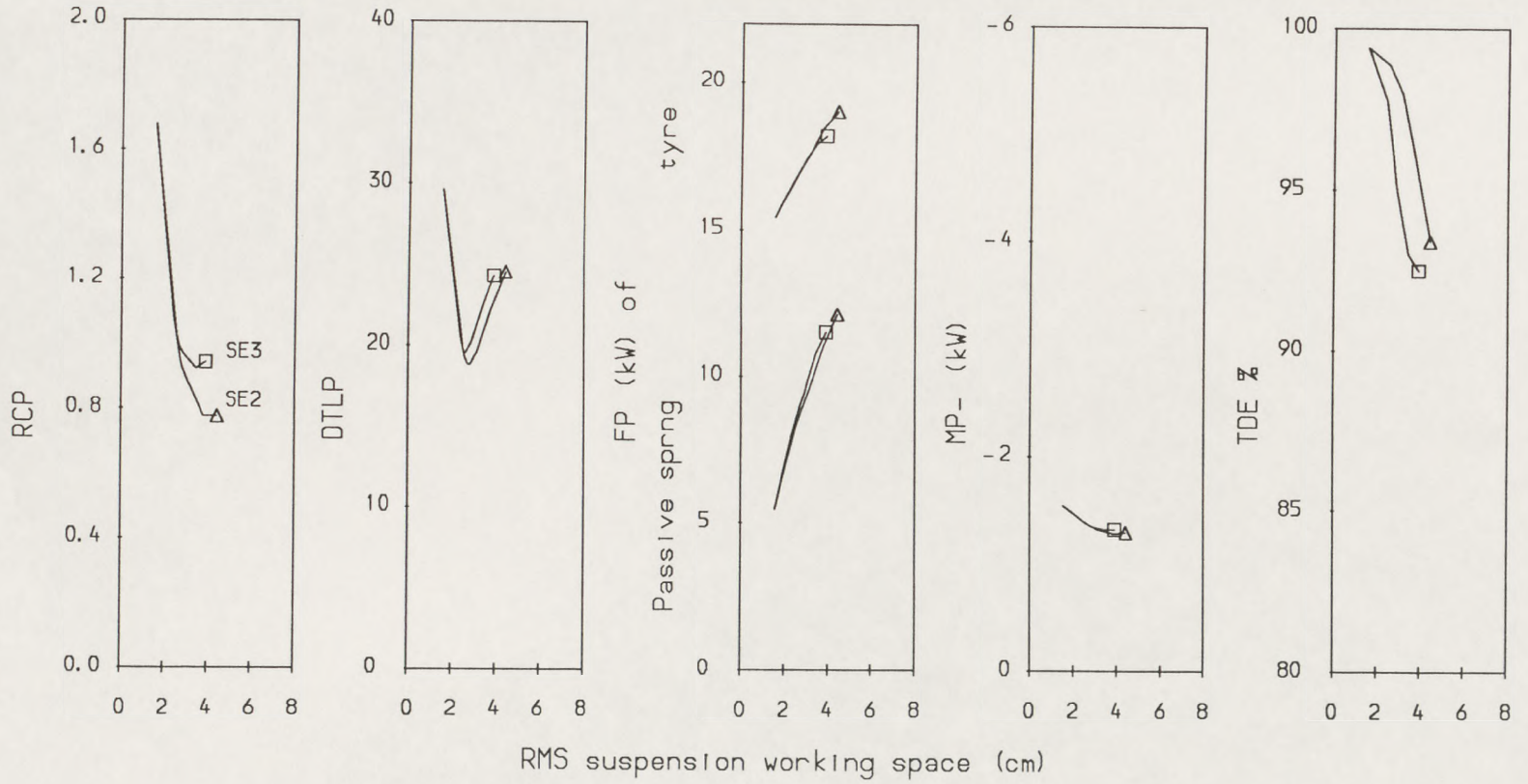

Figure 6.3. Comparison of full state feedback semi-active systems, which are based on the fully active systems in table 5.1, with additional spring Se2 to give a natural frequency of 1.01 Hz and Se3 (1.27 Hz).

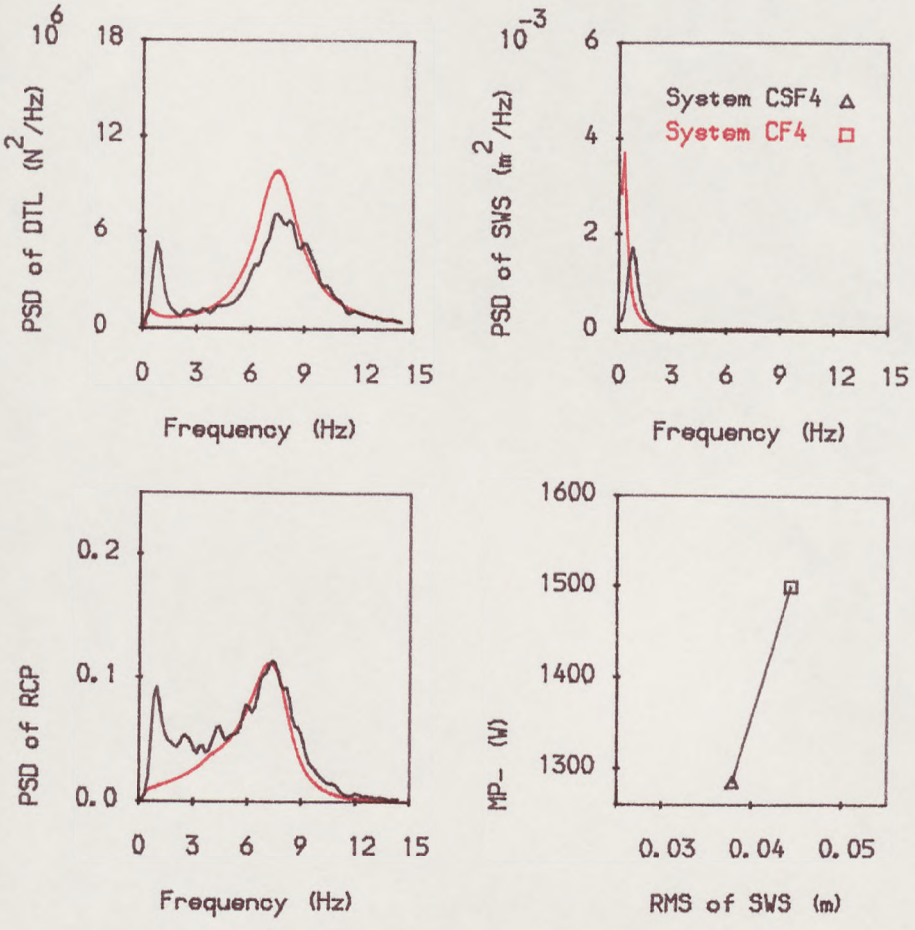

Figure 6.4. Comparison of the PSDs and power dissipation of the full state feedback systems: fully active CF4, table 5.1, and corresponding semi-active CSF4, table 6.1.

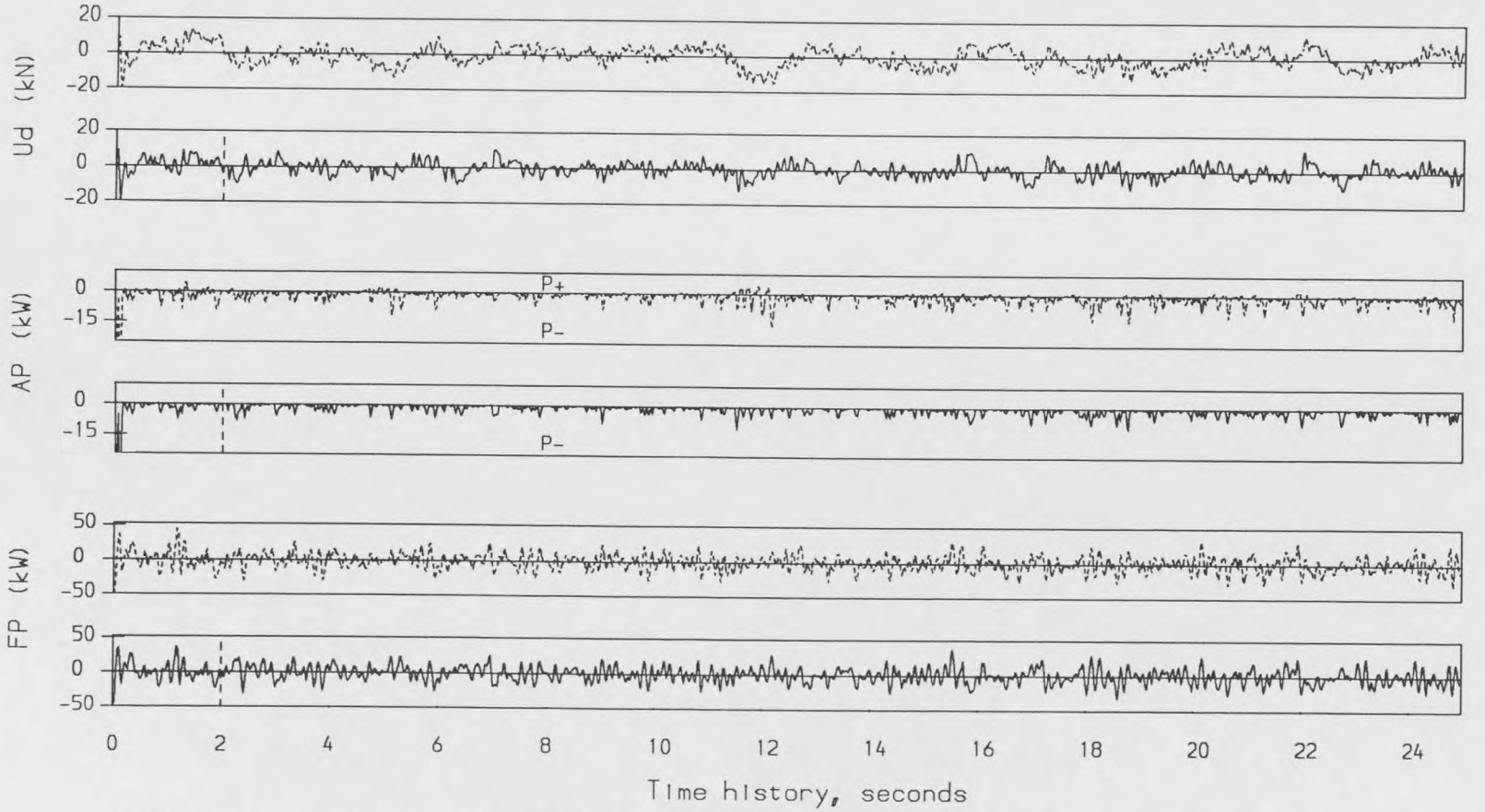

Figure 6.5. Time histories of the control forces and power requirements of the suspension elements of the systems: fully active CF4 {broken line} and corresponding semi-active CSF4 {continuous line}, in tables 5.1 and 6.1.

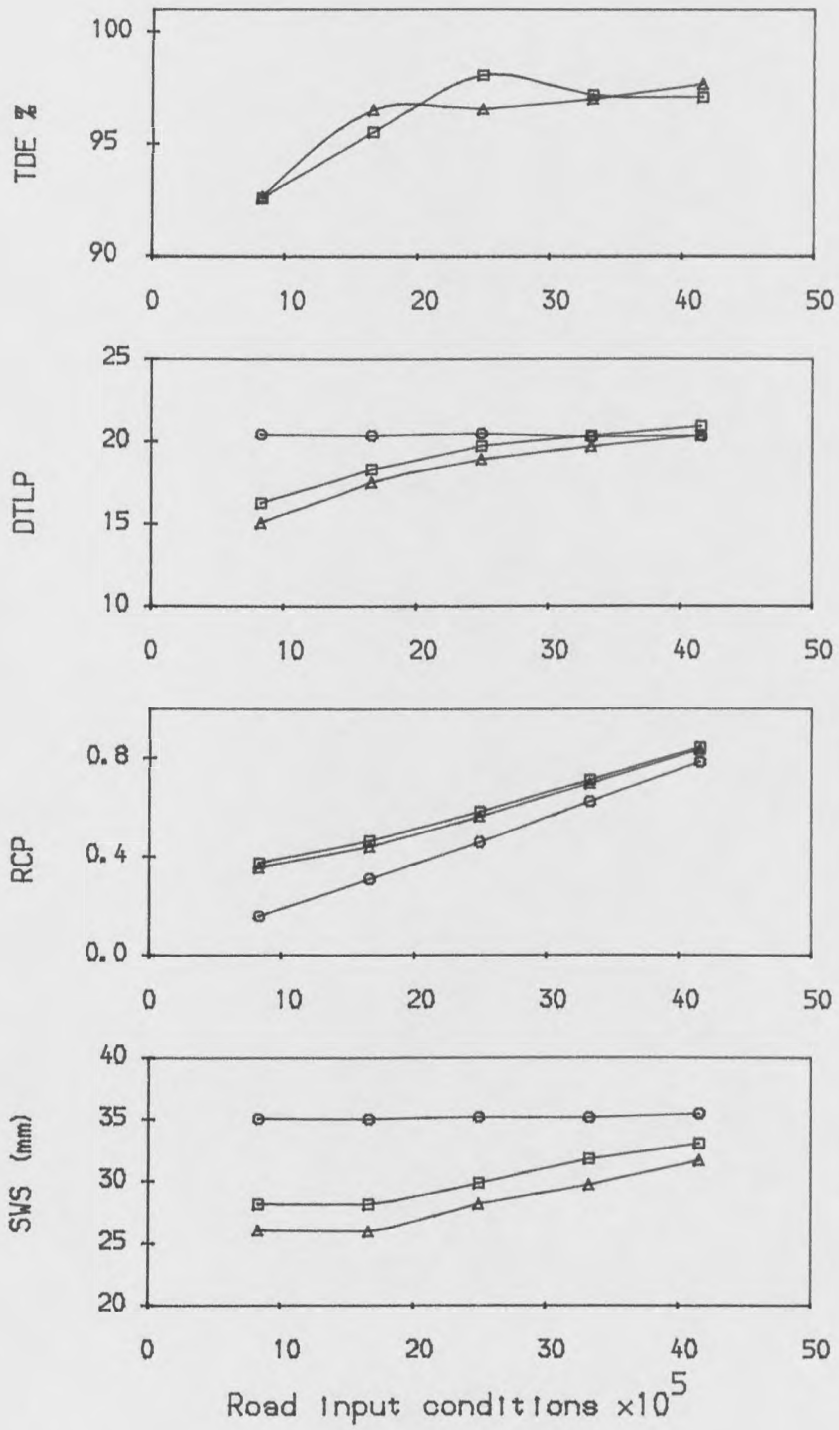

Figure 6.6. Comparison of performances of the full state feedback systems: fully active and corresponding semi-active versus road input.
△ △ Semi-active at forward speed 12 m/s, group DSF
□ □ Semi-active at forward speed 17 m/s
○ ○ Active systems in group DF, table 5.1

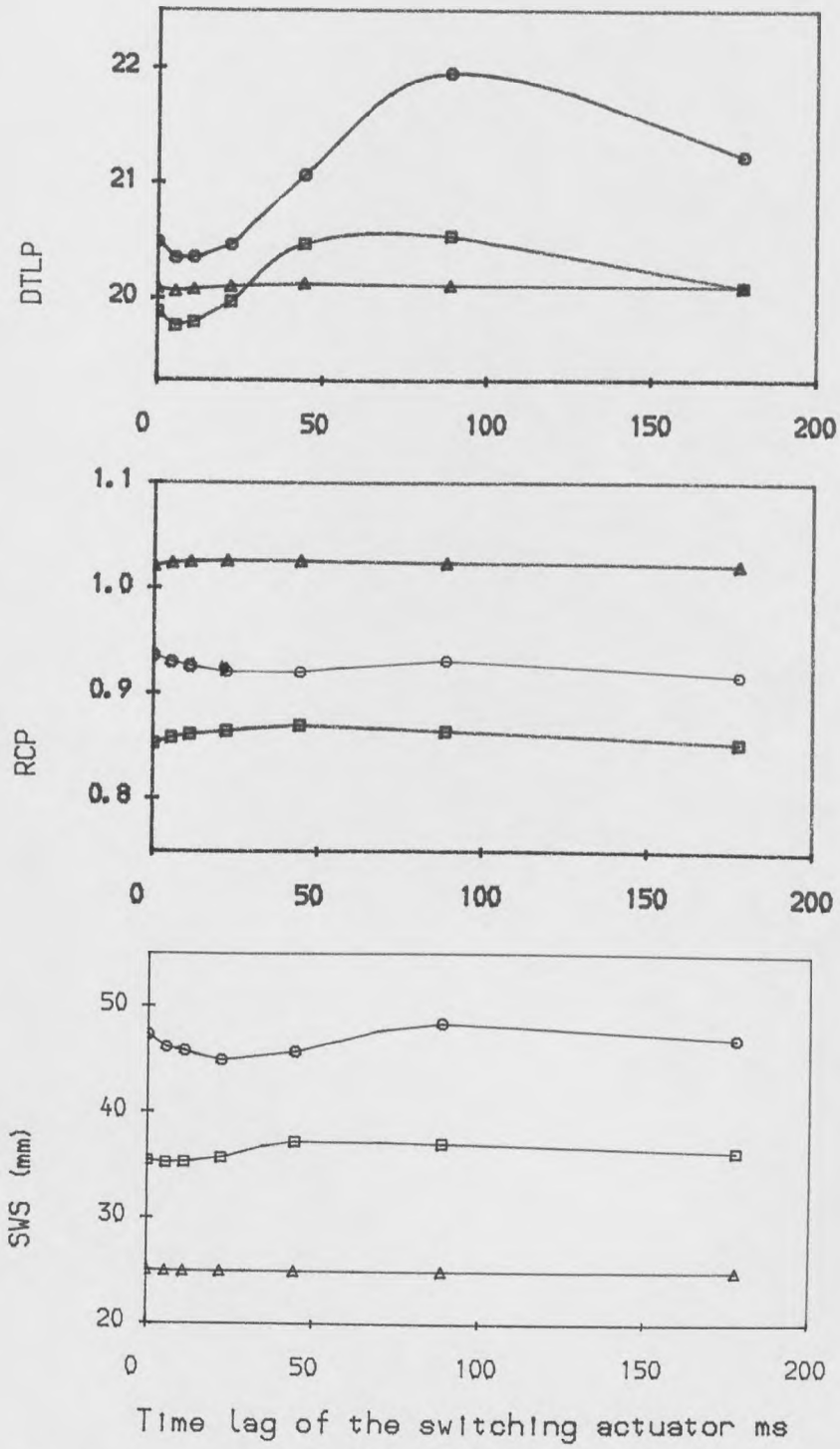

Figure 6.7. Comparison of performances of full state feedback semi-active systems versus time lag of the switching actuator.

△ △ Semi-active system ESF1

□ □ Semi-active system ESF2

o o Semi-active system ESF3

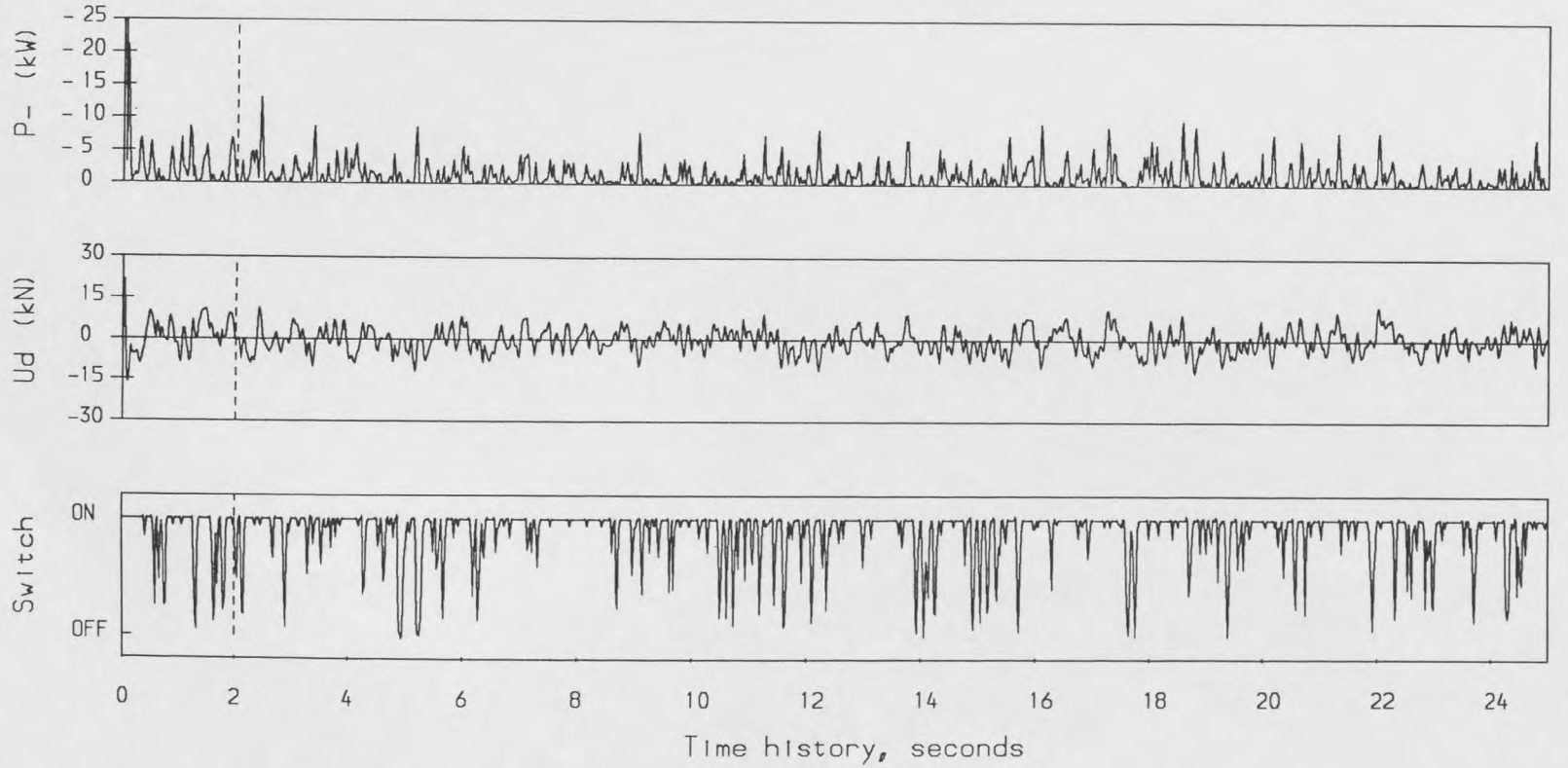

Figure 6.8. Time histories of the active damper characteristic of full state feedback semi-active system ESF1.

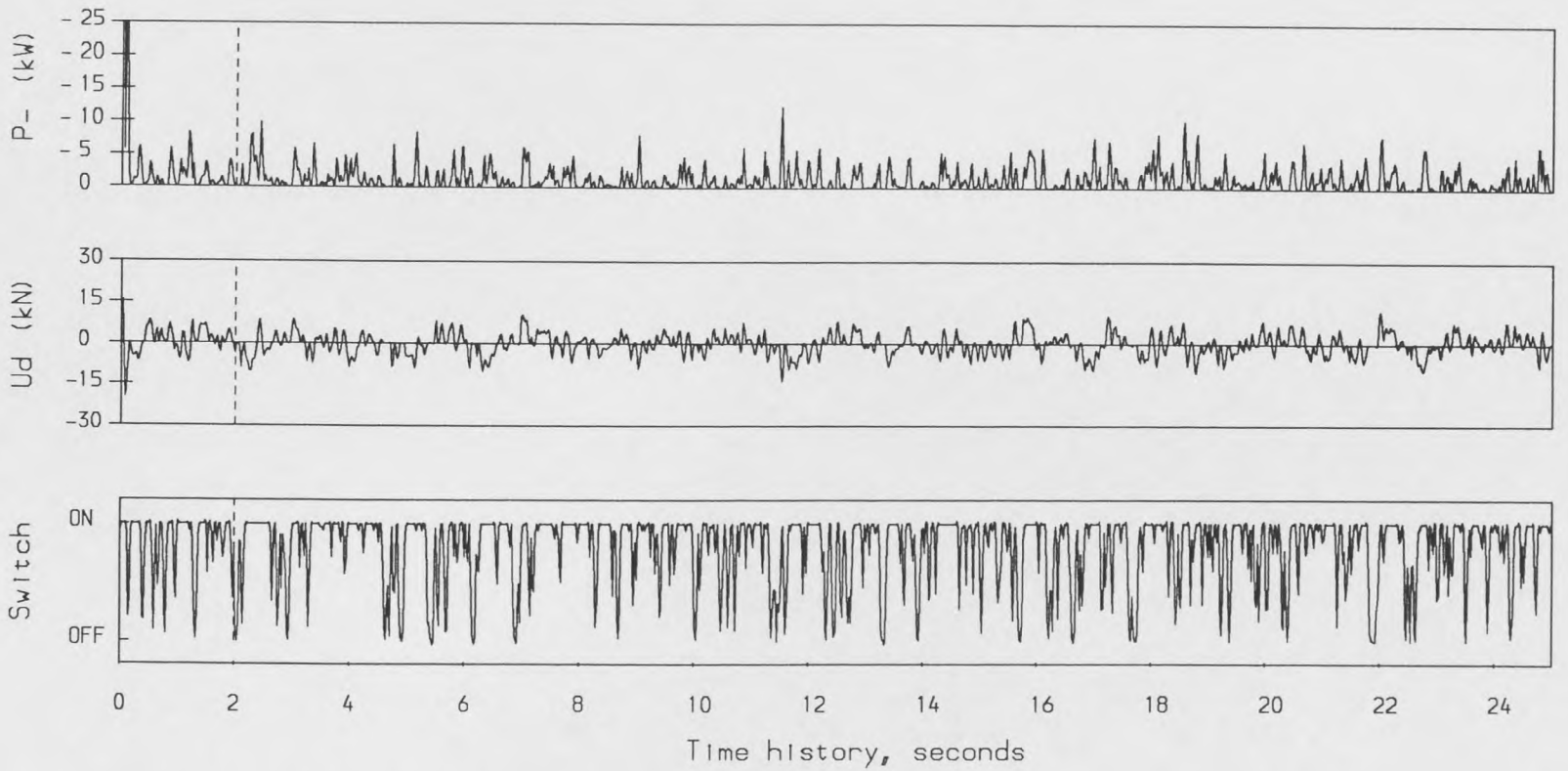

Figure 6.9. Time histories of the active damper characteristic of full state feedback semi-active system ESF2.

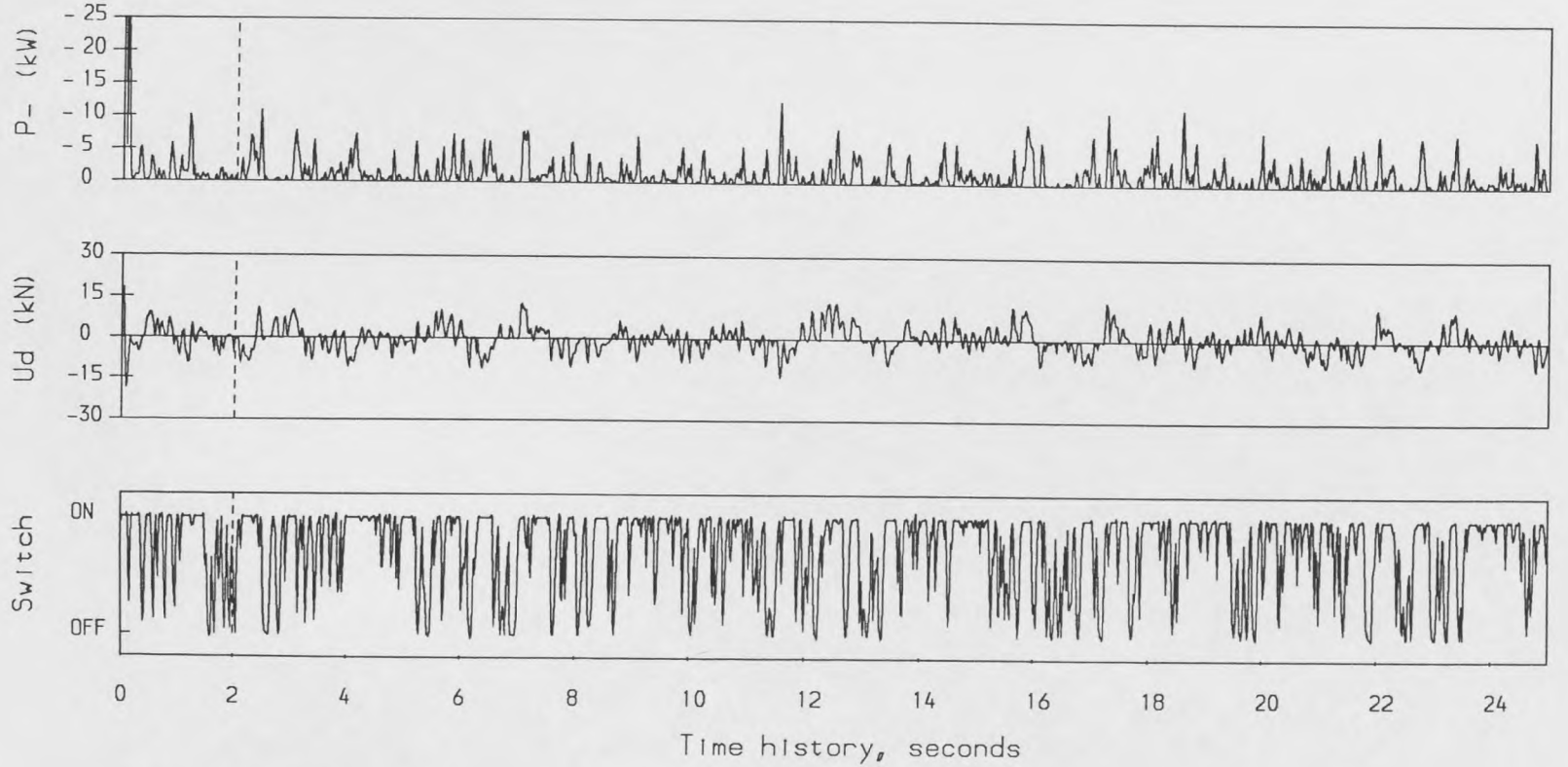

Figure 6.10. Time histories of the active damper characteristic of full state feedback semi-active system ESF3.

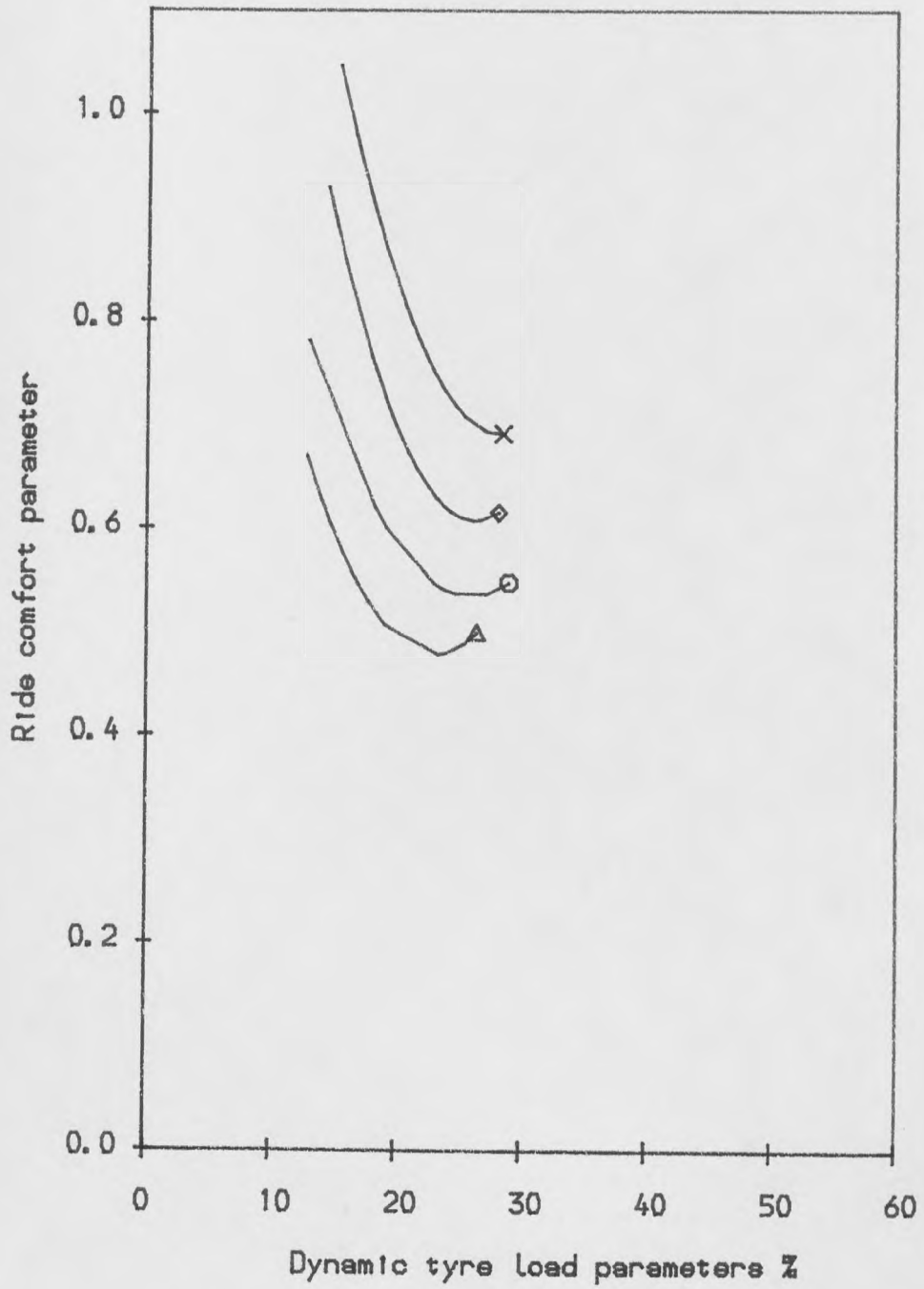

Figure 6.11. Comparison of performances of full state feedback semi-active systems at 3.5 cm RMS working space.

Δ Δ GV= 16.63×10^{-5} o o GV= 24.95×10^{-5}

$\diamond$ $\diamond$ GV= 33.25×10^{-5} x x GV= 41.56×10^{-5}

Group	System	weighting factor $r=10^{-8}$ and		RMS Performance of dynamic tyre load %DTLP, ride comfort RCP, working space SWS (mm) and mean power dissipation MP- (W)				percentage improvement offered by fully active system compared with corresponding semi-active system		
		q_1	q_2	DTLP	RCP	SWS	MP-	DTLP	RCP	SWS
ASL	ASL 1	6667	666.7	20.4	1.10	24.0	1387	1	1	-2
	ASL 2	1667	45	21.9	0.97	32.9	1337	7	18	-8
BSL	BSL 1	16000	100	19.9	1.06	28.9	1371	30	9	-16
	BSL 2	1000	23.3	21.6	0.89	30.8	1332	-4	21	-13
	BSL 3	500	40	22.8	0.77	30.7	1308	-8	18	-13
CSL	CSL 1	400	4000	29.5	1.67	15.4	1539	0	-1	1
	CSL 2	4000	500	20.9	1.05	23.9	1396	1	2	-1
	CSL 3	3333	66.7	21.2	1.00	32.0	1357	13	11	-6
	CSL 4	750	5	26.0	0.91	38.7	1274	12	35	-13
	CSL 5	533	0.2	29.1	1.02	45.9	1366	16	64	-17
DSL	DSL 1	166	0.3	18.8	0.64	27.7	479	-10	110	-24
	DSL 2	480	1.1	19.7	0.77	29.9	768	-2	61	-18
	DSL 3	800	5	21.3	0.88	31.8	1039	2	42	-14
	DSL 4	1857	12.8	22.0	0.97	32.5	1348	5	19	-9
	DSL 5	1857	12.8	22.6	0.97	33.1	1305	9	19	-7
ESL	ESL 1	400	350	21.3	0.91	26.5	1361	0	6	-2
	ESL 2	5000	10	21.1	0.99	34.4	1337	19	10	-8

Table 6.2 Results for various limited state feeback semi-active systems including performances, power dissipation and percentage changes relative to corresponding fully active systems.

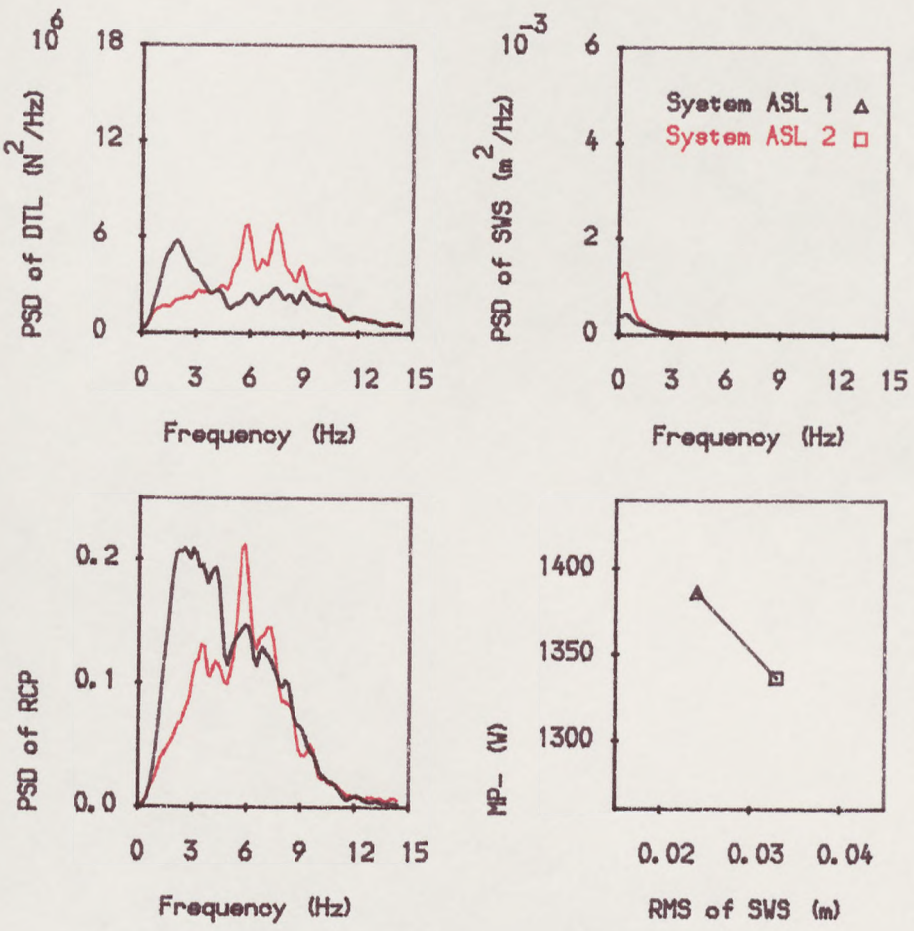

Figure 6.12. The PSDs and power dissipation of the limited state feedback semi-active systems, group ASL.

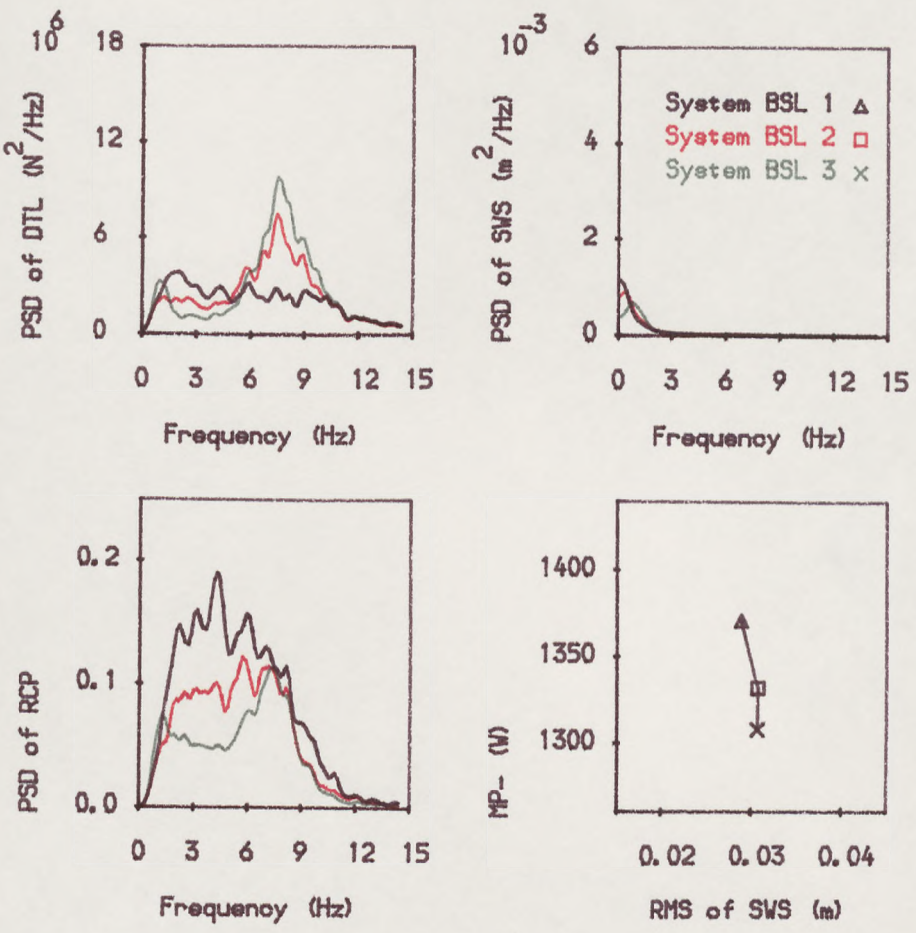

Figure 6.13. The PSDs and power dissipation of the limited state feedback semi-active systems, group BSL.

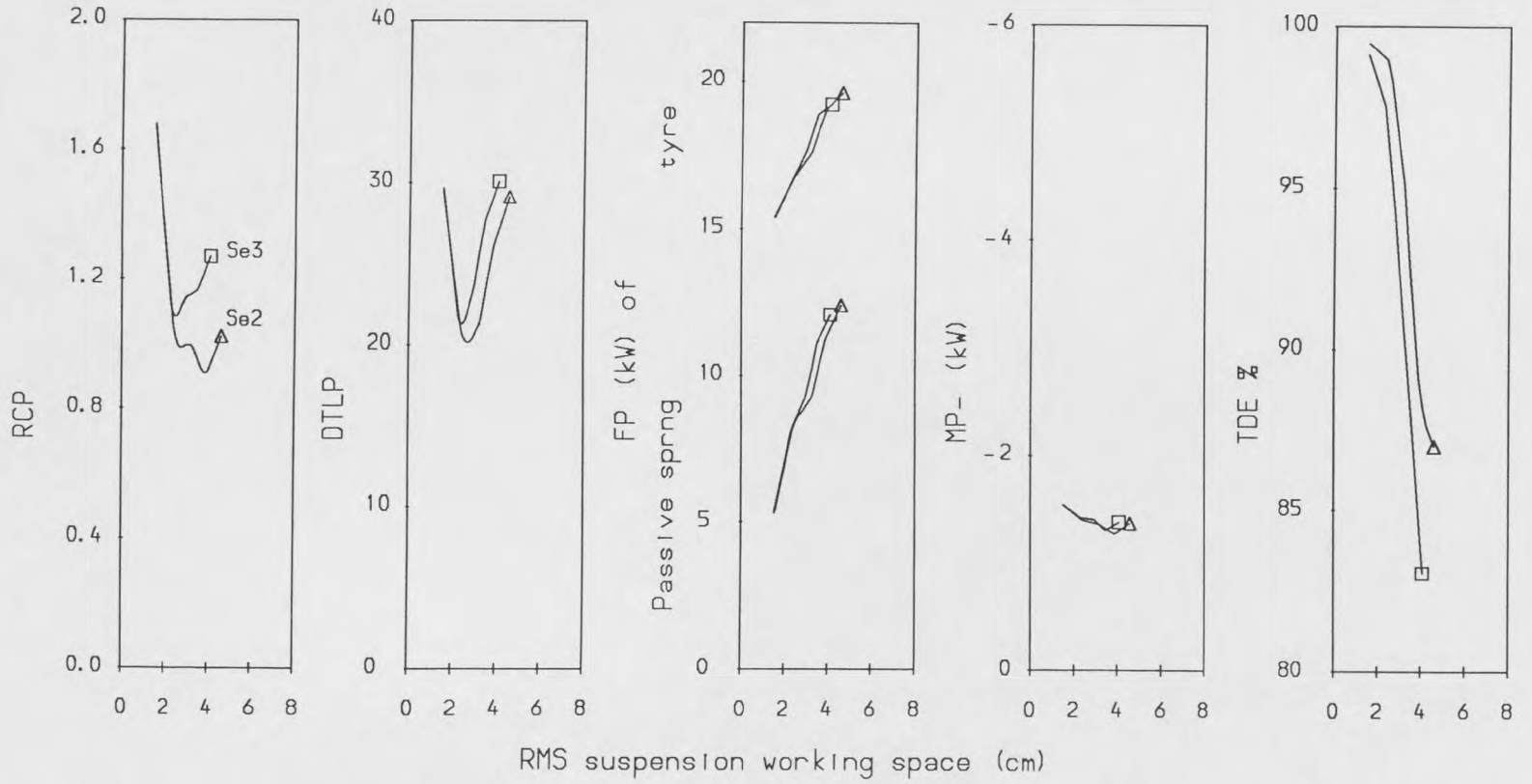

Figure 6.14. Comparison of limited state feedback semi-active systems, which are based on the fully active systems in table 5.2, with additional spring Se2 to give a natural frequency of 1.01 Hz and Se3 (1.27 Hz).

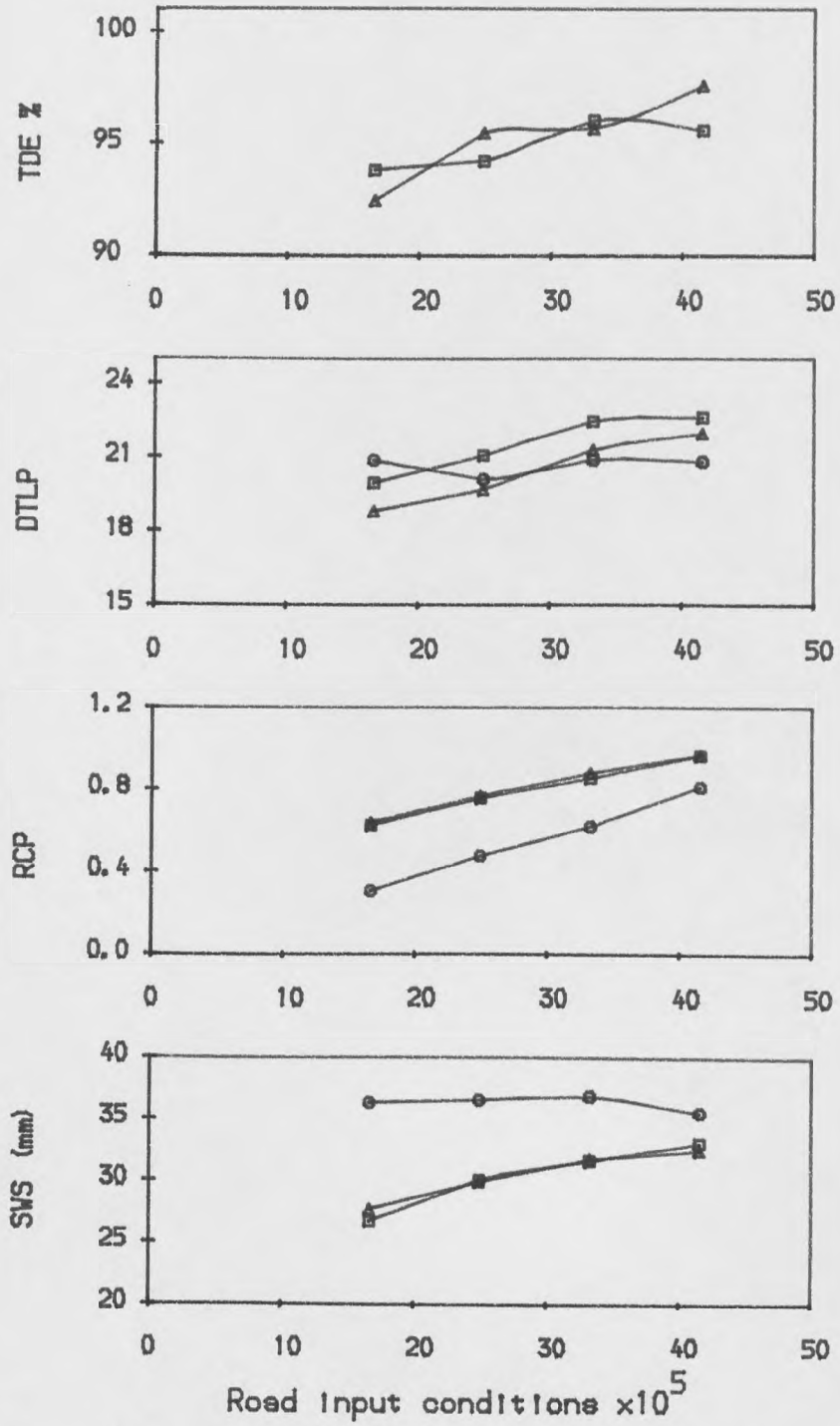

Figure 6.15. Comparison of performances of the limited state feedback systems: fully active and corresponding semi-active versus road input.
△ △ Semi-active at forward speed 12 m/s, group DSL
□ □ Semi-active at forward speed 17 m/s
o o Active systems in group DL, table 6.2

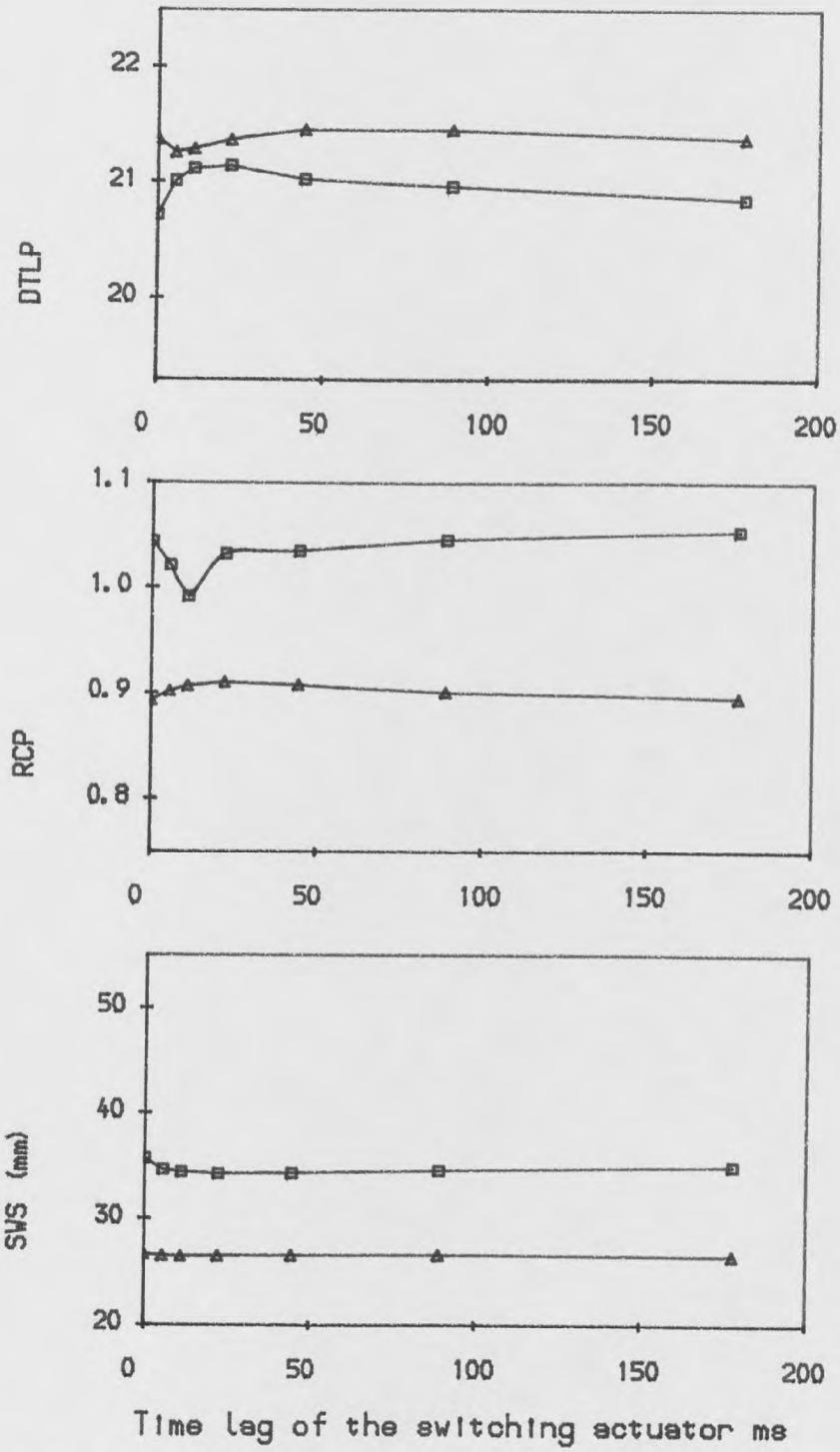

Figure 6.16. Comparison of performances of limited state feedback semi-active systems versus time lag of the switching actuator.

△ △ Semi-active system ESL1

□ □ Semi-active system ESL2

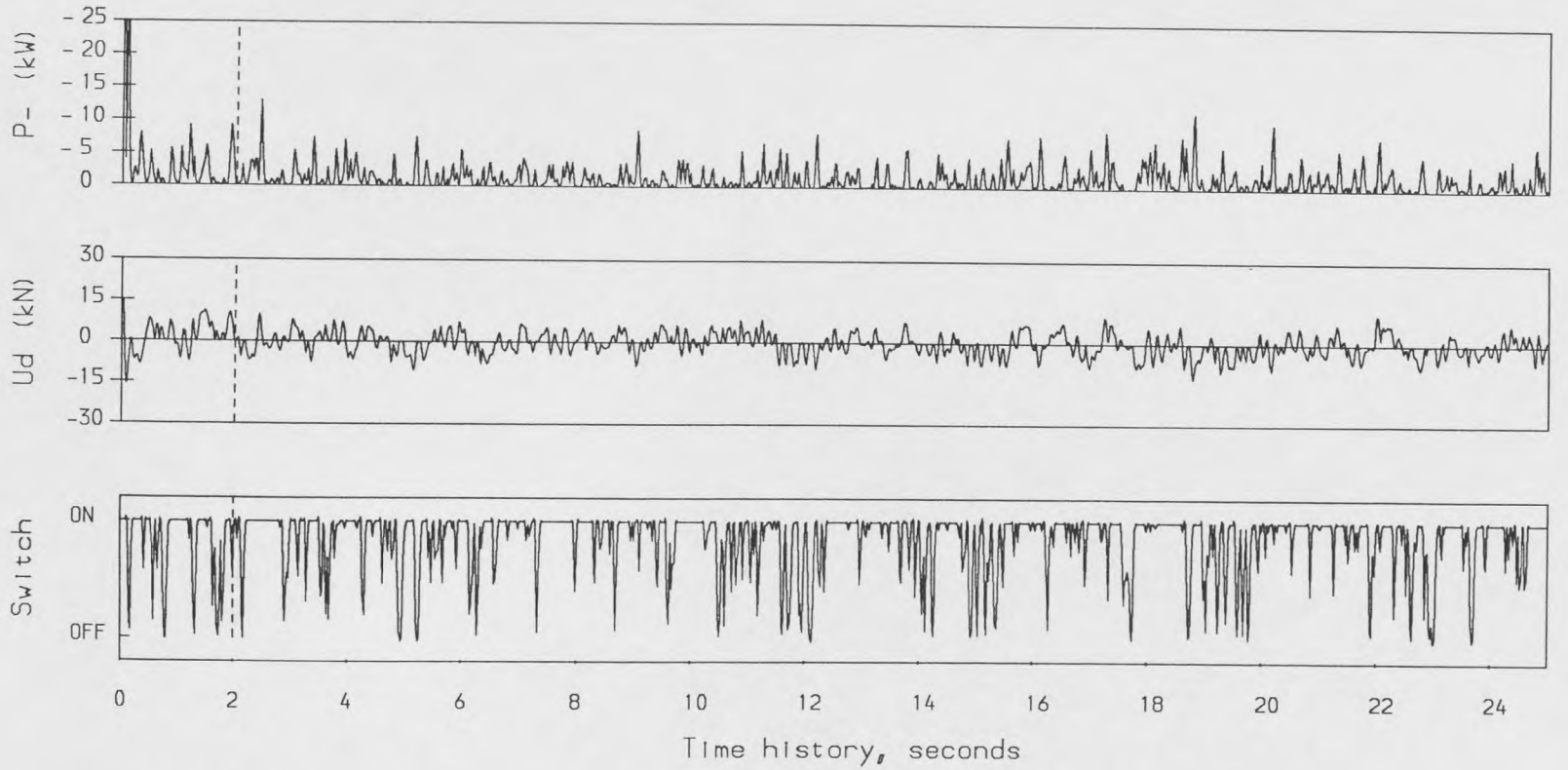

Figure 6.17. Time histories of the active damper characteristic of limited state feedback semi-active system ESL1.

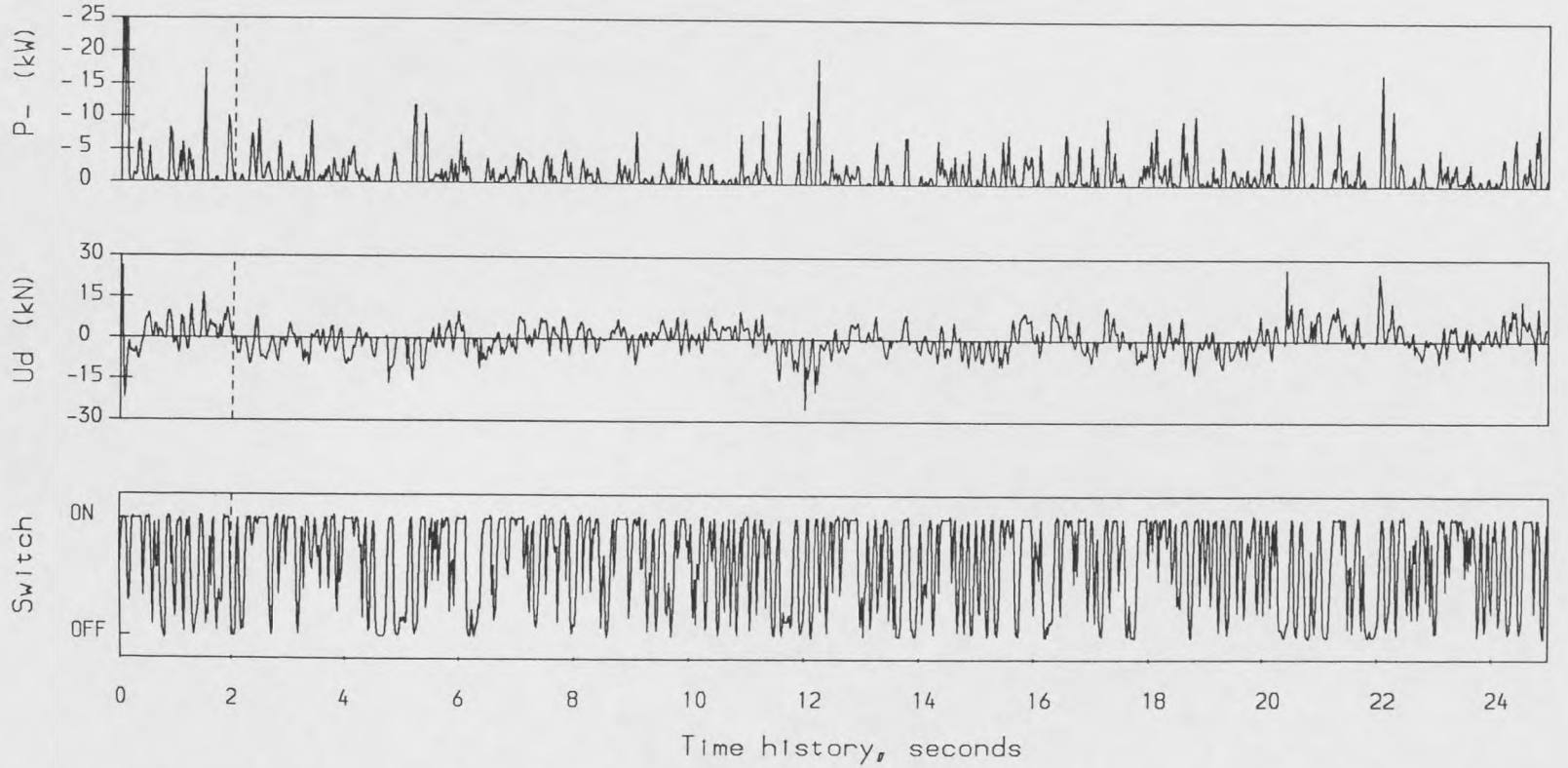

Figure 6.18. Time histories of the active damper characteristic of limited state feedback semi-active system ESL2.

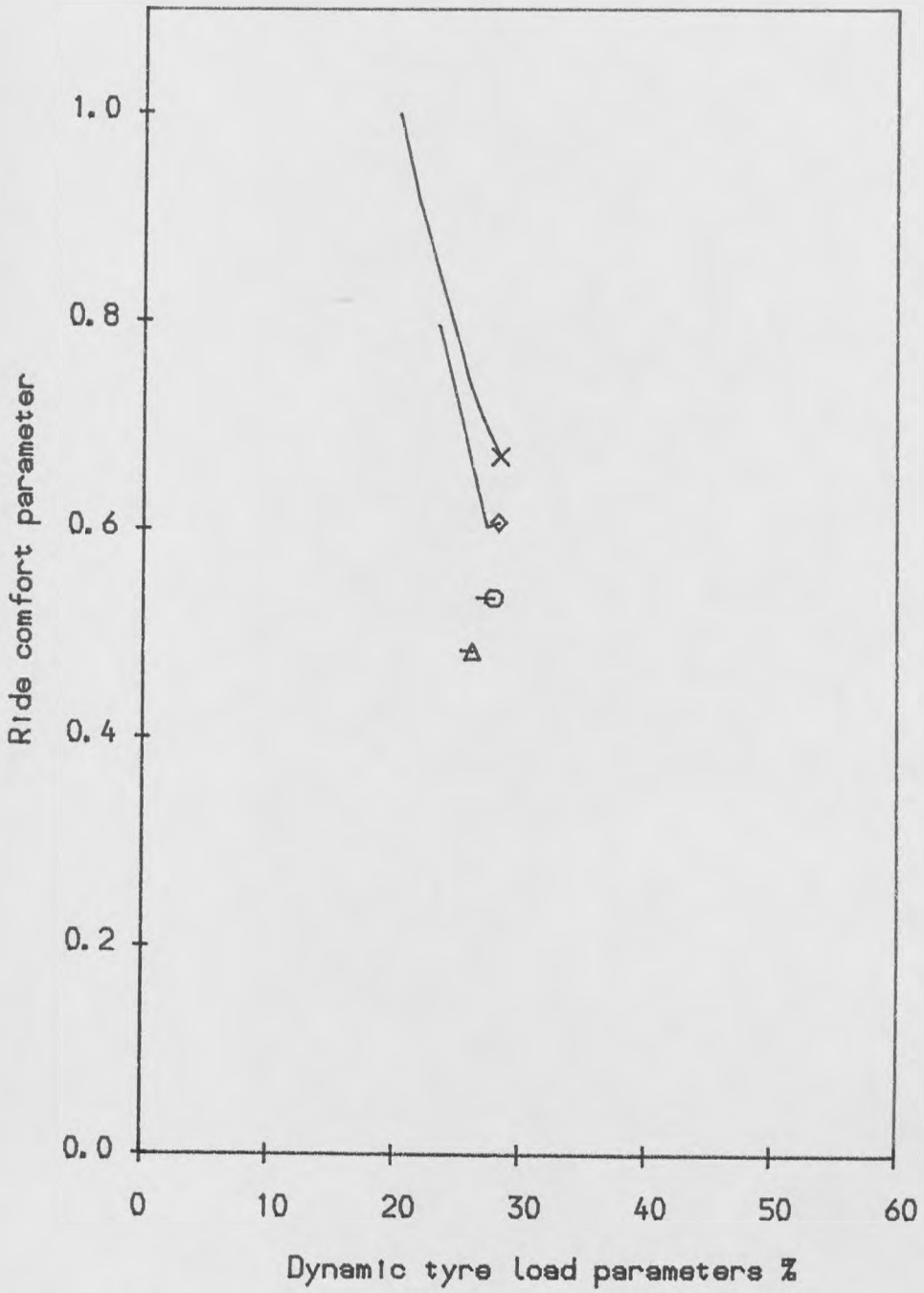

Figure 6.19. Comparison of performances of limited state feedback semi-active systems at 3.5 cm RMS working space.

△ △ GV= 16.63×10^{-5} ○ ○ GV= 24.95×10^{-5}

◇ ◇ GV= 33.25×10^{-5} × × GV= 41.56×10^{-5}

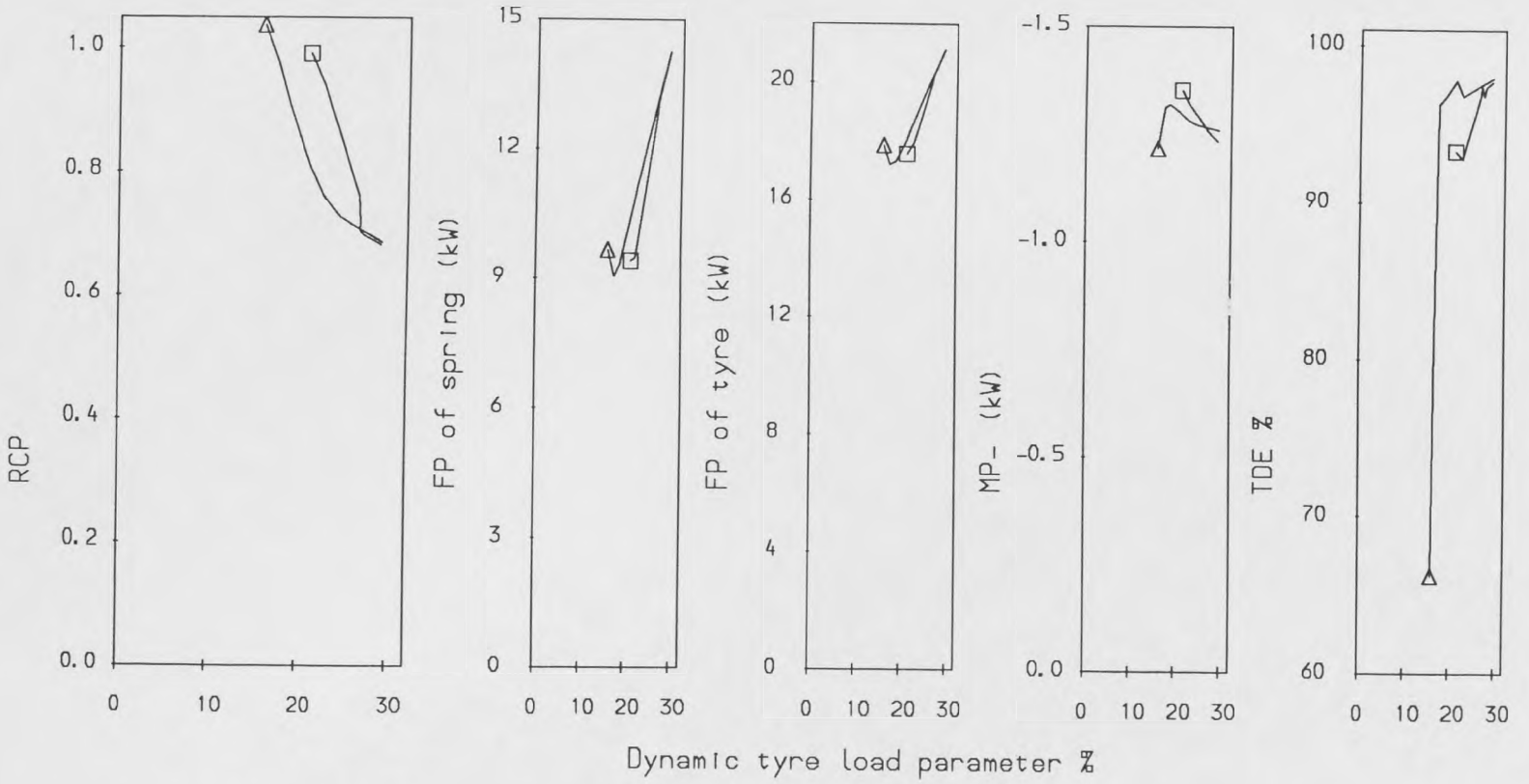

Figure 6.20. Comparison of performances and power requirements of full(Δ Δ) and limited(□ □) state feedback semi-active systems at 3.5 cm working space.

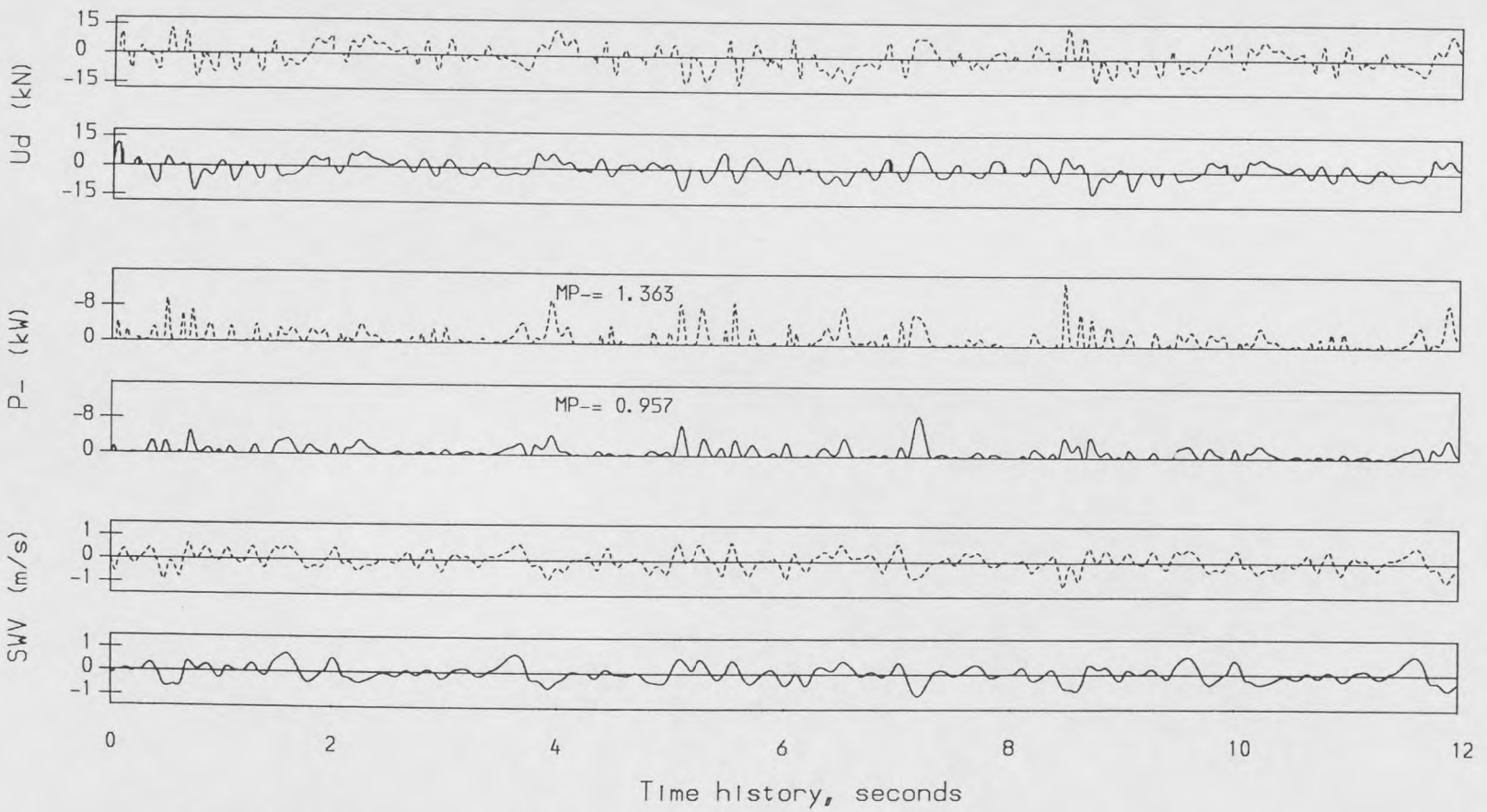

Figure 6.21. Time histories of the active damper characteristic of the semi-active linear (broken line) and non-linear (continuous line) systems.

CHAPTER 7

SLOW-ACTIVE SYSTEMS

7.1 Introduction

The term, slow-active, is used to refer to an active control which has a limited frequency response capability. Thus it is similar to a fully active control in that it is capable of both power input and power dissipation but differs in that it is assumed that the fully active system has no frequency response limitation in following the control law demand. In practice, the frequency response limitation of the slow-active system would be a function of the components, which might typically be pneumatic, hydraulic or electrical. However, in the mathematical model, an idealised frequency response limitation is imposed by a second order low pass filter, which enables the effect of various cut-off frequencies to be investigated. The behaviour of such system is linear and, therefore performance calculations including the total power and actuator space requirements can be done in the frequency domain but the power demand and dissipation of the slow actuator must be obtained by using the time domain.

In this chapter, three different forms of the control laws are used in studying active systems: four, two and single state feedback. The chapter is then divided into five different parts. The first part introduces the slow-active model and control using the four and two state feedback forms. The second part presents the design and performance properties of the four and two state feedback slow-active systems in order to investigate the effect of frequency response limitations in the actuator. The effect of the passive spring and damper rates on the performance are also studied. The third part evaluates the performance capabilities including the power requirements of the slow-active systems. The fourth part introduces the idea of a single state feedback active system, which is based on the principle of the slow-active system. A comparison between the slow-active and single state feedback active systems is also made. The last part summarises the concluding remarks

obtained throughout the calculations of the slow-active systems.

7.2 Slow-active model and control

The slow-active suspension model consists of an actuator connected in series with a passive spring and in parallel with a passive damper between the body and wheel of the vehicle as shown in Figure 7.1. In order to model the frequency response limitations associated with the actuator, a second order low pass filter is introduced into the feedback circuit. This technique actually introduces the response limitation into the control signal rather than the actuator output, but it nevertheless represents a convenient method for enabling the effect of the response limitation to be studied.

The equations of motion of the slow-active system can be rewritten using equations 3-2 and 3-3 as follows,

$$M_w \ddot{X}_w(t) + F(t) - K_t(X_0(t) - X_w(t)) = 0 \qquad 7\text{-}1$$

$$M_b \ddot{X}_b(t) - F(t) = 0 \qquad 7\text{-}2$$

$$\ddot{X}_{sb}(t) + 2\,\gamma\,\omega_f \dot{X}_{sb}(t) + \omega^2_f X_{sb}(t) - C_m\,\omega^2_f U_s(t) = 0 \qquad 7\text{-}3$$

in which,

$$K_s\,(X_w(t) - X_s(t)) + C_d\,(\dot{X}_w(t) - \dot{X}_b(t)) = F(t) \qquad 7\text{-}4$$

$$X_s(t) - X_b(t) = X_{sb}(t) \qquad 7\text{-}5$$

where X_{sb} is the required displacement of the slow actuator, C_m is actuator displacement coefficient which relates to the gain of the actuator (i.e. output/input demand), ω_f and γ are the natural frequency and damping ratio of the second order low-pass filter characteristic. The actuator demand signal $U_s(t)$ can be obtained by using a classical optimal control theory as discussed by Sharp and Hassan (1987). The equations 3-65 and 3-66 can be used to represent the state space form of the

slow-active system so that the matrix A_1, the vectors X, b_1 and d are,

$$A_1 = \begin{pmatrix} -2\pi\alpha V & 0 & 0 & 0 & 0 & 0 & 0 \\ 0 & 0 & 0 & 1 & 0 & 0 & 0 \\ 0 & 0 & 0 & 0 & 1 & 0 & 0 \\ \frac{K_t}{M_w} & \frac{-(K_t+K_s)}{M_w} & \frac{-K_s}{M_w} & \frac{-C_d}{M_w} & \frac{C_d}{M_w} & \frac{K_s}{M_w} & 0 \\ 0 & \frac{K_s}{M_b} & \frac{K_s}{M_b} & \frac{C_d}{M_b} & \frac{-C_d}{M_b} & \frac{-K_s}{M_b} & 0 \\ 0 & 0 & 0 & 0 & 0 & 1 & 0 \\ 0 & 0 & 0 & 0 & 0 & -\omega_f^2 & -2\gamma\omega_f \end{pmatrix}$$

$$X = \begin{pmatrix} X_0 \\ X_1 \\ X_2 \\ X_3 \\ X_4 \\ X_5 \\ X_6 \end{pmatrix}, \qquad b_1 = \begin{pmatrix} 0 \\ 0 \\ 0 \\ 0 \\ 0 \\ 0 \\ C_m\omega_f^2 \end{pmatrix} \text{ and } \qquad d = \begin{pmatrix} GV \\ 0 \\ 0 \\ 0 \\ 0 \\ 0 \\ 0 \end{pmatrix}.$$

The output matrix C and the weighting matrix Q are;

$$C = \begin{pmatrix} -1 & 1 & 0 & 0 & 0 & 0 & 0 \\ 0 & -1 & 1 & 0 & 0 & 0 & 0 \\ 0 & K_s & -K_s & C_d & -C_d & -K_s\omega_f^2 & 0 \end{pmatrix}, \qquad Q = \begin{pmatrix} q_1 & 0 & 0 \\ 0 & q_2 & 0 \\ 0 & 0 & q_3 \end{pmatrix} \qquad 7\text{-}6$$

In this type of suspension system, the body mass is supported on the wheel mass via active and passive elements and therefore, the performance index is formulated as follows,

$$J = \lim_{t\to\infty} E\,[q_1 (X_0 - X_w)^2 + q_2 (X_w - X_b)^2 + q_3 (\ddot{X}_b)^2] \qquad 7\text{-}7$$

In this study, the four and two state feedback forms of the active control law

are used, and the technique to obtain the feedback gains for both forms is based on a numerical solution of the Liapunov equations (Wilson et al (1986)) as discussed previously in section 3.5.3.

7.2.1 Four state feedback control form

The first form of the control law is a function of the displacements and velocities of the vehicle body and wheel,

$$U_s(t) = K_{d1} X_w(t) + K_{d2} X_b(t) + K_{d3} \dot{X}_w(t) + K_{d4} \dot{X}_b(t) \qquad 7\text{-}8$$

where K_{d1} to K_{d4} are feedback gains and $X_w(t)$, $X_b(t)$, $\dot{X}_w(t)$ and $\dot{X}_b(t)$ are the state variables of the model. The auxiliary matrix M of the four state feedback form is,

$$M = \begin{pmatrix} 0 & 1 & 0 & 0 & 0 & 0 & 0 \\ 0 & 0 & 1 & 0 & 0 & 0 & 0 \\ 0 & 0 & 0 & 1 & 0 & 0 & 0 \\ 0 & 0 & 0 & 0 & 1 & 0 & 0 \end{pmatrix} \qquad 7\text{-}9$$

7.2.2 Two state feedback control form

The second form of control law is a function only of the velocities of vehicle body and wheel as follows,

$$U_s(t) = K_{d3} \dot{X}_w(t) + \dot{K}_{d4}(t) \qquad 7\text{-}10$$

The auxiliary matrix M of the two state feedback form is,

$$M = \begin{pmatrix} 0 & 0 & 0 & 1 & 0 & 0 & 0 \\ 0 & 0 & 0 & 0 & 1 & 0 & 0 \end{pmatrix} \qquad 7\text{-}11$$

7.3 Design and performance properties

The design properties of the slow-active systems are defined by the feedback gains of the control law (K_{d1} to K_{d4}) and performance index J and the performance properties by the RMS ride comfort RCP, dynamic tyre load DTLP, suspension working space SWS, actuator force SLAF and actuator working space SLAWS. The actuator working space may be expressed as a percentage ratio of the total suspension working space as follows,

$$SLAWS\ \% = \frac{RMS\ actuator\ working\ space}{RMS\ suspension\ working\ space}\ 100 \qquad 7\text{-}12$$

It is a measure of the required displacement of the slow actuator compared to the workspace usage of the suspension system.

The results of the slow-active systems are generated for the following conditions. Firstly, the road input and basic elements of the model are the same as described in 2-7 and 3-4. Secondly, the actuator is designed to give a displacement coefficient, C_m, of 1. Thirdly, the second order low-pass filter is designed to give a damping ratio, γ, of 0.707. It is also designed to give a cut-off frequency, ω_f, of 3 Hz as a baseline reference. Table 7.1 gives the RMS dynamic tyre load, ride comfort, suspension working space and actuator working space variation as well as the mean values of both the actuator power demand/dissipation and the damper power for five groups of the two state feedback slow-active systems. These systems refer to different sets of the weighting parameters in the performance index, denoted q_1, q_2 and q_3. They also refer to different sets of the body natural frequencies and damper coefficients denoted by F_n and C_d.

For the two state feedback slow-active systems ASL1, ASL2 and BSL1 to BSL6 in table 7.1, the corresponding four state feedback slow-active systems

CASL1, CASL2 and CBSL1 to CBSL6 are also calculated using all the same parameters in order to compare directly the two and four state feedback control forms of the slow-active system. The design and performance properties of the two state feedback systems in group ASL are compared with the corresponding four state feedback systems as shown in Figures 7.2 and 7.3 for cut-off frequencies, ω_f, of up to 30 Hz. The results indicate that the performance of the four state feedback form is similar to that obtained by using the two state feedback form and, therefore, the latter control form is preferable in view of its reduced requirements in measured parameters.

The effect of the spring stiffness and damper coefficient on the design and performance properties of the two state feedback slow-active systems is calculated in group BSL, which is designed to include stiff, conventional or soft passive springs as well as hard or soft dampers. Results for the corresponding four state feedback slow-active systems CBSL1 to CBSL6 are shown in Figures 7.4, 7.5 and 7.6 for cut-off frequencies, ω_f, of up to 30 Hz. The results merit the following points. Firstly, the performance categories of the four state feedback systems are similar to those obtained for the two state feedback systems in group BSL at 3 Hz cut-off frequency. Secondly, for the stiff spring systems a lower performance index is obtained by using a hard damper, whereas for the soft spring a lower performance index is obtained with the soft damper. Thirdly, the hard damper systems increase the actuator working space and decrease actuator force. Fourthly, the performances of the slow-active systems are related to the passive elements in a similar way to that obtained for passive systems, i.e. the stiff spring or hard damper systems increase the ride discomfort and reduce the working space. Finally, the optimal cut-off frequency of the second order low-pass filter overall is 3 Hz and therefore, this value was used as a baseline reference in this study.

7.4 Performance and power requirements

The performance and power requirements of the two state feedback slow-active systems will be concentrated on in this section. Figures 7.7 and 7.8 show the transfer functions and PSD performances including the actuator working space of systems in groups ASL and CSL. The systems in group ASL are chosen to give equal dynamic tyre loads of 21.5% whereas the systems in group CSL are chosen to give equal suspension working spaces of 3.5 cm. Figure 7.7 shows the conflict between the ride comfort and working space whereas in Figure 7.8 the conflict between the ride comfort and dynamic tyre load is highlighted. The PSD working space or actuator space requirements of the slow-active system give one resonant peak and the actuator workspace is only affected by the road input conditions within the frequency range of up to 3 Hz because of the actuator's frequency response limitations whereas the other performance figures are not.

In terms of the power requirement, the force levels demanded from the actuator of the slow-active system are likely to be high because the actuator always supports the static vehicle weight unless a method can be found of supporting the static vehicle weight by placing an additional spring in parallel with the actuator. The resulting equations of motion of this form of the slow-active system remain exactly the same, although the forces generated by the actuator will now be different. Thus, the overall performance of the system with a spring in parallel with the actuator is exactly the same as described in the previous section but the actuator forces, and hence, powers are changed. The actuator remains as before- driven by a displacement demand signal- and the force it has to produce changes by an amount exactly equal to the fluctuating force in the parallel spring (i.e. dynamic force - static force due to the body weight). In practice, the parallel spring arrangement appears attractive from a power consumption viewpoint and although the design appears imprac-

tical with metallic spring elements, it could in principle be achieved in pneumatic or hydro-pneumatic systems. The requirements of the actuator force can be summarised by the following equations.

$$SLAF(t) = K_s\,(X_w(t) - X_s(t)) + \textit{Static load of vehicle body} \qquad 7\text{-}13$$

$$SLAF(t) = K_s\,(X_w(t) - X_s(t)) - \textit{Additional spring force} \qquad 7\text{-}14$$

The calculation of the power requirements therefore reveal how much power would be used by a slow actuator and damper which are assumed to be 100% efficient. These idealised calculations reveal the fundamental differences between competing layouts of the slow-active concept. Further power losses due to the inevitable inefficiencies in the components would depend on the detail design of the components used in a practical design. Results for slow-active systems over a wide range of suspension workspace are included in group DSL. The alternative implementations of the systems are (i) an actuator only mounted between the body and the spring (SAc1), (ii) an actuator in parallel with an additional spring designed to give a natural frequency of 1.27 Hz (SAc2) or (iii) 1.01 Hz (SAc3). In all cases, the performance is the same but the power flows are different as shown in figure 7.9. In particular, the actuator in version SAc1 must generate higher forces, as in equation 7-13, since it carries the static load of the vehicle. As expected, the incorporation of the parallel spring results in a substantial reduction in required actuator power for SAc1, the mean power demand is always between 1 and 2 kW, whereas for SAc2 it is less than 0.3 kW and for SAc3 less than 0.2 kW. The mean power dissipation is the sum of the powers dissipated in the actuator and the damper. The mean level is around 3 kW for SAc1, whereas it is only half this value for SAc2 and SAc3. The mean power demand of the actuator, RMS fluctuating powers of the passive spring and tyre all in general increase as the working space increases whereas the lowest power dissipation is obtained at the largest working space of 3.5

cm.

In fact, the power dissipation of the passive damper, the actuator relative displacements and velocities for all the versions are the same whereas the actuator forces and powers are not. To complete the comparison, the time histories of the actuator forces, power demand and dissipation of the system DSL2 for both versions SAc1 and SAc3 are calculated as shown in Figure 7.10. The results indicate that the mean actuator force of the version SAc1 is changed by an amount exactly equal to the static force due to the body and therefore, the power demand and dissipation are increased. The time histories of the power demand or dissipation look remarkably similar and high peak levels occur for both versions.

To complete the story, the time histories of the control force, actuator relative velocity, power demand and dissipation of the systems in groups ASL are calculated as shown in Figures 7.11 and 7.12. The results indicate that in addition to the power requirements, the peak values of actuator relative velocity also increase as working space increases. The peak values of control force for all the systems in group ASL are, however, similar. The time histories of the power demand and dissipation for the systems in group CSL are shown in figures 7.13 and 7.14. The results indicate that the values of power demand and dissipation all in general increase as dynamic tyre load decreases. This is in contrast to the fully active systems in which the power demand and dissipation increased as the working space or dynamic tyre load increased as shown earlier in tables 5.1 and 5.2.

The systems in group ESL are chosen to give 3.5 cm suspension working space and 22% dynamic tyre load RMS when operating on three different road surface/ vehicle speed (GV) combinations. The power demand and dissipation of the systems ESL1, ESL2 and ESL3 are shown in Figure 7.15 and 7.16. The slow-active systems give similar results to those obtained by the fully active systems when

operating on different road input conditions GV, as shown already in figure 5.9 and 5.10. Again, the mean power dissipation of the systems is increased by operating on a rough road, while the mean power demand is increased by operating on a smooth road. The outputs are proportional to the input condition, GV, but the power demand and dissipation are not related in a similar way. The curves look remarkably similar and high peak power demand and dissipation levels occur. Ignoring the transient features during the initial two seconds of the trace, peak values of around twenty times the mean power and the peak power demands up to 4 kW and peak power dissipation up to 20 kW are indicated.

The performance properties of the two state feedback systems are displayed in Figure 7.17 for two types of road input conditions at a working space of 3.5 cm. The responses of all the systems are proportional to the road input conditions, so that the performance of any slow-active system, studied for smoother or rougher road surface/vehicle forward speed combinations than that assumed are scaled down or scaled up in a similar way to the other linear suspension systems.

7.5 Single state feedback active system

The idea of the single state feedback, SSFB, active system is based on a hypothetical suspension system which only uses passive elements. The layout of the hypothetical and slow-active systems are the same except that the slow actuator of the latter is replaced by a passive damper. Equations 7-1 and 7-2 then remain the same to represent the equations of motion of the hypothetical system together with the following equation,

$$K_s\,(X_w(t) - X_s(t)) - AC_d\,(\dot{X}_s(t) - \dot{X}_b(t)) \qquad = 0 \qquad \text{7-15}$$

where AC_d, Ns/m, is the coefficient of the passive damper which replaces the slow actuator. In practical terms, the damper alone in series with a passive spring could

not support the static vehicle weight. It could in principle achieved by the single state feedback active system shown in Figure 7.18 which uses a group of passive and active elements in parallel, i.e. spring, damper and actuator instead of the actuator of the slow-active system. The SSFB active system uses an additional passive spring to support the static vehicle weight but it also needs an actuator to provide a force against the additional spring force. Therefore, the equations of motion of the hypothetical and SSFB active systems are the same. The control law of the SSFB active system is then a function of the relative displacement feedback, i.e. it can be calculated as follows,

$$U_a(t) = - \textit{Additional spring force} \qquad 7\text{-}16$$

It might be noted that the actuator is now different from those in previous slow-active layouts in that it is driven by a force (rather than a displacement) demand signal.

The performance of the single state feedback active system is compared with the two state feedback slow-active system for the following conditions. Firstly, the road input and the basic elements of the model are the same as described in 2-7 and 3-4. Secondly, the stiffness of the passive spring is 160 kN/m and the stiffness of the additional spring is the same. Thirdly, the power requirements calculated for a 100% efficient system with a flat frequency characteristic up to 15 Hz, which is the upper frequency limit of the calculations are: the fluctuating powers of spring/tyre elements, power dissipation of damper elements and actuator power generated against the dynamic force in the spring which is used to support the static vehicle weight. Fourthly, the feedback coefficient, AC_d, of the SSFB active systems is 160 kNs/m. Fifthly, the weighting factors of the slow-active systems are q_1= 5000, q_2= 5000 and q_3= 10^{-8}. The RMS ride comfort, dynamic tyre load and working space as well as the mean values of the power demand and dissipation for both SSFB active

and slow-active systems are plotted versus the damping ratio of the systems as shown in Figure 7.19. The damping ratios depend on the damper coefficients C_d and spring stiffnesses K_s of the systems. The SSFB active and slow-active systems give similar performance but the SSFB active systems give a reduction of the power dissipation over the slow-active systems. The power demand of the SSFB active system is less than for the slow-active system for damping ratios up to 0.2.

Another comparison of the performance capabilities of the single state feedback active and two state slow-active systems is made for different workspace usage. Figure 7.20 shows the ride comfort parameter versus the dynamic tyre load parameter at three values of working space: 2.5, 3.5 and 4.5 cm. The results indicate that the performance capabilities of the slow-active and SSFB active systems are the same. The SSFB system outlined in Figure 7.18 has the obvious practical drawback of requiring 5 separate components in the limited space available for the suspension. It also requires an actuator with a frequency response capability up to 15 Hz, although the forces demanded of the actuator are modest. However, if the actuator is removed and assuming that the spring is of conventional stiffness to support the body weight, then the performance reverts to that of a passive system. If the actuator is retained to provide a force against the dynamic force in the additional spring, then the system becomes similar to the slow-active system described earlier in this chapter.

7.6 Concluding remarks

The two and four state feedback versions of the slow-active systems give similar overall performance. Also, the performances of these systems relative to their passive elements vary in a similar way to that for conventional passive systems. The optimal performance index is obtained at 3 Hz cut-off frequency of the second order law pass-filter, the practical implication of this result being that the actuator

would only require a frequency response capability up to 3 Hz. The power demand and dissipation were reduced substantially by using an additional passive spring placed in parallel with the actuator without any change in the performance. The power demand is increased whereas power dissipation is decreased when operating on a smoother road. The single state feedback active systems give the same performance as the slow-active systems. The performances of the slow-active and SSFB active systems are proportional to the road input conditions GV whereas the power demand and dissipation of the slow-active systems are not related in a similar way. The single state feedback active system is attractive in that it requires the smallest number of measurements but in practice it would be difficult to fit all the necessary components into the limited space normally available for the suspension. It also demands an actuator with a higher frequency response than the other slow-active systems.

Overall, the slow-active arrangement looks attractive from the viewpoints of both performance and practical feasibility. Further investigations of such suspensions should be based on prototype design in which the component design, for example, electrical, hydraulic, pneumatic etc. is specified.

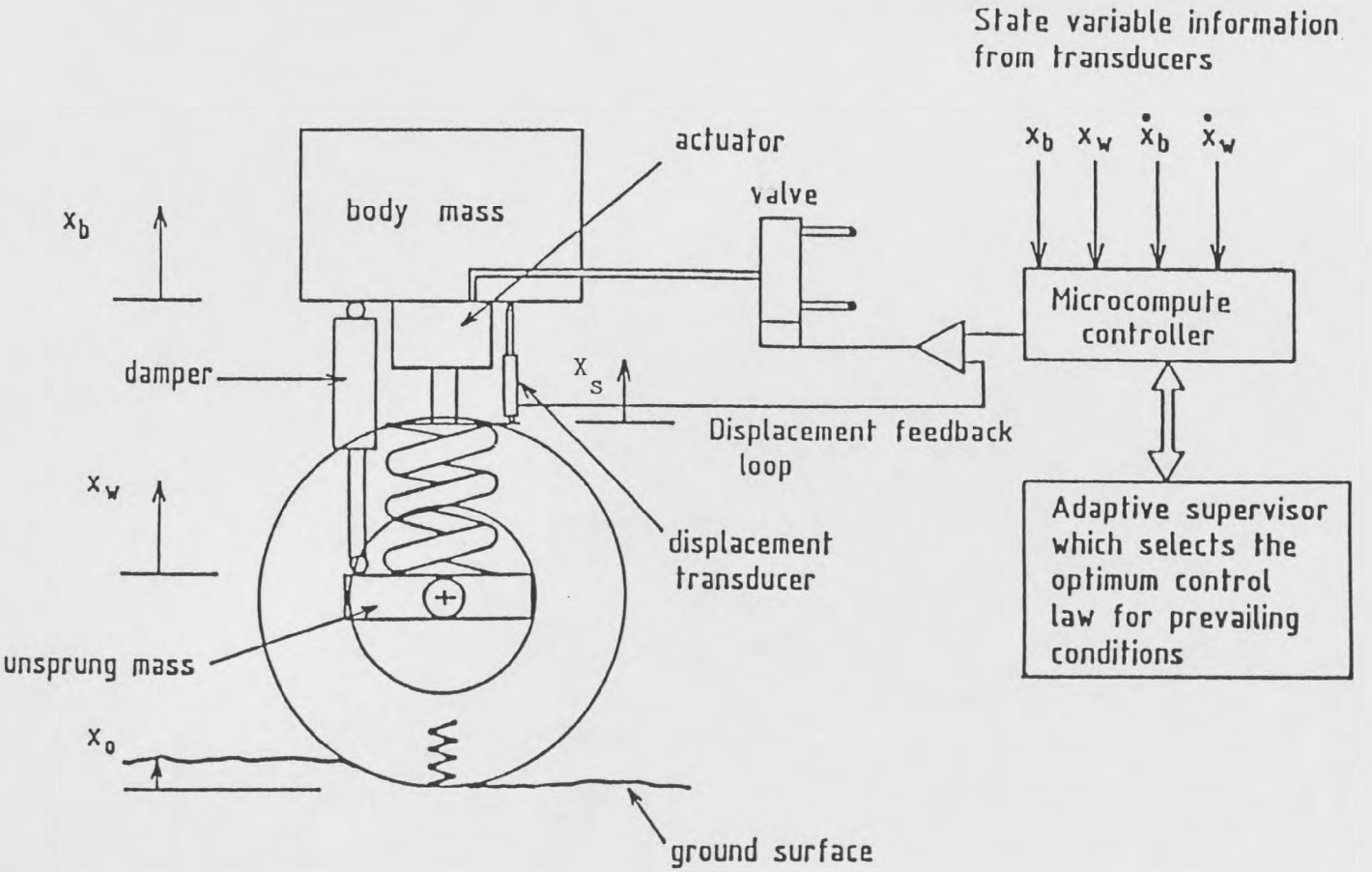

Figure 7.1 Quarter car slow-active suspension system.

Group	System	Weighting factors $q_3=10^{-8}$ and		F_n	C_d	RMS Performance of dynamic tyre load% DTLP, ride comfort RCP, working space SWS mm, actuator space SLAWS%, mean power demand MP+, mean power dissipation of actuator MP- and damper DP W						
		q_1	q_2	Hz	kNs/m	DTLP	RCP	SWS	SLAWS	MP+	MP-	DP
ASL	ASL 1	500000	20000	1.01	8.0	21.3	0.94	25.3	78	45	291	1137
	ASL 2	21.5	59.5	1.27	4.0	21.8	0.78	35.0	95	168	653	800
BSL	BSL 1	50000	500000	1.27	16.0	23.4	1.29	19.7	79	13	284	1195
	BSL 2	50000	500000	1.27	8.0	21.3	1.01	23.8	74	13	368	1046
	BSL 3	50000	50000	1.01	12.6	21.3	1.10	23.5	80	33	226	1215
	BSL 4	250	2000	1.01	6.3	21.6	0.83	28.5	72	27	286	1084
	BSL 5	500	5000	0.64	12.0	21.1	1.03	26.3	86	116	202	1283
	BSL 6	166.7	166.7	0.64	6.0	22.8	0.74	31.0	75	62	176	1192
CSL	CSL 1	800	5	1.01	8.0	20.7	0.93	34.2	98	298	549	1066
	CSL 2	4	18	1.01	4.0	23.6	0.70	35.6	87	152	494	933
	CSL 3	12500	3000	1.01	2.0	30.9	0.62	35.9	82	97	541	817
DSL	DSL 1	5000	5000	1.27	28.0	29.0	1.66	16.1	75	7	203	1345
	DSL 2	215	134.5	1.27	8.0	20.8	0.98	25.2	77	20	368	1038
	DSL 3	5000	5000	0.84	2.0	35.1	0.60	36.1	76	76	329	1014
	DSL 4	5000	5000	0.64	2.0	35.5	0.47	44.6	69	156	360	1011
ESL	ESL 1	21.5	59.5	1.27	4.0	21.8	0.78	34.7	95	159	641	790
	ESL 2	1700	1	1.01	2.0	22.3	0.47	34.7	95	291	598	418
	ESL 3	21.5	59.5	1.27	4.0	21.8	0.78	35.0	95	168	653	800

Table 7.1 Comparison of performances and power requirments for five groups of the two state feedback slow-active systems.

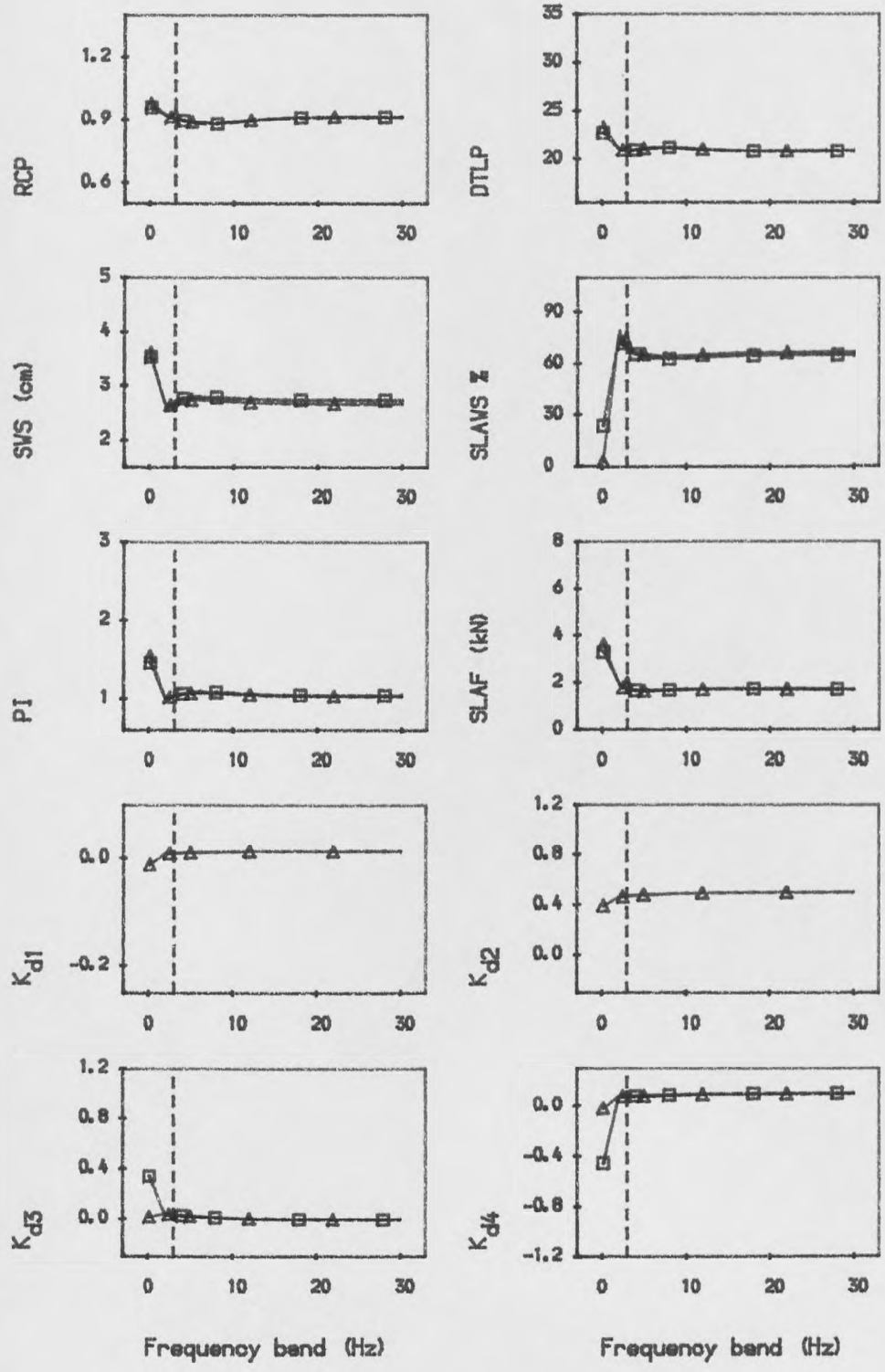

Figure 7.2. Comparison of the design and performance properties of the four and two state feedback of the slow-active systems.

△ △ Four state feedback system CASL1

□ □ Two state feedback system ASL1

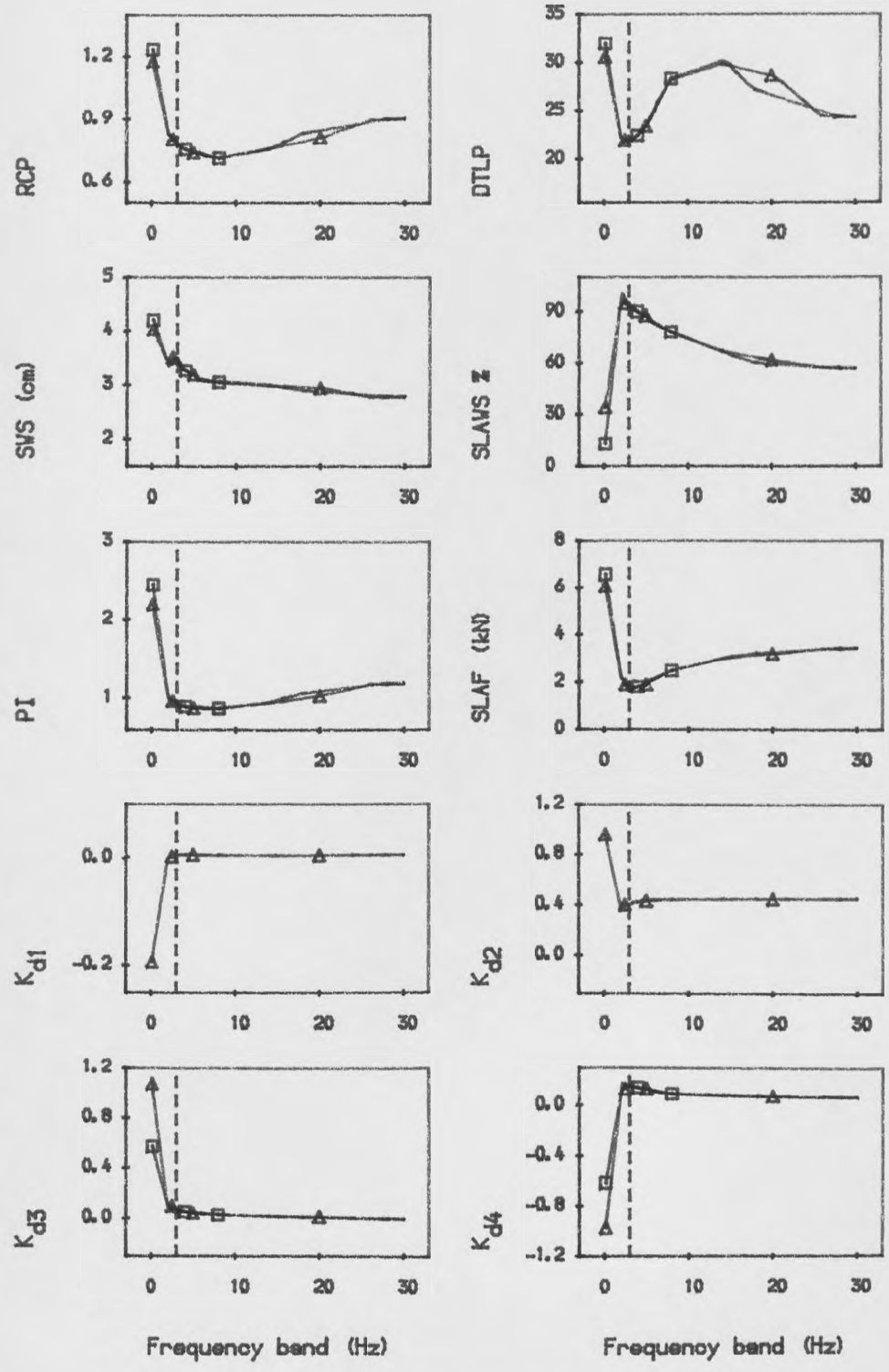

Figure 7.3. Comparison of the design and performance properties of the four and two state feedback of the slow-active systems.

△ △ Four state feedback system CASL2

□ □ Two state feedback system ASL2

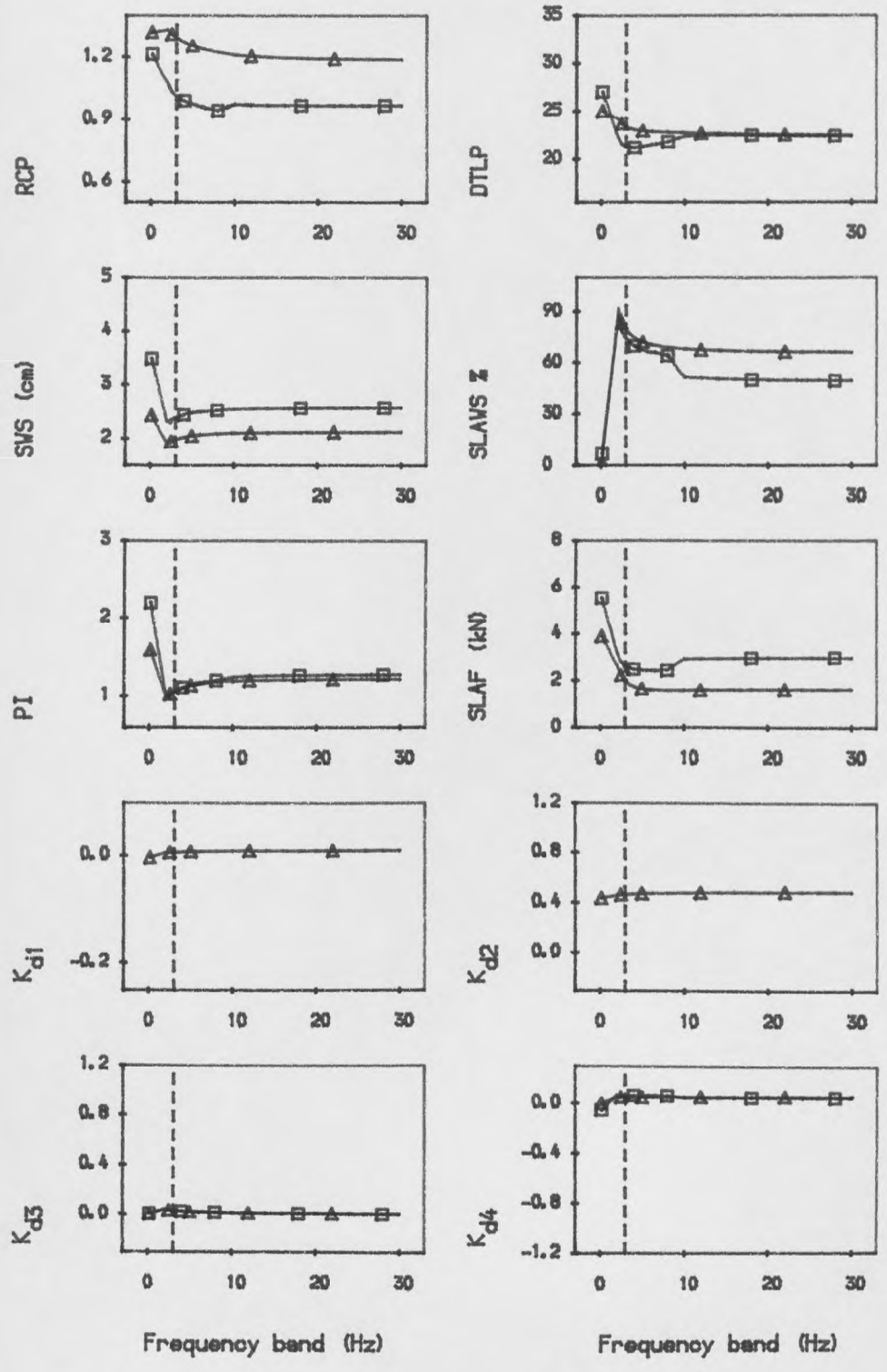

Figure 7.4. Design and performance properties of the slow-active systems versus cut-off frequency of the low-pass filter.

△ △ Four state feedback system CBSL1

□ □ Four state feedback system CBSL2

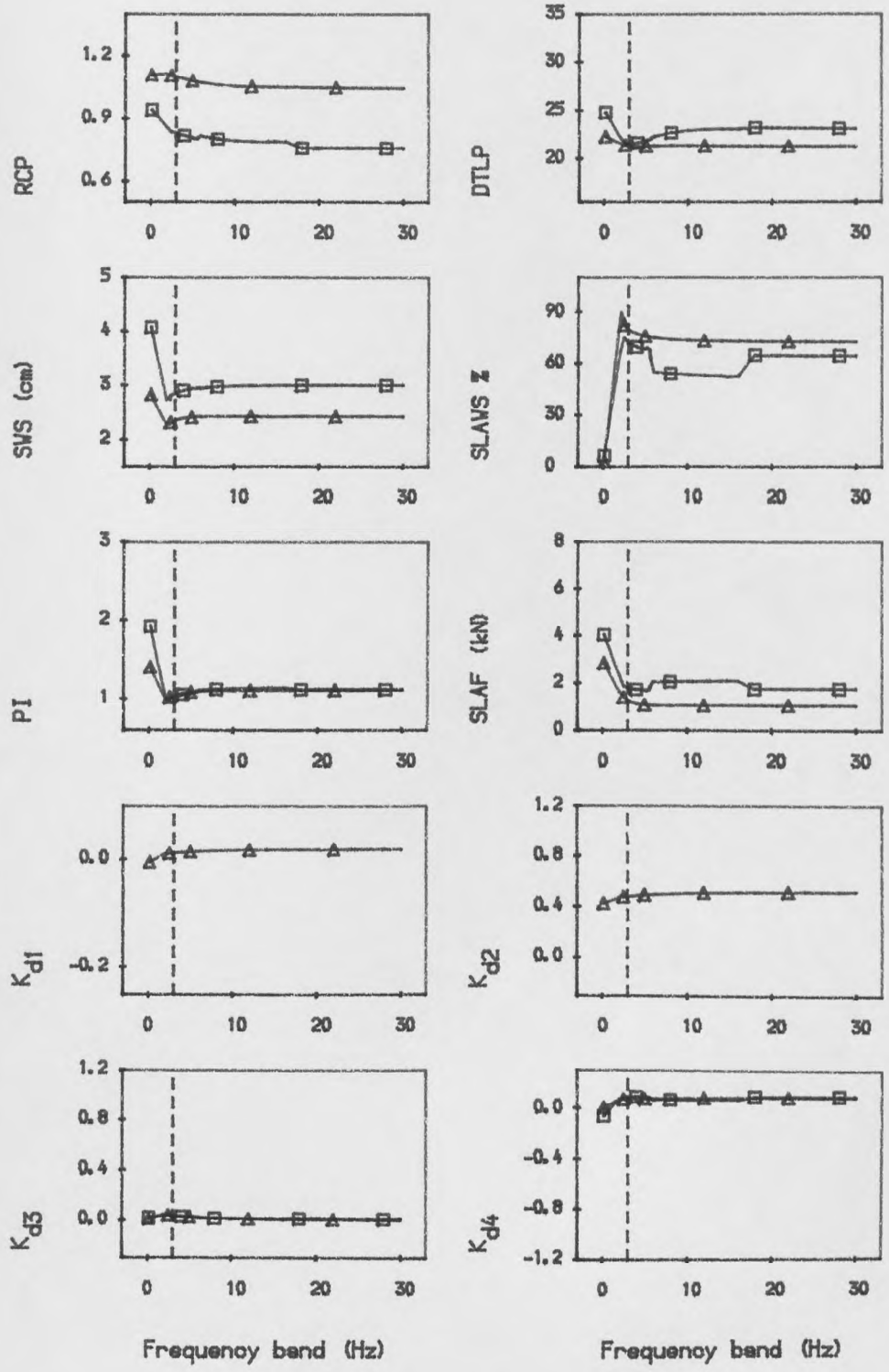

Figure 7.5. Design and performance properties of the slow-active systems versus cut-off frequency of the low-pass filter.

△ △ Four state feedback system CBSL3

□ □ Four state feedback system CBSL4

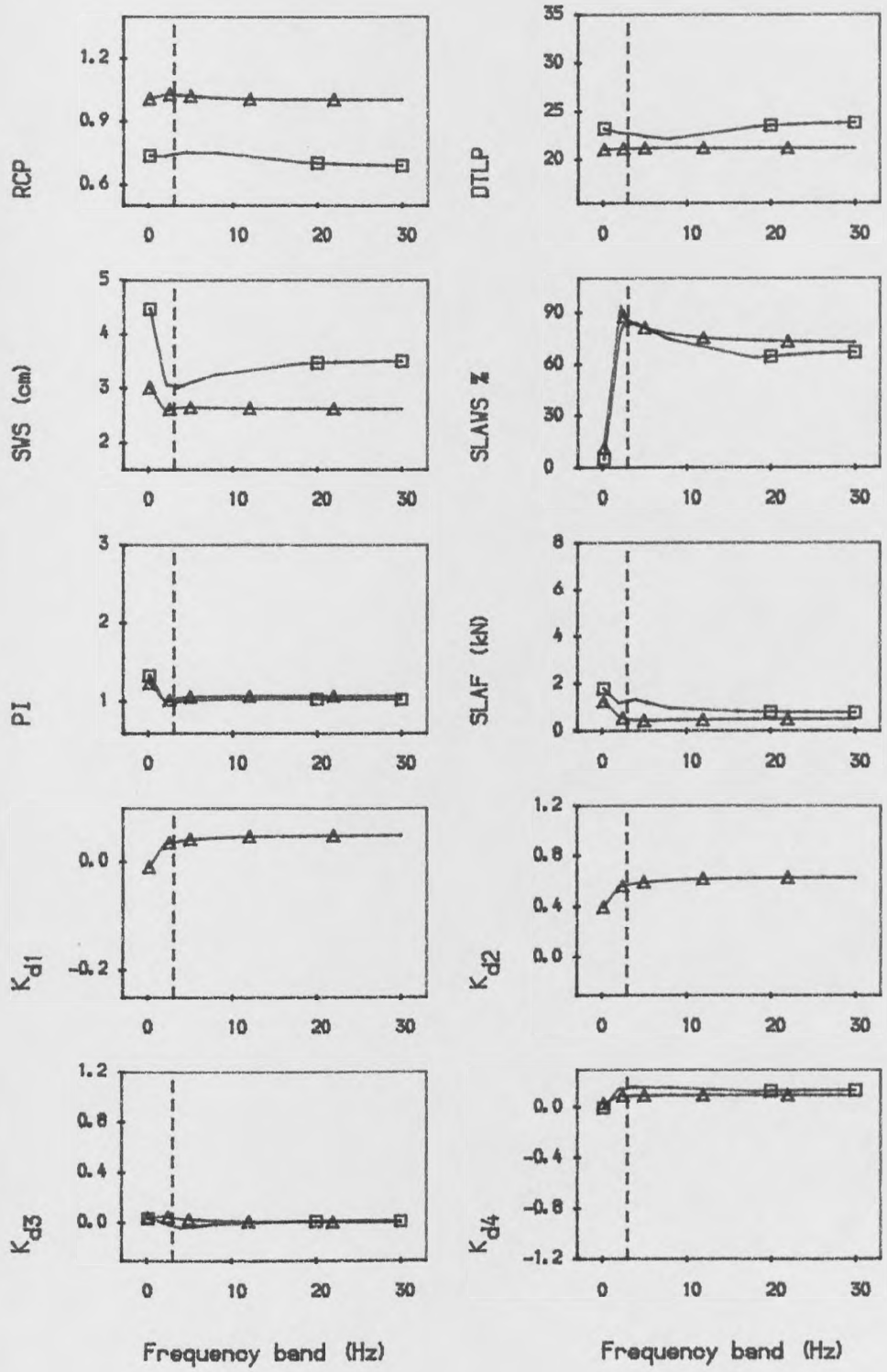

Figure 7.6. Design and performance properties of the slow-active systems versus cut-off frequency of the low-pass filter.

△ △ Four state feedback system CBSL5

□ □ Four state feedback system CBSL6

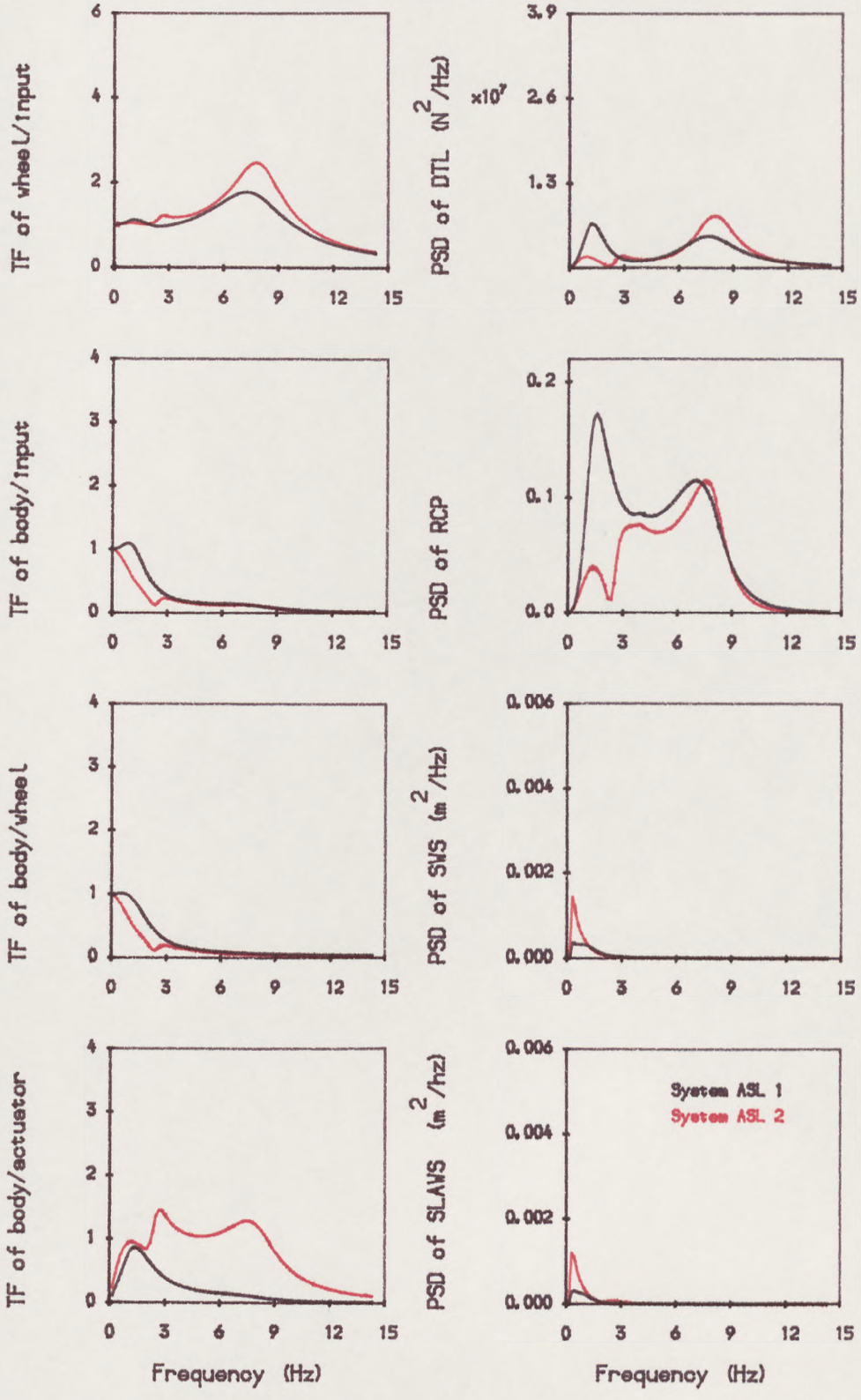

Figure 7.7. The transfer functions and PSDs of the two state feedback slow-active systems in group ASL.

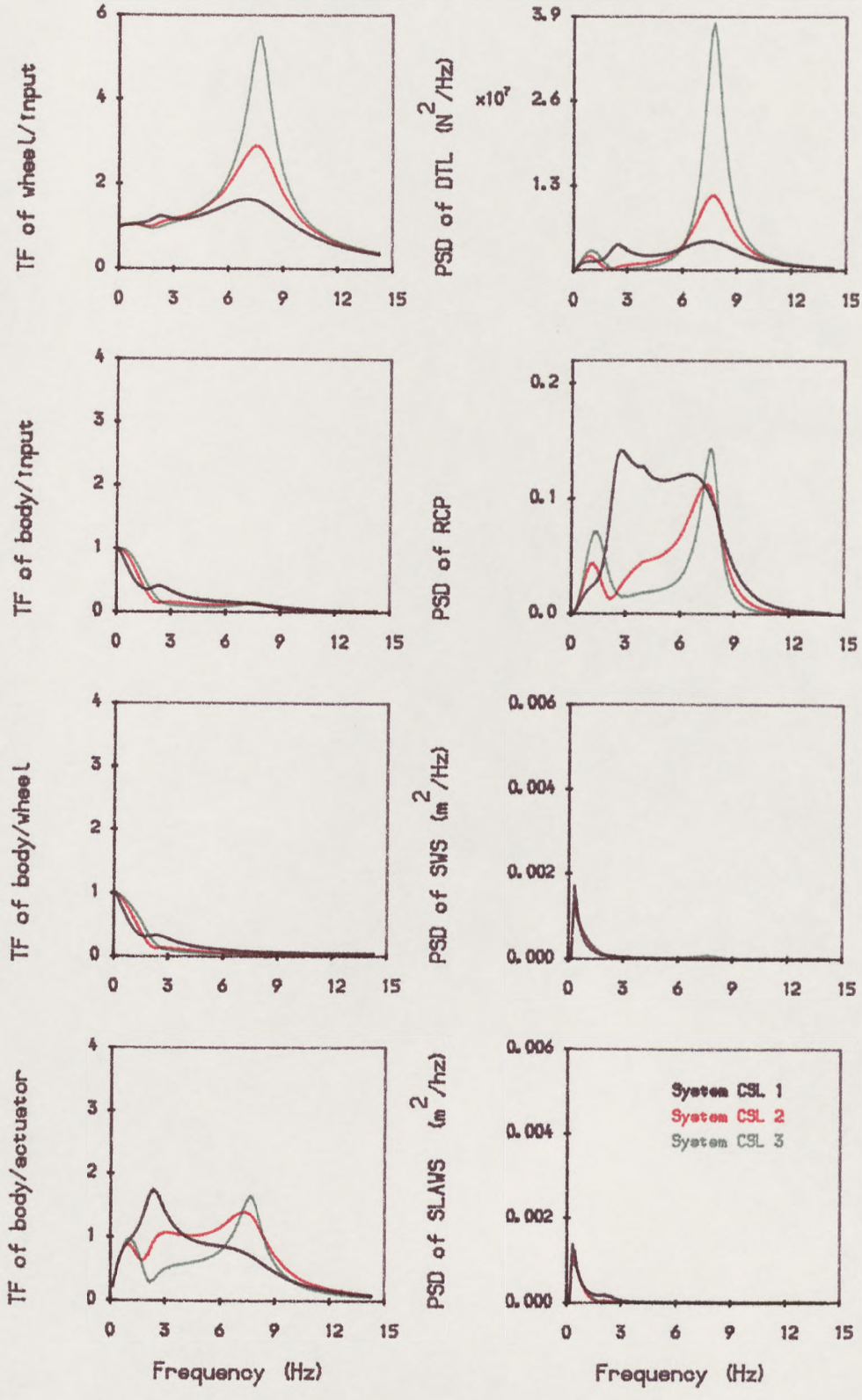

Figure 7.8. The transfer functions and PSDs of the two state feedback slow-active systems in group CSL.

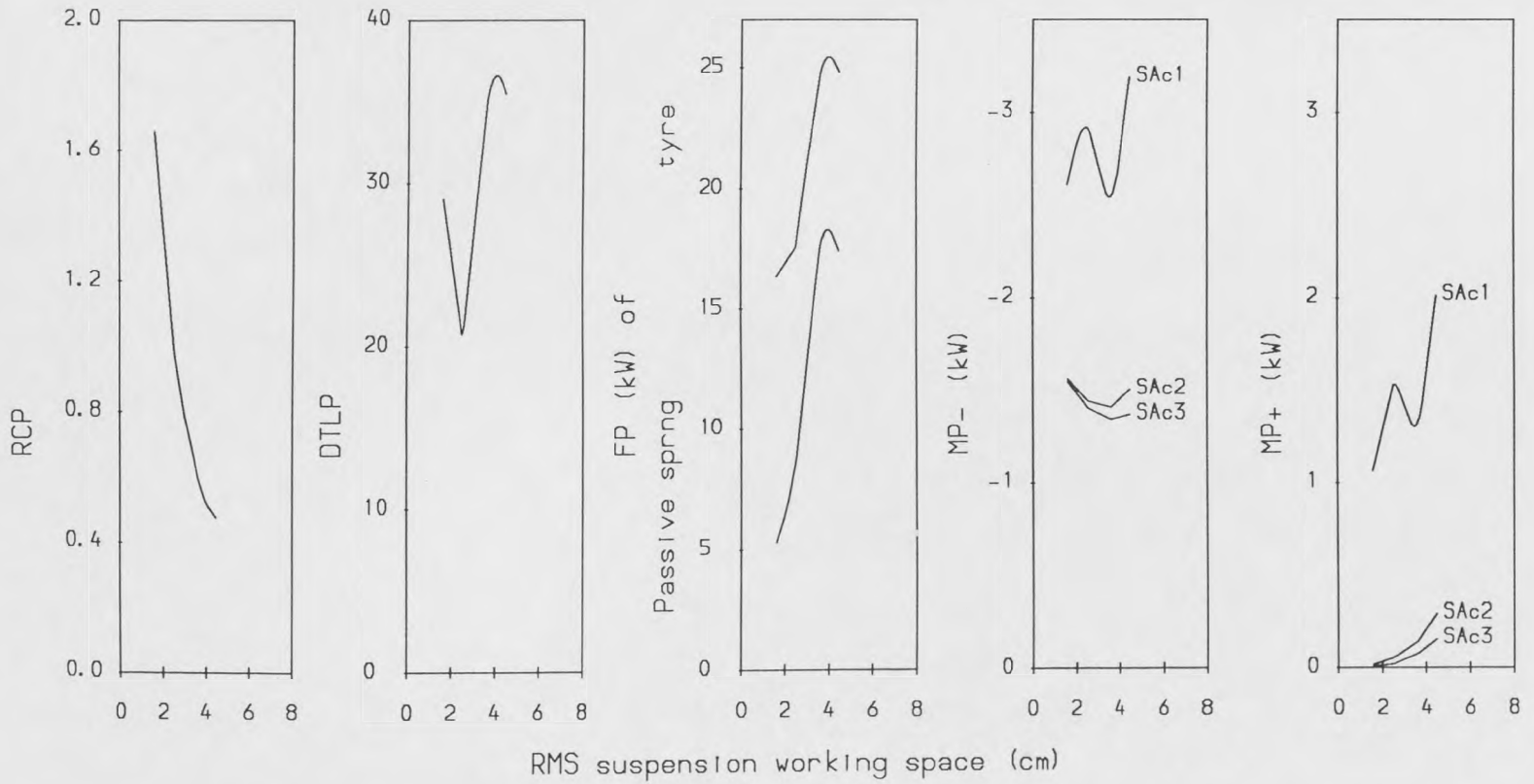

Figure 7.9. Comparison of various two state feedback slow-active systems: no passive spring SAc1, with additional spring SAc2 to give a natural frequency of 1.27 Hz and SAc3 to give a natural frequency of 1.01 Hz.

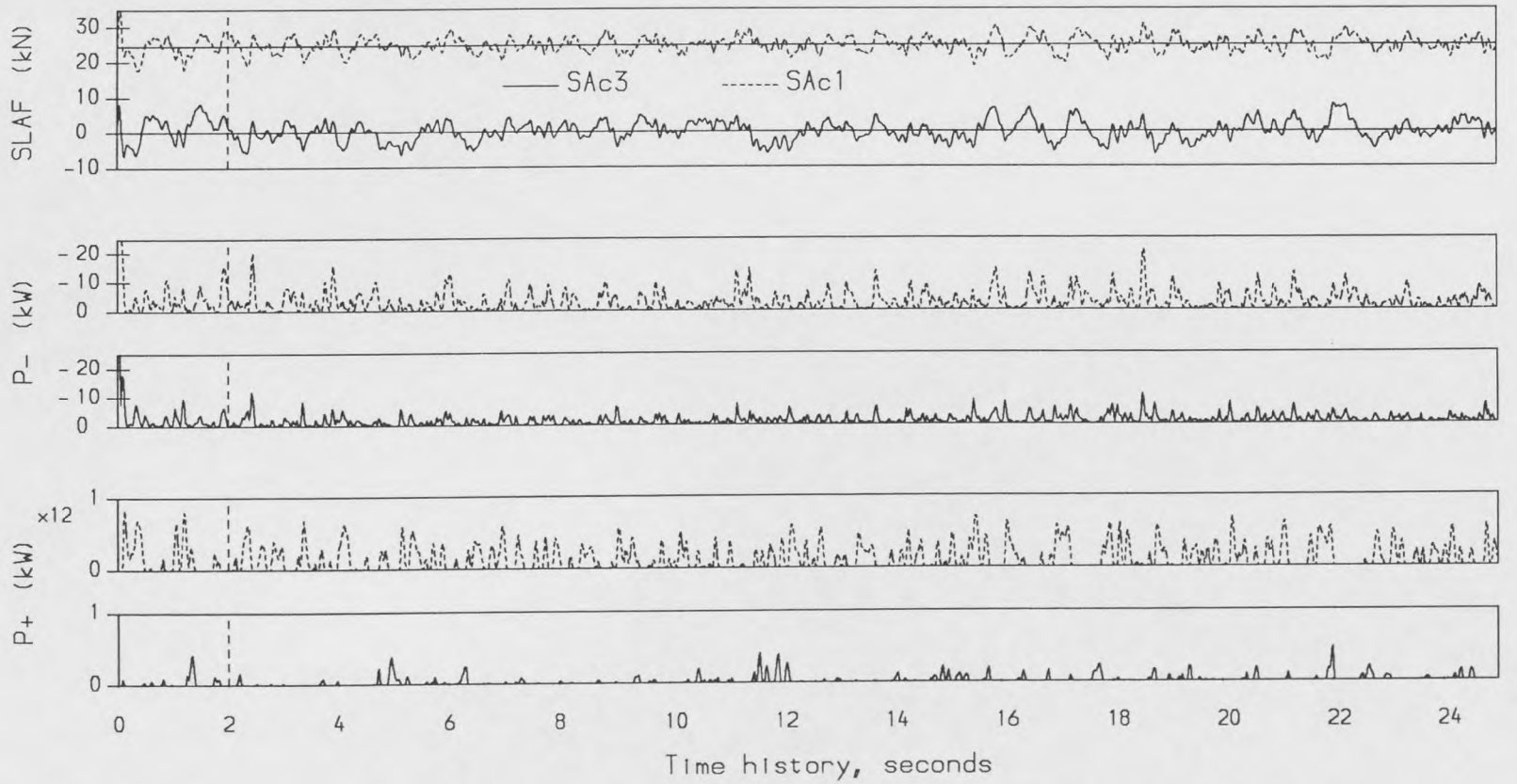

Figure 7.10. Time histories of the control forces, power demand and dissipation of the two state feedback slow-active system DSL2 versions: SAc1 and SAc3.

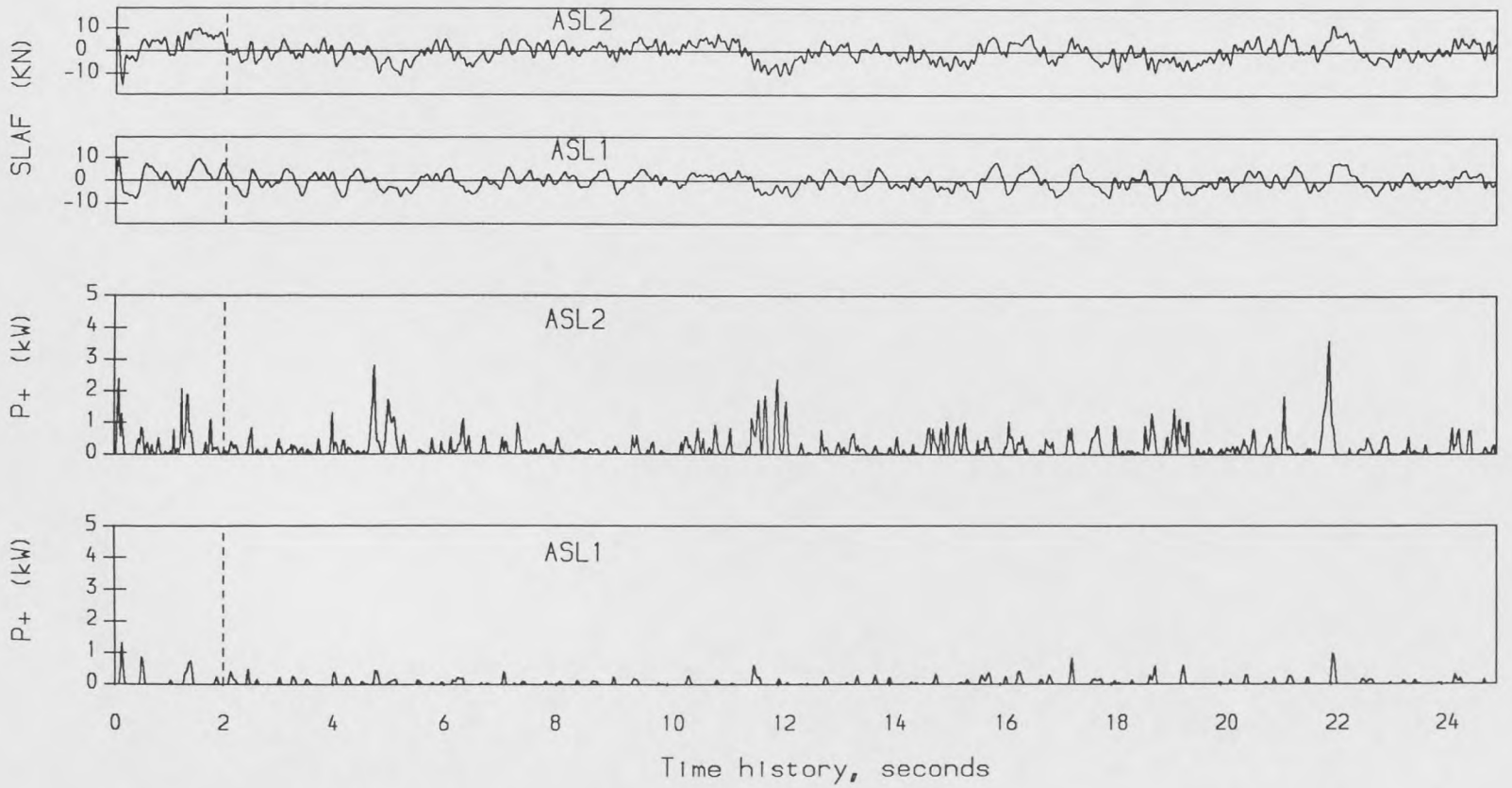

Figure 7.11. Time histories of the power demands and control forces of the two state feedback slow-active systems: ASL1 and ASL2.

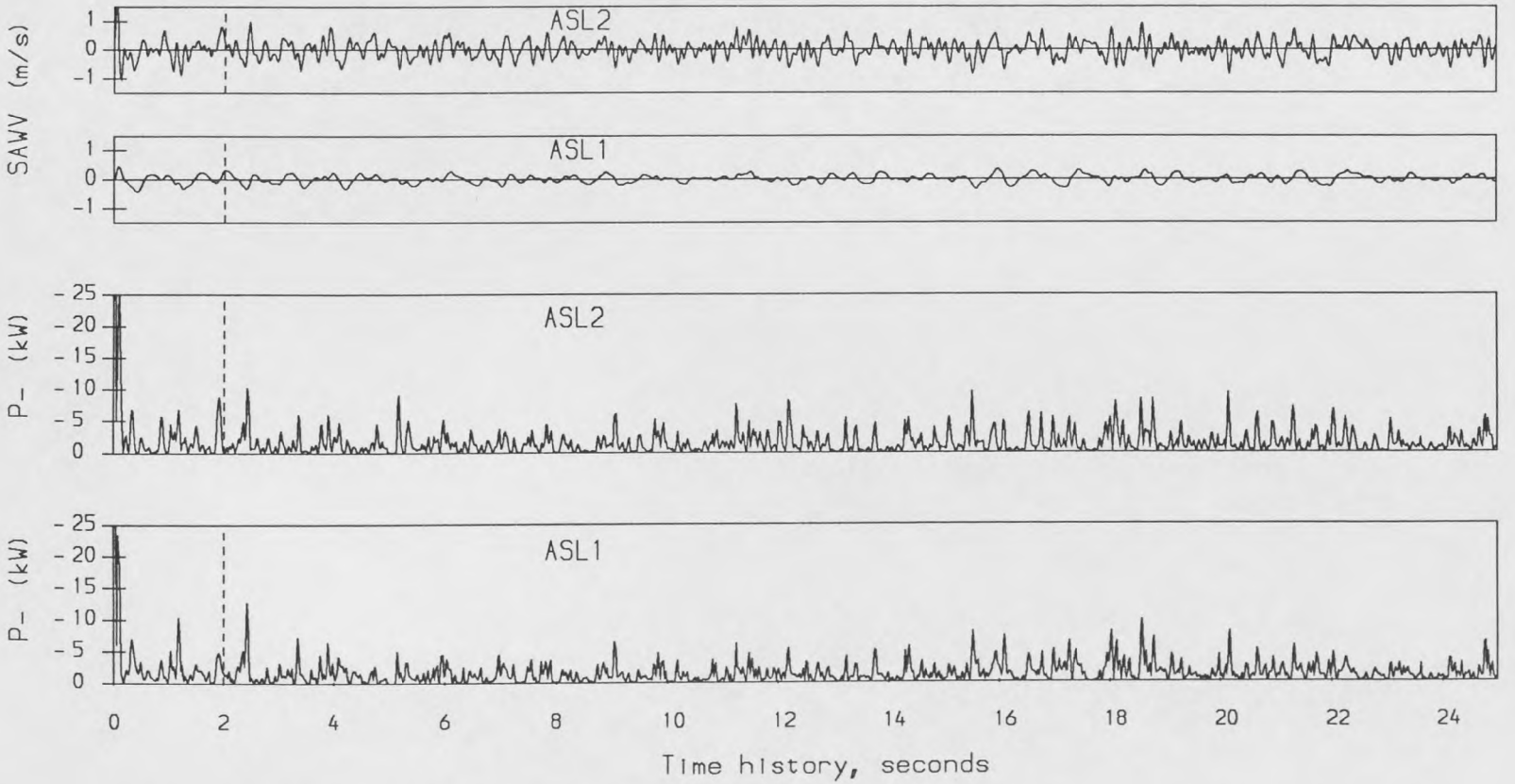

Figure 7.12. Time histories of the power dissipation and actuator relative velocity of the two state feedback slow-active systems: ASL1 and ASL2.

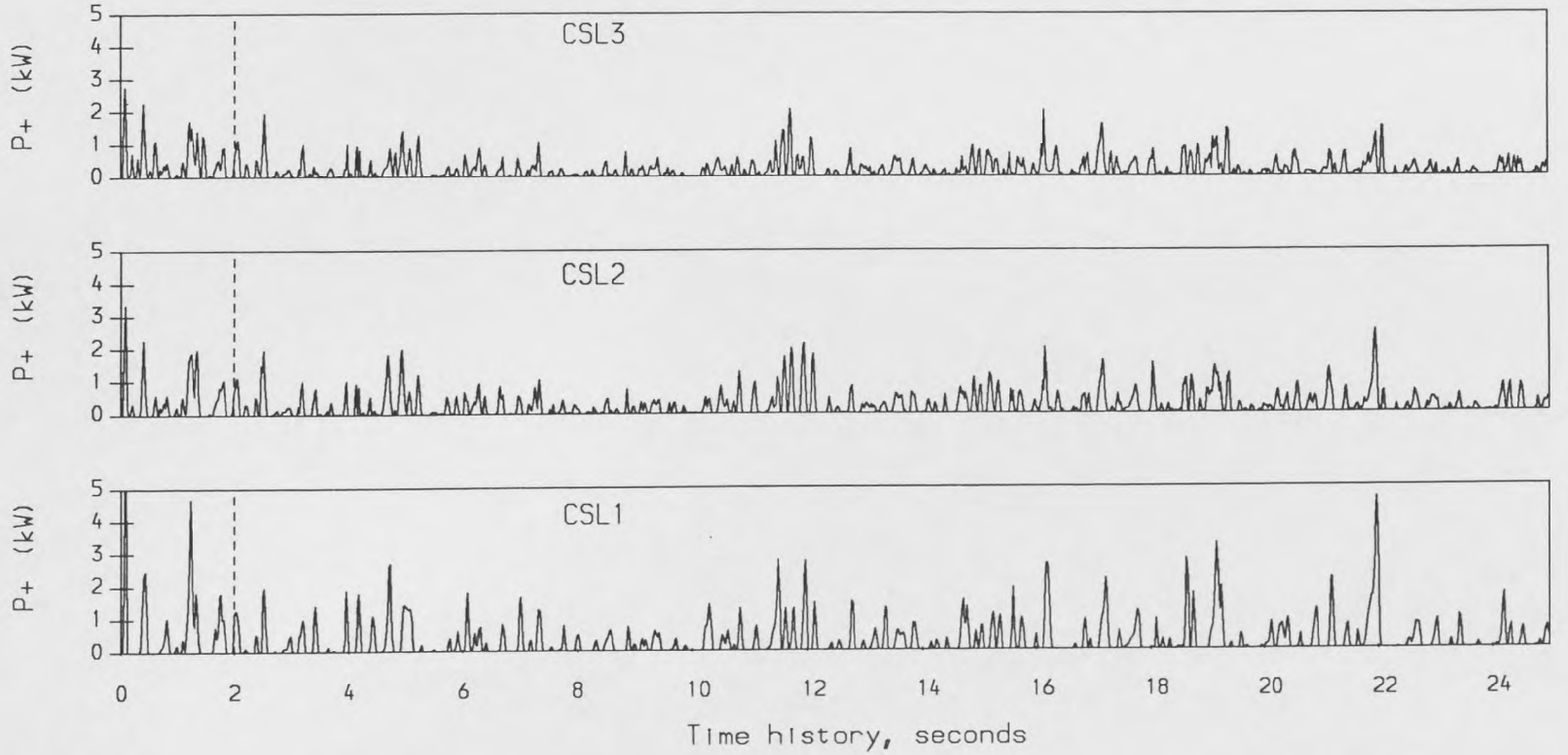

Figure 7.13. Time histories of the power demands of the two state feedback slow-active systems: CSL1, CSL2 and CSL3.

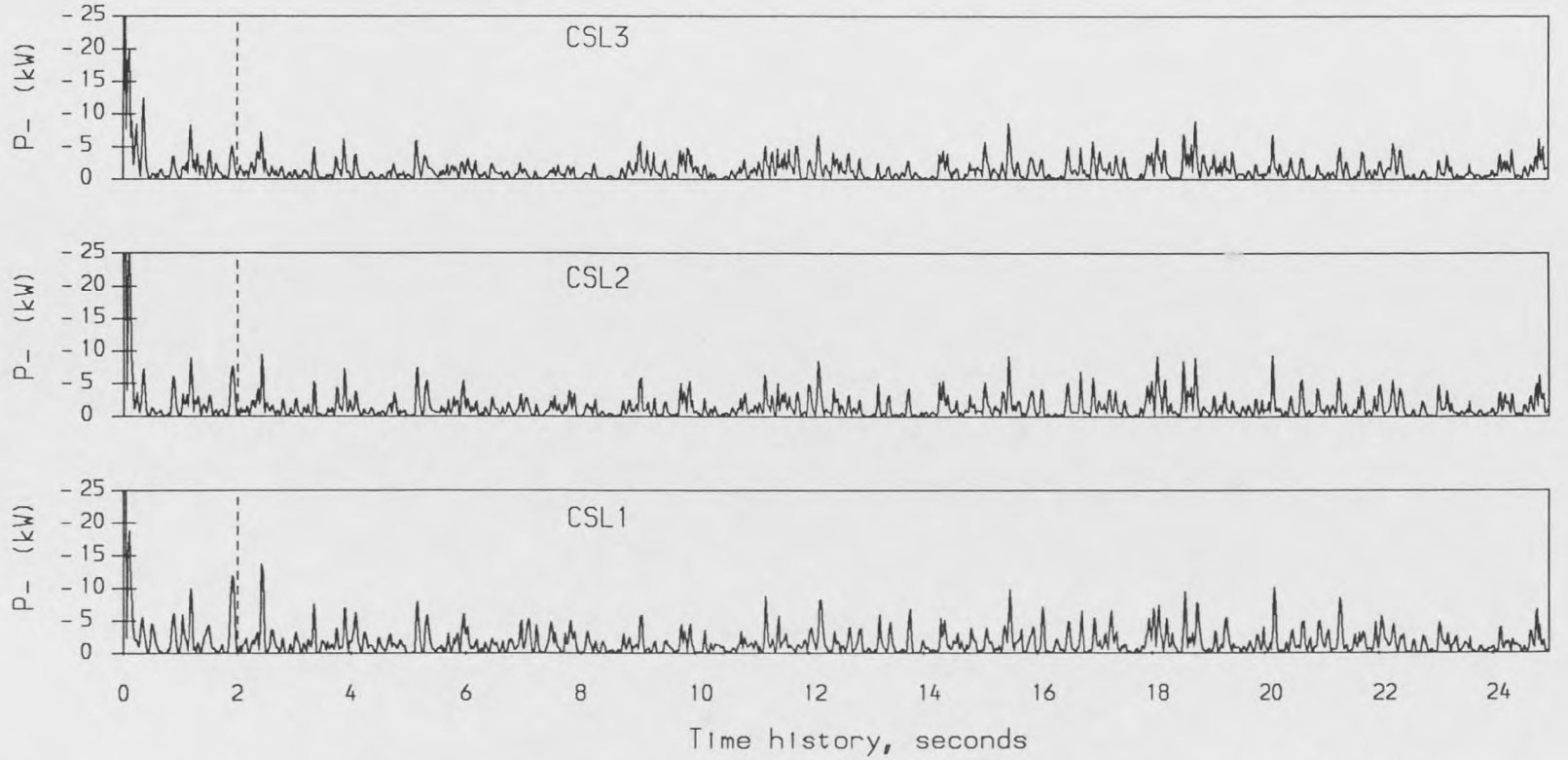

Figure 7.14. Time histories of the power dissipation of the two state feedback slow-active systems: CSL1, CSl2 and CSL3.

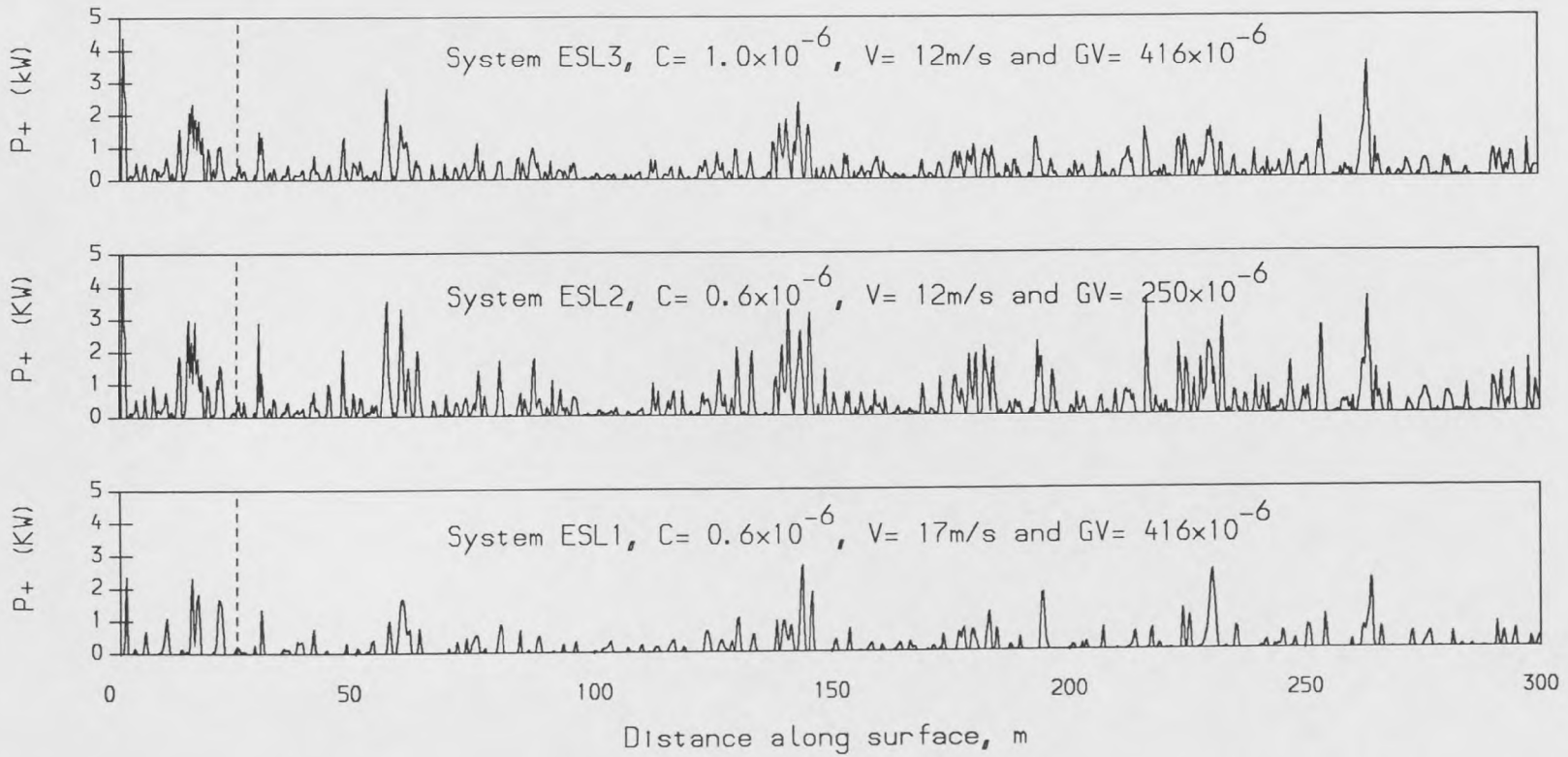

Figure 7.15. Power demands of the two state feedback slow-active systems at 3.5 cm RMS working space and 22% DTLP, group ESL, for 3 road input conditions.

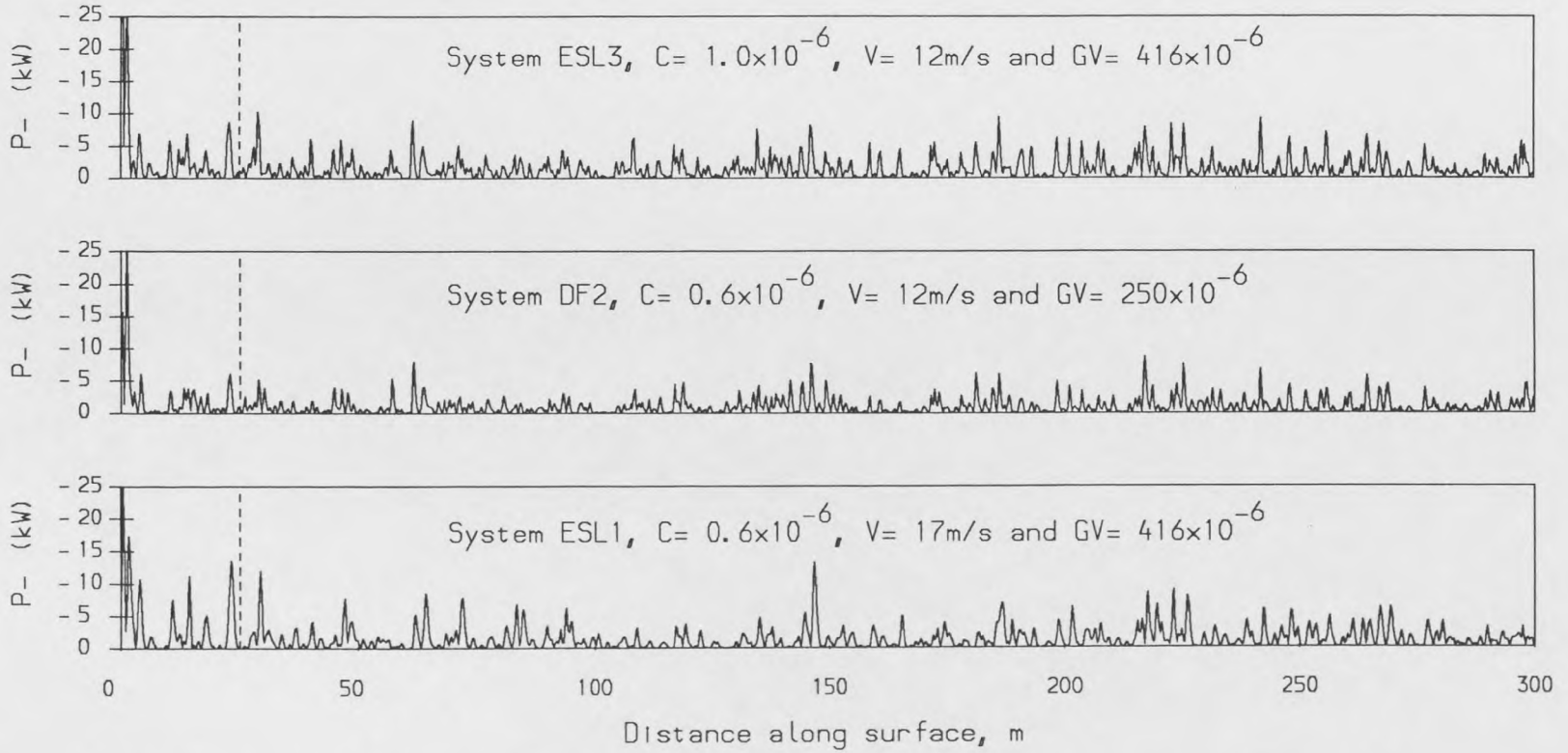

Figure 7.16. Power dissipation of the two state feedback slow-active systems at 3.5 cm RMS working space and 22% DTLP, group ESL, for 3 road input conditions.

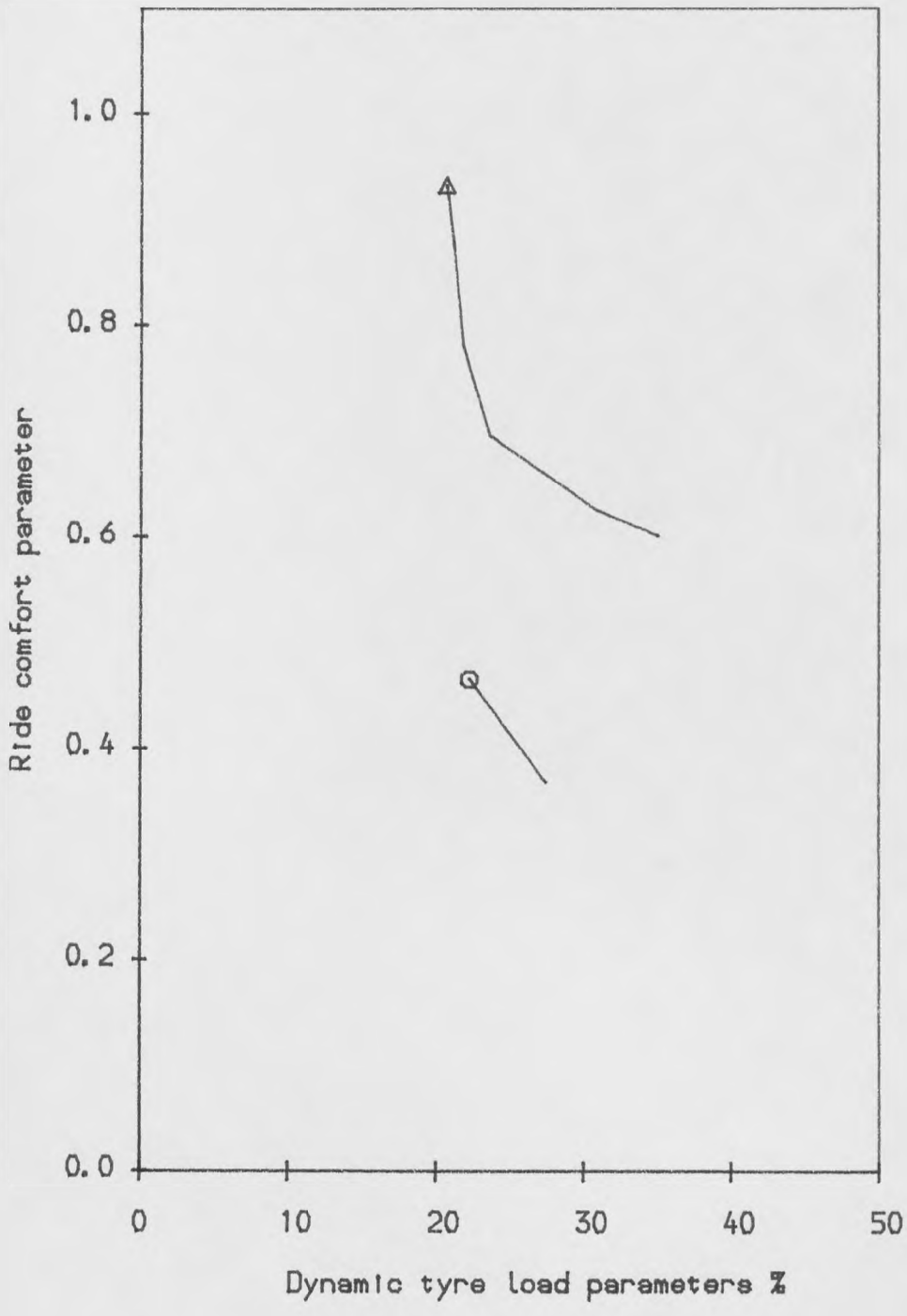

Figure 7.17. Comparison of performance of two state feedback slow-active systems at 3.5 cm RMS working space.

△ △ GV= 41.56×10^{-5} o o GV= 24.94×10^{-5}

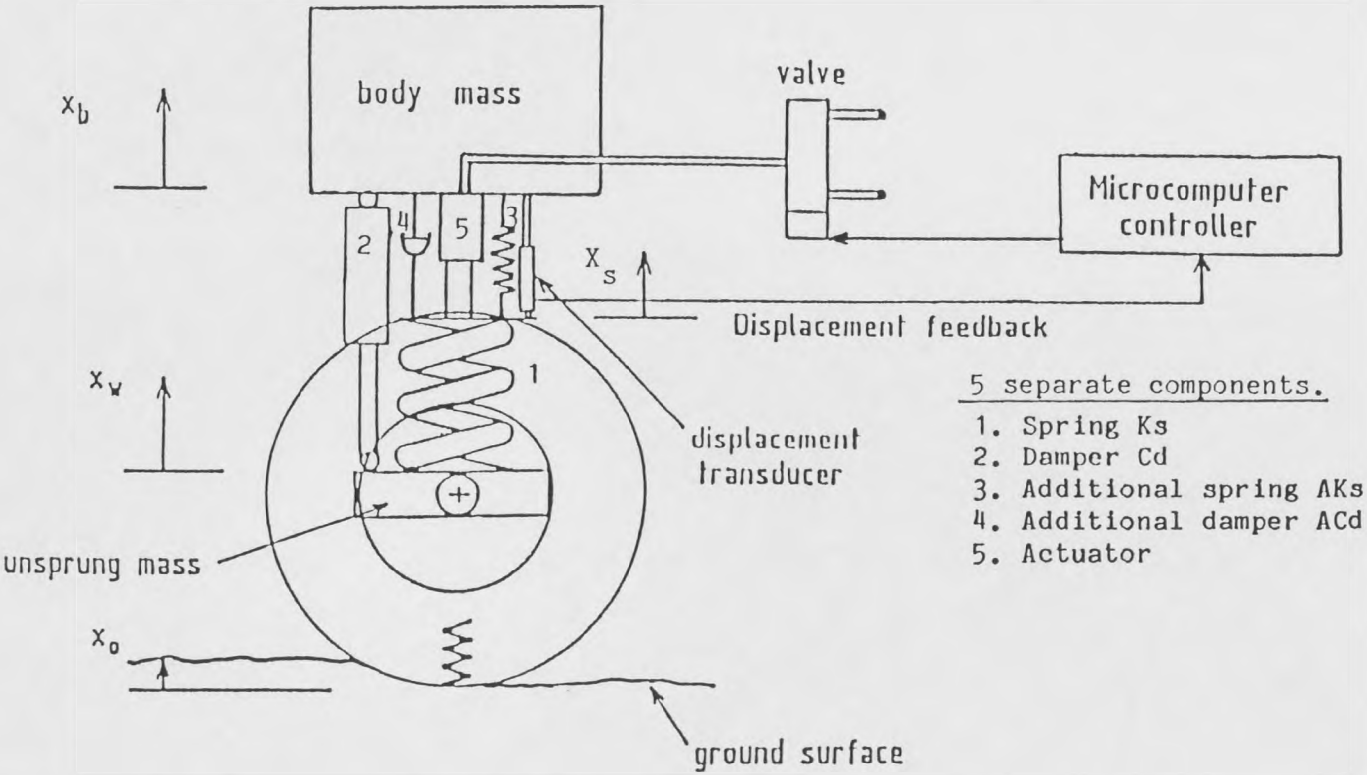

Figure 7.18 Quarter car single state feedback fully active suspension system.

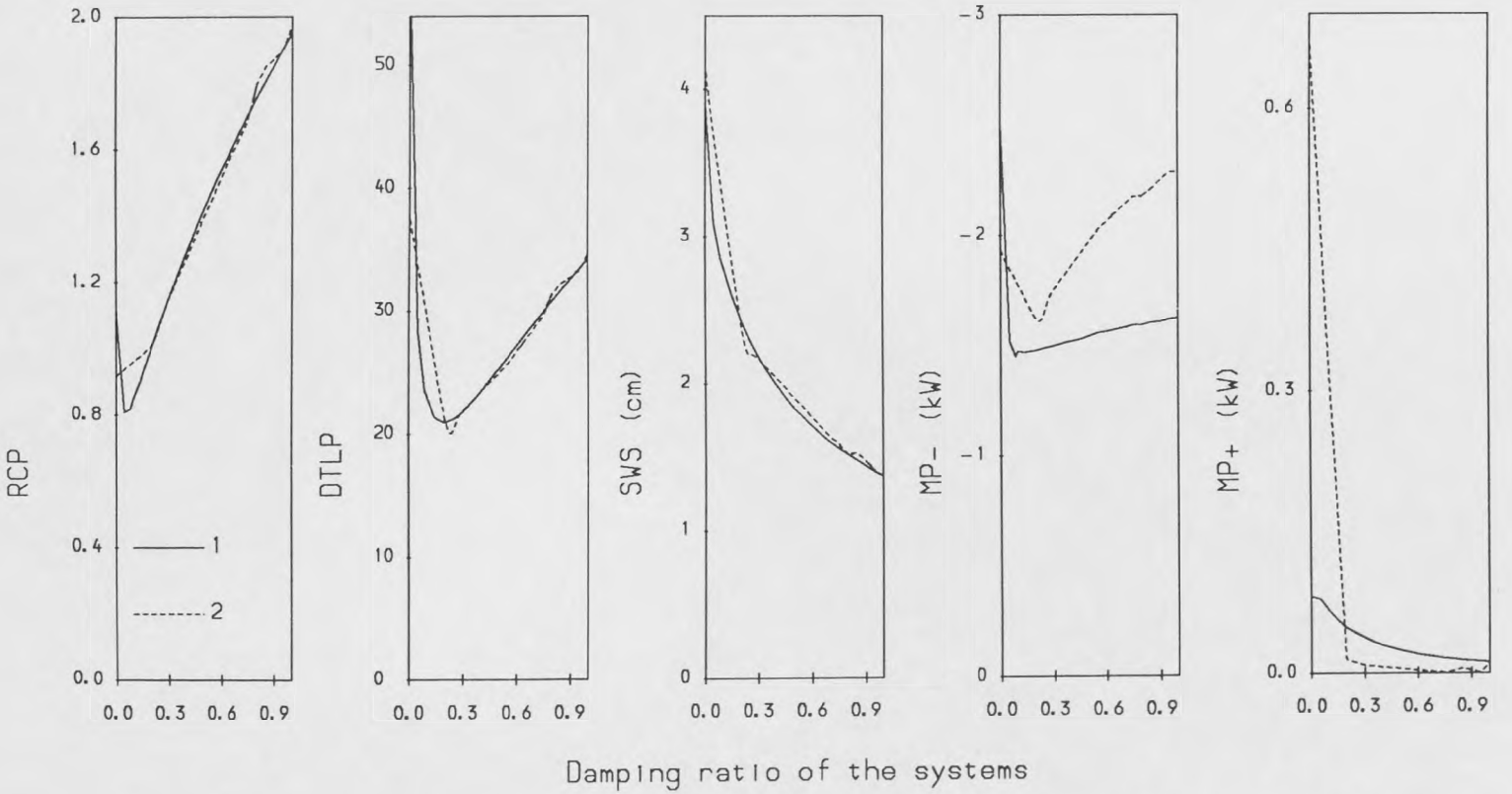

Figure 7.19. Comparison between the single state feedback active systems {1} and two state feedback slow-active systems {2} in terms of the performance and power requirements.

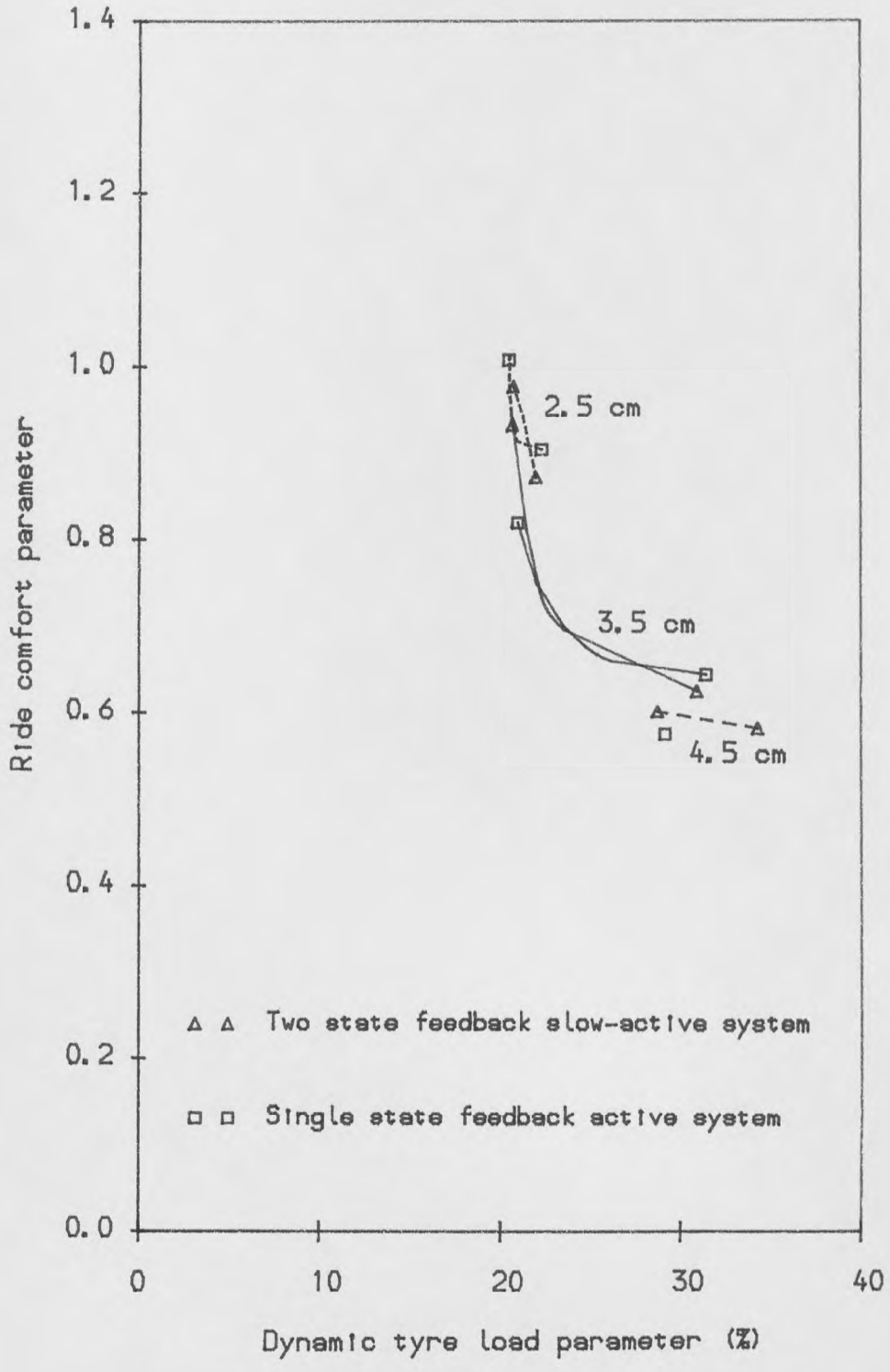

Figure 7.20. Comparison of the performance capabilities of the two state feedback slow-active and single state feedback active systems at 2.5, 3.5 and 4.5 cm RMS working space.

CHAPTER 8

COMPARISON OF THE PERFORMANCE CAPABILITIES OF ALL SYSTEMS

8.1 Introduction

In this chapter, five competing systems of intelligent suspensions will be compared with each other using predicted results based on the well known quarter car model. The systems are classified as: passive, two state switchable damper, fully active, semi-active and slow-active. The active control law of the fully active and semi-active systems is a function of all the state variables, but the control law of the slow-active one is a function only of the vertical velocities of the vehicle body and wheel. Details of all these systems have already been outlined in the preceding chapters.

In general, the most difficult step is to interpret such results, which without some well-founded strategy can become an overwhelming task in view of the large volume of results which may easily be generated for a random ground input. One efficient method of comparing performance is based on the practical viewpoint that the suspension designer is essentially allocated a given amount of working space and must optimise the suspension within this constraint. Hence, competing systems have been compared on the basis of equal workspace contours in two different parts in this chapter. In the first part, the frequency and time history responses of all systems are compared with each other. In the second part, the overall performance capabilities of all systems are compared in terms of the RMS values calculated.

8.2 Frequency and time history responses of all systems

The results are generated for the road input and basic elements of the model as described in sections 2-7 and 3-4. Details of the specific systems compared are as follows:

PAS- passive systems with natural frequency, F_n, and damper coefficient, HC_d. The PAS1 and PAS2 systems use a conventional passive spring to give a body

natural frequency of 1.03 Hz with damper coefficients of 16.3 kNs/m, hard, and 8.15 kNs/m, soft, respectively.

SWD- two state switchable damper system with natural frequency, Fn, and damper coefficients of the hard setting, HC_d, and soft setting, SC_d.

FAC- full state feedback fully active system with the range of results being generated by putting different weighting parameters in the performance index denoted by q_1, q_2 and r.

SAC- full state feedback semi-active system with a control law based exactly on the active control of the fully active system, except that no power input is allowed.

SLA- two state feedback slow-active system with natural frequency F_n, and damper coefficient, HC_d. The actuator of the slow-active system has a limited frequency response capability of up to 3 Hz. Different weighting parameters in the performance index, denoted by q_1, q_2 and q_3, are used to generate a range of results.

A first order lag with time constant of 0.011 second is included in the two state switchable damper and semi-active systems to model the switching characteristic between the states of the active damper since this cannot occur instantaneously in practice. The fully active, semi-active and slow-active systems use an additional passive spring placed in parallel with the active elements to support the static vehicle weight, this spring is designed to give a body natural frequency of 1.01 Hz. These systems are chosen then compared within 3 groupings: CA, CB and CC designed to give RMS workspaces of 2.5, 3.5 and 4.5 cm. Also, in order to ensure that the comparison is done on an equitable basis, all the systems provide the same value of dynamic tyre load, i.e. 23% within ± 0.6. Table 8.1 gives the RMS dynamic tyre load, ride comfort, suspension working space and actuator working space variation% as well as the mean values of the actuator power

demand/dissipation and damper power for these three groups of intelligent suspension systems.

Figures 8.1, 8.2 and 8.3 show the PSD performances of all the suspension systems in groups CA, CB and CC respectively. These suspension systems all have the same RMS values of dynamic tyre load and suspension working space, but the ways in which the responses are distributed throughout the frequency range are different. The overall differences in terms of RMS ride comfort values are shown in Table 8.1 and the corresponding frequency distributions in Figures 8.1 to 8.3. There are three frequency ranges of interest; 0-2 Hz containing the body resonance, 2-6 Hz which is an intermediate range and 6-15 Hz containing the wheel hop resonance. Looking first at group CA indicates the following. First, the fully active system achieves dynamic tyre load improvements in the 0-6 Hz range but is the worst system in the wheel hop range around 8 Hz. The passive system provides the best dynamic tyre load control in this wheel hop range. This performance results from having high damping of 0.54 critical in the wheel hop mode. However, this relatively heavy damping has a disadvantage when looking at the PSD of ride comfort, where it is the worst performing system in the 2-6 Hz range. Second, the switchable damper system achieves ride comfort improvements at 2-6 Hz and dynamic tyre load improvements at up to 6 Hz compared to the passive system. Finally, the semi-active system gives a similar performance to the active system except for frequency distributions of the working space. The frequency distributions of working space, however, are not very important because the suspension designer is only really interested in total workspace usage.

These curves change considerably as the available workspace increases for groups CB and CC (figures 8.2 and 8.3). For group CB, the passive system has lower damping than that in group CA so the resonant peaks are much higher. It

still offers the best control of tyre load at wheel hop resonance however. The fully active and slow-active systems achieve all their improvement performance in terms of ride comfort by controlling the body resonance mode better than the other systems. For systems CC (figure 8.3) where plenty of working space is available, there is less difference between all the systems, except for the semi-active systems. However, since this semi-active control is actually inferior to the passive system in these conditions, it does not represent a feasible system. The frequency distributions of the other systems do not show any significant differences.

Despite all the obvious differences between the layouts and control laws of these five systems, the PSD curves show some remarkable similarities for the two lower workspaces (systems CA and CB). For example, the dynamic tyre load and ride comfort parameter curves always contain both the body and wheel hop resonant peaks, whereas the suspension working space curve only ever has a peak at body resonance.

The calculations of PSD ride comfort do not, however, tell the complete story. The raw time histories of the dimensionless body acceleration (expressed as ratio of the acceleration due to gravity g) for all the su spension systems in group CB: passive, switchable damper, fully active, semi-active and slow-active are shown in Figures 8.4 to 8.8 respectively. The results indicate the improvement of the body acceleration obtained by the fully active system over the other systems which in order of merit from the highest to lowest are: slow-active, semi-active, switchable damper and passive for the same workspace and dynamic tyre load. In terms of body acceleration, the low frequency components of the passive system are clearly shown in figure 8.4 whereas the high frequency components of the fully active system are highlighted in figure 8.6. The raw time histories of body acceleration look remarkably similar for the active, semi-active and slow-active systems and high

peak levels occur.

8.3 RMS performance capabilities of all systems

A summary of the performances of the five competitive systems is given for three working space restrictions: 2.5, 3.5 and 4.5 cm in Figures 8.9 to 8.11, Crolla and Abouel-Nour (1988a-b). Tables 8.2 to 8.6 give more specific details of all the systems compared i.e. passive, two state switchable damper, fully active, semi-active and slow-active. A typical value of total available working space for the type of vehicle considered would be 20 cm and so the above RMS values cover the range either side of this value (assuming that total working space is six times the RMS value).

Although summaries of the performance capabilities of these systems have been attempted previously e.g. Crolla and Abouel-Nour (1988a-b), some further comments about the relative performance of competing suspensions include the following. Fully active systems provide the best overall performance of all the systems in the case of using equal working space as the same fair basis for comparison. Semi-active systems, particularly under limited working space conditions, offer performance which is nearly as good as fully active systems. The above finding suggests that the most of the gain associated with an active system relates to its ability to control the dissipation of power rather than its ability to put power into the system. Also, slow-active systems give performance which is nearly as good as that for the fully active systems. Switchable damper systems lie between the passive and active systems. They clearly offer advantages over passive systems but, perhaps not surprisingly in view of their relative simplicity, they are not as good as either of the active systems.

The benefits in performance offered by active systems over passive systems

appear to be very modest when first looking at the results presented in figures 8.9 to 8.11. For example, for the conditions under which the active system offers most advantage (limited working space condition figure 8.9), the improvement in terms of a reduction in ride comfort parameter over an equivalent passive system which uses the same working space and gives the dynamic tyre load is around 25%. However, there are a number of other factors which must be considered.

First, the best passive system indicated in figure 8.9 involves a spring stiffness value which is much lower than conventional and which would not be stiff enough for controlling body attitude angles. Hence, a realistic "optimum" passive design would actually lie further up the line representing all the passive systems. In contrast, any of the active systems shown on this graph are achievable because a separate part of the control algorithm when implemented on a full vehicle would involve controlling the body attitude angles.

Second, the "optimum" passive system for the road roughness and working space conditions of figure 8.9 is not the same as that for the conditions of figures 8.10 and 8.11. The only method of overcoming this problem of obtaining the best passive system over all conditions would be to have adaptable spring stiffness and damping coefficients which could be changed depending on the road conditions. Some commercial systems already achieve part of this requirement by providing a limited choice of damper settings. In practice, with a conventional non-adjustable passive system, the stiffness and damping parameters are chosen on the basis of compromising between all the road/speed conditions over which the vehicle typically operates. In contrast, the active system suffers from no such compromise, and the optimum control law can be selected for particular condition as shown previously in figure 5.8. This adaptive ability is, in principle, at least easy to arrange - it requires that a set of gains, e.g. the K_f values in equation 5.1, are first calculated

then set within the microcomputer controller. Some supervisor algorithm would continually monitor the average values of the conditions under which the vehicle is operating and would then update the control law settings. In summary, the two features discussed above mean that the practical benefits obtained from active suspension control would be substantially greater than indicated in figures 8.9 to 8.11.

Previous comparative results have not considered the case of the switchable damper and the results shown in figures 8.9 to 8.11 suggest that the performance of the switchable damper systems lies between the passive and active systems. Whilst the results in these figures attempt to provide the overall flavour of what might be achieved by the various systems using a fair basis for comparison, some further details about the parameters of the switchable damper systems are necessary as discussed previously in section 4.4. In terms of overall performance the switchable damper offers a worthwhile improvement in performance, over the fixed damper, indicated here by an improvement in ride comfort for the same values of dynamic tyre load and working space.

The system described here requires continuous switching of the damper and it offers improved performance over a wide range of road roughness conditions, according to figures 8.10 to 8.11. It must be contrasted with adaptive systems with two state dampers which are beginning to appear in prototype form on vehicles. Typically, these involve strategies such as switching to the soft damper setting for straight (and smooth and moderate roughness) road running and switching rapidly to hard for handling manoeuvres and possibly rough roads and discrete, severe events like potholes. The continuously switchable damper system described here would probably also need to include additional features such as switching to its hard setting for manoeuvres. From a practical viewpoint, however, the continuously switchable system places a bigger demand on the damper hardware by virtue of its much greater number of switching cycles.

Group	System	Weighting factors $r=q_3=10^{-8}$ and q_1	q_2	F_n Hz	HC_d and SC_d kNs/m	RMS Performance of dynamic tyre load % DTLP, ride comfort RCP, working space SWS (mm), actuator workspace% SLAWS, mean values of actuator power demand MP+, dissipation MP- and mean values of damper power DP (W)						
						DTLP	RCP	SWS	SLAWS	MP+	MP-	DP
CA	PAS 1	ND	ND	1.03	16.3	23.2	1.23	24.7	NR	NR	NR	1490
	SWD 1	ND	ND	1.27	18.0 0.0	23.4	1.10	25.4	NR	NR	NR	2632
	FAC 1	200	485	1.01	ND	23.0	0.92	25.3	100	36	1431	NR
	SAC 1	200	485	1.01	ND	22.8	0.96	25.0	100	NR	1410	NR
CB	PAS 2	ND	ND	1.03	8.1	23.5	1.00	35.8	NR	NR	NR	1430
	SWD 2	ND	ND	0.80	10.0 2.5	23.3	0.80	35.3	NR	NR	NR	2006
	FAC 2	600	50	1.01	ND	23.5	0.69	35.4	100	132	1415	NR
	SAC 2	500	5	1.01	ND	23.1	0.74	35.1	100	NR	1274	NR
	SLA 2	4	18	1.01	40.0	23.6	0.70	35.6	87	152	494	933
CC	PAS 3	ND	ND	0.32	6.5	22.9	0.73	45.6	NR	NR	NR	1280
	SWD 3	ND	ND	0.32	10.0 5.0	23.0	0.79	44.9	NR	NR	NR	1781
	FAC 3	88.9	0.1	1.01	ND	22.6	0.69	45.4	100	259	1507	NR
	SAC 3	892.9	0.1	1.01	ND	22.9	0.82	45.5	100	NR	1317	NR

Table 8.1 Comparison of performances and power requirments of the passive, switchable damper, active, semi-active and slow-active suspension systems.

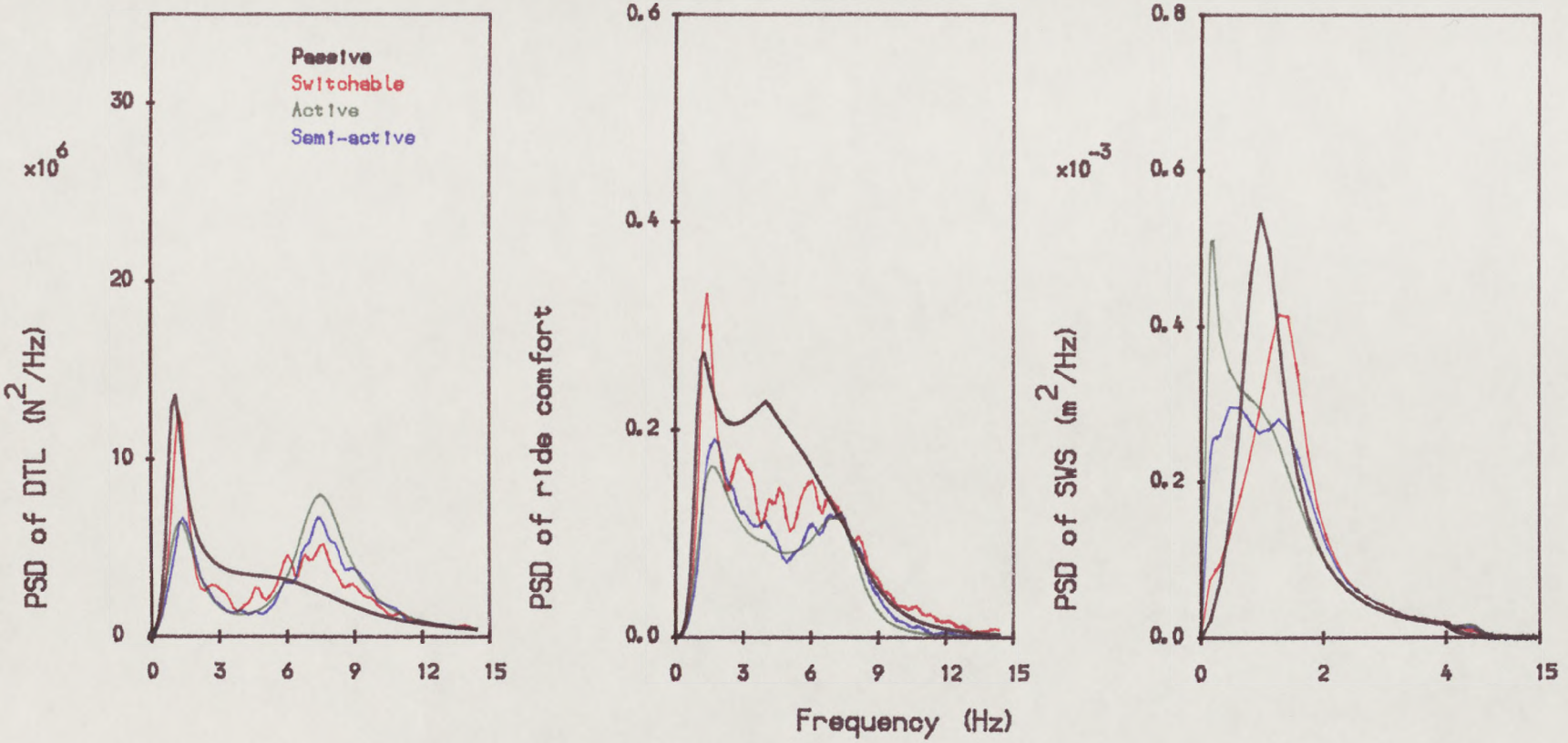

Figure 8.1 The PSDs of the passive, switchable damper, fully active and semi-active suspension systems in group CA.

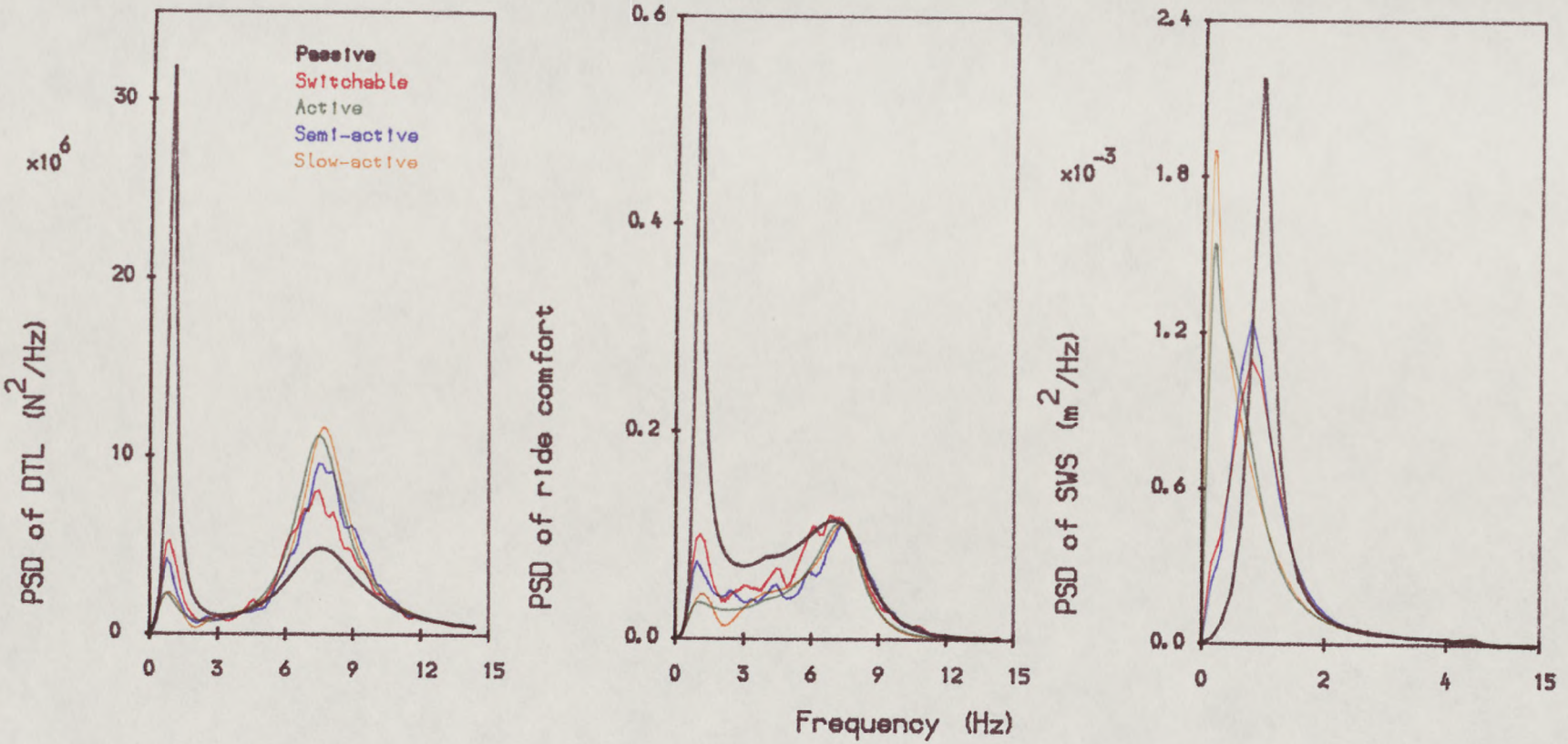

Figure 8.2 The PSDs of the passive, switchable damper, fully active, semi-active and slow-active suspension systems in group CB.

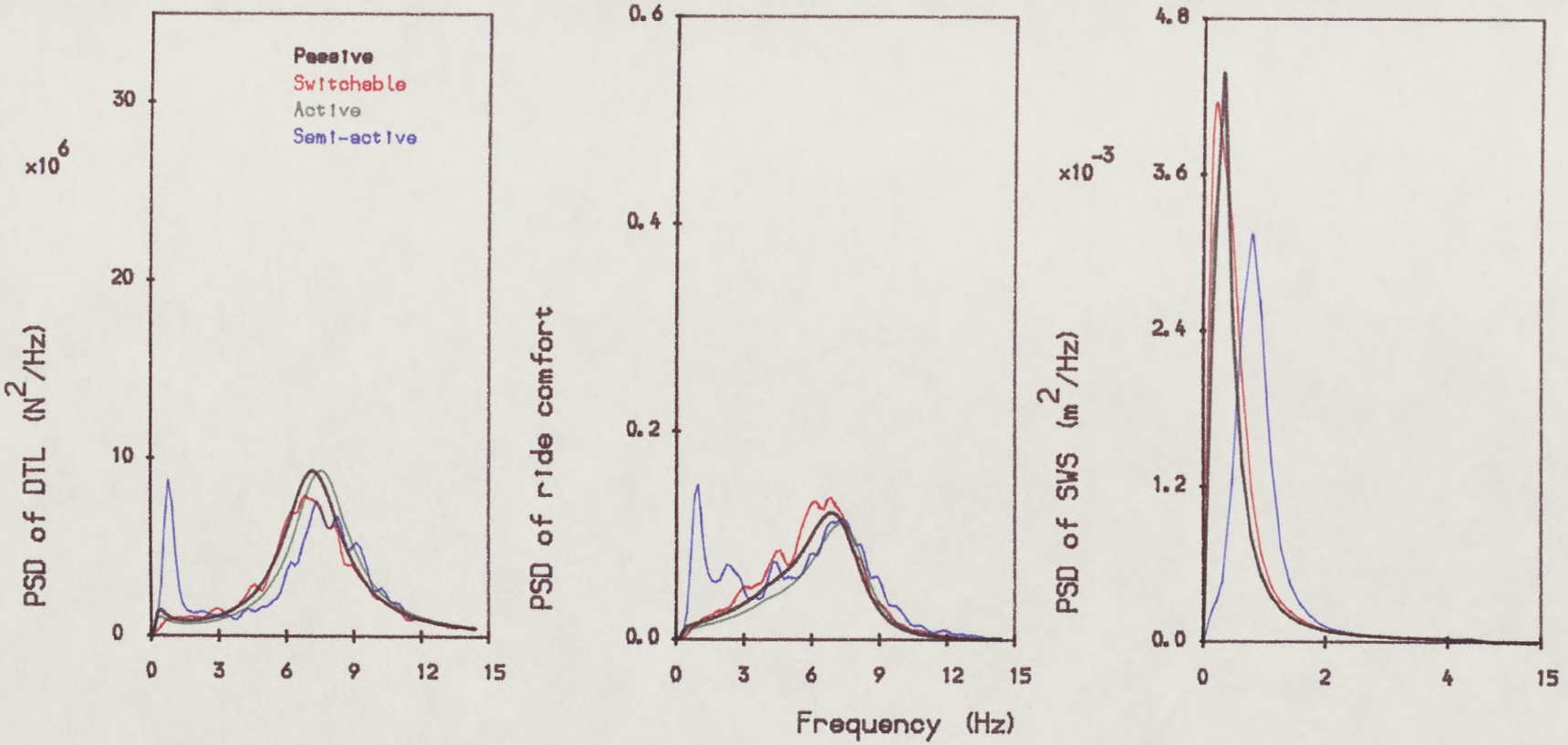

Figure 8.3 The PSDs of the passive, switchable damper, fully active and semi-active suspension systems in group CC.

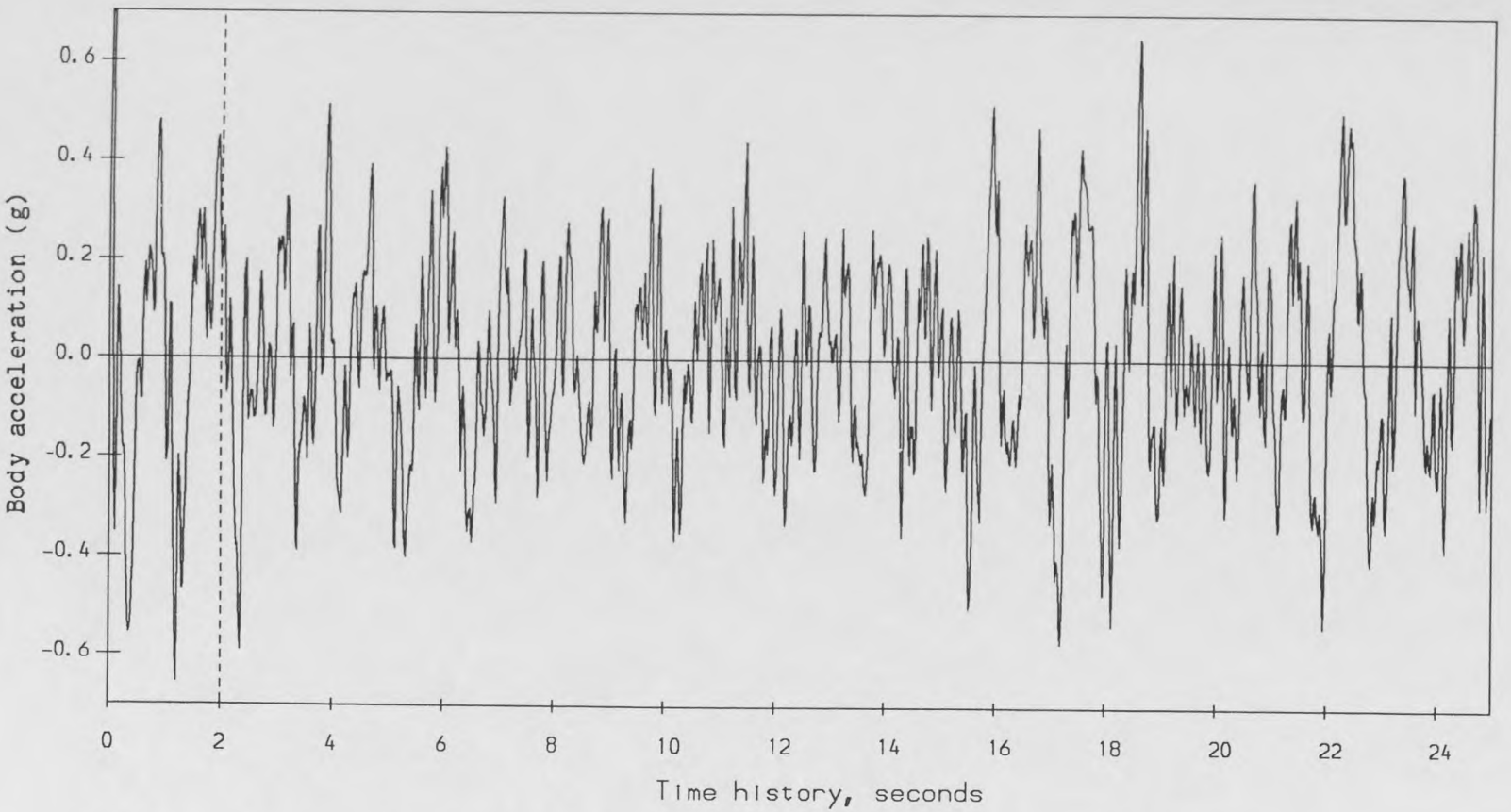

Figure 8.4. Time histories of the body acceleration for the passive system PAS2 in group CB at the RMS working space of 3.5 cm and dynamic tyre load of 23%.

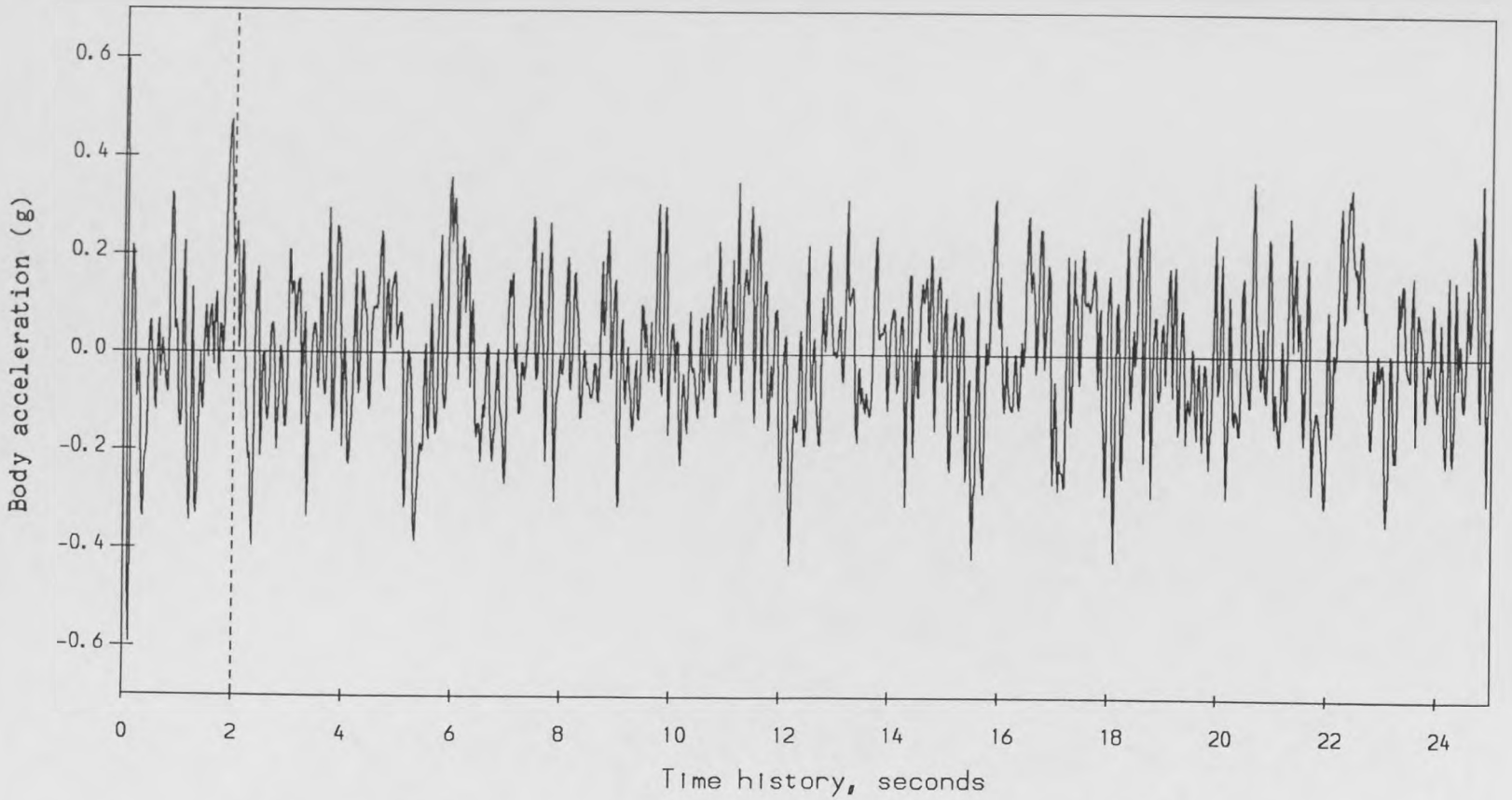

Figure 8.5. Time histories of the body acceleration for the switchable damper system SWD2 in group CB at the RMS working space of 3.5 cm and dynamic tyre load of 23%.

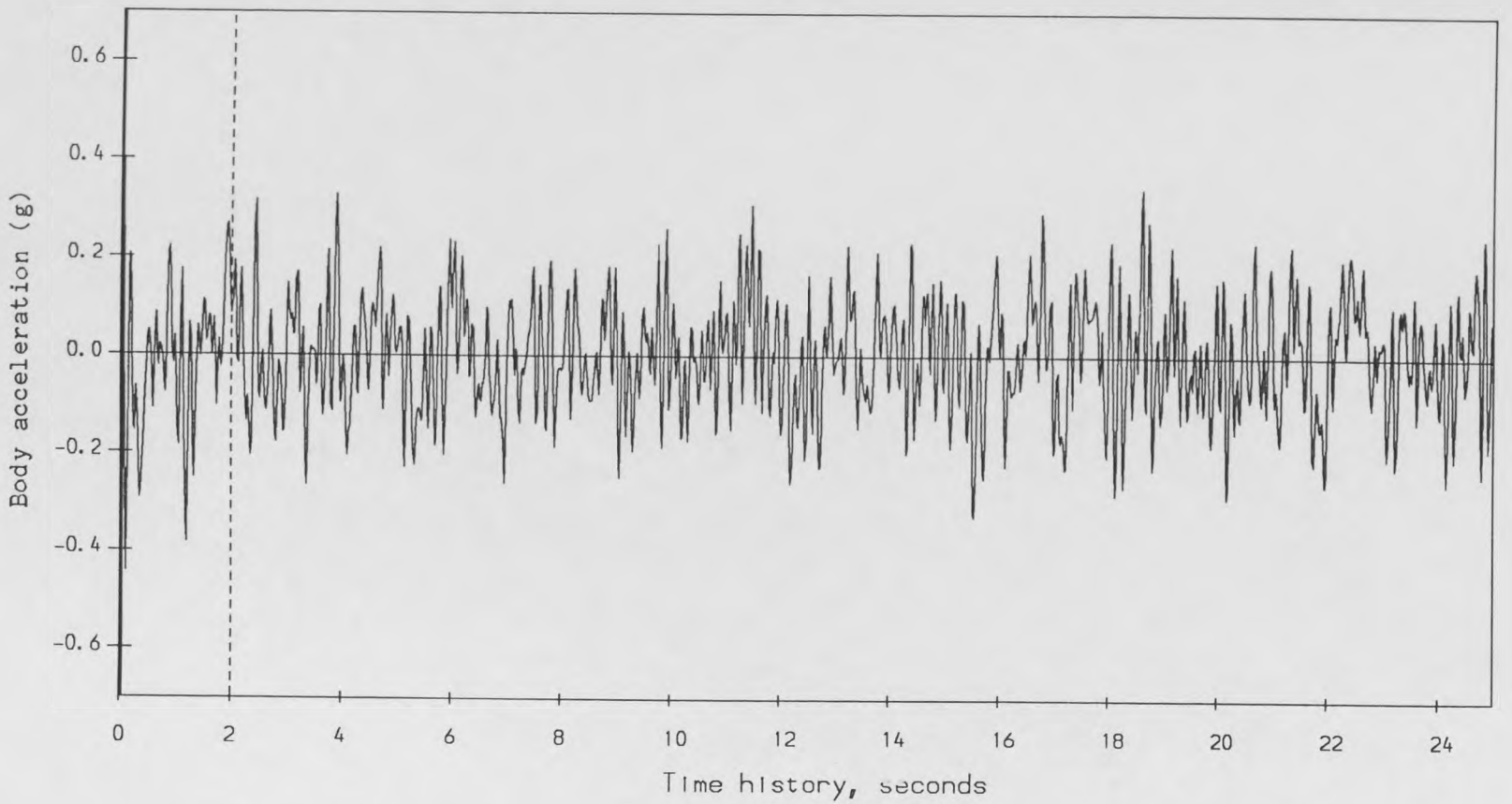

Figure 8.6. Time histories of the body acceleration for the active system FAC2 in group CB at the RMS working space of 3.5 cm and dynamic tyre load of 23%.

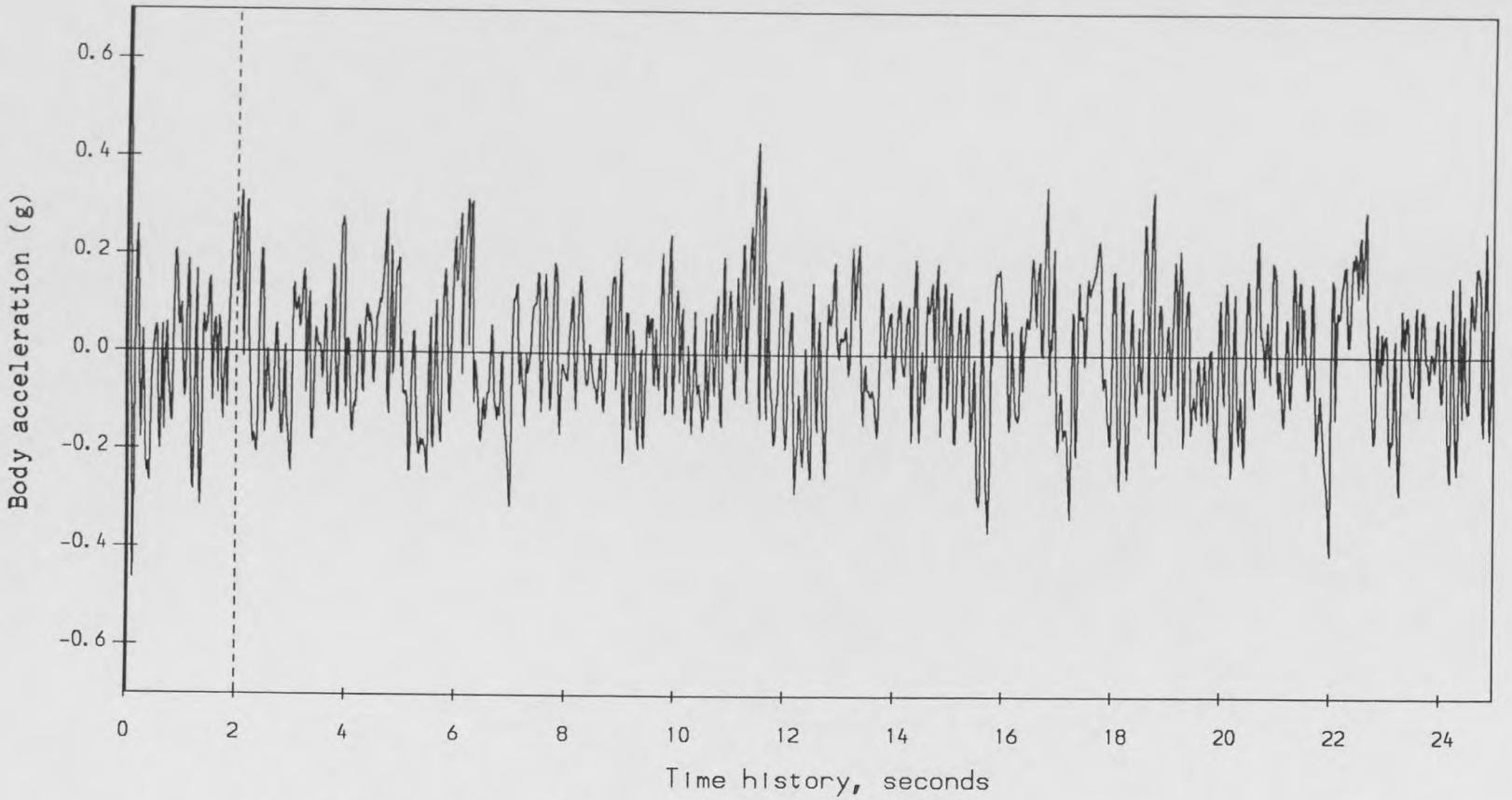

Figure 8.7. Time histories of the body acceleration for the semi-active system SAC2 in group CB at the RMS working space of 3.5 cm and dynamic tyre load of 23%.

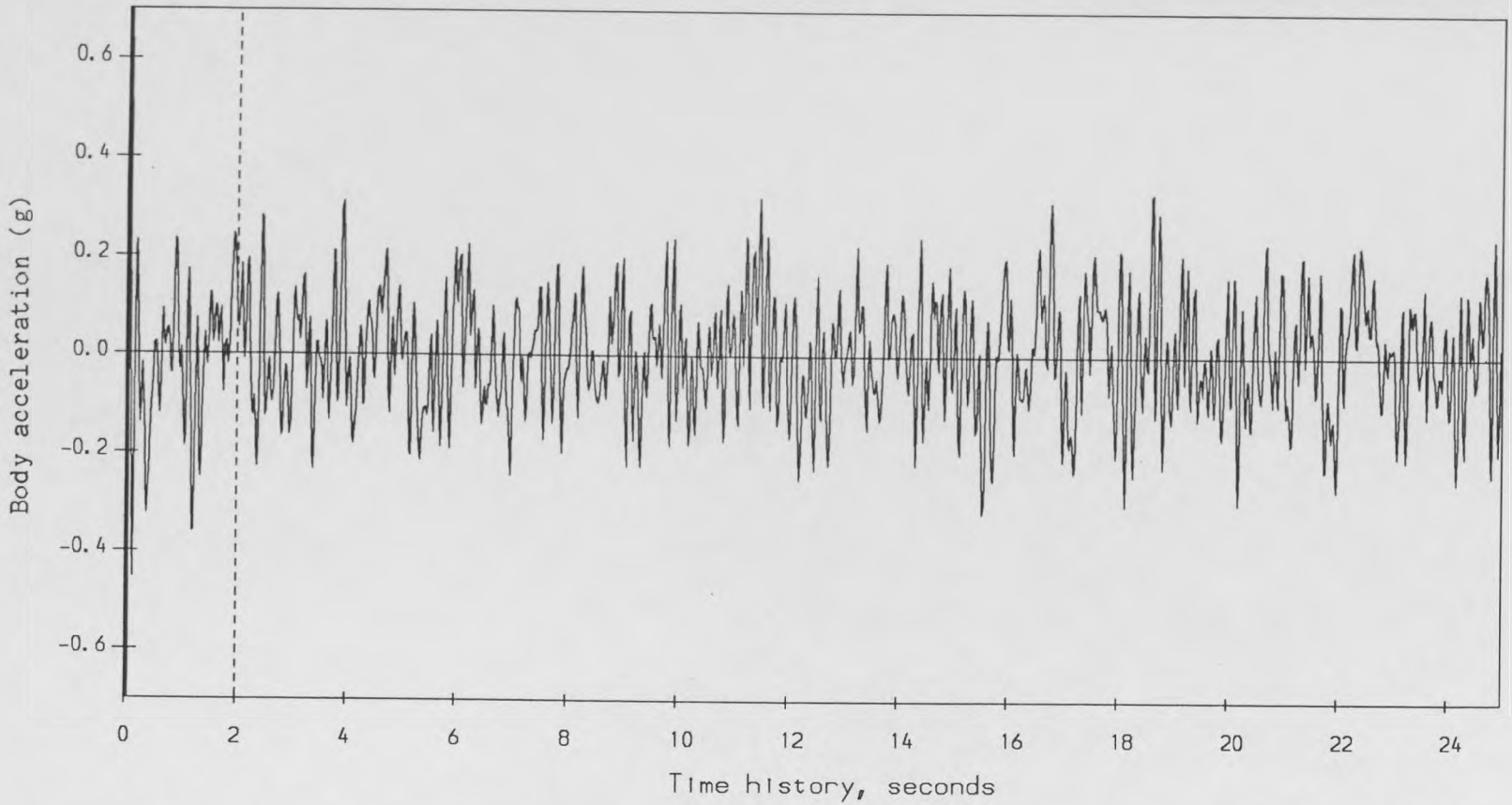

Figure 8.8. Time histories of the body acceleration for the slow-active system SLA2 in group CB at the RMS working space of 3.5 cm and dynamic tyre load of 23%.

Group	System	F_n Hz	ζ	RMS Performance of dynamic tyre load% DTLP, ride comfort parameter RCP and suspension working space SWS (cm)		
				DTLP	RCP	SWS
CA	1	0.56	0.95	22.3	1.18	2.5
	2	0.72	0.75	22.5	1.20	
	3	1.11	0.45	23.6	1.24	
	4	1.19	0.40	24.1	1.26	
	5	1.35	0.35	25.9	1.35	
CB	1	0.72	0.40	21.3	0.89	3.5
	2	0.56	0.55	21.0	0.90	
	3	0.40	0.75	21.1	0.91	
	4	1.11	0.25	24.0	1.07	
	5	1.27	0.20	27.2	1.23	
CC	1	0.24	0.85	23.2	0.73	4.5
	2	0.56	0.35	23.1	0.73	
	3	0.64	0.30	23.2	0.74	
	4	0.72	0.25	23.9	0.75	
	5	1.11	0.15	28.3	1.07	

Table 8.2 Comparison of performances of three groups of the conventional passive systems at the RMS suspension working space of 2.5, 3.5 and 4.5 cm.

Group	System	F_n Hz	ζ	Csoft/ Chard ratio	RMS Performance of dynamic tyre load% DTLP, ride comfort parameter RCP and suspension working space SWS (cm)		
					DTLP	RCP	SWS
CA	1	1.19	0.50	0.00	23.2	1.05	2.5
	2	1.11	0.45	0.25	22.1	1.06	
	3	0.88	0.60	0.50	21.5	1.07	
	4	1.19	0.40	0.25	22.7	1.09	
	5	1.19	0.70	0.00	24.3	1.12	
CB	1	0.88	0.30	0.25	24.3	0.79	3.5
	2	0.80	0.35	0.50	22.5	0.82	
	3	0.48	0.70	0.75	21.2	0.88	
	4	1.03	0.25	0.25	24.5	0.90	
	5	1.19	0.20	0.00	27.8	1.03	
CC	1	0.80	0.20	0.00	32.2	0.65	4.5
	2	0.72	0.25	0.25	28.3	0.65	
	3	0.64	0.30	0.50	25.8	0.67	
	4	0.40	0.55	0.75	23.5	0.71	
	5	0.32	1.00	0.50	23.0	0.80	

Table 8.3 Comparison of performances of three groups of the two state switchable damper systems at the RMS suspension working space of 2.5, 3.5 and 4.5 cm.

Group	System	Weighting factors $r=10^{-8}$ and		Control law = $-(K_{f1}+K_{f2})X_0+K_{f1}X_w+K_{f2}X_b+K_{f3}\dot{X}_w+K_{f4}\dot{X}_b$				RMS Performance of dynamic tyre load% DTLP, ride comfort parameter RCP and suspension working space SWS (cm)		
		q_1	q_2	K_{f1}	K_{f2}	K_{f3}	K_{f4}	DTLP	RCP	SWS
CA	1	800000	100000	9397000	-3162000	28240	-395800	15.5	1.23	
	2	40000	3000	1771000	-547700	23430	-86740	16.3	1.14	
	3	15000	1000	944100	-316200	18280	-54770	17.3	1.08	2.5
	4	4000	500	393700	-223600	11790	-37280	19.3	1.02	
	5	700	450	146500	-212100	6640	-31000	21.8	0.94	
CB	1	17500	25	891500	-50000	21250	-23460	15.2	0.99	
	2	5000	10	352200	-31620	13330	-15180	17.6	0.90	
	3	2500	22.50	215900	-47430	9846	-17150	19.2	0.84	3.5
	4	800	40	96880	-63250	5931	-18210	22.5	0.72	
	5	400	66	65570	-81240	4466	-19930	24.8	0.67	
CC	1	1500	1	121200	-10000	7989	-7612	20.6	0.76	
	2	1071.43	1.07	91540	-10350	6827	-7600	21.8	0.72	
	3	666.67	1.67	63120	-12910	5443	-8317	23.9	0.65	4.5
	4	500.00	3.33	52630	-18260	4735	-9786	25.3	0.62	
	5	333.33	6.67	41090	-25820	3903	-11490	27.5	0.57	

Table 8.4 Comparison of performances of three groups of the full state feedback fully active systems at the RMS suspension working space of 2.5, 3.5 and 4.5 cm.

Group	System	Weighting factors $r=10^{-8}$ and		Control law = $-(K_{f1}+K_{f2})X_0+K_{f1}X_w+K_{f2}X_b+K_{f3}\dot{X}_w+K_{f4}\dot{X}_b$				RMS Performance of dynamic tyre load% DTLP, ride comfort parameter RCP and suspension working space SWS (cm)		
		q_1	q_2	K_{f1}	K_{f2}	K_{f3}	K_{f4}	DTLP	RCP	SWS
CA	1	11000000	1000000	3462400	-10000000	-23509	-1344900	16.8	1.11	2.5
	2	15000	1000	944080	-316230	18279	-54766	18.4	1.09	
	3	7333.33	666.67	591810	-258200	14561	-43661	19.1	1.06	
	4	3000	500	329830	-223610	10664	-35885	20.1	1.02	
	5	700	450	146530	-212130	6640	-31004	21.8	0.97	
CB	1	25000	18.75	1122600	-43301	24193	-23459	16.8	1.01	3.5
	2	14285.71	10.71	759790	-32733	20046	-18266	17.4	0.98	
	3	8000	7.50	496260	-27386	16168	-15121	18.0	0.96	
	4	2295.08	4.10	183720	-20244	9616	-11174	19.8	0.86	
	5	400.00	5.83	46546	-24152	4255	-11164	24.5	0.73	
CC	1	11666.65	0.75	624700	-8660	19133	-9022	19.0	1.01	4.5
	2	3000.00	0.27	208760	-5164	10995	-5773	20.3	0.93	
	3	1888.89	0.20	139590	-4472	8937	-5165	21.1	0.89	
	4	892.86	0.14	71640	-3779	6299	-4553	22.9	0.83	
	5	625	0.10	51519	-3162	5312	-4111	24.0	0.80	

Table 8.5 Comparison of performances of three groups of the full state feedback semi-active systems at the RMS suspension working space of 2.5, 3.5 and 4.5 cm.

Group	System	Weighting factors $q_3=10^{-8}$ and		Control law = $K_{d1}X_w+K_{d2}X_b$ $K_{d3}\dot{X}_w+K_{d4}\dot{X}_b$, within a limited bandwidth of 3 Hz				RMS Performance of dynamic tyre load% DTLP, ride comfort parameter RCP and suspension working space SWS (cm)		
		q_1	q_2	K_{d1}	K_{d2}	K_{d3}	K_{d4}	DTLP	RCP	SWS
CA	1	215	134.50	0	0	-0.04588	-0.06359	20.8	0.98	2.5
	2	500000	20000	0	0	0.00105	-0.10860	21.3	0.94	
	3	40	900	0	0	-0.02227	-0.10020	24.2	0.91	
CB	1	800	5	0	0	-0.06152	-0.20280	20.7	0.93	3.5
	2	21.50	59.50	0	0	-0.07451	-0.16270	21.8	0.78	
	3	4	18	0	0	-0.06633	-0.15550	23.6	0.70	
	4	12500	3000	0	0	-0.04327	-0.16170	30.9	0.62	
CC	1	1700	1	0	0	-0.09237	-0.27100	28.8	0.60	4.5
	2	400	400	0	0	-0.10370	-0.20210	34.3	0.58	

Table 8.6 Comparison of performances of three groups of the two state feedback slow-active systems at the RMS suspension working space of 2.5, 3.5 and 4.5 cm.

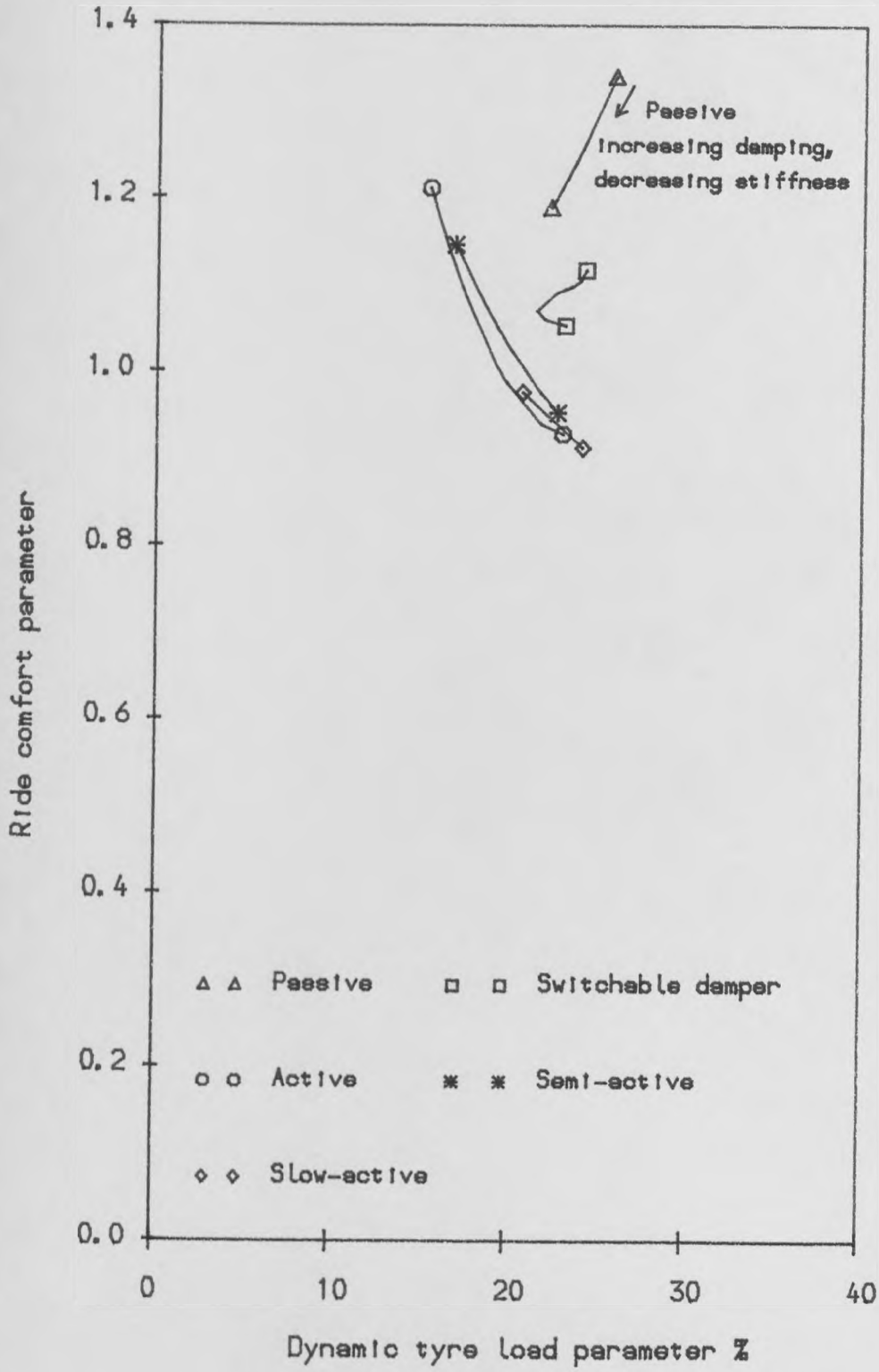

Figure 8.9. Comparison of all the suspension systems at the RMS working space of 2.5 cm.

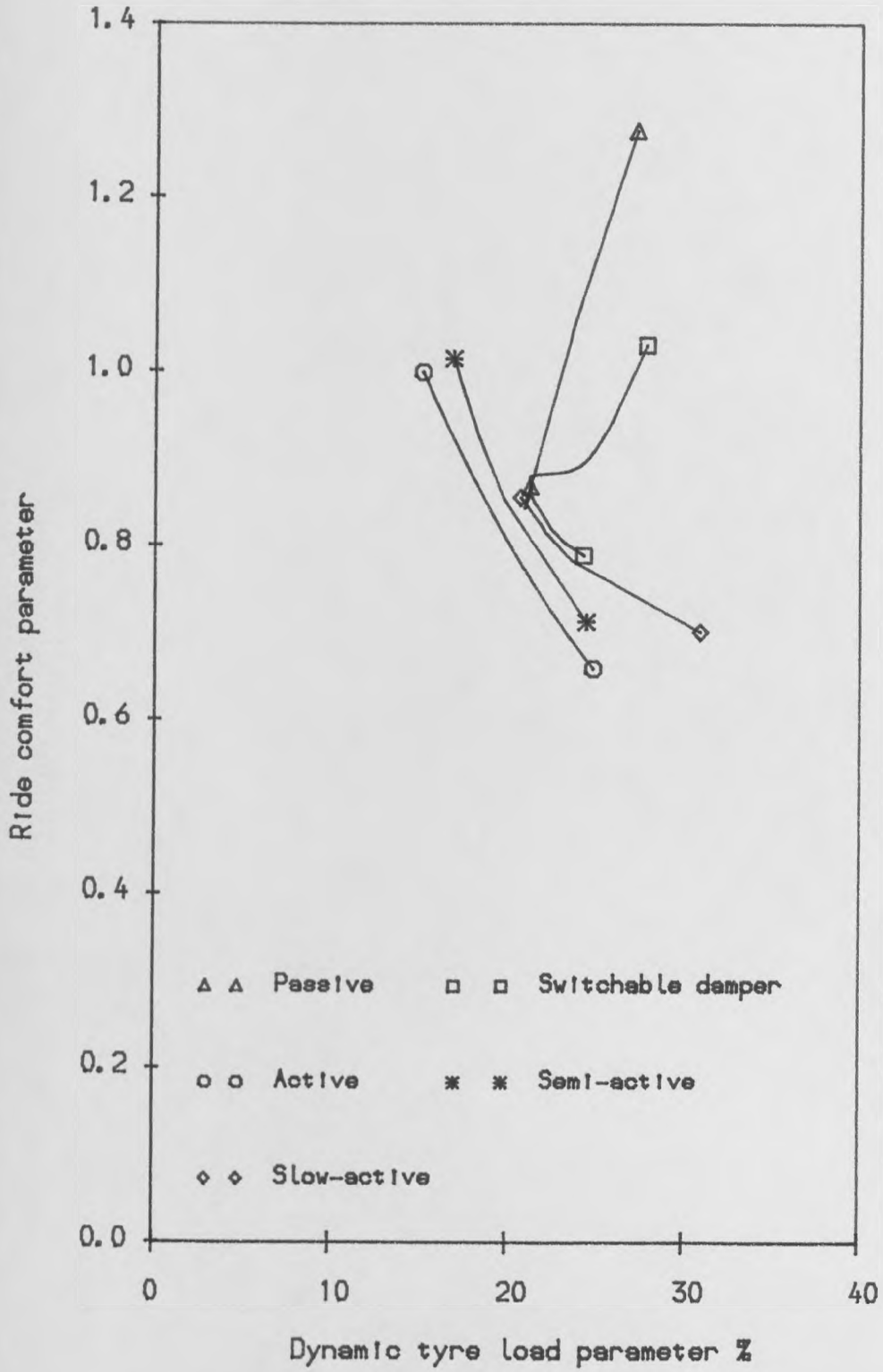

Figure 8.10. Comparison of all the suspension systems at the RMS working space of 3.5 cm.

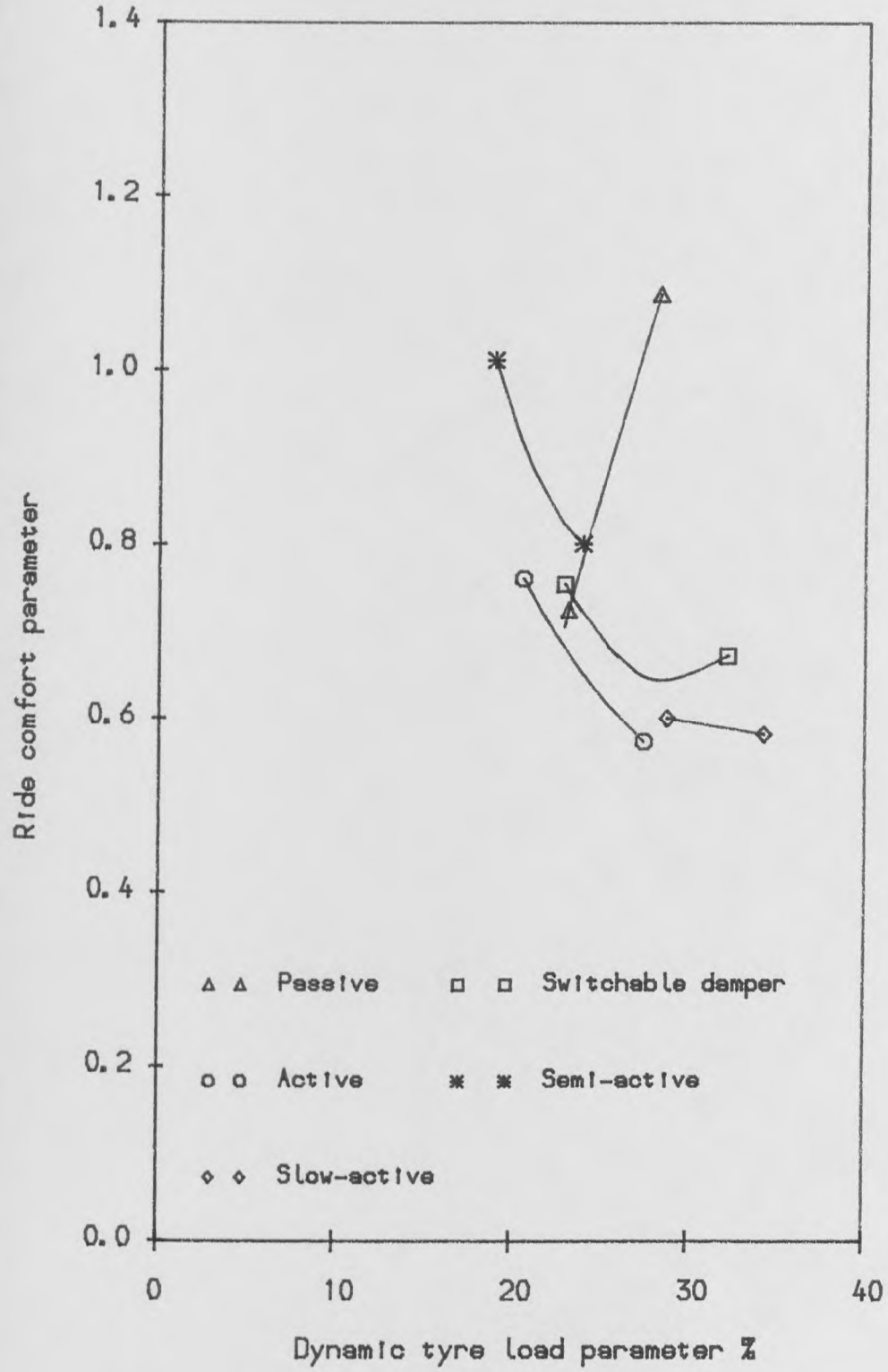

Figure 8.11. Comparison of all the suspension systems at the RMS working space of 4.5 cm.

CHAPTER 9

COMPARISON OF THE POWER REQUIREMENTS OF ALL SYSTEMS

9.1 Introduction

The power requirements of the suspension systems are defined by: mean power dissipation of the passive damper and active actuator elements, mean power demand of the active actuator element as well as the RMS fluctuating powers of the passive spring and tyre. They are considered as a part of the main load on the vehicle power supply. In this chapter, the power requirements of the five competing systems of intelligent suspensions will be compared with each other using predicted results based on the quarter car model. Details of all the systems compared in this chapter and the previous chapter are the same. The power requirements of all the suspension systems can be correlated as parts of the vehicle rolling and acceleration resistances.

This chapter is divided into two different parts. The first part presents the practical implications of the power requirements which are power dissipation, power demand and fluctuating powers of the passive spring and tyre. The correlation of the power requirements with respect to the vehicle power losses are also discussed. In the second part, two different strategies are used to compare the power requirements of all competing systems. The first strategy is used to compare the power requirements of the systems in table 8.1 when operating on different road input conditions GV whereas the second strategy is used to compare the power requirements of the systems in tables 8.2 to 8.6 for three RMS working space restrictions: 2.5, 3.5 and 4.5 cm.

9.2 Practical implications of power requirements

The three features of greatest interest in understanding the behaviour of the suspension systems are first, power input (demand) to the actuator second, power dissipated in the damper or actuator third, power fluctuation in the passive spring

and tyre. These power requirements are a part of the main load on the vehicle power supply, i.e. the engine. For the power demand, the actuator and control systems would, therefore, have to meet the instantaneous force and velocity requirements and design issues relating to a low overall power rating coupled with an accumulator system to meet peak demands would be important, i.e. the sizing of the components are related to the mean power value and the high peak demand levels can then be obtained by using an accumulator. Further simulations to test the ability of alternative system designs to meet these requirements should now be based on modelling the components and hardware used in any proposed system design. For the power dissipation, a high value is compatible with a good isolation system although it appears as a part of the vehicle power loss. The fluctuating powers of the passive spring and tyre are not important for the following reasons: first, this effect on the power supply is only during the acceleration periods and second, the RMS differences between all the suspension systems are limited.

In general, the power requirements of the suspension elements can be calculated as a part of the vehicle power losses as follows. Firstly, when the vehicle is driven at a constant forward speed, under steady state conditions, the power demand is supplied by a device driven directly from the engine and the power dissipation appears as an increase in the vehicle rolling resistance. Secondly, when the vehicle increases its forward speed, during unsteady state conditions, the fluctuating power of the spring and tyre appears as a part of the vehicle resistance to acceleration. The driving force, F, and power, P, relationships for a single wheel station can then be formulated as follows;

$$F = m_f (M_b + M_w)\, g \qquad 9\text{-}1$$

$$P = F\, E_v \qquad 9\text{-}2$$

Where m_f is the dimensionless mass factor, M_w and M_b are the masses of the

vehicle body and wheel, g is the acceleration due to gravity and E_v is the RMS value of the PSD road input velocities which can be obtained from equation 2-7 as follows;

$$E_v = \sqrt{\int_{\omega=1}^{90} PSD(\omega)\, \omega^2\, d\omega} \qquad 9\text{-}3$$

where ω is the frequency content. The mass factor m_f of a vehicle rolling or acceleration resistance due to suspension is dependent on the basic elements of the suspension and road surface/vehicle forward speed combination (GV).

The power losses of the vehicle due to the vehicle rolling, Prr, and acceleration, Par, resistances can be obtained by the following equations,

$$P_{rr} = C_r\,(M_b + M_w)\, g\, V \qquad 9\text{-}4$$

$$P_{ar} = (M_b + M_w) \sum_{V=V_{min}}^{V=V_{max}} a_v\, V \qquad 9\text{-}5$$

where C_r is the coefficient of the vehicle rolling resistance which can be considered as 0.02 for a smoother road or 0.1 for a rough road, Inns and Kilgour (1978), and a_v is the vehicle acceleration which is assumed to be 1 m/s^2 in this study. The power losses in the suspension are compared with the other power losses of the vehicle for the various suspension systems (table 8.1) operating on an off and on - road surface in Tables 9.1 and 9.2 respectively. The power loss due to the rolling resistance of the quarter vehicle model is 6.66 kW on the road and 33.31 kW for the off road conditions. The power loss due to the acceleration resistance of the quarter vehicle is 220.74 kW for both surfaces for a constant acceleration of 1 m/s^2 as the vehicle speed increases from 1 to 12 m/s.

The results indicate the following important points. In the steady state condi-

tions, the rough road increases the power losses due to the suspension by 85% compared with the smoother road. In the non-steady state conditions, the rough road increases the power loss due to the spring and tyre by 35% compared with the smoother road. The power dissipation of the suspension is up to 22% of that of the total power due to rolling resistance for the smoother road whereas it is up to 8% for the rough road. The percentage fluctuating power of the suspension and tyre relative to the total power due to acceleration resistance is up to 11% for smoother road and up to 15% for rough road.

9.3 Power requirements of all systems

The results described here refer to the power calculated according to the power equations which were specified previously for each suspension element. They are intended to form a basis for comparing the fundamental power levels implied by the various systems and their control laws. Because of this emphasis on comparative behaviour, the systems are assumed to have ideal behaviour, with none of the losses associated with practical components. In this section, two different strategies are used to compare the overall power losses from the vehicle power supply due to the suspensions of the five competing systems: passive, switchable damper, fully active, semi-active and slow-active. The first strategy compares the power requirements of the systems when operating on different road surface and forward speed combinations. The second strategy compares power requirements of all the systems at 2.5, 3.5 and 4.5 cm RMS working space.

9.3.1 First strategy for comparison of systems

The aim of this strategy is to compare the power requirements of all systems for different road input conditions. The systems in Table 8.1 are chosen to be used in this comparison. Figure 9.1 to 9.3 show the mean dissipation power of the sus-

pension and the fluctuating powers of the passive spring and tyre versus road input conditions GV for the systems in groups CA, CB and CC respectively. The results indicate the following important features. Firstly, there is little difference between the mean dissipation powers of active, semi-active, slow-active and passive systems although the detailed way in which power is dissipated must be different to account for differences in performance. Secondly, the switchable damper system stands out in that it consistently dissipates more power in achieving its improved performance over the passive system. Thirdly, the passive systems give the lowest fluctuating powers of the spring and tyre. Finally, the power dissipation and fluctuation values for the fully active and slow-active systems are similar.

In terms of the power demand, Figure 9.4 shows the mean demand power of the fully active and slow-active suspension systems in group CB versus road input conditions GV. The results indicate that the lower power demand is always obtained with the fully active systems. To illustrate the comparison, the time histories of the power demand and control forces and velocities for the active elements of the fully and slow active systems are given in Figures 9.5 and 9.6 respectively. The time histories show two important features as follows: first, the curves of the active elements characteristics for the systems look remarkably similar when operating over the same ground profile, and second, high peak forces, relative velocities and power demand levels occur. Ignoring the transient features during the initial two seconds of the trace in the steady state conditions, peak power demands of up to 3 kW are predicted. Peak forces of up to 10 kN and peak relative velocities for the fully active system of up to 2 m/s are predicted whereas for the slow-active system, similar forces but somewhat reduced velocities (up to 1 m/s) are predicted. Hence, despite the low values of mean power demand predicted for the active suspension, peak values are much higher. For example, peak values occur which are around twenty times the mean power levels indicated in table 8.1. In practical

terms, the actuator control systems would, therefore, have to meet these requirements and design specifications relating to a low overall power rating coupled with an accumulator system to meet peak demands would appear appropriate.

9.3.2 Second strategy for comparison of systems

The power requirements of all the competing systems are compared with each other in Figures 9.7 to 9.9 for the same working space used earlier, i.e. 2.5, 3.5 and 4.5 cm RMS. Further details of these systems are specified in tables 8.2 to 8.6. The results confirm some of the comments which have already been made in the first strategy comparison. However, some additional points emerge. Firstly, for the most restricted suspension working space case (2.5 cm), the power dissipation of the switchable damper systems increases dramatically as dynamic tyre load increases. The power demand of the fully active systems increases as dynamic tyre load is reduced. Secondly, for all three different suspension working space conditions, the mean power dissipation of all the systems stays almost constant at around 1 to 2 kW, whereas the mean power demand of the fully active and slow-active systems increases as more suspension working space is available.

Group	System	Weighting factors $r=q_3=10^{-8}$ and q_1	q_2	F_n Hz	HC_d and SC_d kNs/m	MP- W	FP W	Total power dissipated in suspension relative to power consumed in vehicle rolling resistance %	Total fluctuating power in suspension and tyre relative to vehicle acceleration resistance %
CA	PAS 1	ND	ND	1.03	16.3	1490	24120	4.5	10.9
	SWD 1	ND	ND	1.27	18.0 0.0	2632	27435	7.9	12.4
	FAC 1	200	485	1.01	ND	1431	27814	4.3	12.6
	SAC 1	200	485	1.01	ND	1410	26700	4.2	12.1
CB	PAS 2	ND	ND	1.03	8.1	1430	28200	4.3	12.8
	SWD 2	ND	ND	0.80	10.0 2.5	2006	29920	6.0	13.6
	FAC 2	600	50	1.01	ND	1415	30978	4.2	14.0
	SAC 2	500	5	1.01	ND	1274	30826	3.8	14.0
	SLA 2	4	18	1.01	40.0	1427	31448	4.3	14.2
CC	PAS 3	ND	ND	0.32	6.5	1280	29800	3.8	13.5
	SWD 3	ND	ND	0.32	10.0 5.0	1781	28950	5.3	13.1
	FAC 3	88.9	0.1	1.01	ND	1507	30863	4.5	14.0
	SAC 3	892.9	0.1	1.01	ND	1317	29660	4.0	13.4

Table 9.1 Comparison between powers consumed in the suspension and those involved in vehicle rolling and acceleration for an off - road condition (roughness $C=10^{-5}$ and vehicle forward speed V=12 m/s).

Group	System	Weighting factors $r=q_3=10^{-8}$ and q_1	q_2	F_n Hz	HC_d and SC_d kNs/m	MP- W	FP W	Total power dissipated in suspension relative to power consumed in vehicle rolling resistance %	Total fluctuating power in suspension and tyre relative to vehicle acceleration resistance %
CA	PAS 1	ND	ND	1.03	16.3	812	17420	12.2	7.9
	SWD 1	ND	ND	1.27	18.0 0.0	1433	19922	21.5	9.0
	FAC 1	200	485	1.01	ND	780	20299	11.7	9.2
	SAC 1	200	485	1.01	ND	752	19435	11.3	8.8
CB	PAS 2	ND	ND	1.03	8.1	777	20530	11.7	9.3
	SWD 2	ND	ND	0.80	10.0 2.5	1093	21835	16.4	9.9
	FAC 2	600	50	1.01	ND	779	22791	11.7	10.3
	SAC 2	500	5	1.01	ND	707	22839	10.6	10.3
	SLA 2	4	18	1.01	40.0	792	23094	11.9	10.5
CC	PAS 3	ND	ND	0.32	6.5	700	22850	10.5	10.4
	SWD 3	ND	ND	0.32	10.0 5.0	971	21175	14.6	9.6
	FAC 3	88.9	0.1	1.01	ND	829	22704	12.4	10.3
	SAC 3	892.9	0.1	1.01	ND	727	22098	10.9	10.0

Table 9.2 Comparison between powers consumed in the suspension and those involved in vehicle rolling and acceleration for an on - road condition (roughness $C= 0.544\times10^{-5}$ and vehicle forward speed V=12 m/s).

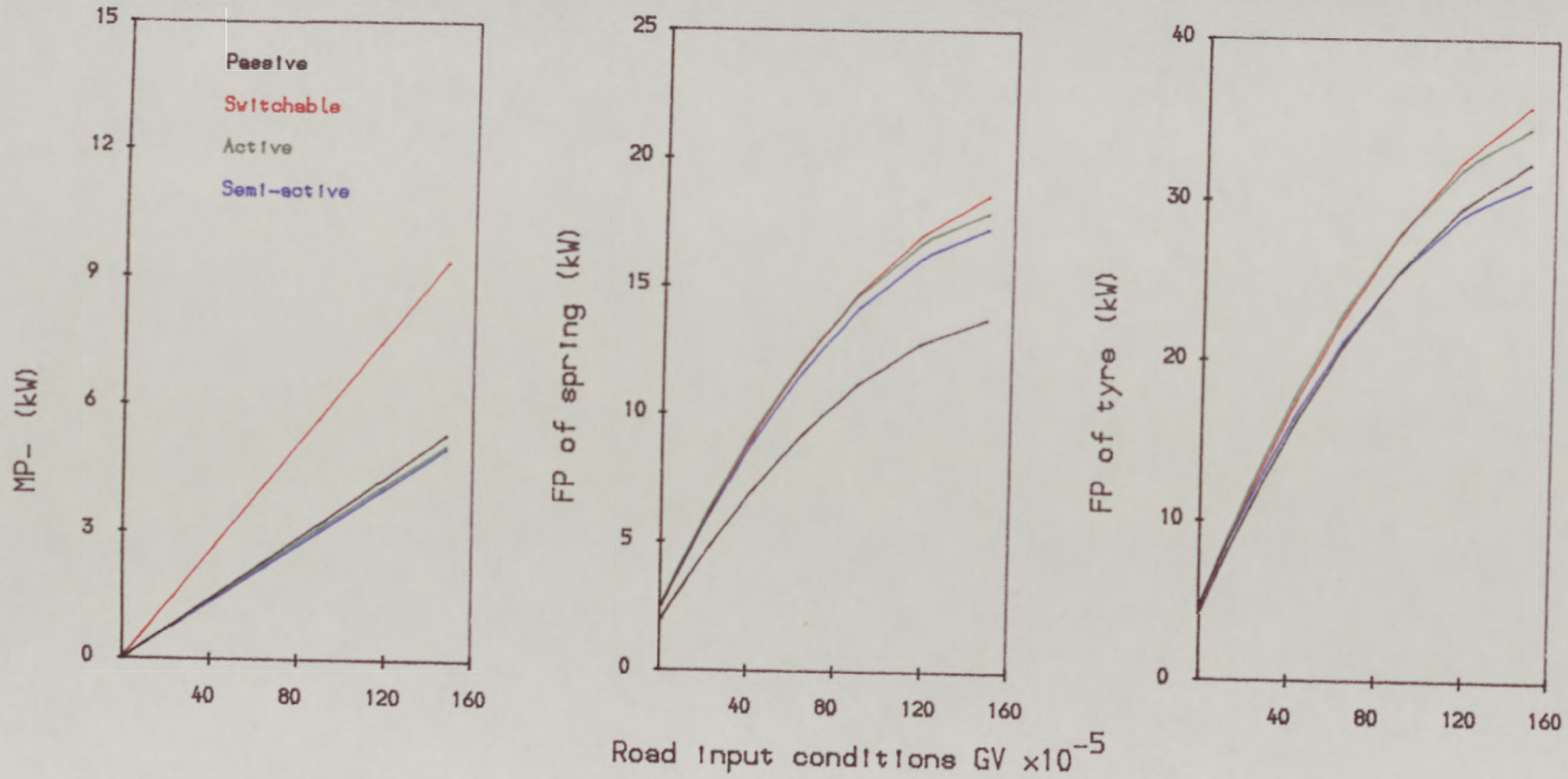

Figure 9.1 Mean power dissipation and fluctuating powers of the passive spring and tyre for all competitive systems in table 8.1 group CA.

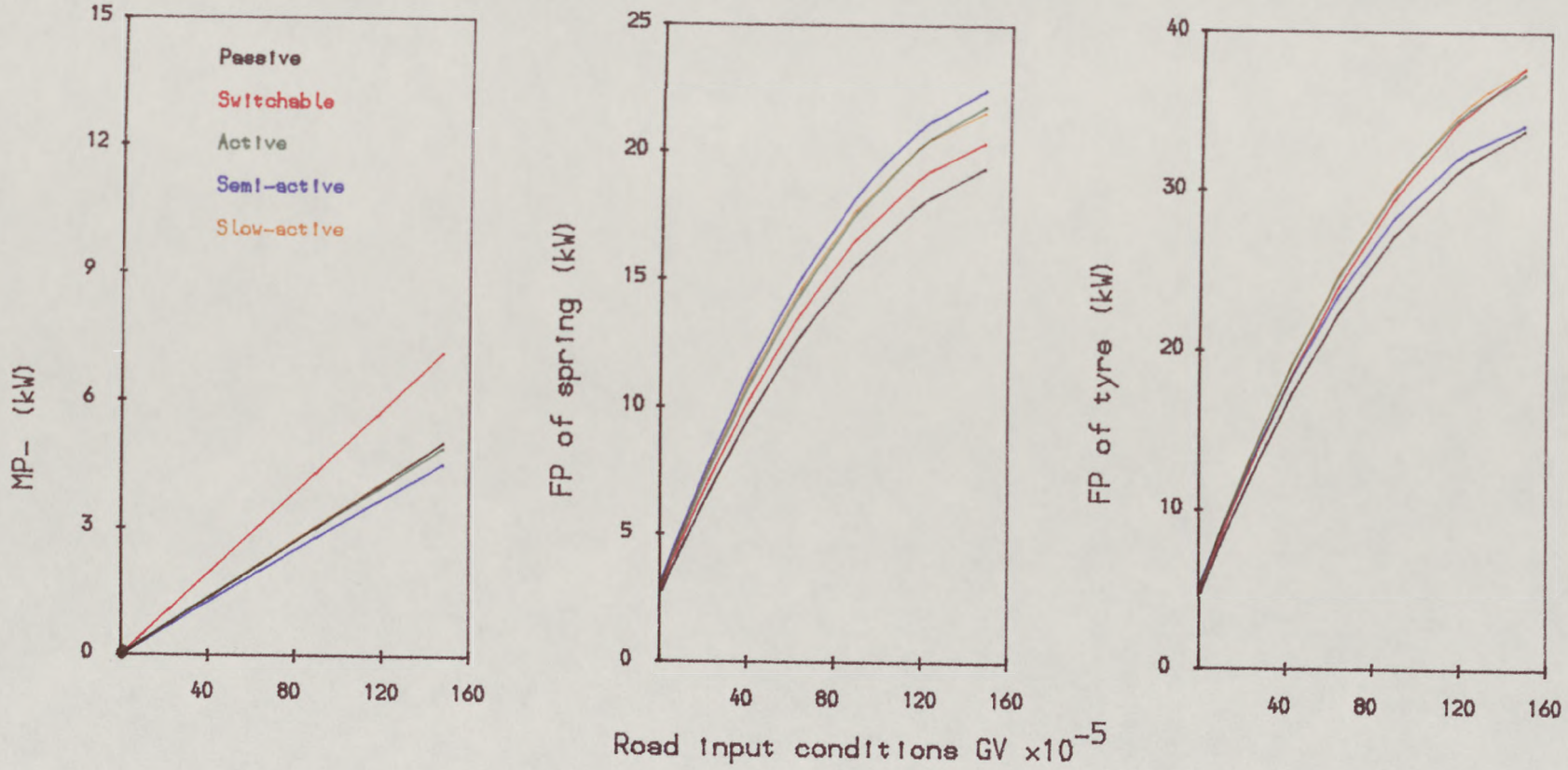

Figure 9.2 Mean power dissipation and fluctuating powers of the passive spring and tyre for all competitive systems in table 8.1 group CB.

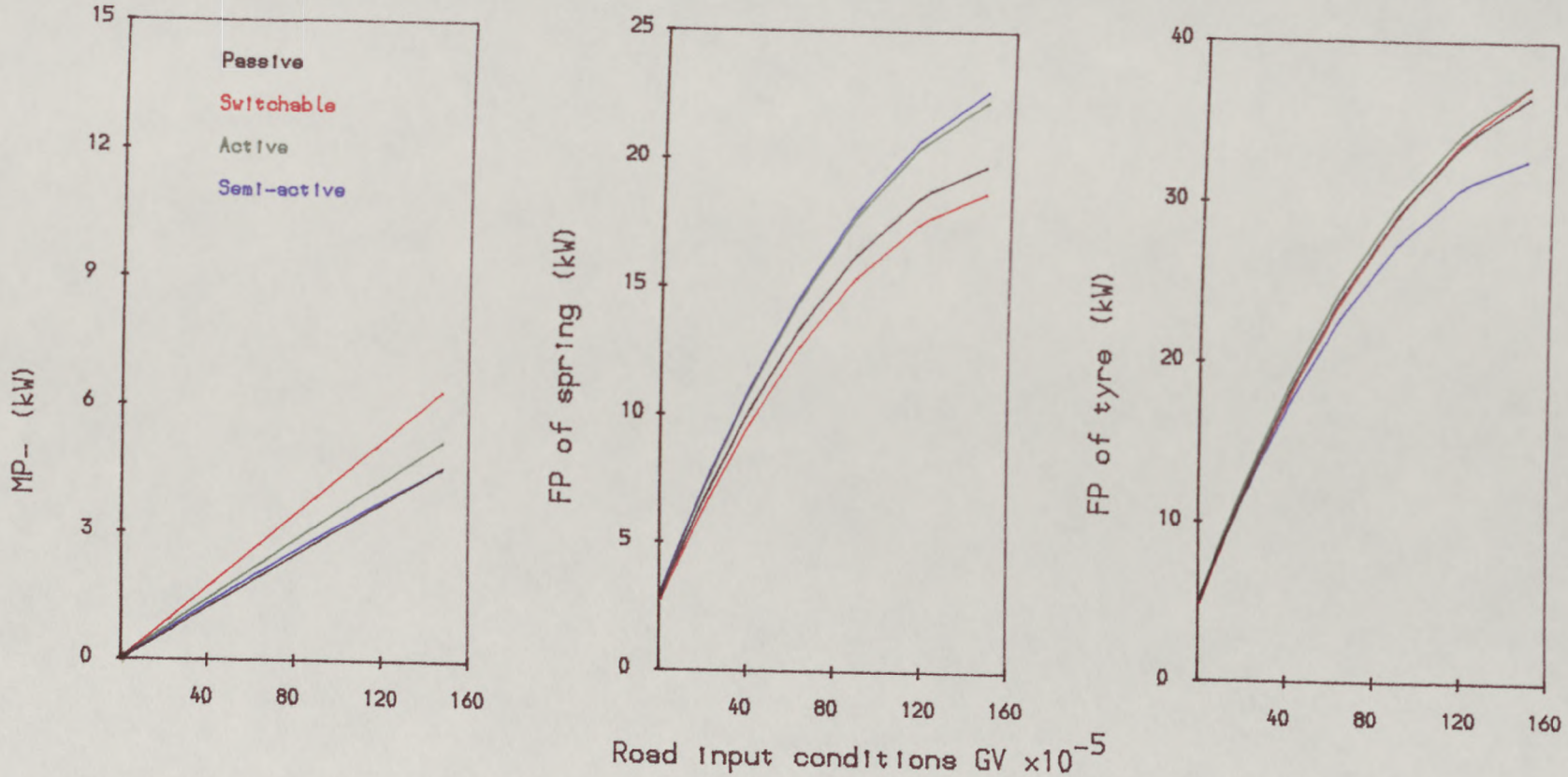

Figure 9.3 Mean power dissipation and fluctuating powers of the passive spring and tyre for all competitive systems in table 8.1 group CC.

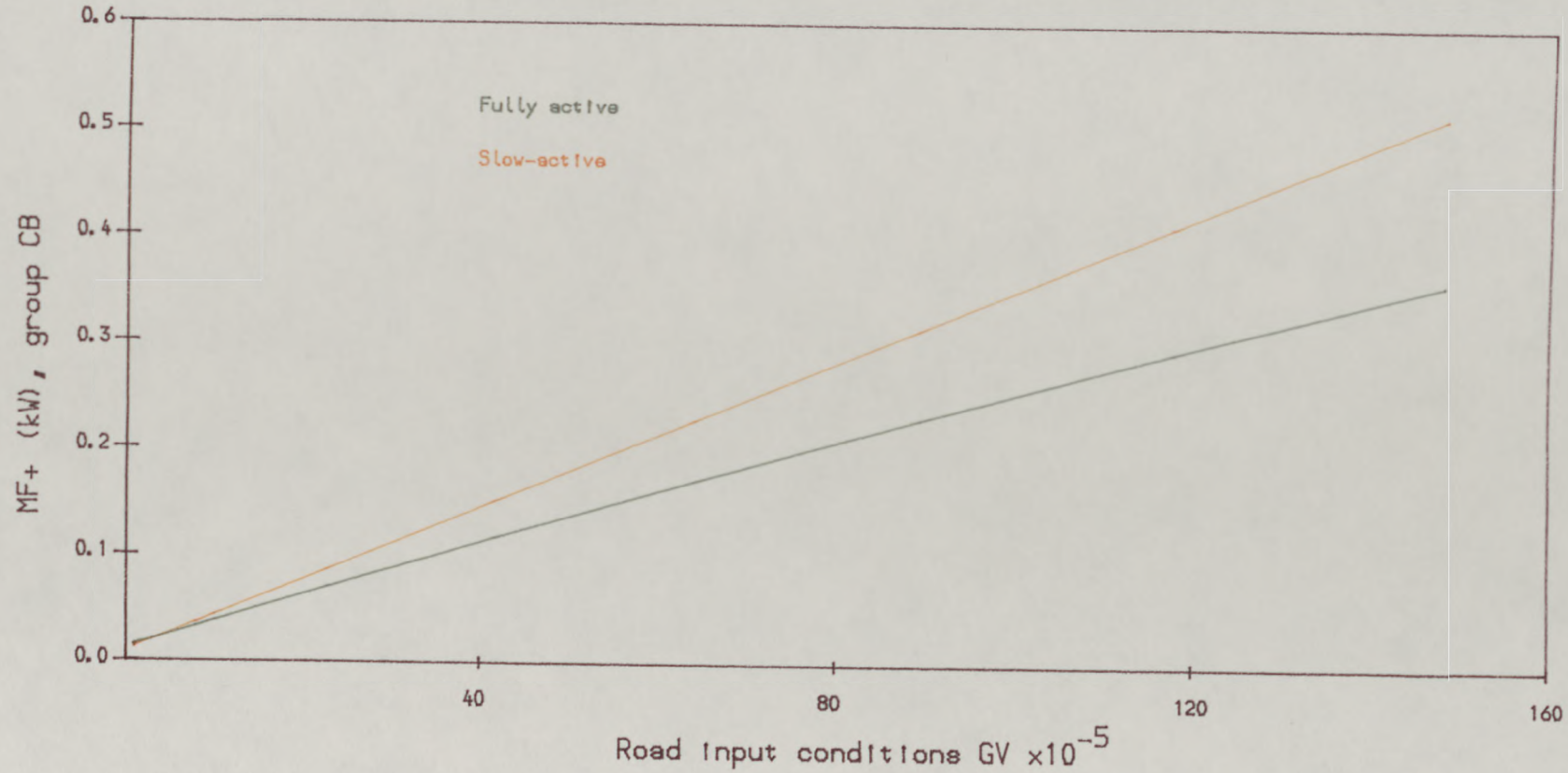

Figure 9.4 Mean power demand for the fully active and slow-active systems in group CB.

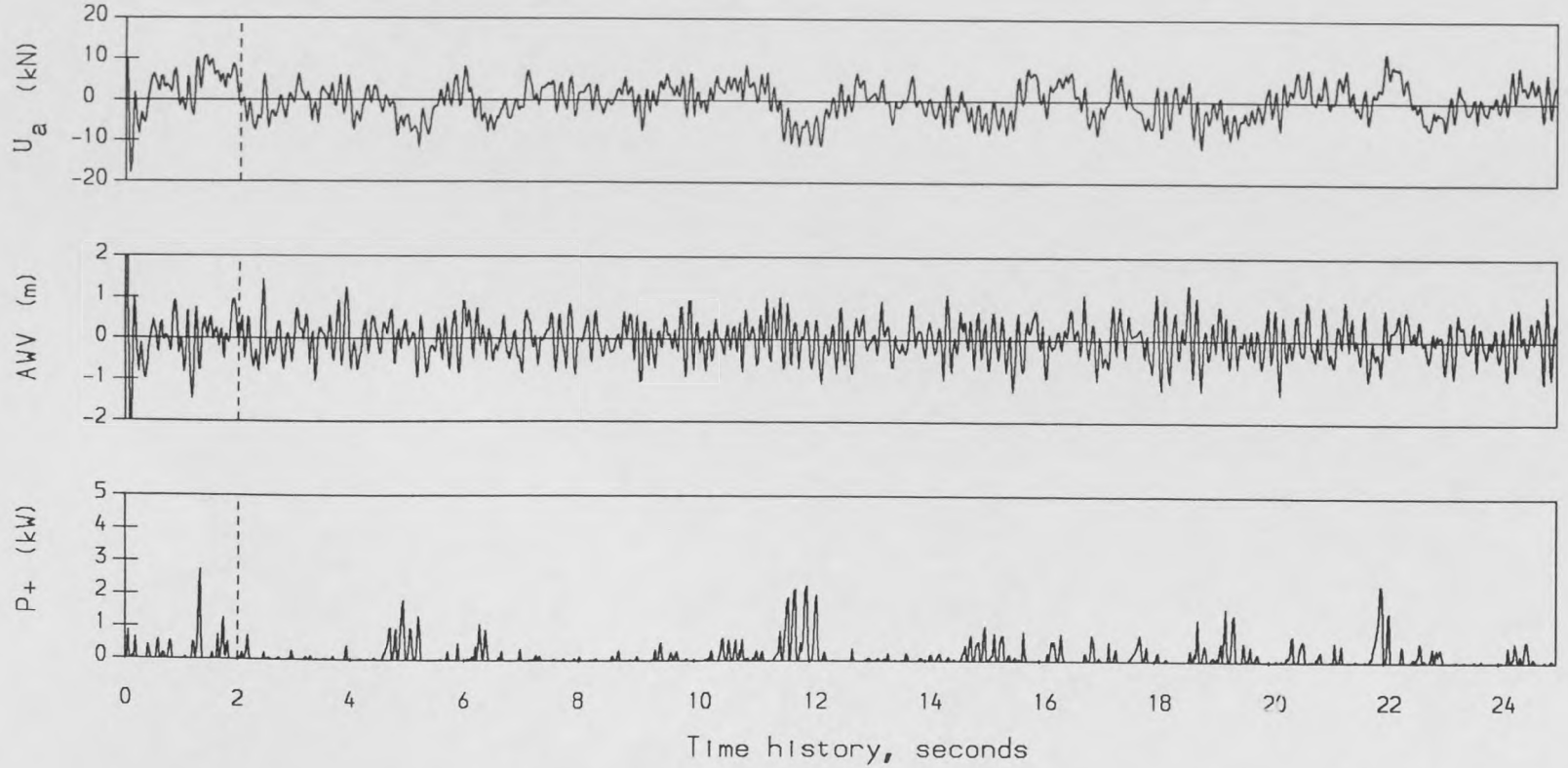

Figure 9.5. Time histories of the power demand, control force and velocity of the fully active system in group CB.

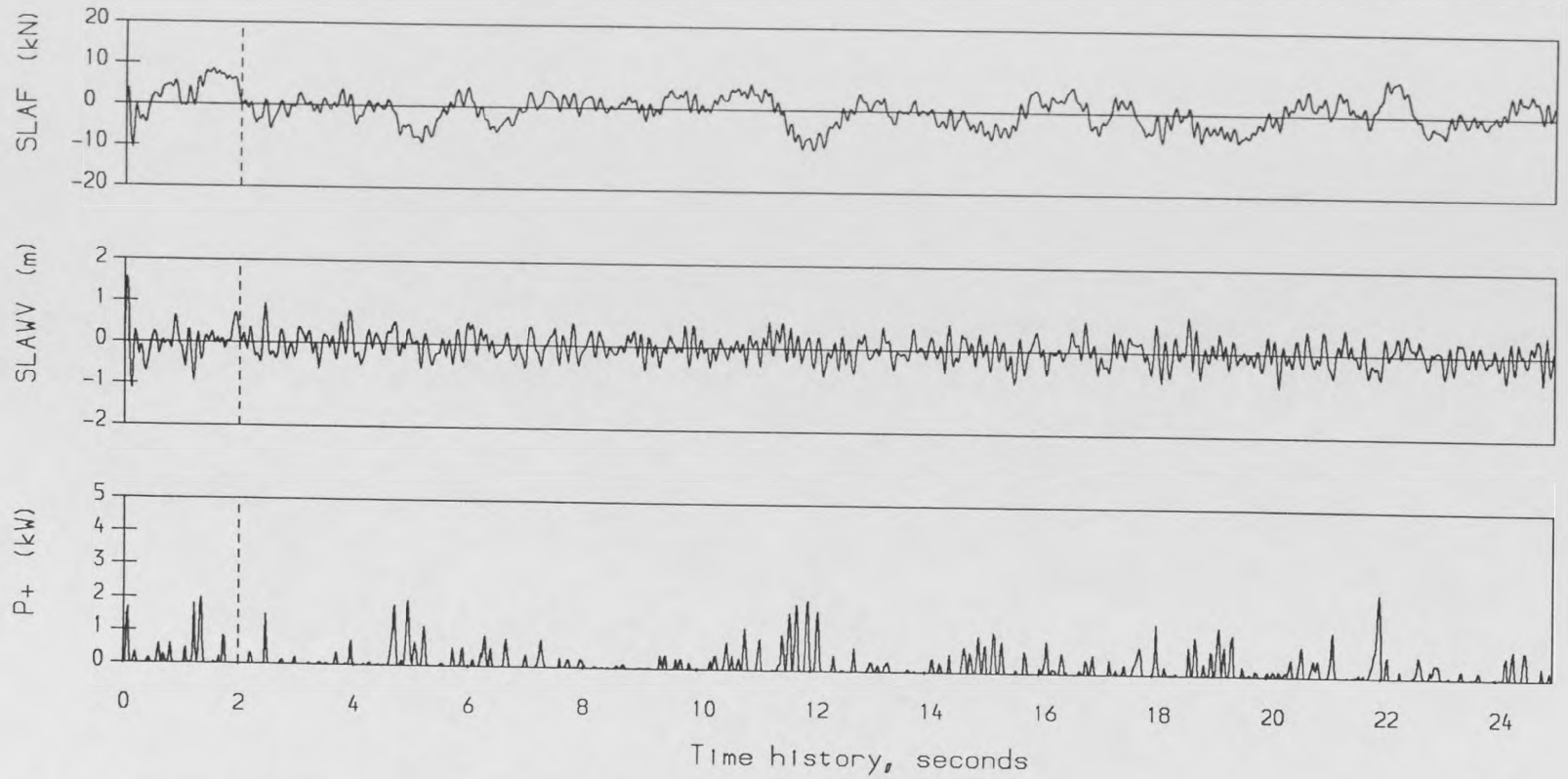

Figure 9.6. Time histories of the power demand, control force and velocity of the two state feedback slow-active system in group CB.

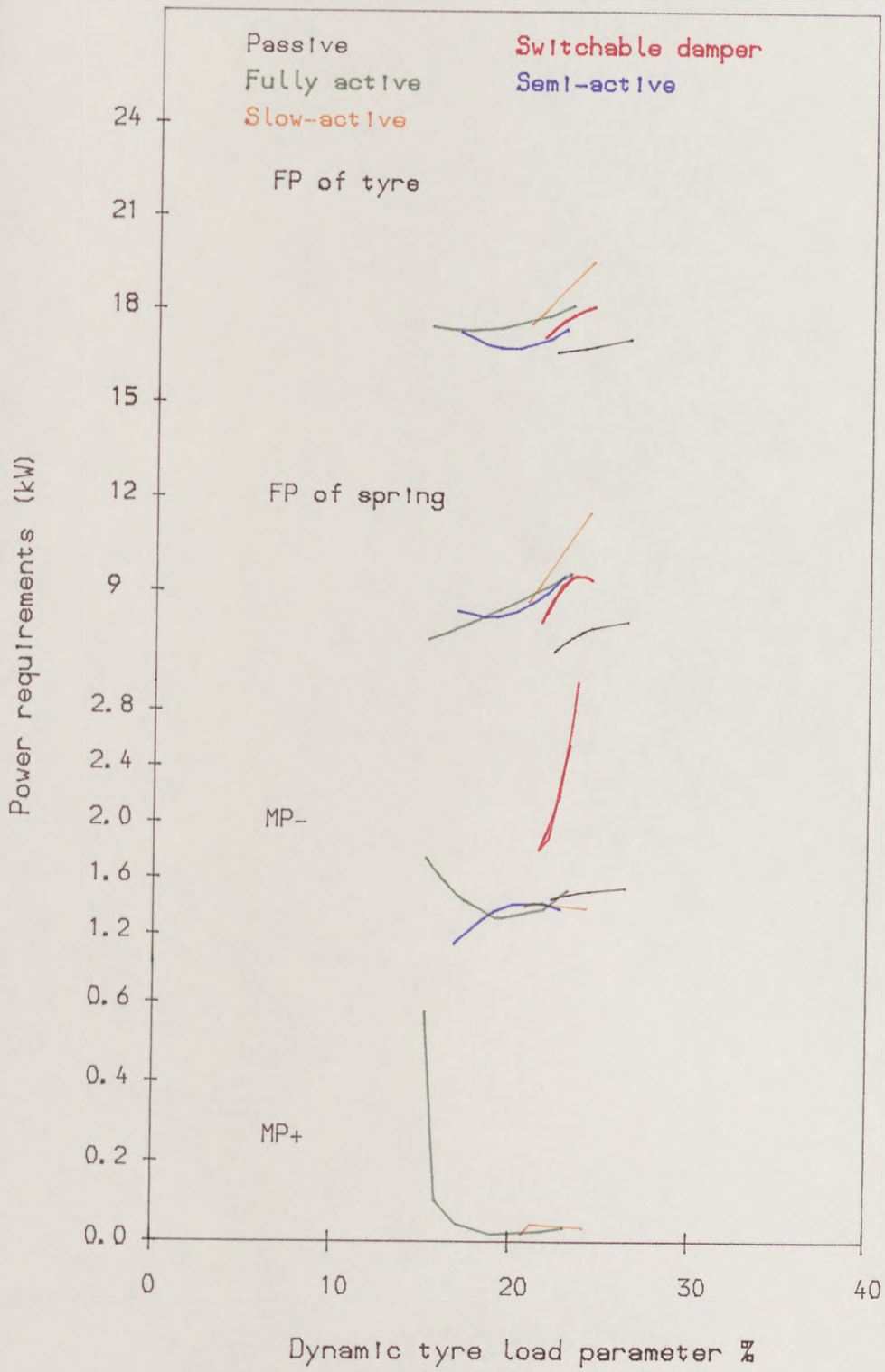

Figure 9.7. Comparison of the power requirements of all suspension systems at 2.5 cm RMS suspension working space.

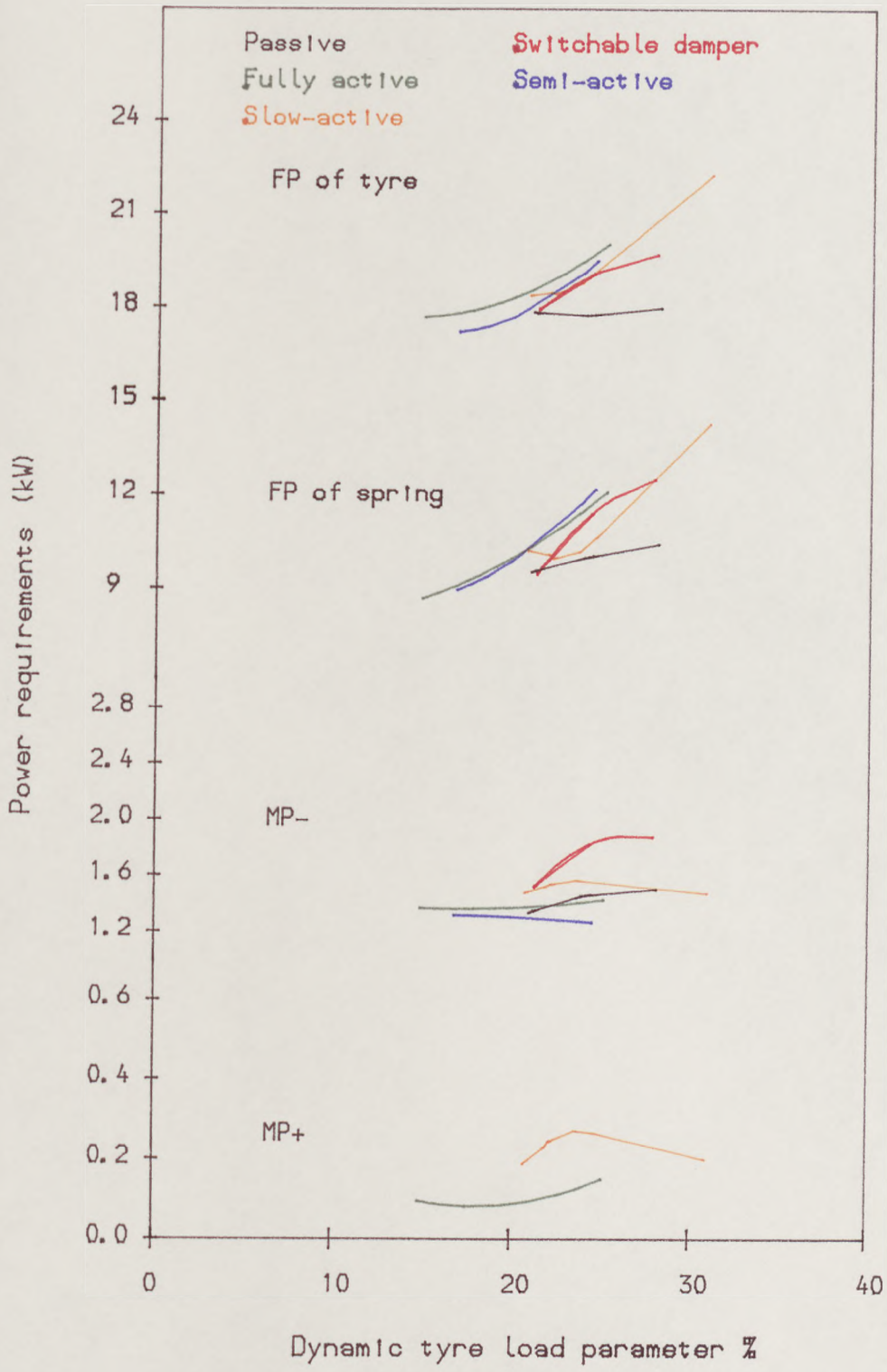

Figure 9.8. Comparison of the power requirements of all suspension systems at 3.5 cm RMS suspension working space.

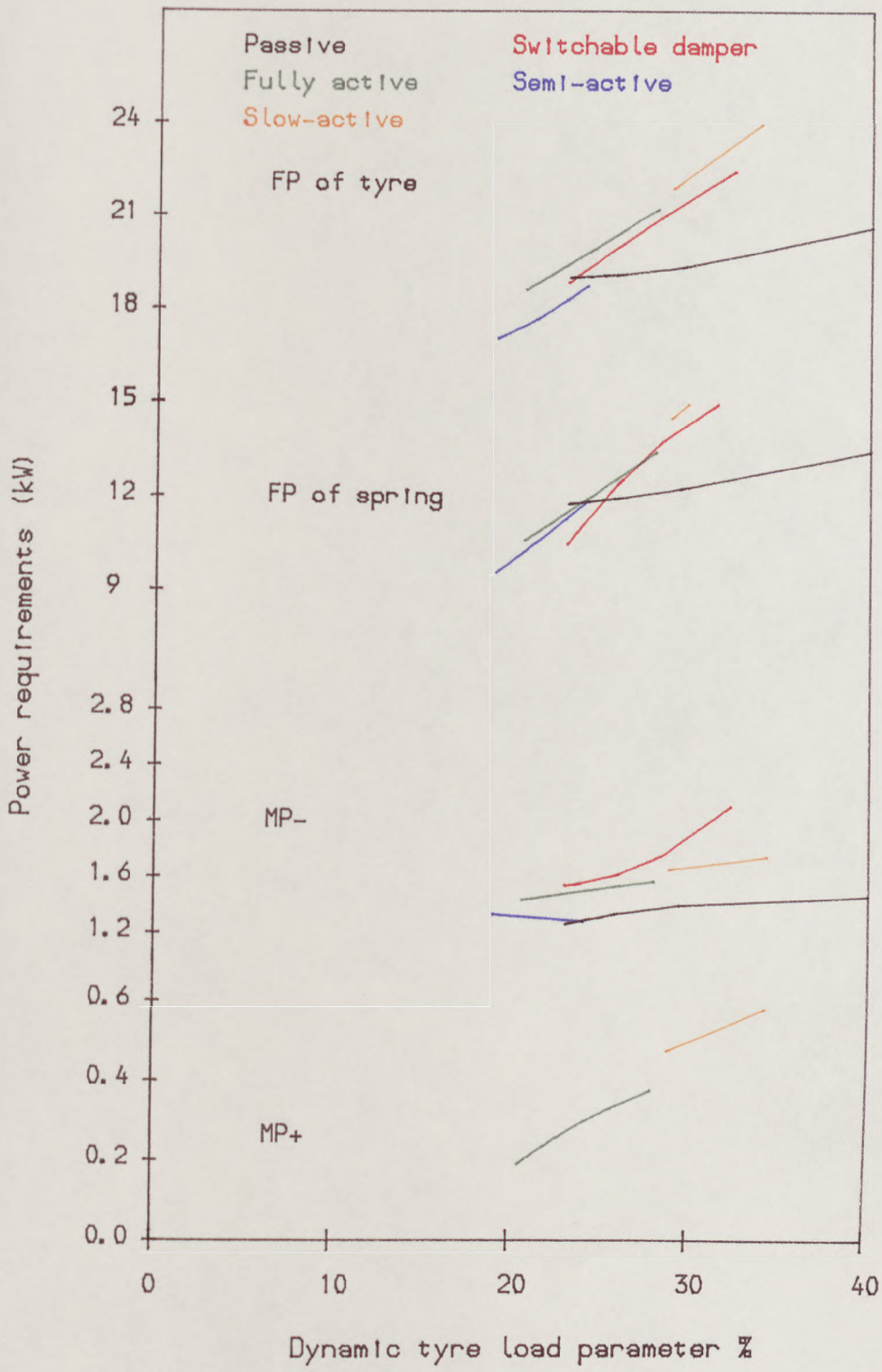

Figure 9.9. Comparison of the power requirements of all suspension systems at 4.5 cm RMS suspension working space.

CHAPTER 10

CONCLUSIONS AND SUGGESTIONS FOR FURTHER WORK

10.1 Conclusions

The fundamental conflict between the RMS dynamic tyre load, ride comfort and working space of all the suspension systems, for example as shown in figures 4.5, 5.3, 5.16, 6.3, 6.14, 7.9 and 7.19, is the main problem relating to suspension system design. In addition, the optimum suspension system for different ratios between the working space and road roughness/vehicle speed conditions, for example as shown in figures 5.11, 5.18, 6.11, 6.19, 7.17, 7.20, 8.9, 8.10 and 8.11, is not the same. The only method of overcoming this problem of obtaining the best suspension system over all conditions would be to have adaptable passive or active suspension elements which could be changed depending on the road conditions because the suspension system with fixed parameters cannot possibly be optimum over a wide range of road surfaces and vehicle forward speed. Also, although this thesis has concentrated on ride behaviour, the suspension must control body attitude. Hence it is not appropriate to select the best system from a ride point of view in isolation because it must be stiff enough to react changes in static loading and control attitude under manoeuvring, hard braking, cornering etc. In general, the suspension designer is essentially allocated a given amount of working space and must optimise the ride and handling behaviour within this constraint.

The best passive system simply from a ride point of view theoretically involves suspension elements which have very low stiffness and light damping in order to use all available workspace. But the soft spring system, which is softer than conventional, would not be stiff enough for static load changes and controlling body attitude angles. The optimum passive system over all road roughness/speed conditions would be to have adaptable spring stiffness and damping coefficients which could be changed depending on the road conditions. Some commercial systems already achieve part of this requirement by providing a limited choice of damper

settings. In practice, with a conventional non-adjustable passive system, the stiffness and damping parameters are chosen on the basis of compromising between all the road conditions over which the vehicle typically operates. Also, the passive suspension designer is restricted by the fact that changes in static loading condition use up a significant proportion of the available workspace usage. Self-levelling can be used to ensure that the full working space is available for any loading condition but it would not control vehicle attitude during cornering or braking, Crolla et al (1987). For a given working space, improvements in RMS ride comfort and dynamic tyre load can generally be obtained by reducing the spring stiffness and increasing the damper coefficient as shown in table 8.2. Finally, small improvements can be obtained by reducing the tyre stiffness or reducing the wheel/body mass ratio.

A significant improvement in ride performance can be obtained using a switchable damper with two settings and a control law as shown in figure 4.6. The continuously variable damper with a control law as shown in equations 4-6 and 4-7 offers a further improvement in ride performance over a two state switchable damper. The results suggest that improvements may be obtained over a wide range of road roughness/speed conditions. The continuously variable damper system offers an improvement in the performance even for time lag constants as high as 150 ms because it derives most of its benefit from controlling the low frequency range around the body resonant peak of approximately 1 Hz. Furthermore, it only requires measurements of the relative displacements and velocities between the body and wheel. The two state switchable damper system is much more sensitive to the time lag and improvements in the performance start to reduce if the time lag constant is greater than 11 ms. It requires measurements of the absolute velocities of the body and wheel which in practice are more difficult to obtain than the relative velocities.

The fully active system involves replacing the conventional suspension elements with a hydraulic actuator which is controlled by a high frequency response servovalve and which involves a force feedback loop. The force demand signal, typically generated in a microprocessor, is governed by a control law which is normally obtained by application of various forms of optimal control theory. The results suggest that the full state feedback linear control strategy, method 2, gives the biggest improvement in the performance index compared with the optimum passive system (which is represented the limited state feedback, type 2) as shown in tables 3.1 and 3.2. However, this system involves practical difficulties relating to measuring all the state variables of the system. The performances of the full (method 1) and limited (type 1) state feedback active systems were close to each other for a limited range of values of the ratio between the RMS working space and road input conditions GV as shown in figure 5.19. In practical terms, the control law of the active system was rearranged so that a conventional spring could be placed in parallel with the actuator. This design has obvious practical benefits since the passive spring can then be used to support the static vehicle weight and the force demanded from the actuator is vastly reduced. Hence, the power demand was significantly reduced without any change in the performance as shown in figures 5.3 and 5.16. The active non-linear control system provided significant improvements in performance and power requirements over the linear control system, although it involves practical difficulties relating to ground profile measurements and amount of data processing required.

The fully active system can be modified so that the actuator is only capable of dissipating power rather than supplying it as well. Typically, the semi-active system involves replacing the external power supply and active suspension elements with a continuously variable damper which is theoretically capable of tracking a force demand signal independently of instantaneous velocity across it as simulated

in equations 6-2 and 6-3. The semi-active systems are therefore similar to the switchable and variable damper systems but the control strategies are different. The results suggest that the semi-active system is as good as the fully active when the available suspension working space is restricted relative to the ground/speed conditions, even when the time lag constant is up to 180 ms, and it is also satisfactory to use a passive spring of conventional stiffness. The full state feedback semi-active systems give improvements in the ride comfort relative to the limited state feedback systems for the same working space, as shown in figure 6.20. In practical terms, the main difficulties would be in using a continuously variable orifice damper to generate a force demand signal independently of instantaneous velocity across it, and in particular generating either a very small force when velocity is high or very high force when velocity is small.

The actuator of the slow-active system acts in series with a passive spring and in parallel with a passive damper. The crucial, practical implication of this design is that the actuator need only have a limited frequency response capability, typically up to 3 Hz. This value was used as a baseline reference and it was established that no significant gains occur beyond this value. The control law is now based on a displacement demand signal of the different forms. The two and four state feedback slow-active systems give a similar overall performance and the performance of these systems relative to their passive elements varies in a similar way to that for conventional passive systems. The power demand and dissipation were also reduced substantially by using a conventional spring placed in parallel with the actuator without any change in the performance, as shown in figure 7.9. The slow-active arrangement then looks attractive from the viewpoints of performance, power requirements and practical feasibility.

The single state feedback fully active system is as good as the slow-active sys-

tem over a wide range of road roughness/speed conditions. It is attractive in that it only requires measurement of the relative displacement across the actuator, but in practice it would be difficult to fit all the necessary components into the limited space normally available for the suspension. It also demands an actuator with a higher frequency response than the other slow-active systems.

In comparison of all the systems, the results indicate the best performance is obtained by the fully active systems and the other systems in order of merit from the highest to lowest are: slow-active, semi-active, switchable damper and passive for the same working space, as shown in figures 8.9 and 8.10. Assuming that the fully active and slow-active systems are implemented with a conventional passive spring in parallel with the actuator, the mean and peak power demands are similar and the power dissipation is increased when operating on a rougher road while the power demand is increased when operating on a smoother road. In terms of the mean power dissipation, all the suspension systems are surprisingly similar although the detailed way in which power is dissipated during normal suspension operation must clearly be different in order to achieve differences in overall performance levels.

The fully, semi and slow active systems offer the significant advantage that the optimum control law can be selected for particular road conditions. This adaptive ability is, in principle, at least easy to arrange- it requires those sets of gains, e.g. the feedback values in equations 5.1, 7.8 and 7.10, are first calculated for various operating conditions and then stored within the microcomputer controller. Some supervisor algorithm would continually monitor the average values of the conditions under which the vehicle is operating and then update the control law settings.

Finally, a short comparison of three suspension systems is also made to illustrate all aspects of the vehicle ride criteria including the power requirements. The

systems are classified as: fully active, conventional passive and with no suspension elements, i.e. the body mass of the vehicle is directly supported on the tyre. In agricultural applications, these three systems span the extreme conditions of a conventional, unsuspended tractor through to an actively suspended version. The conventional passive systems (PAS1 and PAS2) and fully active systems (FAC1 and FAC2) in table 8.1 groups CA and CB are chosen to be used in this comparison. These passive and fully active suspension systems all have the same body natural frequency of 1.03 Hz as well as the same RMS values of dynamic tyre load and working space but significantly different values of the ride comfort and power requirements. The passive, active and unsuspended systems all have the same tyre stiffness of 700 kN/m. Figures 10.1 and 10.2 show the RMS ride comfort of all the systems and power requirements of passive and active systems versus the vehicle forward speed. The fluctuating power represents the total power of the passive spring and tyre.

The results are now viewed in a slightly different way to those discussed previously, i.e. for a given level of ride comfort the suspended systems offer the opportunity of an increased forward speed relative to the unsuspended vehicle. Hence, for the same ride comfort parameter, the passive and active systems enable the vehicle forward speed to be increased relative to the unsuspended system by 92% and 184% respectively for the systems in group CA and by 116% and 260% respectively for the systems in group CB. The active system also permits an increase in vehicle forward speed relative to the passive system of 48% and 67% for the systems in groups CA and CB respectively. The power dissipation for the both passive and active systems are similar.

Overall, the results presented in this thesis have established the potential gains in performance offered by a variety of controlled suspension systems. The pre-

dicted performances have been based entirely on the quarter car model, the main justification for this being that many other research workers support the idea that although simple it does capture all the features of the vehicle suspension problem. It has enabled progress to be made with the tasks of developing possible control laws and judging the comparative merits of the various systems. Against these predicted gains must be weighted the practical costs associated with implementing the systems. It has not been possible to predict these costs precisely because of uncertainties about prototype hardware currently under development and the economies possible with large scale production. However, comments regarding the relative practical feasibility of the systems have been made throughout.

Although the work is a continuation of previous theoretical studies, many original issues have been investigated including; power and energy calculations, non-linear active and semi-active control strategies, various new control laws for the slow-active systems and generation of results in the context of an on/off road transport vehicle.

10.2 Suggestions for further work

Further work should be aimed at investigating the ride performances including the power requirements over a wide range of the on -and off- road input conditions as follows.

1- Investigation the optimum ratios of the damper setting for the two state switchable and continuously variable damper systems. These were selected in this study on an empirical basis in that they provided good -but not necessarily optimum- performance. Also, further calculations to predict the effect of introducing realistic practical limitations such as switching dynamics, maximum and minimum available setting etc. are required.

2- For the fully, semi and slow active systems, many aspects of the ride performances are similar suggesting that further comparison between the systems will be dictated by features such as system cost, attitude control performance, handling qualities, adaptation strategies when the road surface quality changes, reliability, maintainability, failure modes, noise, harshness, packaging and etc. Further calculations of performance relating to ride behaviour or power consumption should now incorporate the response characteristics of the actual components which make up the suspension system.

3- For the slow-active and single state feedback active systems, further investigation should be based on prototype design in which the components, for example, electrical, hydraulic, pneumatic etc. are specified.

4- The fully active linear system gives the best overall performance over the other suspension systems and therefore, a potential way to obtain further improvements in performance is the active non-linear system. Further investigations aimed at methods of overcoming the practical difficulties relating to ground profile measurements and the amount of data processing are required. Progress in the development of transducers and more powerful, on-board computers may make this system a practical possibility.

5- This work has concentrated entirely on the quarter vehicle model to judge the competing systems. For the most attractive systems, the work should be extended to model half and full vehicle versions, investigating such issues as (a) the extent to which the results and control strategies are applicable to the more relaistic representations of a vehicle and (b) using power dissipated at one wheel station to feed other wheel stations where power is required.

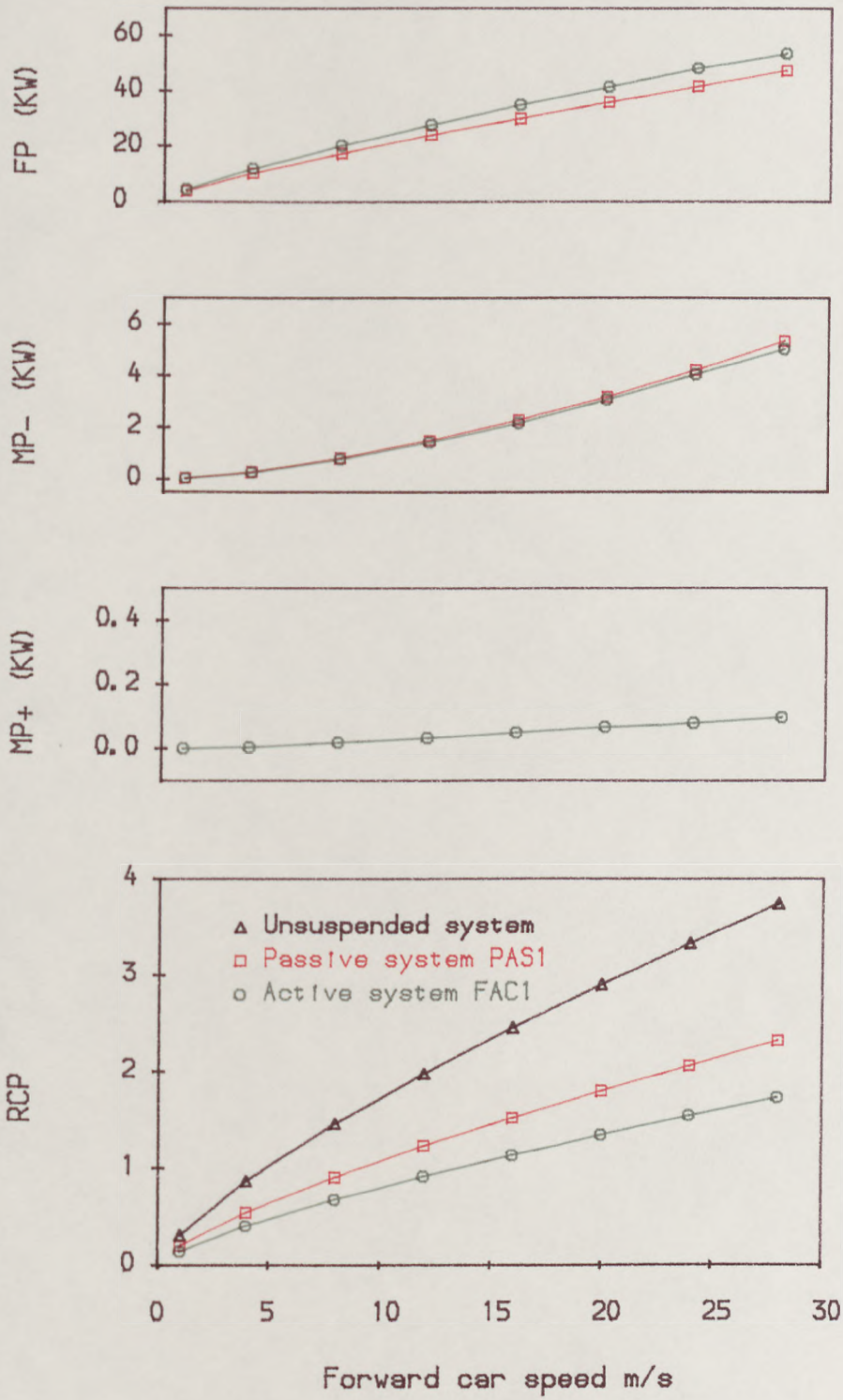

Figure 10.1 Performance capabilities and power requirements of the systems: passive, fully active and no suspension.

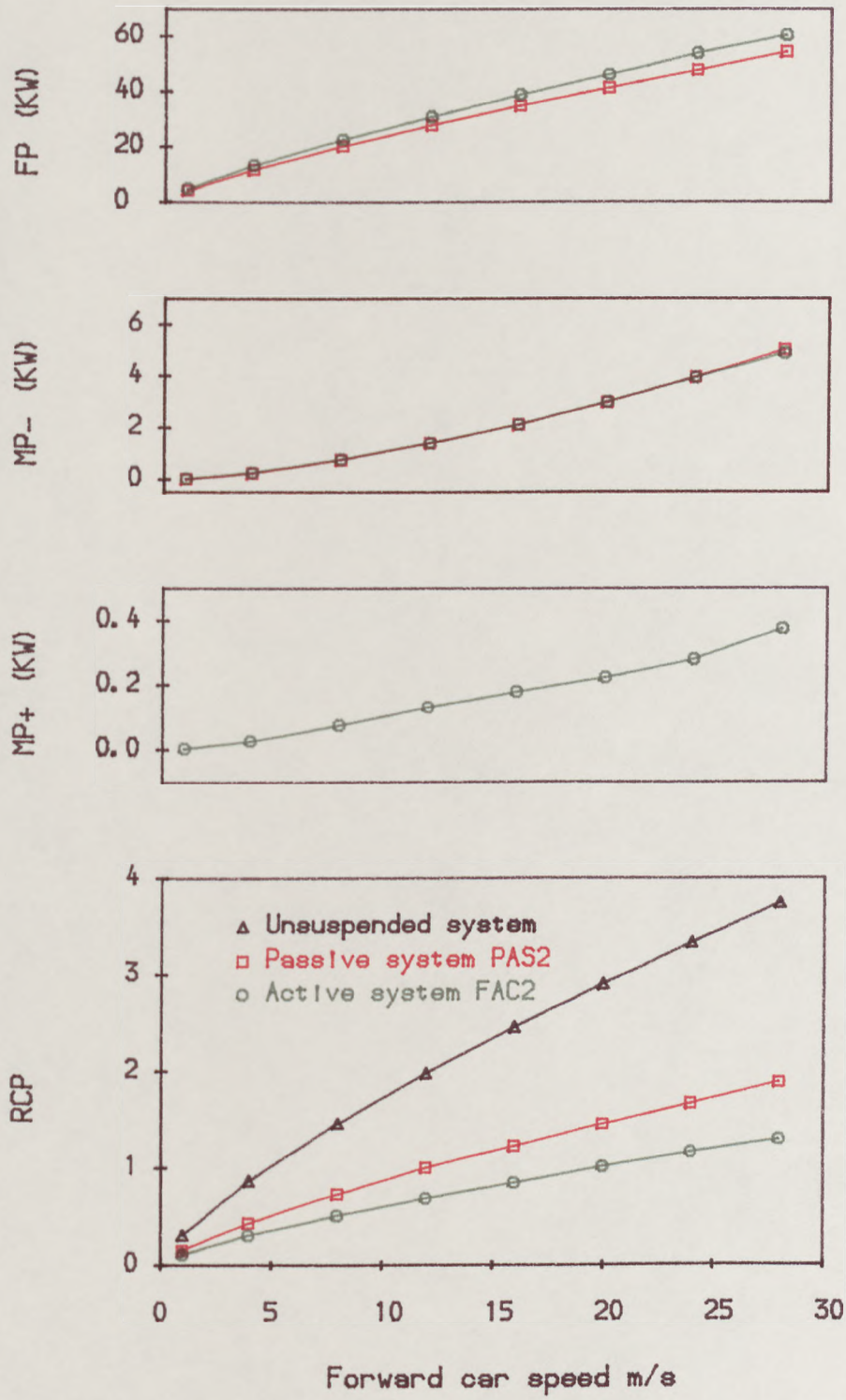

Figure 10.2 Performance capabilities and power requirements of the systems: passive, fully active and no suspension.

LIST OF REFERENCES

Abouel-Nour, A.M.A. and Crolla, D.A. [1988b] "Active control of automotive suspensions". The Eleventh Annual Operations Research Int. Con. (Technology, Productivity and Environment Development) Cairo. November 28-30.

Abdel Hady, M.B.A. and Crolla, D.A. [1989] "Theoretical analysis of active suspension performance using a four-wheel vehicle model". Proc. Instn. Mech. Engrs vol 203 pp (125-135).

Bastow, D. [1975] "The human problem in relation to vehicle suspension". The J. of Automotive Engineering, February, pp (19-20).

Bulman, D.N. [1979] "Cross-country vehicle ride simulation, details of a device for measuring cross-country ground profiles for use in vehicle ride simulation". IMechE, Automotive Engineer, February/March, pp (66-67).

Cebon, D. and Newland, D.E. [1983] "The artificial generation of road surface topography by the inverse FFT method". Proc. 8th IAVSD Symposim, Cambridge, England, MA, pp (24-42).

Clarke, M.J. [1979] "A study of the available evidence on duration effects on comfort and task proficiency under vibration". J. of Sound and Vibration, 65(1), pp (107-123).

Crolla, D.A., Horton, D.N.L., Pitcher, R.H. and Lines, J.A. [1987] "Active suspension control for an off-road vehicle". Proc. Inst. Mech. Engrs. 201(D1), pp (1-10)

Crolla, D.A. and Abouel-Nour, A.M.A. [1988a] "Theoretical comparison of various active suspension systems in terms of performance and power requirements". International Conf. on Advanced suspensions, London, October, pp (1-9).

Crolla, D.A., Firth, G.R., Hine, P. and Pearce, P.A. [1989] "Performance of suspensions fitted with controllable dampers". Proc. of the Ninth I.A.V.S.D. Conf., Kingston, Canada.

Crawford, I.L. [1987] "Semi-active suspension system". Proc. EAEC Int. Con. on New Developments in Power Train and Chassis Engineering, Strasbourg, 2 , pp (602-619)

Dodds, C.J. and Robson, J.D. [1972] "Simulated road testing". The J. of Automotive Engineering, April, pp (17-20).

Fletcher, R. and Reeves, C.M. [1964] "Function minimization by conjugate gradients". Computer J., 7, p. 149.

Gill, P.E. and Murray, W. [1979] "Conjugate-gradient method for large-scale nonlinear optimization". Dep. of operations Research, Stanford University, Technical Report SOL 79-15

Gill, P.E. and Murray, W. [1981] "Practical Optimization". Academic Press, New York.

Goodall, R.M. and Kortum, W. [1983] "Active controls in ground transportation - A review of the state-of-the art and future potential". Vehicle System Dynamics, vol. 12, pp (225-257).

Griffin, M.J. and Whitham, E.M. [1976] "Duration of whole-body vibration exposure: its effect on comfort". J. of Sound and Vibration, 48(3), pp (333-339).

Griffin, M.J. and Whitham, E.M. [1977] "Assessing the discomfort of dual-axis whole-body vibration". J. of Sound and Vibration, 54(1), pp (107-116).

Griffin, M.J. and Lewis, C.H. [1978] "A review of the effects of vibration on

visual acuity and continuous manual control, part I: visual acuity". J. of Sound and Vibration, 56(3), pp (383-413).

Griffin, M.J. and Whitham, E.M. [1978] "Individual variability and its effect on subjective and biodynamic response to whole-body vibration". J. of Sound and Vibration, 58(2), pp (239-250).

Griffin, M.J. [1986] "Evaluation of vibration with respect to human response". Society of Automotive Engineering, 860047, pp (11-34).

Hac, A. [1985] "Suspension optimisation of a 2-dof vehicle model using a stochastic optimal control technique". J. Sound and Vibration, 100(3), pp (343-357).

Healy, A.J., Nathman, E. and Smith, C.C. [1977] "An analytical and experimental study of automobile dynamics with random roadway input". Transaction of the ASME, Journal of Dynamic Systems, Measurement, and Control, December, pp (284-292).

Hedrick, J.K. and Wormley, D.N. [1975] "Active suspension for ground transport vehicles - a state of the art and review". Mechanics of Transportation AMD., A.S.M.E., vol. 15, pp (21).

Hine, P.J. and Pearce, P.T. [1988] "A practical intelligent damping system". International Conf. on Advanced Suspensions, London, October, pp (141-147).

Hrovat, D. and Margolis, D.L. [1981] "An experimental comparison between semi-active and passive suspension for air - cushion vehicles". Int. J. Vehicle Design, 23, pp (308-321).

Innocent, P.R. and Sandover, J. [1972] "A pilot study of the effects of noise and vibration acting together, subjective assessment and task performance". Human

Response to Vibration Conference, University of Sheffield, Sheffield, U.K., September.

Inns, F.M. and Kilgour, J. [1978] "Agricultural tyres". Dunlop Limited, London.

ISO, International Standards Organization. [1985] "Evaluation on human exposure to whole-body vibration". 1970, 1974, 1978.

Jacobson, M. [1976] "Road surface effects on braking and steering". IMechE, Automotive Engineer, October/November.

Jones, A.J. and Saunders, D.J. [1972] "Equal comfort contours for whole body vertical pulsed sinusoidal vibration". J. of Sound and Vibration, 23(1), pp (1-14).

Jones, A.J. and Saunders, D.J. [1974] "A scale of human reaction to whole body, vertical, sinusoidal vibration". J. of Sound and Vibration, 35(4), pp (503-520).

Kamash, K.M.A. and Robson, J.D. [1978] "The application of isotropy in road surface modelling". J. of Sound and Vibration, 57(1), pp (89-100).

Karnopp, D., Crosby, M.J. and Harwood, R.A. [1974] "Vibration control using semi-active force generators". J. of Engineering for Industry, May, 92(2), pp (619-626)

Krasnicki, E.J. [1981] "The experimental performance of an 'on-off' active damper". Shock and Vibration Bulletin Vol. 51, May.

Krishna, M. B. and Hullender, D.A. [1976] "Analytical model for guideway surface roughness". J. of Dynamic Systems, Measurement, and Control, December, pp (425-431).

Kuo, B.C. [1981] "Automatic control systems". Prentice - Hall

Lewis, C.H. and Griffin, M.J. [1978] "A review of the effects of vibration on visual acuity and continuous manual control, part II: continuous manual control". J. of Sound and Vibration, 56(3), pp (415-457).

lizell, M. [1988] "Semi-active damping" International Conf. on Advanced suspensions, London, October, pp (83-91).

Lu, X.P. and Segel, L. [1985] "Vehicular energy losses associated with the traversal of an uneven road". Proceedings 9th IAVSD- Symposium, the dynamic of vehicles on roads and on tracks, Sweden, June 24-28, pp (342-352).

Margolis, D.L., Tylee, J.L. and Hrovat, D. [1975] "Heave mode dynamics of a tracked air cushion vehicle with semiactive airbag secondary suspension". J. of Dynamic Systems, Measurement and Control, ASME Publication, December.

Margolis, D.L. [1982a] "Semi-active heave and pitch control for ground vehicles". Vehicle System Dynamics, 11, pp (31-42).

Margolis, D.L. [1982b] "The response of active and semi-active suspension to realistic feedback signals". Vehicle System Dynamics, 11, pp (267-282).

Margolis, D.L. [1983] "Semi-active control of wheel hop in ground vehicles". Vehicle System Dynamics, 12 pp (317-330)

Margolis, D.L. and Goshtasbpour, M. [1984] "The chatter of semi-active on-off suspensions and it's cure". Vehicle System Dynamics vol. 13.

Meller, T., Fruhauf, F. and Boge, A.G. [1988] "Variable damping - philosophy and experiences of a preferred system". International Conf. on Advanced suspensions, London, October, pp (113-118).

Miller, L.R [1988] " The effect of hardware limitations on an on/off semi-active

suspension". International Conf. on Advanced suspensions, London, October, pp (199-206).

Mitschke, M. [1961] "influence of road and vehicle dimensions on the amplitude of body motions and dynamic wheel loads". S.A.E. preprint 310C.

Moore, J.H. [1988] "Linear variable inductance position transducer for suspension systems". International Conf. on Advanced suspensions, London, October, pp (75-81).

NAG. [1987] "The numerical algorithms group Fortran library - mark 13". Europe and elsewhere, excluding North America and Australasia. NAG Ltd, Wilkinson House, Jordan Hill Road, Oxford, U.K. OX2 8DR.

Newland, D.E. [1984] "An introduction to random vibrations and spectral analysis". Ch. 8 Second addition, longman.

Parker, G.A. and Lau, K.S. [1988] "A novel valve for semi-active vehicle suspension systems". International Conf. on Advanced suspensions, London, October, pp (69-74).

Pollard, M.G. and Simons, N.J.A. [1984] "Passenger comfort - the role of active suspension". Proc. Instn. Mech. Engrs, Vol. 198D, PP (1-15).

Robson, J.D. [1979] "Road surface description and vehicle response". International J. of Vehicle Design, vol. 1, pp (25-53).

Ryba, D. [1973] "Possible improvements in ride comfort". Vehicle System Dynamics, 2, pp (1-32).

Ryba, D. [1974] "Improvements in dynamics characteristics of automobile suspension systems". Vehicle System Dynamics, 3, pp (17-46).

Sharp, R.S. and Hassan, S.A. [1984] "The fundamentals of passive automotive suspension system design". Proc. of the Society of Environmental Engineers conf. on Dynamics in Automotive Engineering, Cranfield Inst. Tech., pp (104-115).

Sharp, R.S. and Hassan, S.A. [1986] "The relative performance capabilities of passive, active and semi-active car suspension systems". Proc. Instn. Mech. Engrs, 200, D3, pp (219-228).

Sharp, R.S. and Hassan, S.A. [1986] "An evaluation of passive automotive suspension systems with variable stiffeness and damping parameters". Vehicle System Dynamics, 15, pp (335-350)

Sharp, R.S. and Crolla, D.A. [1987a] "Road vehicle suspension design - a review". Vehicle System Dynamics, 16, pp (167-192).

Sharp, R.S. and Crolla, D.A. [1987b] "Intelligent suspension for road vehicles - current and future developments". Proc. EAEC Int. Con. on New Developments in Power Train and Chassis Engineering, Strasbourg, 2, pp (579-601).

Sharp, R.S. and Hassan, S.A. [1987] "On the performance capabilities of active automobile suspension systems of limited bandwidth". Vehicle System Dynamics, 16, pp (213-225).

Sharp, R.S. and Hassan, S.A. [1987] "Performance and design considerations for dissipative semi-active suspension systems for automobiles". Proc. Instn. Mech. Engrs, 201(D2), pp (1-5).

Smith, C.C. McGehee, D.Y. and Healey, A.J. [1978] "The Prediction of passenger riding comfort from acceleration data". J. of Dynamic Systems, Measurement, and Control, vol. 100, March, PP (34-41).

Thompson, A.G. [1969] "Optimum damping in a randomly excited non-linear suspension". Proc. Instn. Mech. Engrs, 184(2A), pp (196-178)

Thompson, A.G. [1976] "An active suspension with optimal linear state feedback". Vehicle System Dynamics, 5, pp(187-203).

Velinsky, S.A. and White, R.A. [1980] "Vehicle energy dissipation due to road roughness". Vehicle System Dynamics, 9, pp (359-384).

Wilkinson, J.H. and Reinsch, C. [1971] "Handbook for automatic computation". Volume II, Linear Algebra, pp (339-358 and 372-395).

Wilson, D.A., Sharp, R.S. and Hassan, S.A. [1986] "Application of linear optimal control theory to the design of automobile suspensions". Vehicle System Dynamics, 15, pp (103-118).